The metabolic consequences of gene knockout to pathway flux in trypanosomes

Maria Fatarova

Université de Toulouse

THÈSE

En vue de l'obtention du

DOCTORAT DE L'UNIVERSITÉ DE TOULOUSE

Délivré par :
Institut National des Sciences Appliquées de Toulouse (INSA de Toulouse)

Cotutelle internationale avec :

Présentée et soutenue par :
Maria Fatarova
Le mardi 23 mai 2017

Titre :
The metabolic consequences of gene knockout to pathway flux in Trypanosomes

---

ED SEVAB : Ingénieries microbienne et enzymatique

Unité de recherche :
LISBP - MetaSys

Directeur(s) de Thèse :

Prof. Jean-Charles Portais

Rapporteurs :

Prof. Michael Boshart
Dr. Sophie Colombié

Autre(s) membre(s) du jury :

Dr. Frédérick Bringaud
Dr. Patrick Kiefer
Dr. Patrick Moreau

Abstract

Unusual metabolism of protozoan parasite causing deadly sleeping sickness, *Trypanosoma brucei*, has been enigmatic for many years. In the past decades, targeted genetic perturbations combined with metabolic analysis have advanced the view on complex compartmentalized metabolism of this organism, but acyl-CoA metabolism on the crossroad between catabolic and anabolic pathways, remains largely uncharacterized. Present work aims at clarifying mitochondrial operation and topology of acyl-CoA network of *T. brucei*, as well as its interconnections with the rest of metabolism. This has required the development of a complete framework for investigation of acyl-CoA metabolism in *T. brucei* integrating isotope labeling experiments with metabolite quantification.

Sensitive LC-MS method for identification and quantification of acyl-CoAs based on high-resolution mass spectrometry (*HRMS*) with LTQ-OrbiTrap has been established. In presented work, the LC-HRMS method was applied to investigate acyl-CoA metabolism in the protozoan parasite *Trypanosoma brucei*, as well as in the model bacterium *Escherichia coli*. Appropriate sampling protocols were set up and validated for these two organisms. Absolute quantification was based on application of isotope dilution method that prevents biases during sampling and analysis. Parameters of analytical method have been characterized and method has been validated for 9 short-polar acyl-CoA thioesters. Validation criteria of acyl-CoA thioesters of interest included accuracy, precision, linear range, detection and quantification limits.

Knowledge of the composition and absolute concentrations of Acyl-CoAs is important for understanding the interaction with metabolic pathways as well as analysis of their *in vivo* conversion rates. This approach paves the way for study of the topology of the metabolic network. Complete workflow from cell cultivation, measurement of extracellular fluxes and analysis of isotopic profile which is result of enzyme-specific incorporation of isotopic tracer allowed modeling of metabolic network and calculation of metabolic fluxes. The entire workflow has been biologically validated and has clarified the link between acyl-CoA and central carbon metabolism in *E. coli,* model organism in systems and synthetic biology.

The proposed framework has been adapted to *T. brucei*, for which several sample collection methods have been evaluated thoroughly. It was possible to extract, identify and quantify main acyl-CoA species produced from glucose catabolism. This optimised setup for acyl-CoA analysis will allow collection of data for NMR-based analysis of metabolic end products as well as collection of intracellular metabolites from same sample. Applied genetic modifications and instationary ^{13}C analysis is yet to be resolved.

Keywords

Polar Acyl-CoA thioesters, quantification, method validation, isotope profiling, ^{13}C-MFA, *Escherichia coli*, *Trypanosoma brucei*

Acknowledgements

This work was funded by the European Commission FP7 Marie Curie Initial Training Network 'ParaMet' (290080)

Resumé

Cette thèse s'est déroulée dans le cadre du projet ParaMet, qui s'inscrit dans un réseau de formation initiale Marie Sklodowska-Curie financé par la Commission européenne. Ce projet ParaMet s'est focalisé sur l'analyse du métabolisme de nombreuses espèces parasitaires affectant des millions de personnes dans des régions pauvres du monde : Le *Trypanosoma brucei* (*T. brucei*) africain provoque la maladie du sommeil, le *Trypanosoma cruzi* sud-américain provoquant la maladie de Chagas, *Leishmania major* causant des déformations cutanées sévères et le *Plasmodium falciparum* qui cause le paludisme. Le contexte de ce projet de thèse était d'approfondir la compréhension du métabolisme de *Trypanosoma brucei*. Historiquement, le métabolisme du trypanosome a été étudié dans des milieux riches en glucose, et l'organisme réorganise significativement son métabolisme en l'absence de glucose. Les trypanosomes utilisent différents types de sources de carbone, des hydrates de carbone ainsi que des acides aminés pour alimenter leurs besoins énergétiques et biosynthétiques (conditions imitant réellement l'environnement dans la mouche tse-tse). Les différences de thioesters d'acyl-CoA sont encore inconnues dans ces conditions. Une telle élucidation est essentielle pour comprendre les adaptations métaboliques de l'organisme au cours de son cycle de vie.

Cet objectif pourrait être complété par une combinaison d'analyses sensibles de divers groupes de métabolites, de délétions dirigées de gènes ou de régulations négatives. Leur combinaison induit des changements métaboliques et aboutit finalement à la description de la fonction des gènes et à la réponse des organismes à ces conditions particulières.

Dans ce contexte, l'objectif de recherche spécifique de ce travail était d'acquérir une vue quantitative et la topologique détaillée duréseau métabolique mitochondrial des thioesters d'acyl-CoA à chaines courtes des trypanosomes à la lumière de différentes perturbations génétiques. Plusieurs voies anaboliques s'appuient sur l'utilisation de la biosynthèse de l'acétyl-CoA-FAS II, de l'ELO et des stérols. Le taux de conversion in vivo de l'acétyl-CoA provenant de diverses sources de carbone dans ces voies reste à caractériser. Cela nécessitait d'établir et de valider une méthodologie pour une étude fonctionnelle détaillée et complète du métabolisme cellulaire dans les trypanosomes. Ces derniers développements intègrent un flux de travail complet d'analyse des flux métaboliques par ^{13}C à l'état-instationnaire. Ce flux

de travail combine les méthodes existantes pour la collecte d'échantillons, la métabolomique quantitative basée sur MS et l'analyse isotopique d'acides organiques, d'acides aminés, de composés phosphorylés en plus des thioesters d'acyl Coenzyme A (acyl-CoAs), qui représentent un point central entre le métabolisme central du carbone et les voies anaboliques. Ce flux de travail a d'abord été évalué et validé sur l'organisme modèle *Escherichia coli* et a fourni de nouvelles idées sur son fonctionnement métabolique. Par la suite, ce flux de travail a ensuite été exploité pour étudier le métabolisme de *T. brucei*, pour lequel les résultats préliminaires sont décrits et discutés dans cette thèse.

Les thioesters d'Acyl-CoA représentent un pont entre les voies cataboliques et anaboliques et participent également à la production d'énergie. Mais malgré l'importance du coenzyme A dans les études sur le métabolisme, le réseau métabolique des acyl-CoA de *T. brucei* n'a pas été complètement résolu. Les rapports d'acides aminés différents en tant que sources de carbone ont soulevé des questions concernant leur incorporation dans les acides gras et les stérols par des intermédiaires d'acyl-CoA. Dans le cadre de cette thèse, l'objectif est d'obtenir une description détaillée du métabolisme des thioesters d'acyl-CoA dans le métabolisme central du carbone et la biosynthèse des lipides et des stérols. L'accent a été mis sur les thioesters polaires courts d'acyl-CoA, car ces composés représentent le lien le plus étroit entre les réactions cataboliques et la biosynthèse des lipides et des stérols. L'objectif est de définir le réseau de réactions biochimiques qui opère réellement dans le *T. Brucei* procyclique. Les données métaboliques qualitatives et quantitatives sont informatives mais cependant, ne permet pas de résoudre la topologie des réactions. Le profilage ^{13}C seul ou en combinaison avec des perturbations génétiques (KO, RNAi mutants) fournit des informations détaillées sur la topologie du réseau métabolique et la fonction des gènes et cette stratégie sera appliquée afin d'examiner l'incorporation du ^{13}C dans les intermédiaires métaboliques de *T. brucei*.

Le choix de la méthode d'échantillonnage des métabolites est crucial dans la métabolomique car il peut déterminer à la fois le contenu des métabolites observé et l'interprétation ultérieure des données. Idéalement, la préparation des échantillons devrait être rapide et fiable, éviter la sous-estimation des niveaux de métabolites pendant l'échantillonnage et prévenir leur dégradation ou leur perte lors de l'extraction. Cette tâche nécessitait de mettre en place un cadre méthodologique complet pour l'étude fonctionnelle du métabolisme de

l'acyl-CoA, présenté dans le chapitre 2. La méthode d'analyse adaptée permet une quantification précise des thioesters courts d'acyl-CoA basés sur le principe de la spectrométrie de masse par dilution isotopique (IDMS). Tous les acyl-CoAs court-polaires ciblés pour la description de l'acide gras mitochondrial et de la biosynthèse des stérols de trypanosome ont été validés selon les critères définis. La quantification absolue ne décrit qu'un seul paramètre du réseau métabolique, pour déchiffrer les expériences de traceur de topologie ^{13}C. Afin d'évaluer l'aptitude de la méthode analytique à détecter sept thioesters, un profil isotopique a été obtenu avec *E. coli* cultivé sur un mélange défini d'acétate marqué produisant tous les intermédiaires métaboliques avec un profil isotopique prédéfini. Ce profil peut être simulé et la distribution des isotopologues de carbone peut être comparée aux valeurs mesurées. Pour les thioesters acyl-CoA, les isotopologues les plus lourds et les plus légers étaient inférieurs à la limite de détection (LOD). Les isotopologues au milieu du modèle étaient en accord avec les valeurs simulées, à l'exception de la butyryl-CoA qui se révélait être coéluée avec une molécule inconnue. Dans le chapitre 3, nous validons l'applicabilité biologique de la méthodologie sur la bactérie *E. coli*, un organisme modèle dans les systèmes et la biologie synthétique. Un flux de travail complet pour l'étude du métabolisme de l'acyl-CoA a été développé, validé et appliqué sur *E. coli*, un organisme modèle utilisé en biologie des des systèmes et synthétique et aussi un organisme largement utilisé dans les plate-formes de biotechnologie. Ce flux de travail intègre une métabolomique optimisée et des expériences de marquage isotopique avec une modélisation quantitative. À notre connaissance, ce travail explore pour la première fois l'interconnexion fonctionnelle entre le métabolisme central et le métabolisme de l'acyl-CoA chez *E. coli*. Malgré le grand nombre d'études de flux effectuées sur *E. coli*, il n'existe aucun modèle qui relie le métabolisme central au métabolisme des acyl-CoAs. Nous avons donc développé un tel modèle, qui a été utilisé i) pour valider l'approche proposée et ii) étudier le métabolisme de l'acyl-CoA dans *E. coli*. Outre la validation de la métabolomique et des données isotopiques obtenues à l'aide des méthodes présentées, nous avons clarifié les voies qui produisent de l'acétyl-CoA, malonyl-CoA, succinyl-CoA et propionyl-CoA dans des cellules d'*E. coli in vivo* en culture avec du glucose.

Enfin, dans le chapitre 4, nous présentons les premiers résultats obtenus sur le métabolisme de *T. brucei*. *T.brucei* se caractérise par la présence d'organites métaboliquement importants

- tels que le glycosome et les mitochondries qui répondent aux changements environnementaux (i.e. changement de substrat de carbone) en réorientant le flux métabolique (glycolyse du glucose, de la gluconeogénèse de la proline, de la glutamine) et sont intéressant dans l'étude des capacités d'adaptation pendant un cycle de vie assez complexe. Certaines des voies métaboliques actives sont situées dans plusieurs organites. L'utilisation du traçage des isotopes est une manière élégante de résoudre la topologie ainsi que les conversions métaboliques in vivo dans les flux de compartiments et leur distribution à la lumière des modifications génétiques appliquées. Ces raisons ont inspiré le sujet de cette thèse, qui visait à résoudre la topologie et le fonctionnement du réseau métabolique des thioesters d'acyl-CoA, qui sont sur le carrefour entre les voies cataboliques et anabolisantes, en utilisant des expériences de traçage isotopique du réseau métabolique.

Les applications de la métabolomique aux trypanosomes ont non seulement fourni des informations nouvelles et précieuses sur leur métabolisme, mais elles ont également mis l'accent sur la forte souplesse métabolique de ces organismes. Jusqu'à présent, les recherches se sont concentrées principalement sur le métabolisme central du carbone, afin de résoudre les caractéristiques métaboliques très inhabituelles de ces organismes. Un défi à l'avenir sera de déchiffrer le réseau métabolique complet, à savoir le réseau cellulaire, de *T. brucei* et plus généralement, les trypanosomes. Avec la disponibilité récente du réseau métabolique complet de *T. brucei* (à l'échelle du génome), l'approche isotopique du profilage est susceptible d'accélérer considérablement les progrès sur le métabolisme parasitaire, ainsi que l'identification de nouvelles cibles de médicaments. À côté de la reconstruction métabolique, un deuxième défi pour le prochain avenir est d'obtenir une meilleure compréhension quantitative du fonctionnement du métabolisme dans les trypanosomes. La mesure des flux métaboliques peut être obtenue à partir d'expériences de marquage isotopique à l'aide de modèles mathématiques pertinents. La forte compartimentation du métabolisme de *T. brucei*, ainsi que l'apparition de doubles réactions, rend actuellement l'analyse du flux métabolique dans cet organisme un véritable défi. Les développements mathématiques récents ainsi que l'application d'expériences d'étiquetage du cours peuvent aider à cet effet. Cette approche permettra d'obtenir des informations plus détaillées sur l'opération et la régulation du métabolisme de *T. brucei*. Ils représenteront également un outil

précieux pour mesurer l'impact réel des médicaments sur leur métabolisme et leurs capacités de croissance.

List of abbreviations

Abbreviation	Meaning
1,3-BPG	1,3-bisphosphoglyceraldehyde
1,3DiPG	1,3-diphosphoglycerate
2-KG	2-ketoglutarate
2KGDH	2-ketoglutarate dehydrogenase
2PG	2-phosphoglycerate
3-HMG-CoA	3-hydroxy-3-methylglutaryl Coenzyme A
3-PG	3-phosphoglycerate
AC	acetate
AcAcCoA	acetoacetyl Coenzyme A (3-oxobutanoyl-CoA)
ACC	acetyl-CoA carboxylase
AcCoA	acetyl Coenzyme A
AceCS	AMP-forming acetyl-CoA synthetase
ACH	acetyl-CoA transferase
ACH	acetyl-CoA thioesterase
ACO	aconitase
Aco	aconitate
ACP	acyl carrier protein
ADP	adenosine diphosphate
AKCL	2-amino-3-ketobutyrate-CoenzymeA ligase
AKGDH	a-ketoglutarate dehydrogenase
AMP	Adenosine monophosphate
AOB	amino-oxobutyrate
ASCT	acetyl: succinyl-CoA trasnferase
ATP	adenosine triphosphate
BSF	Trypanosoma brucei - bloodstream form
ButCoA	Bytyryl Coenzyme A
C16	palmitic acid
C18	stearic acid
C8	octanoate
CE-MS	capillary electrophoresis - mass spectrometry
CID	Carbon isotopologue distribution
Cit	citrate
citsynth	citrate synthase
CoA	coenzyme A
CoASH	free coenzyme A
CrotCoA	crotonyl coenzyme A
CS	citrate synthase
CSF	celebrospinal fluid
CTP	cytidine triphosphate
CV	coefficient of variance
Da	dalton, unit of atomic mass
D-Glu	D-glucose
DHAP	dihydroxyacetone phosphate

Abbreviation	Meaning
DPCK	dephospho-CoA kinase
E. coli	Escherichia coli
EI	electron impact ionisation
EIC	extracted ion chromatogram
ELO	elongase system of fatty acid biosynthesis
eno	enolase
ER	endoplasmic reticulum
Ery4P	erythrose 4-phosphate
ESI	electrospray ionisation
FAB	fast atom bombardment ionisation
FAS	fatty acid synthesis
FF	fast flitration sampling
FHg / FHc	fumarate hydratase (glycosomal /cytosolic)
FRDg / FRDm	NADH-dependent fumarate reductase (glycosomal / mitochondrial)
Fru-1,6-BP	frucoctose -1,6 - bisphosphate
Fru6P	fructose-6-phosphate
FruBP	fructose-1,6-biphosphatase
FTMS	fourier Transform Mass Spectrometry
Fum	fumarate
FUM	fumarase
FWHM	full width at half maximum
G6pdh	glucose-6-phosphate dehydrogenase
GA3P	glyceraldehyde-3-phosphate
GAPD	glyceraldehyde-3-phosphate dehydrogenase
GC-MS	gas chromatography - mass spectrometry
gDW	gram dry weight
Glc6P	glucose-6-phosphate
GLU	glutamate
GPDH	glycerol-3-phosphate dehydrogenase
GPI	glycophosphatidylinositol anchor
HBDH	3-hydroxy-3-butyrate dehydrogenase
HCD	higher energy collisional induced dissociation
HESI	heated electrospray ionisation
HGML	3-hydroxy-3-methyl-glutaryl CoA lyase
HGMR	3-hydroxy-3-methyl-glutaryl CoA reductase
HGMS	3-hydroxy-3-methyl-glutaryl CoA synthase
HILIC	hydrobilic interaction liquid chromatography
HPCE	high performance capillary electrophoresis
HPLC	high performance liquid chromatography
HXK	hexokinase
ICL	isocitrate lyase
IDH	isocitrate dehydrogenase
IDMS	isotopic dilution mass spectrometry
IEC	ion exchange chromatography
IS	internal standard

Abbreviation	Meaning
isoCIT	isocitrate
IVDH	isovaleryl-CoA dehydrogenase
χ^2	Khi2, a test of goodness of fit establishes whether an observed frequency distribution differs from a theoretical distribution.
L.mexicana	Leishmania mexicana
LC-MS	liquid crhomatography - mass spectrometry
L-Gln	L-glutamine
LOD	limit of detection
LOQ	limit of quantification
L-Pro	L-proline
M. extorquens	Methylobacterium extorquens
m/z	mass-to-charge ratio
Mal	malate
MalCoA	malonyl Coenzyme A
maldh	malate dehydrogenase
MALDI	matrix assisted laser desorption ionisation
MDH	malate dehydrogenase
Mec / Mem	malic enzyme (cytosolic / mitochondrial)
Metcrot-CoA	methylcrotonyl Coenzyme A (trans-2-methylbut-2-enoyl-CoA)
Metmal-CoA	methylmalonyl Coenzyme A (isosuccinyl-CoA)
MFA	metabolic flux analysis
MID	mass isotopologue distribution
MRM	multiple reaction monitoring
MS	mass spectrometry
MS	mass spectrometry
MS/MS	tandem mass spectrometry
MVAK	mevalonate kinase
NA	not available
n/d	not detected
NAD(P)	nicotinamide adenine dinucleotide phosphate (oxidized)
NAD(P)H	nicotinamide adenine dinucleotide phosphate (reduced)
NAD+	nicotineamide adenine dinucleotide (oxidized)
NADH	nicotinamide adenine dinucleotide (reduced)
NMR	nuclear magnetic resonance
OAA	oxaloacetate
OD	optical density (measured at 600nm)
ODE	ordinary differential equation
OHButCoA	OH-butyryl Coenzyme A
P.falciparum	Plasmodium falciparum
P5P	pentose phosphates
PANK	pantohtenate kinase
PCF	Trypanosoma brucei - procyclic form
PDH	pyruvate dehydrogenase complex
PEP	phosphoenolpyruvate
PEPCK	phosphoenol pyruvate carboxykinase

Abbreviation	Meaning
PFK	phosphofructokinase
PGI	glucose-6-phosphate isomerase
PGKB	phospho-glyceorl kinase (isoform B)
PPAT	phosphopantethine adenyltrasnferase
PPCS	4'-phosphopantothenoylcysteine synthase
PPDK	pyruvate phosphate dikinase
ppm	parts per million (unit)
PPP	pentose phosphate pathway
PRODH	proline dehydrogenase
PropCoA	propionyl Coenzyme A
PYK	pyruvate kinase
Pyr	pyruvate
QC	quality control
QqQ	triple quadrupole mass spectrometer
Q-TOF	quadrupole time of flight mass spectrometer
R2	coefficient of determination
Rib-5-P	ribose-5-phosphate
Ribu-5-P	Ribulose-5-phosphate
RNAi	RNA interference
RP	reversed phase
rpe	ribulose 5-phosphate epimerase
RSD	relative standard deviation
SAG	glutamate semialdehyde
sba	seduheptulose-1,7-bisphosphate aldolase
sbpase	sedoheptulose-1,7-bisphosphatase
SCP2	thiolase isoform 2
SCS (ScoAS)	succinyl-CoA synthetase
SDH	succinate dehydrogenase
Sed7P	sedoheptulose-7-phosphate
SPE	solid phase extraction
SRM	selected reaction monitoring
SUC	succinate
SucCoA	succinyl coenzyme A
T.brucei	Trypanosoma brucei
T.cruzi	Trypanosoma cruzi
tal	transaldolase
TCA	tricarboxylic acid cycle (Krebs cycle)
TDH	threonine dehydrogenase
Thr	Threonine (L-c
TIC	total ion current
TIM	triose-phosphate isomerase
TMS	trimethylsilyl
tpi	triose phosphate isomerase
UPLC	ultra perfomance liquid chromatography
upt	uptake

Abbreviation	Meaning
UV	ultratiolet electromagnetic radiation
VSG	variant surface glycoprotein
Xyl-5-P	Xylose -5-phosphate
WT	wild type

List of figures

List of tables

Contents

Preface

This Thesis has been developed within scope of ParaMet project, a Marie Sklodowska-Curie Initial Training Network funded by European comission. Project focused on analysis of metabolism in numerous parasitic species affecting millions of people in poor parts of the world – african *Trypanosoma brucei* (*T. brucei*) causing *sleeping sickness*, south-american *Trypanosoma cruzi* causing *Chagas disease, Leishmania major* causing severe cutanous deformities of soft tissues and *Plasmodium falciparum* which casues malaria. The general topic of this project was deeper understanding of metabolism of *Trypanosoma brucei*. This goal could be completed by combination of sensitive analysis of various groups of metabolites and directed gene deletions or downregulations. Combination of both captures induced metabolic changes and ultimately results in description of gene function and organisms' response to these particular conditions.

In this context, the specific research objective of this work was to acquire detailed quantitative and topological view on the mitochondrial metabolic network of short polar acyl coenzyme A thioesters of trypanosomes in light of different genetic perturbations. This required establishing and validating a methodology for detailed and comprehensive functional investigation of cellular metabolism in trypanosomes. The latter developments integrate a complete instationary ^{13}C-metabolic flux analysis workflow. This workflow combines existing methods for sample collection and quantitative MS-based metabolomics and isotopic analysis of organic acids, amino acids, phosphorylated compounds in addition to acyl Coenzyme A thioesters (acyl-CoAs), which represent pivotal connection between central carbon metabolism and anabolic pathways. This workflow was first evaluated and validated on the model organism *Escherichia coli* and has provided new insights into its metabolic operation. Subsequently, this workflow was then exploited to investigate *T. brucei* metabolism, for which preliminary results are described and discussed in this Thesis.

The **first chapter**, part of which has been published as a book chapter, comprises a bibliographic introduction of *T. brucei* and presents current methodologies used for functional investigations of its metabolism. The focus of this chapter is to introduce the reader to particularities of *Trypanosoma brucei*, interest of studying acyl-CoA thioesters in this parasite and specific chemistry of acyl-CoA thioesters which were targeted in the scope of the whole thesis.

The **second chapter** introduces previously published methodology for quantitative analysis of acyl-CoAs. This forms the basis of the application and validation of an analytical method enabling quantitation and isotopic profiling of acyl-CoAs for further instationary ^{13}C-metabolic flux studies.

The **third chapter** focuses on the evaluation and validation of the applicability of these developments to investigate biological systems. The entire instationary ^{13}C-metabolic flux analysis

workflow, which is briefly described in this chapter, was tested on the model organism *Escherichia coli*. Metabolomics and isotopic data obtained on acyl-CoAs were integrated with additional data on other classes of metabolites (organic acids, phosphorylated sugars, amino acids) into an instationary isotopic model used for flux calculations. This first ^{13}C-MFA investigation of the interconnection between central metabolism and CoAs metabolism in *E. coli* allowed to validate the present workflow and provided new insights into its metabolic operation.

The present methodology was applied to investigate *T. brucei* metabolism in the **fourth chapter**. The initial aim was to assess the impact of targeted gene deletions on acyl-CoA metabolism. However, sample collection method currently used, has proven unreliable and halted planned flux analyzes. Cell collection protocol had to be adapted and evaluated and preliminary results on metabolic investigations of *T. brucei* are presented.

Finally, the **fifth chapter** summarizes and discusses the results obtained during this thesis and proposes outlook for future flux investigations in trypanosomes.

All the methods and protocols used are detailed in **sixth chapter**.

Acknowledgements

This work would not see the light without support of numerous people in teams of MetaSys, MetaToul (Toulouse, FR) and iMET (Bordeaux, FR). I would like to express my gratitude to everyone who has helped me to progress.

First of all, I would like to thank my supervisor Jean-Charles Portais for his continuous encouragement, amicable guidance and a great deal of patience. Thank you, Jean-Charles, for helping me understand the metabolism, encouraging motivation in my work and all the help during our discussions as well as accepting me in a group where I could see myself grow professionally and personally. Furthermore, I would like to thank Frédérick Bringaud for useful remarks to my project and help during the days spent in Bordeaux.

Dear comitee members Dr. Colombié, Prof. Boshart, Dr. Bringaud, Dr. Kiefer and Dr. Moreau, thank you for accepting an invitation to be my comitee members, reading my thesis and useful comments.

I would like to thank my colleagues, particularly Pierre for his contagious enthusiasm and hours he dedicated for me to meticulously explain and re-explain modelling as well as going far beyond his responsibilities in helping me to finish this thesis. Thank you, Pierre, for being so supportive and never sending me away whenever I came into your office. My thanks belong also to Edern, for answering any possible question I've had over those past years, showing me anything I needed in the laboratory as well as friendly and approachable nature. Thank you, Floriant, especially for the first couple of months when you showed me the LC-MS and many nuances of the French bureaus in order to finish my paperwork. I would also like to thank Anna, Tony and Lucille for support and for becoming close friends of mine. I am grateful to Anna for scarifying her personal time for consultations and countless help with LC-MS troubleshooting. To Tony, who has analysed my NMR samples anytime and I was lucky to be introduced to the *cuisine reunionaise* and to Lucille for catchy optimism and constant smile. Likewise, I would like to thank Serguei for an immediate resolution of any issues or questions I was met with during modeling, for your attention to details as well as interest in my own project. The 3rd chapter would never be completed without work of Mickael. I am grateful, as you gave up own sleep to come very early and prepare all the strains as well as helped me many times with sampling, I wish you all the best in your own doctoral journey! Short-term labeling experiments required plenty of hands, and I would like to thank everyone who volunteered to pitch in numerous times. Thank you, Lara, for your patience to speak French with me very very slowly at the beginning and helping me with my French homeworks for language school! Thank you, Lindsay, for taking over the organisation of the defense day which has lifted a lot of weight off my shoulders. I would aso like to thank Maud for

offering advice regarding method validation and consultations of amino acids. And to Cécilia, without whom the lab would be way too calm :). I cannot omit Stephanie, Fabien, Brice, Florence and Guy who would offer advice to ameliorate this work or its final presentation. During my time in Toulouse, when a number of evenings was spent in Dubliners, which was the main spot to get to know the French way of life that is incomplete without good food and drinks and elaborate discussions about food and drinks!

To my fellow international friends who will soon sail towards their next adventure - Rana, Asma, Xiaomin and Carlos, thank you for making my time in Toulouse a fond memory, I hope our paths will cross again one day. This work was part of ParaMet project and I would like to thank the project coordinator Prof. Sylke Műller, all the attendees and fellow PhD. students – Sanu, Sabine, Ewa, Julie, Marco, Maria, Marion, Freddy, Fernando, Francis and Daniela for making all the meetings memorable events.

V neposlednej rade moje poďakovanie patrí najmä mojej rodine a najbližším za podporu, bez ktorej by som som túto úlohu asi nikdy sama nedokončila. Túto prácu venujem ako pamiatku svojej babičke, ktorá mi bola veľkou oporou počas celej dĺžky mojich štúdii, a ktorá sa s nami navždy rozlúčila krátko pred koncom tejto cesty.

1 *Investigation of Acyl-CoA Metabolism in T. brucei*

This chapter aims to introduce reader to *Trypanosoma brucei* and methods used for functional studies of metabolism, which has been published as chapter in book series "Comprehensive Analysis of Parasite Biology: From Metabolism to Drug Discovery". Since the organism is of medical importance and the infection it causes claims many lives every year, the detailed understanding of metabolic pathways used for energy production and growth is essential for new drug targets discovery. After introducing *T. brucei* metabolism and its unusual features, the function and importance of study of acyl-CoA thioesters in trypanosomes is presented.

Trypanosomes utilize different types of carbon sources, carbohydrates as well as amino acids to feed their energetic and biosynthetic needs. Acyl-CoA thioesters represent a bridge between catabolic and anabolic pathways and are also involved in energy generation. But despite importance of coenzyme A in studies of metabolism, the acyl-CoA network of *T. brucei* has not been fully resolved. Reports of different amino acids as carbon sources have raised questions about their incorporation into fatty acids and sterols through acyl-CoA intermediates.

In the context of this thesis, the aim is to obtain detailed description of acyl-CoA thioesters metabolism within central carbon metabolism and lipid and sterol biosynthesis. The focus was placed on short polar acyl-CoA thioesters, because these compounds represent the closest link between the catabolic reactions and sterol and lipid biosynthesis. The objective is to define the biochemical reaction network that is actually operating in procyclic *T. brucei*. Qualitative and quantitative metabolomics data are informative; however, do not resolve topology of reactions. Combination of ^{13}C profiling alone and in combination with genetic perturbations (KO, *RNAi* mutants) yields detailed information on metabolic network topology and function of genes and this strategy will be applied in order to examine incorporation of ^{13}C into metabolic intermediates in *T. brucei*.

1.1 Methods to Investigate Metabolic Systems in Trypanosoma

M. Fatarova[1,2,3,*] F. Bellvert[1,2,3,*], E. Cahoreau[1,2,3,*], F. Bringaud[4,#] and J.-C. Portais[1,2,3,*]

1 : Université de Toulouse ; INSA, UPS, INP ; LISBP, 135 Avenue de Rangueil, F-31077 Toulouse France

2 : INRA, UMR792, Ingénierie des Systèmes Biologiques et des Procédés, F-31400 Toulouse, France

3 : CNRS, UMR5504, F-31400 Toulouse, France

4 : CNRS, UMR 5234, Microbiologie Fondamentale et Pathogénicité (MFP), Université de Bordeaux, 146, rue Léo Saignat, 33076 Bordeaux, France

**: MetaToul-MetaboHUB, National Infrastructure of Metabolomics & Fluxomics (ANR-11-INBS-0010)*

Abstract

Trypanosoma brucei possess several unconventional metabolic traits due to its parasitic way of life involving complex life cycle and consequent need for redundant metabolic pathways. In the last decade a number of metabolomic studies focused on the functional analysis of *T. brucei* metabolism aiming to find potential new treatments against this parasite. Metabolomics aims at the comprehensive analysis of low-molecular weight species - metabolites - resulting from the operation of metabolism. This review is a general introduction to the field of metabolomics and its application to trypanosomatids, with a focus on *T. brucei* metabolism. It describes the various approaches applied to investigate cellular metabolomes, as well as the main steps of the experimental workflow and the main analytical platforms. It also includes the use of stable isotopes labeling experiments in the investigation of metabolic networks. Over the past years, the application of this approach to mutants impaired for specific metabolic enzymes has allowed significant progress of the topology and operation of metabolism in the parasite.

1.2 Trypanosomes, Unconventional Organisms

Trypanosoma brucei is a unicellular parasitic organism responsible for fatal Human African Trypanosomiasis (*HAT*) and Nagana in cattle. Available HAT treatment currently consists of 4 licensed compounds, which all have drawbacks in low efficacy, toxicity, susceptible to resistance and difficult administration [1]. In order to eradicate the lethal disease new drug targets are intensively being searched for, focusing on features that distinguish parasites and eukaryotic host cells. *T. brucei* survives in two distinct and very different environments: in the midgut and salivary glands of the male or female blood-feeding tsetse fly (genus *Glossina*) and in the blood of a mammalian host. Insect forms, called procyclic forms (PCF) proliferate in the insect midgut and undergo several developmental stages before migrating to the salivary glands, where they differentiate into mammalian infective (metacyclic) forms [2]. From the point of injection parasites traverse into the blood stream and differentiate into long-slender forms. In the late stage of the infection they enter the cerebrospinal fluid (CSF) but remain strictly extracellular. The bloodstream population is pleomorphic as it comprises of both proliferative long slender forms and non-proliferative stumpy forms. The latter are pre-adapted for transition to the insect host [2]. There are several prominent physiological and biochemical features distinguishing trypanosomatids from other eukaryotic cells that have shaped the search for new drug treatments, such as the unusual network of interconnected mini and maxi circles of mitochondrial DNA (kDNA) called kinetoplast, advanced host-defence mechanism through the variable surface glycoprotein (VSG) [3] effective in the mammalian host and the protective protein layer (procyclin) in the insect host [4]. The metabolism of trypanosomatids has been subject of intense research since it was discovered that these organisms possess a peroxisome-like organelle, called glycosome, in which glycolysis takes place [5]. Such an atypical feature has motivated detailed investigations of glucose metabolism, and it was further shown that this organelle contains a broad range of metabolic processes in addition to glycolysis, such as part of pyrimidine biosynthesis, nucleotide synthesis and purine salvage, part of mevalonate pathway, oxidative part of pentose phosphate pathway (PPP) which has dual localization between glycosomes and cytosol [6–8]. *Trypanosomes* contain unusual pathways for lipid metabolism. They synthetize fatty acid *de novo* with 3 endoplasmic reticulum elongases (ELO1, ELO2 and ELO3) instead of canonical type I fatty acid synthetase (*FAS*). To do so, they require malonyl-CoA as two-carbon donor and NADPH as reducing agent. Synthesis starts from butyryl-CoA instead of acetyl-CoA common in other systems [9]. In blood stream form (BSF), the main product of the ELO pathway is myristate (C14), a key molecule exclusively used for the glycophosphatidylinositol (GPI) anchors of VSG, while PCF were found to produce more hydrophobic stearate (C18) [10]. Trypanosomes are also equipped with an unusual thiol redox metabolism based on trypanothione [11]. In respect to these unique physiological and metabolic

features, understanding the organism's metabolism matches the comprehensive understanding of its physiology and adaptation capabilities. In recent years, novel and powerful tools for system-level and comprehensive investigations of metabolism have been developed [12,13]. The emergence of metabolomics, the large-scale analysis of metabolites, has allowed unpreceded investigation of metabolism at the cellular level [14]. Particularly when combined with mutants impaired for specific enzymes or exposed to conditions mimicking various environments encountered during the life cycle [15,16]. As a result, notable progress in the understanding of the metabolism of these organisms and their adaptation capabilities has been achieved. The main purpose of this chapter is to provide an overview of approaches and methodologies in metabolomics, and to illustrate its application to the investigation of trypanosomatid metabolism, with a focus on *T. brucei* PCFs.

1.3 Metabolomics

Metabolomics focuses on the comprehensive -qualitative and quantitative- analysis of the metabolome, *i.e.* all low-molecular-weight species (molecular weight usually <1000 or <1500 Da, non-polymeric) present in an organism or a biological sample [17]. The qualitative and quantitative composition of the metabolome depends on the cellular activity, as it results from the expression of the organism's genome in the considered environment, and hence represents a detailed and functional phenotypic characterization of the interaction between genome and the environment.

There is no absolute cut-off in definitions of metabolomics approaches, but several complementary strategies can be distinguished according to their general purposes and considered analytical strategies. *Targeted analysis* aims at the absolute quantification of a limited number of known metabolites. Because the chemical identity of metabolites is known, highly selective and sensitive analytical methods can be applied for this purpose. *Metabolite profilin*g focuses on the quantitative analysis of a larger group of metabolites that share common chemical properties (MS-based metabolite profiling) or represent the major compounds in a sample (NMR-based metabolite profiling). *Metabolic fingerprinting* (intracellular metabolites) or *footprinting* (extracellular metabolites) refer to the untargeted analysis of metabolites independently of their chemical nature, and are often applied for pattern screening and chemometric [18]. The complete resolution of the metabolome is coined *global metabolomics*, and aims at the identification and quantification of all metabolites. This is currently a challenge. Simultaneous determination of all metabolites is hampered by numerous factors. The first issue is the large number of metabolites (up to thousands in a single sample) and their extreme chemical diversity (*e.g.* sugars and fatty acids have totally opposite chemical characteristics), which can be neither extracted nor analysed all at once with a single

method. A second issue is the high turnover rates of many metabolites (sub-seconds to seconds range). Non-physiological evolution of the metabolite content can occur rapidly if metabolism is not blocked immediately. A third issue is the extremely large amplitude of metabolite concentrations, which can range from trace amounts (picomolar) to highly abundant metabolites (hundreds of millimolar) in the same sample. This concentration range spans well beyond the capabilities of current analytical methods, thus cannot be resolved with a single one from this viewpoint as well. For all above-mentioned reasons, the complete coverage of the metabolome cannot be achieved by a single sampling and analytical method, but through the combination of many sampling and analytical methods. This requires tremendous experimental efforts, and is often carried out by consortia of laboratories with complementary expertise. A more practical approach of global metabolomics is to apply an analytical method allowing "the broadest possible" coverage of the metabolome. With modern analytical instruments, such methods allow the detection of thousands of analytical features, which represent a few hundred compounds.

The extreme heterogeneity of the metabolome explains why analytical techniques with broad chemical coverage are preferred in metabolomics. The two most prominent techniques are the sensitive mass spectrometry (MS) coupled with selective chromatographic techniques, such as gas chromatography (GC-MS) and liquid chromatography (LC-MS), and less sensitive but versatile and robust nuclear magnetic resonance (NMR). These techniques, as well as their application to metabolomics, are detailed later in this chapter. Due to the strong resolutive power of modern instruments, a huge number of analytical data can be collected on a single metabolome sample, providing rich information about the metabolism of investigated organisms. Finally, a fourth major issue in metabolomics is related to the interpretation of such mass of analytical data, since converting the analytical information into identified metabolites is currently a huge challenge whatever the analytical platform considered. More details about these issues and how they are currently addressed are given in the following sections.

In addition to methods aiming at the identification and quantification of metabolites, complementary approaches aim at the resolution of biochemical reactions and networks. The most widespread method in this respect is represented by isotope-labeling studies, which are currently performed mainly with stable isotopes. In metabolomics, the most common tracer is ^{13}C because the wide majority of metabolome components are organic molecules, hence contain one or more carbon atom(s). Other considered isotopes include mainly ^{15}N - to investigate nitrogen metabolism, along with ^{2}H and ^{18}O. The basic principle of isotope labeling studies of metabolism is dating from the pioneering times of biochemistry. Basically, cells, tissues, or organisms are fed with an isotopically-labeled substrate. The label input can be optimized according to the metabolic pathways of interest,

but also to the analytical technique used to measure label incorporation [19]. The label propagates in the metabolites, and leaves a specific pattern that depends on the set of reactions by which the labeled substrate is converted into the compounds. Hence, meaningful information about biochemical reactions and metabolic pathways can be obtained from the measurement (by NMR or MS) of the labeling patterns of metabolites; a strategy termed 'isotopic profiling'. In some favourable cases, especially with cultivated cells, the labeling data can be combined with mathematical models of metabolic pathways to calculate metabolic fluxes ('fluxomics'), which are the actual rates of biochemical reactions *in vivo*. Because they provide functional information about the operation of metabolism, stable-isotope labeling experiments are increasingly used in the field of metabolism. In particular, they have been significantly applied to investigate *Trypanosoma* metabolism, enabling the identification of key metabolic features in these organisms. This is why they will be detailed later in this chapter.

The metabolomics workflow can be divided into 4 parts: experimental design, sample collection and preparation, sample analysis and data processing and interpretation (Fig. 1). All these steps are defined and optimized according to the biological model, to the purpose of the experiment, to the biological model, to the metabolites of interest, and to the considered analytical platform.

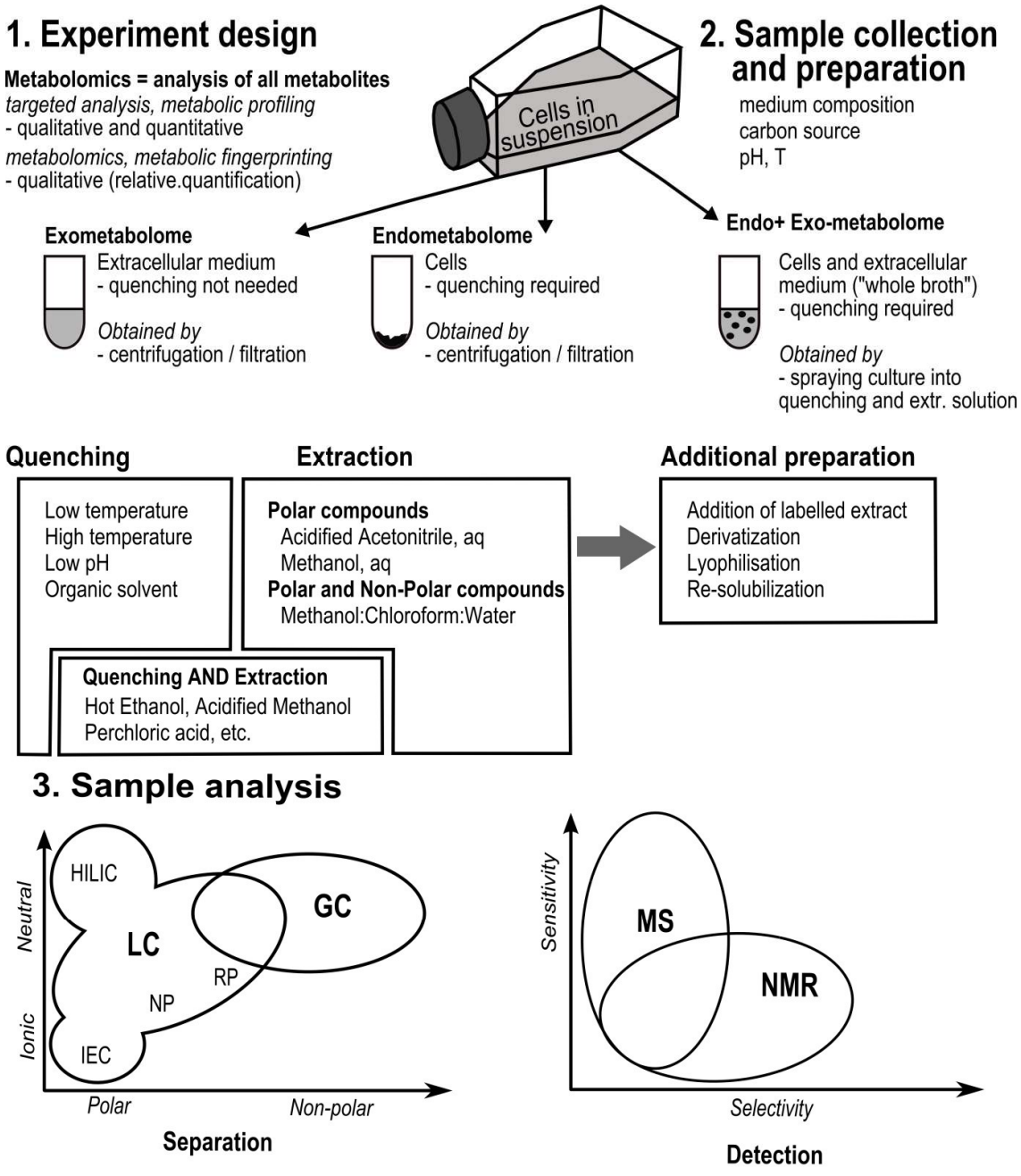

Figure 1: Scheme of workflow in metabolomics

Abbreviations: LC, liquid chromatography; GC, gas chromatography; IEC, ion exchange chromatography; IDMS, isotope dilution mass spectrometry (addition of labeled extract); HILIC, hydrophilic interaction liquid chromatography; NP, normal phase; RP, reversed phase; MS, mass spectrometry; NMR, nuclear magnetic resonance.

1.4 Sample Preparation in Metabolomics

1.4.1 General Considerations

The choice of the metabolite sampling method is crucial in metabolomics because it can determine both the observed metabolite content and subsequent interpretation of data. Ideally, sample preparation should be fast and reliable, avoid under/over-estimation of metabolite levels during sampling and also prevent their degradation or loss during extraction. Overall, the sampling of metabolites consists of three main steps. The first one is the collection of the desired biological material, *i.e.* cells for endo-metabolomics and cultivation medium for exo-metabolomics. The separation of cells from medium is achieved by centrifugation or fast filtration, though in some approach the whole cultivation broth – including both cells and extracellular medium – is directly sampled. During collection of biological material washing step is required to avoid cross-contamination. It also aids in removal of salts present in media that can impede MS detection. Because the rates of metabolic reactions can be very high, the washing solution is supplemented with all nutrients normally present in the cultivation medium to avoid substrate limitation and metabolic perturbations, which can be observed after a few seconds in some systems [20]. Some intracellular metabolites can be detected in the medium, as a result of active metabolite release (especially organic acids) or of cell lysis [21]. They can also result from the non-physiological release of metabolites (metabolite leakage) if cell integrity is not maintained during sampling, thereby leading to underestimation of the intracellular content [22]. A number of strategies to circumvent the leakage problem have been suggested, such as quenching of metabolism before separating the cells from medium, though the quenching method can also itself induce some leakage (*e.g.* some quenching solvents can permeabilize cell membranes). Another alternative strategy consists in the so-called 'differential method', in which the concentrations of intracellular metabolites are measured from the difference between metabolites in total cultivation broth and metabolites in the extracellular medium [23]. The second step of sampling is the blockage of metabolic activity (quenching), to avoid non-physiological alteration of metabolome composition during the sampling process. Quenching should be extremely fast since the turnover of metabolites is in the range of sub-second to seconds. The turnover rate is high especially for the intermediates of central metabolic pathways. In the bacterium *Escherichia coli*, the turnover time of phosphorylated sugars and most organic acids involved in TCA cycle could be measured below 4 sec [23]. Quenching can be achieved by rapidly pouring the samples into liquid nitrogen or cold solvent (*e.g.* methanol at -60°C) to thermodynamically block chemical reactions, or on the contrary in hot solvent (*e.g.* boiling ethanol, boiling water) to denature enzymes, or by directly performing metabolite extraction. Finally, the last step of sampling is metabolite

extraction, which depends on both the targeted metabolites and analytical methods. Because of the very different purposes, organisms, samples, metabolites and analytical platforms considered in metabolomics, a broad range of extraction methods have been developed. Unfortunately, there is no method equally applicable to all metabolites because extraction efficiency depends on the chemical properties of each compound and on cellular characteristics (*e.g.* membrane composition). Classification of metabolites into polar, nonpolar, acidic or alkali-stable translates mainly to the extraction method applied. The various extraction methods can yield different and even contradictory metabolic profiles, emphasizing the importance of testing and optimizing the sampling conditions according to the metabolites of interest [24]. Moreover, metabolite sampling is organism- and strain-dependent [20], meaning that methods should be validated for each particular investigation, and adapted if needed.

1.4.2 Sampling of T. brucei Metabolome

Comprehensive reviews of sampling methods applied to trypanosomatids have been published a couple of years ago [25] and only the main aspects are discussed below. For cells cultivated *in vitro*, the exo-metabolome simply refers to the metabolites detected in the cultivation medium and resulting from cellular activity. The culture medium can be sampled by centrifugation or fast filtration. It is usually analysed by NMR, which allows measurement of both substrate consumption and production of metabolic end-products. The media used for cultivation of *T. brucei* often contain buffers that can be incompatible with analytical methods, such as HEPES or MOPS that can impair the chromatographic separation of metabolites in LC-MS. The buffers in general should not be an issue for the acquisition of NMR spectra; however, their signals can potentially overlap with the signals of analytes of interest. Significant information about the metabolism of *T. brucei* has been collected by isotopic profiling of the exo-metabolome, as is illustrated later in this chapter.

Sampling of intracellular components requires separation of media and cells, which can be achieved by centrifugation or fast filtration. Fast filtration has been successfully applied to *T. brucei* PCFs [8,26,27]. In this method, the cultivation broth is rapidly filtered and cells on the filter are rapidly washed with cold and diluted medium to maintain the salt and nutrient balances during the sampling process. The presence of the carbon source in the washing solution was also shown to prevent substrate limitation during sampling [28]. The metabolites can be extracted immediately after filtration, though for practical reasons in most cases they are quenched in liquid nitrogen or other cold solvents before metabolite extraction is performed. Fast filtration takes 4-10 sec, which is well adapted for maintaining the pools of fast-turnover compounds such as central metabolites (*e.g.* intermediates of glycolysis, TCA cycle, amino acid metabolism and anabolic pathways). However, metabolite leakage was reported to occur in *T. brucei* BSF during fast filtration or aqueous methanol quenching [25]. An

alternative method has been applied to *T. brucei* and *Leishmania* [25,29,30] in which cells are separated from medium by centrifugation. In this approach, cells are rapidly chilling in a bath of dry ice and ethanol at 4°C, centrifuged (5-10 min) at 4°C and subsequently the cell pellet is extracted in methanol: chloroform: water (1:3:1). This protocol is well adapted for the analysis of metabolites with slow turnover, however cells might undergo undefined conditions (substrate or oxygen limitation) during centrifugation [31]. So, as for all other organisms, there is currently no absolute method for sampling trypanosomatid metabolome, but different protocols that are adapted to specific objectives. Fast filtration is well adapted to the investigation of central and energy metabolism, meanwhile centrifugation-based protocols appear better suited for analysing biosynthetic processes. Finally, various methods have been applied to extract trypanosomatid metabolome. Extraction of polar metabolites, organic acids and phosphorylated compounds in *T. brucei* PCF has been performed with boiling water [26,27]. Methanol: chloroform has been used for the simultaneous extraction of both polar and non-polar metabolites [32]. Extraction of whole *T. brucei* PCF culture medium with boiling ethanol has been used for untargeted metabolome [33]. Non-polar lipids were reported to be extracted by chloroform: methanol (2:1) [34–37]. The broad range of methods applied to trypanosomatids is a direct illustration of the current necessity to adapt metabolite extraction according to the investigated metabolism/metabolites.

1.5 Analytical Platforms in Metabolomics

This section provides a brief description of the two main analytical platforms used in metabolomics, NMR and MS. For more details the reader should refer to comprehensive reviews that have been published in recent years on analytical methods in metabolomics [38], MS [39,40] and NMR [41]. The choice of the analytical technique(s) depends on instrument availability and on the particular objectives of the investigations.

NMR allows the detection of any atom nucleus with non-zero magnetic moment (^{1}H, ^{13}C, ^{31}P, ^{14}N, etc.), which are called spins, by applying a radiofrequency pulse to samples placed in a high magnetic field. The nuclei absorb the energy, excite to high-energy state and subsequently emit detectable energy in form of an electromagnetic radiation emitted at a specific frequency. This resonance frequency is altered by electrons surrounding the nuclei in the molecule, hence depends on the chemical environment of the nucleus. For instance, the resonance of a CH_3 group will be different from that of a CH_2 group. This chemical dependence, called chemical shift, is scaled according to known chemical references (*e.g.* trimethylsilyl, TMS, for ^{1}H- and ^{13}C-NMR) and can be used for identification. Additional structural information about the molecules is obtained from the so-called 'scalar coupling'. This phenomenon is due to the interaction between two or more neighbouring spins.

It results in the splitting of the NMR resonances into two or more lines, according to the nature and number of spins in interaction. For instance, the resonance of a proton will be a singlet (one line) if it has no proton neighbour, a doublet (two lines) with one proton neighbour, a triplet (three lines) with two proton neighbours, etc. NMR provides highly detailed chemical information from which the structure of the molecules can be resolved. Furthermore, multi-dimensional NMR methods can be applied to resolve chemically-complex samples - such as those considered in metabolomics - by spreading the signals over 2 (2D-NMR) or 3 (3D-NMR) spectral dimensions. This 'magnetic separation' of chemical groups makes possible the resolution of metabolome samples without the need for physically (chromatographically) separating the compounds. Therefore, very often little sample preparation is needed in NMR, especially for the analysis of bio fluids. In principle all compounds occurring in the sample can be detected by NMR independently of their chemical nature and in a quantitative manner. All these features make NMR very attractive for untargeted (or without a priori) and quantitative approaches in metabolomics, such as metabolic fingerprinting or metabolic profiling, respectively. In practice, NMR has a rather low sensitivity (nanomole range) and allows the detection of predominant metabolites (around one hundred species at a maximum). With current developments in NMR technology, however, the sensitivity of instruments is increasing, which provides better metabolome coverage. Since it requires minimal sample preparation, and is very robust, NMR is well suited for high-throughput metabolomics. Finally, NMR is also a valuable method for the detection of stable isotopes, and is extensively used for isotopic studies of metabolism as developed further in this chapter.

Mass spectrometry detects ionised molecules and separates them according to the mass/charge (*m/z*) ratio using a variety of analysers (quadrupole, time of flight, ion trap, Fourier transform ion cyclotron, etc.). Separation of metabolites in *m/z* dimension depends on the analyser resolution, which is defined by IUPAC as the smallest difference (Δ *m/z*) between two ions that can be separated at a given peak height (10%, 50%, etc.). Within routine instruments, one can differentiate between low-resolution (*e.g.* quadrupoles, with resolution between 1000 and 3000) and high resolution (*e.g.* time-of-flight, OrbiTrap, FT-ICR) detectors, with resolution up to 1 000 000 (FT-ICR). The various analysers are applied for different purposes. For instance, quadrupoles are highly linear analysers and very sensitive in the tandem mode (triple-quadrupoles), so that they are preferred to other instruments for quantitative investigations. High-resolution analysers allow better separation of analytes in the *m/z* dimension, and have become pivotal for the identification of metabolites in complex samples. Mass analysers can be combined in tandem (MS/MS) to enable fragmentation of the molecule. The detailed analysis of the generated fragments provides detailed chemical information about the chemical sub-structures composing the molecule. MS is very sensitive and

modern instruments have detection limits around or below the femtomole range (*i.e.* 6 orders of magnitude better than NMR). This allows the potential detection of hundreds to thousands of compounds; for that reason, MS is a method of choice for gaining the most complete view of the metabolome of a particular organism. Metabolites are mainly identified on the basis of their accurate mass, from which their elemental formula can be determined. Other MS parameters, such as the isotopic cluster, can be used in addition to get a more precise formula. Then chemical databases are searched for potential matches. One accurate mass can correspond to various elemental formulae, and one single formula can correspond to hundreds or thousands of molecules. Moreover, many biological compounds are currently unknown and thus not present in database. Therefore, the unambiguous identification of metabolites from high-resolution MS is extremely challenging and needs complementary information such as MS/MS fragmentation profiles, or complementary analytical methods [42]. The metabolomics community is currently making significant efforts to develop identification strategies based on the information collected by high-resolution MS, in parallel with the development of appropriate annotation tools and (bio) chemical databases.

Though significant progress in analyser technologies, chromatographic separation of metabolites before MS analysis is necessary to resolve the strong chemical complexity of metabolome samples. Separation of metabolites prior to MS detection increases sensitivity and adds information for analyte annotation (*e.g.* retention time). The prevalent separation techniques for coupling with MS are GC and LC. In GC, the analytes are separated based on their boiling point in a flow of carrier gas (nitrogen, helium, or argon). GC is highly relevant to separate volatile compounds but also low-volatile compounds that can be converted into volatile species after appropriate chemical derivatization. An advantage of GC-MS over LC-MS is the availability of reproducible fragmentation patterns enabling identification form spectral databases. In LC compounds are separated based on their interaction with a stationary phase. Because a variety of stationary phases is available, LC (and LC-MS) is very flexible and is a method of choice for separating most polar compounds. For highly polar metabolites, such as phosphorylated sugars or ionic compounds, ion exchange chromatography (IEC) can also be applied [43]. Depending on the purpose of the experiment and instrument availability, the major GC-MS or LC-MS approaches include 'targeted metabolomics, *i.e.* the (quantitative) analysis of specific compounds using a highly selective method, or 'global metabolomics' using a method with broad selectivity. The chromatographic separation of molecules is chemically selective and so far, there is no universal platform that would allow complete separation of all metabolites, *i.e.* global metabolomics is a challenge. Currently the best way to maximize the coverage of the metabolome is to combine multiple analytical platforms and methods (a series of 'targeted approaches').

It is worthy to note from the brief descriptions of MS and NMR given above that the two techniques are very complementary and can be used in combination to increase metabolome coverage both in qualitative and quantitative terms.

1.6 Isotopes and Isotopic Profiling

Some basic information about isotopes and nomenclature of isotopic species are given in the following section before analytical methods relevant for isotopic profiling are discussed. *Isotopes* are defined as chemical elements which differ only in the number of neutrons, such as ^{11}C, ^{12}C, ^{13}C and ^{14}C for carbon. Some are stable (*e.g.* ^{12}C and ^{13}C) and others are radioactive (^{11}C and ^{14}C). Only stable isotopes are further discussed in this chapter. Depending on its chemical formula, a particular molecule can have many different isotopic forms, resulting from all possible combinations of number and positions of isotopes in the molecule. These isotopic forms can be divided into *isotopomers* and *isotopologues.* Isotopomers ('isotopic isomers') are compounds with identical isotopic formula only distinguished by the position(s) of the isotope(s) in the molecule (*e.g.* an alanine labeled with one ^{13}C atom in position 1 and an alanine labeled with one ^{13}C atom in position 3 are isotopomers). *Isotopologues* are chemically identical compounds that differ in the number of isotopes, *e.g.* incorporation of 0, 1, 2, etc., isotopes (*e.g.* an alanine labeled with one ^{13}C atom and an alanine labeled with two ^{13}C atoms are isotopologues, whatever the positions that receive the label atoms).

By MS, species with different numbers of isotopes – *i.e.* with different masses – can de distinguished, meaning that isotopologues are measured. For a three-carbon compound, such as pyruvate or lactate, four ^{13}C-isotopologues can be detected by MS: non-labeled [M0], partially labeled [M+1], [M+2] and fully labeled [M+3] species (where x in [M+x] stands for the mass excess compared to the unlabeled form [M0]). The position(s) of labeled atom(s) in [M+1] and [M+2] forms cannot be determined directly, though some information about this can be obtained after fragmentation of the molecule. The different isotopologues of the molecule give distinct signals separated by one mass unit, and together with the contribution of other, naturally-occurring isotopes (*e.g.* ^{18}O, ^{15}N) they form a cluster of peaks called isotopic cluster. In practice in ^{13}C-labeling experiments the ^{13}C-isotopologue distribution (percentage of each ^{13}C-isotopologue) of labeled metabolites is calculated from their isotopic clusters, after correction for naturally-occurring isotopes [44].

The most classical approach for MS-based isotopologue analysis is a targeted one and relies on the selective detection of pre-defined, molecule-specific ions. These ions are selected from preliminary MS analysis of the metabolites of interest. The labeling pattern of the metabolite is extracted from the isotopic cluster measured for its specific ion. For a long period of time, isotopologue analysis has been performed with single quadrupoles. More sensitive and accurate

targeted measurement of isotopologues can now be achieved by tandem MS (MS/MS) on triple-quadrupoles. In that case, the ion (metabolite) of interest is selected in the first quadrupole, fragmented into 'daughter' ions in the second one, and a daughter ion chosen for its specificity is selected in the third one. This detection mode offers both improved specificity and sensitivity, though determining the labeling pattern of the metabolite from that of its daughter ions is not straightforward [43]. Besides targeted approaches, untargeted approaches can be applied. In these approaches, the complete MS spectrum is collected, which potentially allows the measurement of isotopologues for all detectable compounds. Low-resolution MS detectors are not well suited for such untargeted approaches, and until recently the low sensitivity and quantitative inaccuracy of high-resolution instruments made them poorly suited for (quantitative) isotopic profiling. Modern high-resolution MS instruments have become both more sensitive and more quantitatively accurate, enabling the emergence of powerful untargeted isotopic profiling methods. The first reports of such investigations, which include the study of *T. brucei* PCFs by Creek *et al*. [45] emphasize their huge potential for gaining detailed insights into metabolic networks and their operation.

NMR allows direct determination of isotope position in labeled metabolites, so that this method allows the measurement of isotopomers [46,47]. For instance, a three-carbon molecule will have three distinct signals in ^{13}C-NMR spectra. The intensity of each signal is proportional to the number of ^{13}C atoms, so that the ^{13}C-content of each position can be measured individually. This is usually expressed as 'specific' or 'positional' enrichment, *i.e.* percentage of ^{13}C atoms in a specific position of the molecule. Specific enrichments can be also measured by ^{1}H-NMR by exploiting scalar couplings between ^{1}H and ^{13}C nuclei ('heteronuclear couplings'). Because ^{1}H-NMR is much more sensitive than ^{13}C-NMR, the indirect detection by ^{1}H-NMR of is usually preferred over direct detection by ^{13}C-NMR, except for quaternary carbons that have no proton coupling. Similarly, the exploitation of scalar couplings between two or more adjacent ^{13}C atoms ('homonuclear couplings') allows to measure ^{13}C-^{13}C connectivity in the molecule, and distinguishing the various isotopomer species. For instance, by NMR alanine doubly labeled in positions 1 and 2 can be easily distinguished from alanine doubly labeled in positions 2 and 3. As for the structural resolution of complex metabolite samples, multi-dimensional NMR experiments have been developed to measure either specific enrichments or isotopomers without need for compound separation. For this reason, NMR provides a rich and highly flexible method to measure positional isotopic information, with the benefit that such positional information very often encodes directly active pathways.

1.7 Application of Metabolomics to T. brucei - Selected Illustrations.

In this section, selected applications of metabolomics to trypanosomatids are given to illustrate the interest of these approaches for getting comprehensive understanding of the unique metabolic traits of these organisms. The examples are taken from *T. brucei*, for which significant metabolic knowledge has been recently gathered using metabolomics. More specifically, considerable progress in the identification of metabolic pathways in *T. brucei* was achieved by applying ^{13}C isotopic profiling strategies to mutants impaired for specific enzymes by means of gene silencing (*RNAi* mutants) or deletion (KO mutants). Table 1 provides a list of these investigations, though probably not exhaustive. To help the reader in following the metabolic processes discussed below, a schematic representation of the current view of *T. brucei* central carbon metabolism is given in Fig. 2. For simplicity and consistency reasons, the examples are taken from the investigation of *T. brucei* PCFs.

1.7.1 Exo-metabolomics and Succinate Fermentation

The analysis of the exo-metabolome provides detailed information about the compounds that are either consumed or produced by cells. It gives the global result of cellular metabolic activity since it can be measured which compounds are used by the cells and into which products they are converted in. *T. brucei* PCFs convert glucose into succinate and acetate as major end-products while alanine, lactate and malate as minor ones [27,35]. Succinate is an intermediate of TCA cycle and all enzymes of this pathway can be detected in PCFs [48]. Together with the fact that PCFs have a functional ATP synthase coupled to aerobic respiration, this suggested that pyruvate was oxidized in the mitochondrion to fulfil the cells' energetic needs by oxidative phosphorylation. It also suggested a mitochondrial origin of succinate, which is produced from succinyl-CoA in the TCA cycle. However, succinate could also be produced from fumarate via a controversial NADH-dependent fumarate reductase (FRD) activity, described in *T. brucei* PCFs [49,50]. In 2002, Besteiro *et al.* investigated the metabolic origin of succinate in PCFs by applying isotopic profiling of the exo-metabolome to the study of relevant mutants [51]. First, these authors established the glycosomal localization of FRD (accordingly called FRDg), and generated mutants in which the activity of the enzyme was switched off by using an RNA interference (RNAi) strategy. Then, they incubated PCFs with [1-^{13}C]-labeled glucose, and analysed the labeling patterns of metabolic end-products in the medium using ^{13}C-NMR. In FRDg-depleted parasites, succinate production was decreased by 60% compared to wild-type parasites, whereas a significant increase in both fumarate and malate were observed, indicating that most of succinate was produced via FRDg.

Moreover, detailed analysis of the labeling patterns of the metabolic end-products measured by ^{13}C-NMR provided evidence that the TCA cycle could not be responsible for the production of the

remaining succinate. Briefly, the glycolytic degradation of [1-^{13}C]-glucose generates [3-^{13}C]-pyruvate, which can be further converted into [2-^{13}C]-acetyl-CoA to feed the TCA cycle. The singly-labeled acetyl-CoA entering the TCA cycle produces doubly - or more - labeled species after several turns of the cycle. Given the labeling pattern measured for acetyl-CoA, it was calculated that 15% of succinate molecules should be doubly labeled at both C2 and C3 ([2, 3-^{13}C2]-succinate) if a complete operation of the TCA cycle was assumed. As mentioned above, NMR allows unambiguous discrimination of singly and doubly labeled species. But Besteiro *et al*. could not observe doubly-labeled succinate, but only singly labeled forms, in the exo-metabolome of PCFs incubated with [1-^{13}C]-glucose, showing that the TCA cycle was unlikely to be operating as a complete cycle in *T. brucei* PCFs [51]. One year later, van Weldeen *et al*. confirmed this hypothesis by demonstrating that deletion of the aconitase gene, encoding a TCA cycle enzyme, does not affect central metabolism of the parasite [52], although several branches of the cycle can be used in upon utilization of glucose or proline [53,54].

Table 1: Applications of isotopic profiling to *T. brucei* procyclic forms.

Metabolic perturbation	Sample & sampling protocol	Analytical platform	(Labeled) carbon source	Ref.
PPDK, PYK	Exo-metabolome; medium collected by centrifugation, no quenching, NMR analysis carried out in D_2O	^{13}C-NMR	D-[1-^{13}C]glucose	55
PPDK, PEPCK, PGKC	Exo-metabolome; medium collected by centrifugation, no quenching, NMR analysis carried out in D_2O	^{13}C, ^{1}H –NMR	D-[U-^{13}C]glucose D-[1-^{13}C]glucose L-threonine (*NE*)	56
FRDg	Exo-metabolome; medium collected by centrifugation, no quenching, NMR analysis carried out in D_2O	^{13}C, ^{1}H –NMR	D-[1-^{13}C]glucose	51
FRDg, FRDm1	Exo-metabolome; medium collected by centrifugation, no quenching, NMR analysis carried out in D_2O	^{13}C, ^{1}H –NMR	D-[1-^{13}C]glucose	57
FHm, FHc	Exo-metabolome; medium collected by centrifugation, no quenching, NMR analysis carried out in D_2O	^{13}C-NMR	D-[1-^{13}C]glucose	53
FRD(g, m1), FH (c,m), SDH, PEPCK, PDH, PYK, ASCT, ME(c, m), F_0/F_1-ATP syn.	Exo-metabolome; medium collected by centrifugation, no quenching, NMR analysis carried out in D_2O	^{13}C, ^{1}H –NMR	D-[1-^{13}C]glucose L-[4-^{13}C]proline	58
CL, AceCS, ASCT	Exo-metabolome; medium collected by centrifugation, no quenching, NMR analysis carried out in D_2O	^{13}C-NMR	D-[1-^{13}C]glucose	34
AAT	Exo-metabolome; medium collected by centrifugation, no quenching, NMR analysis carried out in D_2O	^{13}C-NMR	L-[4-^{13}C]proline	59
ASCT	Exo-metabolome; medium collected by centrifugation, no quenching, NMR analysis carried out in D_2O	^{13}C, ^{1}H –NMR	D-[1-^{13}C]glucose	60
PDH, TDH, ACH, ASCT, PEPCK	Exo-metabolome; medium collected by centrifugation, no quenching, NMR analysis carried out in D_2O	^{13}C, ^{1}H -NMR HILIC-MS	D-[U-^{13}C]glucose threonine (NE) [^{15}N]threonine	35
ASCT, ACH, β subunit of F_0/F_1 –ATP synthase	Exo-metabolome; medium and cells separated by centrifugation, no quenching, NMR analysis of supernatant carried out in D_2O	^{1}H-NMR	glucose (NE)	36
TKT	Endo-metabolome; cells collected by fast filtration, quenching in liquid N2 and extraction in boiling water	IC – MS/MS	glucose (NE)	8
MEc, G6PDH, PGI	Endo-metabolome; cells collected by fast filtration, quenching in liquid N2 and extraction in boiling water	IC – MS/MS	[U-^{13}C]proline ± glucose (NE)	26
PEPCK, SDH, β subunit F_0/F_1 –ATP synthase, FAD-GPDH, PDH	Exo-metabolome; medium collected by centrifugation, no quenching, NMR analysis carried out in D_20 Endo-metabolome; cells collected by fast filtration, quenching in liquid N2 and extraction in boiling water	^{13}C-NMR IC-MS/MS	D-[1-^{13}C]glucose L-[4-^{13}C]proline	27
ACO	Exo-metabolome; medium collected by centrifugation, no quenching, NMR analysis carried out in D_20	^{13}C-NMR Scintillator	D-[U-^{13}C]glucose D-[6-^{14}C]glucose L-[U-^{14}C]proline	52
Wild-type	Endo-metabolome; cells collected by centrifugation, quenching in cold ethanol, and extraction in chloroform:methanol:water (1:3:1)	IC-MS	D-glucose, L-proline (separate)	29
Wild-type	Endo-metabolome; cells collected by centrifugation, quenching in cold ethanol, and extraction in chloroform:methanol:water (1:3:1)	LC-MS	[U-^{13}C]glucose (50%)	45

Abbreviations of enzymes: Please see Fig. 2. NE, non-enriched carbon source

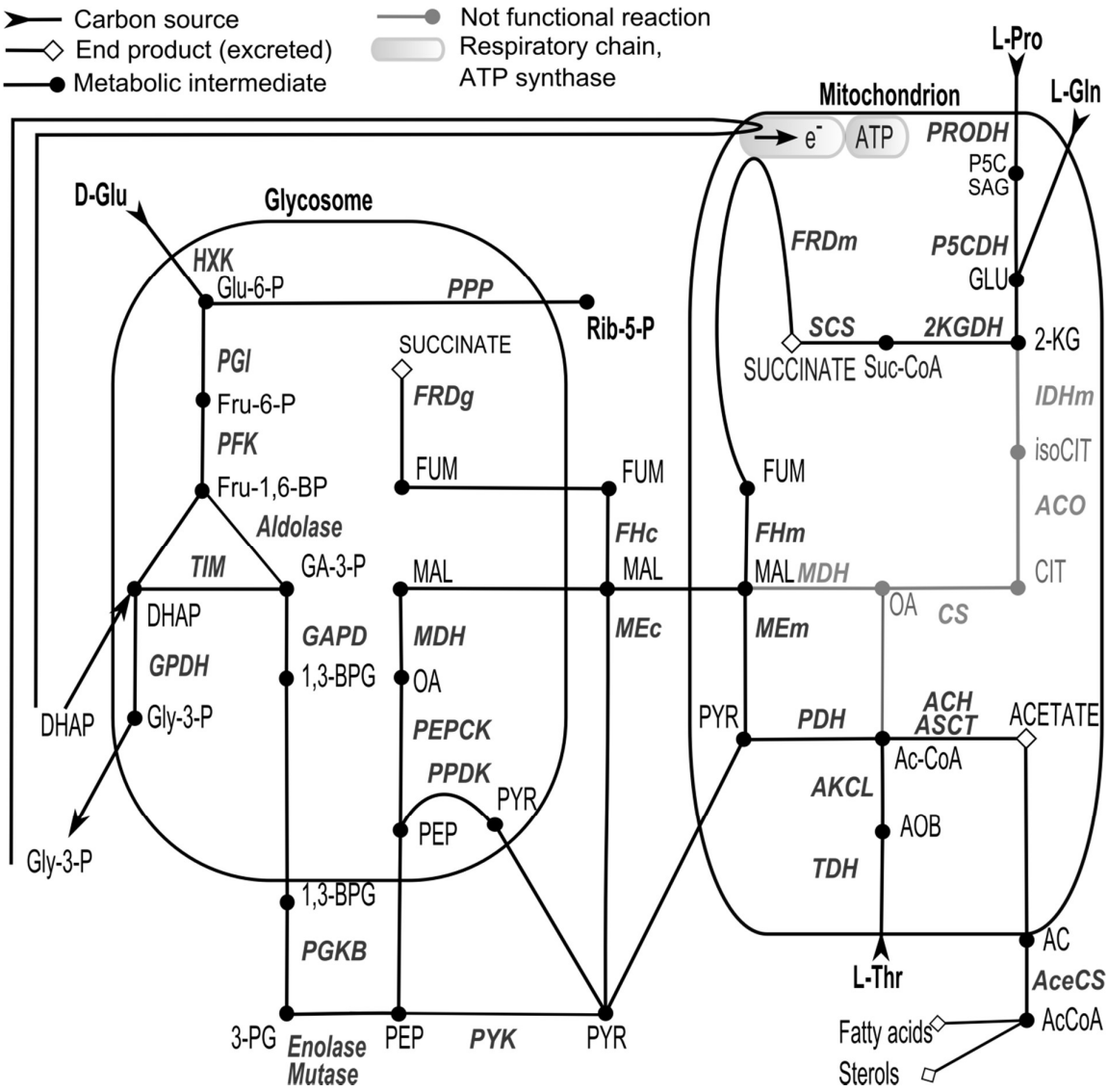

Figure 2: Schematic representation of central carbon metabolism in procyclic T. brucei

Each node represents a metabolite; direction of reactions in glycolytic or gluconeogenetic flux is not indicated. Abbreviations of enzymes (indicated in bold italic): HXK, hexokinase; PGI, glucose-6-phosphate isomerase; PFK, phosphofructokinase; TIM, triose-phosphate isomerase; GAPD, glyceraldehyde-3-phosphate dehydrogenase; GPDH, glycerol-3-phosphate dehydrogenase; PGKB, phospho-glycerol kinase (isoform B); PYK, pyruvate kinase; PPDK, pyruvate phosphate dikinase; PEPCK, phosphoenol pyruvate carboxykinase; MDH, malate dehydrogenase; FHg/ FHc, fumarate hydratase (glycosomal, cytosolic); FRDg/FRDm, fumarate reductase (glycosomal, mitochondrial); SDH, succinate dehydrogenase; MEc/MEm, malic enzyme (cytosolic, mitochondrial); PDH, pyruvate dehydrogenase complex; ACH, acetyl-CoA thioesterase; ASCT, acetyl: succinyl-CoA transferase; CS, citrate synthase; ACO, aconitase; IDH, isocitrate dehydrogenase, 2KGDH, 2-ketoglutarate dehydrogenase; SCS, Succinyl-CoA synthetase; PRODH, proline dehydrogenase; TDH threonine 3-dehydrogenase; AKCL, 2-amino-3-ketobutyrate-Coenzyme A ligase;

Abbreviation of pathway: PPP, pentose phosphate pathway.

Abbreviations of compounds: D-Glu, D-glucose; L-Pro, L-proline; L-Thr, L-threonine; L-Gln, L-glutamine; Glu-6-P, glucose-6-phosphate; Rib-5-P, ribose-5-phosphate; Fru-6P, fructose-6-phosphate; Fru-1,6-BP, fructose-1,6-bisphosphate; DHAP, dihydroxyacetone phosphate; GA-3-P, glyceraldehyde-3-phosphate; 1,3-BPG, 1,3-bisphosphoglycerate; 3-PG, 3-phosphoglycerate; PEP, phosphoenol pyruvate; OA, oxaloacetate; MAL, malate; FUM, fumarate; SUC, succinate; AC, acetate; OA, oxaloacetate; CIT, citrate; isoCIT, isocitrate; 2-KG, 2-ketoglutarate; GLU, glutamate, SAG, glutamate semi-aldehyde; AOB, amino-oxobutyrate.

The complete pathway by which glucose is converted into succinate via FRDg was further established (Fig. 2). Glucose is converted into 1,3-biphosphoglycerate in the glycosomes, and then this metabolic intermediate is converted to phospho*enol*pyruvate (PEP) in the cytosol. PEP is then entering the glycosomes to be converted into oxaloacetate (OAA) by phospho*enol*pyruvate carboxykinase (PEPCK) [56]. Subsequently, OAA is converted by a glycosomal malate dehydrogenase (MDHg) into malate, which is dehydrated into fumarate by a cytosolic fumarate hydratase (FHc) [53], and the latter intermediate is reduced to succinate in the glycosomes by FRDg [51]. The entire process is a fermentation, called glycosomal succinate fermentation, and enables the re-oxidation of glycolytic NADH into NAD^+ within the glycosome by two enzymes, MDHg and FRDg [51]. In addition the glycosomal succinate fermentation is used to maintain the glycosomal ATP/ADP ratio through the PEPCK reaction, together with the PPDK reaction (conversion of PEP into pyruvate with production of ATP) [56]. Following the work of Besteiro *et al*., it was later demonstrated that a mitochondrial form of NAD-dependent FRD (FRDm1) was present and active in PCFs in addition to the glycosomal form (FRDg) [57]. These investigations showed that *T. brucei* PCFs possess two alternative processes for succinate production, one in the glycosome and the other one in the mitochondrion. The pathway by which glucose is converted into mitochondrial succinate includes the same initial reactions as in glycosomal succinate fermentation up to the glycosomal formation of malate (Fig. 2). But instead of being converted into succinate inside the glycosomes malate (or fumarate not yet experimentally confirmed) enters the mitochondrion to be dehydrated to fumarate by a mitochondrial fumarate hydratase (FHm) and/or reduced into succinate by FRDm1. As discussed for the glycosomal succinate fermentation, the mitochondrial production of succinate is likely to be involved in the maintenance of redox balance by oxidation of NADH via FRDm1. By applying the same approach as Besteiro *et al.*, *i.e.* isotopic profiling of the exo-metabolome of selected FRD mutants incubated with ^{13}C-enriched glucose, Coustou *et al*. could determine that the two enzymes FRDg and FRDm1 accounted for the total production of succinate, with FRDg contributing to 56-86% and FRDm1 to 14-44% of total excreted succinate [57]. These data show that the contribution of the mitochondrial process is significant. The reaction catalysed by FRDm1, NADH-dependent reduction of fumarate into succinate, is opposite to the FAD-dependent oxidation of succinate into fumarate catalysed by succinate dehydrogenase (SDH) in the TCA cycle. Since, one may consider that two opposite reactions could not operate simultaneously in the same cellular compartment, the occurrence and significant activity of FRDm1 could be an additional argument against the operation of a complete TCA cycle in PCFs. This is consistent with proline-derived succinate being excreted in the presence of glucose, suggesting that succinate is not further metabolized into fumarate by SDH [58]. However, Turrens *et al.* proposed that the mitochondrial NADH-dependent fumarate reductase and SDH form a cycle transferring electrons from NADH to the

quinone pool of the respiratory chain, through the intermediate fumarate, and may constitute a NADH dehydrogenase-like activity [49]. The occurrence of this hypothetical FRDm1/SDH cycle has not been demonstrated so far in trypanosomatids, or any other organism. This example is an early demonstration of the benefit of (exo-) metabolomics for the understanding of *T. brucei* metabolism. First, it has established a valuable experimental strategy for investigating their metabolism by combining metabolomics with the study of mutants impaired for specific enzyme(s). This strategy was further developed and has very significantly improved our knowledge of trypanosomatid metabolism (Table 1). Second, this approach was helpful to determine the enzymatic reactions involved in the maintenance of the NAD^+/NADH and ATP/ADP ratios inside the organelle [27,51,56] since the glycosomal membrane is not permeable to larges molecules, such as nucleotides and cofactors [5]. Being a very unique feature of trypanosomatids, glycosomes have been the subject of intense experimental research since their discovery. All studies initially focused on determining why these organisms encapsulate glycolysis in a dedicated physical compartment [5]. It was initially thought to allow high glycolytic flux by packing the glycolytic enzymes in very small volume [61], or to protect from the particular design of glycolysis, which can cause growth defect [62]. It is now believed that glycosomal glycolytic sequestration is used to provide a high level of metabolic flexibility, by rapidly changing the glycosomal content through autophagy in response to environmental changes [63]. The occurrence of two alternative pathways for succinate production is certainly part of the metabolic flexibility of trypanosomatids.

1.8 Endo-metabolomics, Redox Balances and Gluconeogenesis

The example given above shows the benefit of exo-metabolomics for the understanding of *T. brucei* metabolism, not only to resolve the metabolic pathways that operate, but also to provide valuable insights into the vital redox processes. Indeed, the two succinate fermentation mechanisms occurring in *T. brucei* PCFs are involved in the maintenance of NAD^+/NADH balances. Some valuable insights into the methods of NADPH balancing, but also into gluconeogenesis, were resolved by applying isotopic profiling to the *T. brucei* endo-metabolome (*i.e.* intracellular metabolites). The production of NADPH is essential for biosynthetic processes and oxidative stress defence. The possible sources of NADPH in the cytosol of *T. brucei* are the pentose phosphate pathway (PPP) and malic enzymes. The PPP appears to be essential in BSFs [64], but not in PCFs, suggesting different mechanisms for NADPH balancing in the two parasite forms. In 2013, Allmann *et al.* [26] investigated the metabolism of cytosolic NADPH in mutants impaired for glucose-6-phosphate dehydrogenase (G6PDH) activity, the first committed step of PPP, or impaired for the cytosolic malic enzyme (MEc). When PCFs were cultivated in glucose-rich

medium, no significant growth alteration was observed in mutants impaired for only one of the two enzymes. In contrast, the double mutant impaired for both enzymes died after a few days of cultivation. These observations showed that the two NADPH-producing processes have a redundant function in glucose-rich conditions. This redundancy may compensate in trypanosomatids for the lack of a transhydrogenase, which catalyses the reversible conversion of NADH into NADPH in other organisms. Based on their data, the authors propose the occurrence of a NADH/NADPH converting cycle (or transhydrogenase-like shunt) in *T. brucei* PCFs [26]. In this cycle, electrons are transferred from NADH to malate by MDHg in the glycosomes, and then malate transfers back the electrons to NADPH either in the cytosol via MEc or in the mitochondrion via MEm. The pyruvate released by the MEs is then recycled to glycosomal PEP via PPDK, and then to OAA via PEPCK (Fig. 2), to complete the NADH/NADPH cycle. By this process, there is a net transfer of electrons from glycosomal NADH to either cytosolic NADPH or mitochondrial NADPH.

Besides the transhydrogenase-like cycle, an intriguing observation of Allmann *et al*. was that the redundancy of PPP and MEc for NADPH production was also observed when PCFs were grown in glucose-depleted medium that contained proline [26], which is closer to the conditions found in the insect digestive tract [65]. The contribution of malic enzyme to cytosolic NADPH production upon growth on proline was expected, since malate was a known product of proline metabolism in PCFs. The contribution of the PPP to NADPH production in glucose-depleted medium was more surprising. It requires a flux through the PPP in the absence of glucose, suggesting the occurrence of gluconeogenesis from proline, a process that was not reported to occur in *T. brucei*. To investigate such hypothesis, Allmann *et al*. incubated PCF cells with [U-^{13}C]-proline and measured the incorporation of label into intermediates of glycolysis and PPP. As emphasized above, MS is a very sensitive analytical method and allows the isotopic profiling of intracellular metabolites. For these experiments, the endo-metabolome of PCFs was collected in a few seconds by fast-filtration of cells, which is appropriate for glycolytic and PPP intermediates that have high turnover rates. The metabolites were separated by ionic-exchange chromatography, a method that is particularly well suited for separation of highly polar compounds such as sugar-phosphates and phosphorylated organic acids. The distribution of ^{13}C-isotopologues was measured by MS/MS on a triple quadrupole to ensure accurate quantitative measurement of labeling patterns. Using such approach, Allmann *et al*. could measure that the incorporation of label into glycolytic and PPP intermediates from [U-^{13}C]-proline was very low in the presence of (unlabeled) glucose [26]. In contrast, very significant label was incorporated from [U-^{13}C]-proline into these compounds in the absence of glucose. The fraction of labeled molecules was above 85% for all measured glycolytic intermediates. These data provided direct evidence that proline can be used by gluconeogenesis in PCFs, and hence can feed the PPP for

NADPH production. The redundancy of cytosolic NADPH-producing processes is a further illustration of the strong metabolic flexibility of *T. brucei*, since they allow adaptation to diverse carbon sources and environmental conditions.

1.9 Concluding Remarks

The applications of metabolomics to trypanosomes has not only provided novel and valuable insights into their metabolism, it has also emphasized the strong metabolic flexibility of these organisms. So far, investigations have mainly focused on central carbon metabolism, in order to resolve the highly unusual metabolic features of these organisms. A challenge is now to decipher the complete – *i.e.* cellular wide - metabolic network of *T. brucei* and more generally, trypanosomatids. In this respect, the untargeted isotopic profiling approach developed by Creek *et al*. is very promising for system-wide elucidation of *T. brucei* metabolism [45]. Based on high-resolution MS, these authors could detect a large number of labeled metabolites after addition of 50% [U-^{13}C]-glucose to cultivations of *T. brucei* PCFs. From the detailed analysis of the metabolites and their labeling patterns, they could assign the biosynthetic routes of many of the detected compounds, thereby building up parts of the PCF metabolic puzzle. They could also identify a new compound, octulose-phosphate, as part of the PPP. Together with the recent availability of the genome-scale metabolic network of *T. brucei* [66], this approach is likely to accelerate significantly the progress on the parasite metabolism, as well as the identification of novel drug targets. Beside metabolic reconstruction, a second challenge for the next future is to get more quantitative understanding of the operation of metabolism in trypanosomatids. Measurement of metabolic fluxes can be achieved from isotope-labeling experiments with the help of relevant mathematical models [67] [68]. The strong compartmentation of *T. brucei* metabolism, as well as the occurrence of duplicate reactions, currently makes metabolic flux analysis in this organism a true challenge. Recent mathematical developments as well as the application of time-course labeling experiments might help for this purpose. This approach will allow getting more detailed information about the operation and regulation of *T. brucei* metabolism. They will also represent a valuable tool for measuring the actual impact of drugs and drug candidates on their metabolism and growth capabilities.

1.10 CoA Thioesters Metabolism in Trypanosomes

This thesis aims at obtaining comprehensive understanding of *Trypanosoma brucei* metabolism, with a focus on its acyl Coenzyme A thioesters (acyl-CoA) metabolism. These metabolites are at the cross road between several catabolic and anabolic pathways and participate in a large number of reactions. Acyl-CoA thioesters support essential cellular functions such as energy generation, lipid and sterol biosynthesis. However, the topology and the operation of acyl-CoA metabolism in *T. brucei* remain largely uncharacterized.

This section first presents general considerations of the structure and function of acyl-CoA thioesters, before focusing on their metabolism in *T. brucei*. In light of this information, the specific objectives of this thesis are presented.

1.11 General Considerations

Coenzyme A (CoA) is ubiquitous cofactor and part of vitamin B family together with biotin, cobalamin, folate, niacin, pantothenate, pyridoxine, riboflavin and thiamin. In the cell metabolome, CoA can be found as a free cofactor (CoA-SH, Fig. 3) or conjugated with various carboxylic acids (acyl-CoAs). CoA and acyl-CoA thioesters play signifant roles in metabolism. Thanks to reactivity of the sulphur atom Coenzyme A participates in numerous reactions. CoA-SH, its thioersters, or parts of the molecule (4'-phosphopantetheine) are utilized in estimated 4% of reactions [69,70]. In *E. coli,* there are approximately 1577 enzymes catalyzing metabolic reactions[71], therefore at least 60 reactions will use CoA as cofactor or acyl carrier. The interest in study of these compounds emerged in second half on 20th century as microbial cell cultures were extensively used for study of CoA moiety biosynthesis. Interest in acyl-CoA profile in mammalian cells has origins in study of fatty acid biosynthesis / degradation, metabolism of cholesterol and when connection between acyl-CoAs and diabetes, insulin resistance and obesity have been observed [72, 73].

CoA functions as activator of carbonyl groups and acyl group carrier, this function is mostly recognized in process of citrate synthesis from oxaloacetate in TCA cycle, biosynthesis and degradation of fatty acids. CoA is also involved in amino acid metabolism (*i.e.* TCA cycle intermediate succinyl-CoA is produced from isoleucine, valine, and methionine). Furthermore, CoAs participates in numerous secondary metabolic pathways, such as in production of anti-carcigenic drug Taxol[74], phenylacetyl-CoA is a precursor of β-lactam antibiotic pencillin[75], propionyl-CoA is an intermediate metabolite of polyketide[76] biosynthesis, acetyl-CoA is key metabolite for biosynthesis of neutrotransmitter acetylcholine[77] in the brain, etc. Detoxification of xenobiotics uses pool of free CoA because many drug candidates carry carboxylic functional group which conjugates with –SH group of CoA to form xenobiotic-CoA[78,79]. Apart from functioning as an acyl carrier to various conjugated

carboxylic acids which is important for biosynthetic reactions, CoA is also involved in energy metabolism of the cell because hydrolysis of thioester bond (between carboxylic acid and CoA) releases energy comparable to hydrolysis of ATP[80]. Main functions of CoA have been reviewed by numerous authors [81,82,83].

1.12 Acyl-CoA structure

CoA is a sulfur containing biomolecule first discovered and described by German biochemist Fritz Lipmann in 1940s during study of acetylation of amino group of drug sulfonamide. Discovery of CoA, where "A" stands for activation of acetate was awarded the Nobel Prize in 1953 [84].

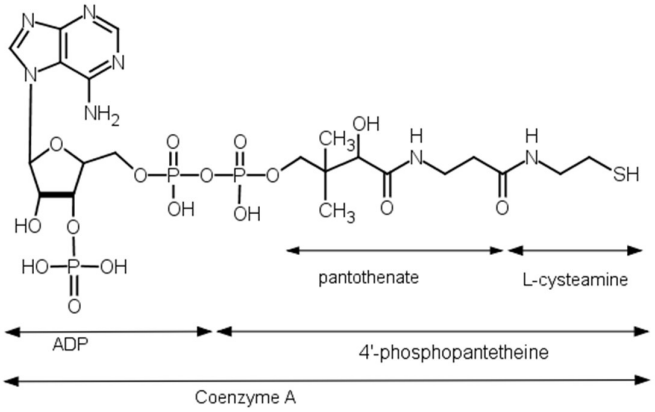

Figure 3: Structure of Coenzyme A

Coenzyme A is complex molecule constructed from adenine nucleotide (ADP), pantothenic acid and cysteamine that is a decarboxylated product of amino acid cysteine.

Thioesters of CoA fall into a large heterogenous group of metabolites that consist of CoA moiety and flexible acyl moiety which contains from 2 up to to 18 carbons. Traditionally, acyl-CoAs are divided to short polar, medium and non-polar long CoAs (also named fatty-acyl CoAs) depending on the character of the acyl moiety. Due to different chemical properties of the acyl, the extraction is generally performed specifically for short polar or fatty-acyl CoAs. Polar acyl-CoAs are extracted in aqueous polar solvents while long acyl-CoAs are mostly extracted with non-polar solvents and are frequently purified using solid phase extraction (SPE, C-18 type)[85]. Long-chain acyl-CoAs contain hydrophilic part (the CoA moiety) and hydrophobic acyl. Due to this chemical difference, unbiased extraction and chromatographic separation of all acyl-CoA thioesters is routinely not perfomed due to diverse solubility - albeit several authors have pursued this query by using biphasic extraction[86] (limit of detection of fatty-acyl CoAs 16x higher than polar CoAs) or buffered isopropanol and use of online SPE[87].

1.13 CoA Biosynthesis

CoA is assembled from three precursors – cysteine, ATP and pantothenate (Fig 4). The CoA assembly starts with uptake of pantothentate and its subsequent phosphorylation to 4'-phosphopantothenate by pantothenate kinase (PANK), its structure is well-known [88, 89]. In the next reaction cysteine is added to 4'-phosphopantothenate producing peptide bond in 4'-phospho-N-pantothenoylcysteine. This reaction is catalysed by 4'-phosphopantothenoylcysteine synthase (PPCS) and reaction is fuelled by CTP rather than ATP[90]. Molecule undergoes further decarboxylation of cysteine's carboxylic group into 4'-phosphopantetheine. The last two steps involve transfer of 5'-AMP (adenylyl from ATP) to 4'-phosphopantetheine to form 3'-dephospho-CoA, and this is then phosphorylated on the 3'-hydroxyl position of ribose to give CoA. Final two steps of CoA biosynthesis are catalysed by phosphopantethine adenyltransferase (PPAT) and dephospho-CoA kinase (DPCK), respectively.

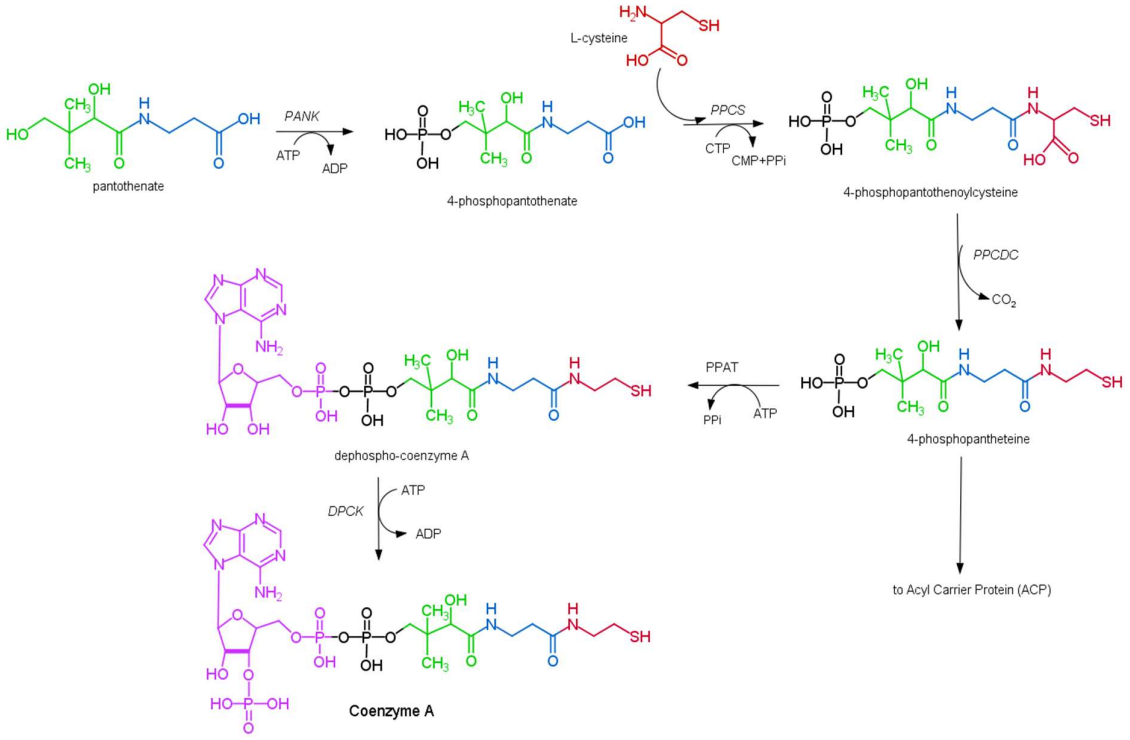

Figure 4: Assembly of Coenzyme A

Abbreviations: PANK, pantothenate kinase; PPCS, phosphopantothenoylcysteine synthase; PPCDC, phosphopantothenoylcysteine decarboxylase; PPAT, phosphopantetheine adenylyltransferase; DPCK, Dephospho-CoA kinase.

CoA precursors ATP and cysteine are readily produced in any cell, however pantothenate biosynthesis is native only to bacteria, fungi and plants[91,92]. The most studied pathway of pantothenate and CoA synthesis is in *E. coli,* where pantothenate is produced by two separate branches from pyruvate via 2-ketoisovalerate (intermediate of L-valine biosynthesis) and L-aspartate. Pantothenate uptake is

essential for all organisms that lack pantothenate biosynthesis panthway. Each tissue of the body seems to be able to transport pantothenic acid into the cell and synthetize CoA from this precursor[93]. Grenschel *et al.,* notes that CoA biosynthesis from common precursors has been largely conserved in kingdoms, however some eukaryotic pathogens (such as *Plasmodium falciparum* – causing malaria, or *Giardia lambia* – intestinal parasite) have various mechanisms of uptake of CoA precursors[94] and since they are cultivated in rich media often containing foetal bovine serum it is not clear which precursor they require.

CoA biosynthesis pathway was targeted as potential drug target in *Plasmodium falciparum* - structural analogue of pantothenate, pantothenol, was found to be an inhibitor of PANK in this organism[95]. Assays with compounds from malaria box were tested also on *T. brucei* (which is not closely related to *P. falciparum*) and obtained results showed similar growth inhibitory effects and rescue behaviour after addition of coenzyme A into culture broth. These results imply that same targets of the CoA biosynthesis pathway were affected[96]. Gerdes et al., suggests that some eukaryotic parasites may share a conserved CoA transporter[97]. Such CoA transporter was implied based on study of isolated potato mitochondria where such CoA transport system could function[98] as exogenous coenzyme A was observed to accumulate inside the mitochondria. Furthermore, in yeast, mitochondrial carrier Leu5p has been identified as a CoA transporter. Its deletion lead to strong growth phenotype and and low levels of mitochondrial CoA pools[99]. Acyl-CoA is membrane-impermeant molecule, thus CoA moiety is typically not transported between intracellular compartments and only acyl part is being transported, *e.g.* via acylcarnitine system. In eukaryotic organisms, ubiquitous L-carnitine can be reversibly acetylated by acetyl-CoA; its main function is to carry activated fatty acyls from cytosol across the mitochondrial membrane to feed β-oxidation. It is involved in acyl-carnitine/carnitine transporter: Acyl-CoA + L-carnitine ↔ Acyl-L-carnitine + CoA.

Cellular levels of CoA are tightly regulated by biosynthesis and degradation, degradation of CoA is less studied than its biosynthesis. Degradation of acyl-CoA thioesters is facilitated by acyl-coa thioesterases, which catalyze the hydrolysis to free acyl (carboxylic acid) and free CoA. These enzymes are present in almost all cellular compartments. Degradation can be catalysed by reverse activity of phosphopantetheine adenyltransferase (PPAT)[100], which yields 4'-phosphopantetheine and ATP. Another possibility of CoA degradation is via nudix hydrolases (nucleoside diphosphate X)[101,102]. This protein family is found in bacteria, archaea and eukaryotes. In *E. coli* one of the proteins (Orf192) has CoA pyrophosphatase motif, however its function has not yet been experimentally defined[102].

1.14 Functions of CoA and Acyl-CoAs in Metabolism

1.14.1 Acyl Acceptor in Central Metabolism

CoA functions as essential cofactor in many enzyme catalysed reactions. It is required by pyruvate dehydrogenase complex (PDH), which catalyses dehydrogenation and decarboxylation of pyruvate into acetyl-CoA. This enzyme uses CoA as acceptor of two carbon residues from decarboxylated pyruvate. Acetyl-CoA produced from decarboxylation of pyruvate and other sources *i.e.* β-oxidation of lipids or breakdown of proteins, is completely oxidized into CO_2 and H_2O in TCA cycle. The α-ketoglutarate dehydrogenase complex (AKGDH) operates in similar manner as PDH. AKGDH catalyses conversion of α-ketoglutarate into succinyl-CoA and CO_2. The enzyme is metabolically important, because it also reduces NAD^+ to NADH. In trypanosomes, AKGDH participates on catabolism of amino acids L-glutamine and L-proline. In this reaction, NAD^+ functions as electron acceptor and CoA carries succinyl group. Succinyl-CoA then undergoes reversible reaction by succinyl-CoA thiokinase (succinyl-CoA synthetase, SCS or SCoAS) to form succinate and free CoA. The thioester bond in succinyl-CoA is energy-rich, its hydrolysis leads to energy release which is subsequently stored in form of phosphate bond of ATP.

1.14.2 Fatty Acid and Polyketide Biosynthesis

One of the intermediates in CoA biosynthesis, 4'-phosphopantetheine, is required for activation of acyl carrier protein (ACP) for fatty acid and polyketide biosynthesis[103]. ACP are autonomous domains or proteins of 80-100AA and they function as stabilization of acyl groups in fatty acid and polyketide biosynthesis. This protein link assures covalent catalysis in multistep processes of sequential condensation reactions [104,105] because it carries intermediates of fatty acid biosynthesis. Acyl groups are attached to the sulfhydryl terminus of 4'-phosphopantetheine prosthetic group [106]. Inactive apo-form of ACP is activated by attack of β-OH-sidechain of serine residue onto pyrophosphate bond in CoA, which releases the 4'-phosphopantetheinyl moiety. Released moiety is transferred by 4'-phosphopantetheine transferase onto serine residue of ACP and free thiol may be esterified by substrate, *i.e.* acetyl-CoA or malonyl-CoA [107]. In higher organisms, this synthetic function is taken over by fatty acid synthetase complex (FAS) where the carrier domain is also called ACP.

1.14.3 Degradation of Lipids and Branched Amino Acids

Another metabolically important process which requires participation of Coenzyme A, are catabolic pathways – such as β-odixation of fatty acids which is source of energy or catabolism of amino acids (proteins). Conjugation of fatty acid with CoA (activation) is a pre-requisite needed for their participation in catabolism. This reaction is catalysed by ATP-dependent acyl-CoA synthetases[108]. CoA conjugated fatty acids also play role in cell signalling and metabolic control[109]. In process of β-oxidation, two-carbon residues are cyclically cleaved from the fatty acyl chain which is catalysed by acyl-CoA synthetases. Eukaryotic organisms possess acyl-CoA synthetases of various chain length specificity, while *E. coli* contains only one synthetase (*fadD*).

Degradation of branched amino acids proceeds through acyl-CoA thioesters, in mammals branched amino acids feed the pool of propionyl-CoA which is then converted to succinyl-CoA. Mitochondrial enzyme responsible for conversion of propionyl-CoA and succinyl-CoA (methylmalonyl-CoA mutase) seems to be absent in *T. brucei*. Furthermore, L-threonine is converted into acetyl-CoA and glycine by activity of threonine dehydrogenase (TDH) because threonine dehydratase (threonine ammonia lyase) is missing – it would convert threonine into 2-oxobutyrate and ammonia[110].

1.14.4 Global Control of Metabolism

The sheer amount of reactions which involve CoA and its thioesters indicates that these compounds will also exhibit regulatory functions. These are demonstrated at enzyme and gene level. Acetyl-CoA is imporant precursor of biosynthetic pathways and is also involved in cellular regulation by acetylation of nuclear and cytosolic proteins. Acetylated ξ-Lysine residues were first described on histones [111]. Acetylation of histones has numerous regulatory functions, such as modifying folding of chromatin that alters gene expression or assembly of nucleosomes affecting DNA replication during cell cycle[112]. Similar covalent modifications were found in mitochondrial and cytosolic proteins. Lysine acetylation is likely acting as regulatory mechanism affecting activity of these enzymes[113]. Acyl moiety can be also transferred onto α-amino group of N-terminal amino acid residue in proteins by activity of N-acetyltransferase. Such N-terminal acetylation affects majority of proteins and determines for example their localisation[114]. Ratio of $\frac{Acetyl-CoA}{CoA-S}$ controls protein acetylation and influences important cell processes, such as growth, cell death or autophagy[115].

Generally, biosynthetic pathways are regulated at the level of gene expression or at level of enzymatic activity, or both. A typical mechanism of biosynthetic pathway regulation is feedback inhibition at the first committed step of the pathway by the end product which controls the metabolic flux. Intracellular level of CoA is modulated by activity of PANK and degradation of CoA and ACP to 4'-phosphopantetheine. The overall CoA biosynthesis pathway is regulated by feedback inhibition of

PANK[116] which responds to CoA and its esters. PANK is more sensitive towards CoA-SH, less potent inhibitors are acetyl-CoA and succinyl-CoA [117] (in bacteria).

1.14.5 Metabolism of Acyl-CoAs in T. brucei

Acyl-CoA network is in many instances unknown in trypanosomes compared to metabolism of other metabolic intermediates. Acyl-CoA thioesters have been only partially targeted in previous studies. First notes on coenzymes, appeared when existence of the TCA cycle and unusual fatty acid biosynthesis were examined. Acyl-CoAs participate in four main essential processes of *T. brucei* metabolism:

1. mitochondrial acetate production, involved in energy generation and
2. fatty acid biosynthesis through the ELO pathway, and
3. mitochondrial lipid biosynthesis through the FASII pathway, and
4. mevalonate pathway leading to sterol biosynthesis.

However, both the topology of the acyl-CoAs metabolism and functions remain experimentally uncharacterized in *T. brucei*. The hypothetical acyl-CoAs metabolic network is depicted in Fig 5. The main functions of acyl-CoAs metabolism in the different processes are described in following section.

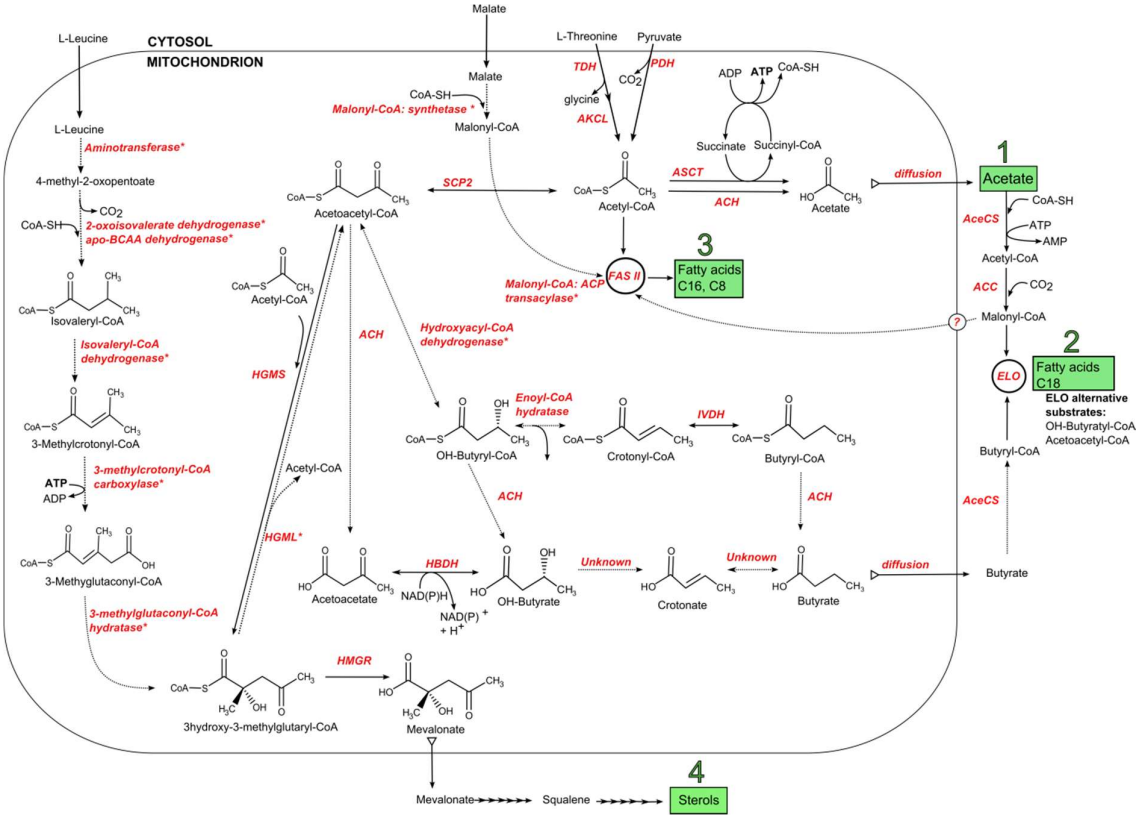

Figure 5: Mitochondrial model of acyl-CoA network in *T. brucei* PCF

Current hypothetical model of the lipid and sterol de novo biosynthesis in the subcellular compartments of procyclic Trypanosoma brucei. Adapted with permission from F. Bringaud (Acetotryp, 2014), [118]

Sections described further in the text: 1, acetate production; 2, fatty acid production ELO pathway; 3, fatty acid production FAS II pathway; 4, sterol production.

Abbreviations of enzyme names: ACH, acetyl-CoA transferase; ASCT, acetyl-CoA: succinate CoA transferase; AceCS, acetyl-CoA synthase; SCP2, thiolase isoform; IVDH, isovaleryl-CoA dehydrogenase; HBDH, 3-hydroxy-butyrate dehydrogenase; HGMS, 3-hydroxy-3-methyl-CoA synthase; HGML, 3-hydroxy-3-methyl-glutaryl lyase; HGMR, 3-hydroxy-3-methyl-CoA reductase.

Enzymes labeled with asterisk (*) are identified putatively. End products of these pathways are highlighted in green boxes. Dotted reaction arrows have not been proven experimentally in T. brucei.

1.14.5.1 Mitochondrial Production of Acetate

As mentioned previously, the TCA cycle is not fully operational in trypanosomes even though all enzymes are expressed[52]. Therefore, the two-carbon moiety in acetyl-CoA is not decarboxylated in the TCA cycle, but instead it is converted to acetate. Production of acetate is a well-known phenomenon in parasitic organisms. This adaptation responds to need for survival during anoxic conditions, where O_2 cannot be used as electron acceptor during oxidative phosphorylation, and ATP production relies on converting acetyl-CoA to acetate[119].

Conversion of acetyl-CoA to acetate is catalysed by two enzymes, that are Acetate: Succinate CoA-Transferase (ASCT)[60,120] and Acetyl-CoA Thioesterase (ACH)[36]. While ACH releases free CoA, the ASCT releases succinyl-CoA. Succinyl-CoA is subsequently hydrolysed by succinyl-CoA transferase (SCS, also abbreviated as SCoAS) to succinate and CoA-SH. Energy of hydrolysis of thioester bond is stored in 1 molecule of ATP per turn of this reaction. Mitochondrial pool of acetyl-CoA is supplemented from pyruvate or L-threonine by activity of pyruvate dehydrogenase (PDH) or L-threonine dehydrogenase (TDH), respectively and possibly through L-homoserine and homoserine lactones because trypanosomes have kept enzymes to produce L-threonine from these precursors[121].

Acetate is one of main end products of fermentative catabolism of glucose in trypanosomes and it is also essential precursor for lipid biosynthesis[34]. Production of acetate via ACH is not essential as its knockdown produces no growth phenotype, and its contribution to acetate production is rather minor because *Δach* cell line strain excretes similar amounts of acetate than wild type cells[36]. ACH is also not coupled to ATP production since addition of oligomycin (specific inhibitor of ATP synthase) does not significantly affect viability of cells. *Δasct* strain is sensitive towards oligomycin, what is in agreement with ATP production associated with ASCT-SCS cycle. In *Δasct* cell line 30% decrease of acetate production compared to wild type cells was observed, implying that ASCT is the main enzymatic activity participating on production of acetate from acetyl-CoA. Abolition of both ASCT and ACH enzymes producing acetate is lethal [36], the phenotype has not been reversed by addition of acetate into cultivation media. This suggests other essential role of acetate, which could be related to maintaining membrane potential[15].

Trypanosomes do not use conventional citrate/malate shuttle which is a way how to transport acetyl-CoA from mitochondrion to cytosol (as citrate). This transport system relies on cleavage of citrate in cytosol into acetyl-CoA which subsequently enters the fatty acid biosynthesis and remaining oxaloacetate is recycled back to mitochondrion. This cycle requires functional citrate lyase. However, disruption of citrate lyase caused no effect on *de novo* fatty acid biosynthesis[34] because *T. brucei* has evolved alternative way of acetyl-CoA transport through mitochondrial membrane. As described, acetyl-CoA is first converted to acetate, which is membrane permeable molecule that diffuses into cytosol. Then in the cytosol, AMP-dependent acetyl-CoA synthetase (AceCS) converts acetate back to acetyl-CoA to enter the fatty acid biosynthesis.

In strains which accumulated acetyl-CoA, ketone compound β-OH-butyrate was detected as minor excreted product. Production of this compound was observed when acetate production via ASCT and ACH was downregulated[60]. Additionally, it was observed also in *Δpepck* cell line where the carbon flux from catabolism of glucose is directed towards mitochondrial acetate production without partitioning into glycosomal succinate branch[56] or in glucose depleted conditions when PCF survives on L-proline as main carbon source[58]. The existence of β-OH-butyrate was explained by redistribution of the carbon flux, because this molecule has not been observed in wild type *T. brucei*. Its origins are presumed to be acyl-CoA thioesters. β-OH-butyrate is thought to originate from acetoacetyl-CoA via activity of putative hydroxyacyl-CoA dehydrogenase, which would convert acetoacetyl-CoA to OH-butyryl-CoA. This reaction has been putatively identified to be catalysed by trifunctional enzyme (Tb.927.2.4130) in dissertation work of Yoann Millerioux [122] who was interested in origin of ELO pathway primer, butyryl-CoA. Subsequently, β-OH-butyrate is thought to be produced from β-OH-butyryl-CoA via activity of ACH, which is substrate-specific towards acyl-CoAs with 2 and 4 carbons [36]. Substrate specificity of ACH has been tested *in vitro*; the highest activity was observed with C2 compounds (acetyl-CoA) and C4 compounds (butyryl-CoA, β-OH-butyryl-CoA and acetoacetyl-CoA) but very little specificity towards crotonyl-CoA (also C4 compound). Group of these C4 carboxylic acids with potential to relocate to cytosol have been suggested as potential primers for ELO pathway[118]. ACH does not exhibit significant activity towards malonyl-CoA and other acyl-CoAs of medium length to fatty-acyl CoAs[36]. Furthermore, in his work Yoann Millerioux identified isovaleryl-CoA dehydrogenase (IVDH), that catalyses dehydratation of isovaleryl-CoA to methylcrotonyl-CoA (in mevalonate production pathway) and could also catalyse reduction of structurally similar crotonyl-CoA to butyryl-CoA. *RNAi* mediated downregulation of IVDH and incubation of cells with radioactive acetate lead to decrease of radiolabel found in fatty acids, which was redistributed to sterols proving the theory that butyryl-CoA is produced via IVDH from crotonyl-CoA[122].

1.14.5.2 Biosynthesis of lipids

Parasites have significant requirement for biosynthesis of cell membrane phospholipids during differentiation. In addition, their protective layers are changing during life cycle and both procyclin and variant surface glycoprotein (VSG) are attached by glycosylphosphatidylinositol anchor (GPI) that contains two molecules of fatty acids – myristic (14:0) for VSG of bloodstream forms[123] and palmitic (16:0)/stearic (18:0) for procyclin in procyclic forms. Presence of VSG is essential for survival of BSF, and procyclin layer is important (but not imperative) for successful colonization of tse-tse midgut by PCF. Therefore, these are the major fatty acids produced by each life form [124]. Lipid biosynthesis in both life forms has been reviewed in detail [118, 125]. Apart from production of fatty acids for growth, trypanosomes possess lipid droplets comprised of di- and tri-acylglycerols and sterol esters used as energy storage during development of procyclic forms[126]. Trypanosomes readily scavenge lipids from their host environment, because it is less energy demanding - ATP cost of uptake is 6-times less than synthesis of a new 16C long fatty acid[10]. Cultivation media SDM-79 contain fetal bovine serum (5-10%) which is composed also of fatty acids. Upon feeding PCF with either radioactively labeled glucose, glycerol, proline or threonine the only way how could trypanosomes incorporate ^{14}C into their fatty acids was to synthetize them *de novo* and include acetyl-CoA (acetate) into the building chain for fatty acid[54].

Fatty acid biosynthesis is comprised of four repetitive steps: condensation, reduction, dehydration and second reduction. These reactions are catalyzed by β-ketoacyl-ACP synthase which condenses ACP with primer molecule. Product is reduced by β-ketoacyl-ACP reductase, dehydrated by β-hydoxyacyl-ACP dehydratase and again reduced by trans-2-enoyl-ACP reductase. Each turn of this cycle results in two-carbon addition which are donated by malonyl-CoA. There are two types of fatty acid synthesis in organisms - FAS I and FAS II. Both FAS systems elongate the carbon chain of the fatty acid by adding two carbon residues to a primer, which is linked to acyl carrier protein (ACP). Both FAS I and FAS II perform similar set of reactions, but there are two principal differences: eukaryotic FAS I type uses multifunctional polypeptide with several domains, it is found in animal and fungi, while type FAS II uses four individual monofunctional proteins catalyzing distinct reactions for elongation of the chain and it is primarily found in plants and bacteria. Enzymes of FAS II are of prokaryotic origin, if present in eukaryotic organisms, they are located in mitochondria, apicoplasts or plant chloroplasts. In trypanosomes, components of FAS I are missing and enzymes related to FAS II are located in mitochondrial matrix. In addition to mitochondrial FAS II system, trypanosomes possess elongase pathway (ELO) associated with endoplasmic reticulum. Generally, in eukaryotic organisms ELO pathway is used for prolongation of medium/long fatty acids, however parasites have adapted this pathway for *de novo* fatty acid biosynthesis[127].

The majority of produced fatty acids is synthetized through ELO pathway, FAS II contributes only with 10% to the total fatty acids production[127]. Final products of FAS II and ELO pathways differ: FAS II produces C8 (octanoate) and C16 (stearate) [127]. Octanoate is precursor of lipoic acid which is a cofactor covalently bound to one of catalytic domains of mitochondrial pyruvate dehydrogenase. ELO was found to produce C18 (palmitate) in procyclic trypanosomes.

ELO pathway

ELO pathway comprises of three elongases (ELO 1-3) that increase the fatty acid chain in stepwise fashion. ELO uses same set of reactions as FAS but with several particularities – it preferentially uses CoA moiety as carrier of reactions instead of ACP[10]. In addition, the pathway requires butyryl-CoA as primer, instead of acetyl-CoA [10,124]**.** Transport of butyryl-CoA into cytosol is thought to be facilitated in similar manner as transfer of acetyl-CoA. Malonyl-CoA serves as donor of two carbons and NADPH as reducing agent[124]. Inhibition of ELO pathway in PCF causes growth defect which could be reversed by addition of stearate into cultivation broth[10,128], therefore essentiality of ELO is dependent on the environment. Ability to control fatty acid biosynthesis in response to environment might be important for host adaptation and maximal use of host resources. Cytosolic acetate is vital precursor for fatty acid biosynthesis because AMP-forming acetyl-CoA synthetase (AceCS)[34] ablation effectively terminated its incorporation into fatty acids synthetized *de novo*. Such notable phenotype hints that AceCS represents a unique step for biosynthesis of fatty acids, and no parallel pathways are available. AceCS is essential for de novo FA biosynthesis in both life forms[34]. First step of fatty acid biosynthesis in cytosol is carboxylation of acetyl-CoA to malonyl-CoA via activity of cytosolic acetyl-CoA carboxylase (ACC). Based TriTrypDB, trypanosomes are predicted to encode only one gene of ACC (based on homology with ACC from other organisms)[129]. Enzymatic product of this gene was found to be cytosolic and distributed in numerous non-specific aggregates which were not co-localized with markers of organelles (golgi, ER, mitochondria or cytoplasmic HSP70)[128]. ACC is biotin dependent enzyme with two catalytic functions so the reaction proceeds via two-step mechanism. First, the biotin carboxylase activity catalyzes ATP-dependent carboxylation of cofactor biotin and in second step; the carboxyl transferase activity moves the carboxyl group onto acetyl-CoA to form malonyl-CoA. Since ATP is used, this reaction is considered to be first committed step of fatty acid biosynthesis[130]. Downregulation of ACC produces stage-specific phenotype – ^{RNAi}ACC in bloodstream forms resulted in little to no difference, while in procyclic forms cultivated in low-lipid media this gene perturbation resulted in 64% reduction of growth[128] which could be reversed by addition of stearate (C18:0) into cultivation broth. The product of ACC, malonyl-CoA, is the two carbon donor for fatty acid biosynthesis in both ELO and FASII.

FAS II system

Despite lesser contribution to fatty acid pools, FAS II is essential component for proper mitochondrion functioning[127,131]. RNAi downregulation of the beta-*enoyl*-ACP reductase in low-lipid media caused procyclic growth arrest and limited multiplication after 3 days since induction. Addition of fatty acids (C14, C16, and C18) in the cultivation broth did not reverse the growth phenotype. Impaired mitochondrial fatty acid biosynthesis caused increased sensitivity towards inhibitors of cytochrome c mediated respiration. Furthermore, it also caused change in levels of phospholipids. These changes could modify formation of mitochondrial membranes which were reflected in modified shape of mitochondria observed under electron microscope[131]. By FAS II acetyl-CoA is converted into palmitic acid or octanoate. FAS II uses malonyl-CoA as donor of two-carbon units; but since only one gene having acetyl-CoA carboxylation function has been identified and localized in cytosol, mitochondrial malonyl-CoA is likely not to be produced by this enzymatic activity. It is not clear, what would be the mitochondrial source of malonyl-CoA. In trypanosomes, malate enters the mitochondria in order to be converted either to pyruvate (via MEm) and feed fatty acid biosynthesis as acetyl-CoA/acetate via PDH/AceCS, or malate is converted to fumarate (via FHm) and produces mitochondrial succinate. Stephens et al. [127] suggests plant-like production of mitochondrial malonyl-CoA by transport of malate into mitochondria where the molecule is activated to malonyl-CoA by malonyl-CoA synthetase. Then activated malonyl would participate on fatty acid biosynthesis, as enzyme that attach malonyl-CoA to ACP has been putatively identified in the *T. brucei* genome[54] (Malonyl-CoA:ACP transacylase, Tb09.211.3020). However, Stephens et al. [127] notes that using [^{14}C]-malate *in vitro* in incubations with isolated mitochondria, no radioactive label incorporation was observed in fatty acids. Although this non-functional incorporation of radiolabeled substrate could be explained by damage of FAS system in preparation of cell lysates as noted by the author.

1.14.5.3 Biosynthesis of Sterols

Sterol composition differs between *T. brucei* procyclic and bloodstream forms. BSF relies on uptake of cholesterol from the host, while PCF produces mainly ergosterol [132], however if cholesterol is available PCF will incorporate it into the membrane[133].

De novo biosynthesis of sterols is facilitated by mevalonate pathway, which provides essential blocks (isoprenoids) for sterol biosynthesis, also other compounds (carotenoids, dolichols) and ubiquinone which essential for cellular functions. The pathway spreads over several organelles – glycosome, mitochondrion, endoplasmic reticulum as well as cytosol. Mevalonate pathway begins with thiolase-catalyzed (SCP2) condensation of two molecules of acetyl-CoA producing acetoacetyl-

CoA and free CoA-SH. SCP2 removes acyl moieties from acyl-CoA during β-oxidation; however, it could also catalyze condensation reactions in anabolic processes, such as biosynthesis of sterol and ketone bodies. Trypanosomal thiolase shows activity in synthetic direction. Gene transcript of SCP2 was found in both PCF and BSF trypanosomes, but the protein is much more highly expressed in PCF. SCP2 activity is experimentally found mostly in mitochondria. *RNAi* mediated downregulation of enzyme does not produce growth phenotype in either glucose rich or glucose depleted media[134]. Localization of SCP2 in mitochondria corresponds with localization of other β-oxidation related enzymes, such as 2-enoyl-CoA hydratase, 3-hydroxyacyl-CoA dehydrogenase (NADP+ dependent), *enoyl*-CoA hydratase. Acetyl-CoA produced by β-oxidation or otherwise (as intermediary product of pyruvate and threonine degradation) may not be used by TCA cycle, but could participate in mevalonate pathway for synthesis of sterol and ketone bodies. Cultivation media in this experiment also contained leucine, what could explain why SCP2 knockout is viable. In insect midgut where leucine is abundantly present, SCP2 may not be essential in this stage. Subsequent reaction involves condensation of third acetyl-CoA to acetoacetyl-CoA form 3-hydroxy-3-methylglutaryl-CoA which is catalyzed by 3-HMG-CoA synthase (HGMS). This intermediate is further reduced to mevalonate by $NADP^+$ dependent 3-HMG-CoA reductase (HGMR) which is associated with mitochondria in *T. brucei*, small fraction with glycosomal membrane and possibly also endoplasmic reticulum[135, 136]. Genome of *T. brucei* also contains a putative 3-HMG-CoA lyase (HGML) which catalyzes the reverse reaction. However, activity this enzyme has not been yet experimentally proven in *T. brucei*. Uttaro suggests that HGML and HMGS represent a balance between sterol and fatty acid biosynthesis[118]. Mevalonate is subsequently phosphorylated to mevalonate-5-phosphate by activity of mevalonate kinase (MVAK) which was found to be associated with glycosomal matrix[135]. Phosphorylated mevalonate is converted in several metabolic steps into squalene, direct precursor of sterols.

Alternative source of sterols is degradation of branched amino acids, which can be converted to acyl-CoAs in the mitochondrion. This degradation pathway was observed in related trypanosomatid - *Leishmania mexicana.* It uses intact carbon skeleton of L-Leucine as major carbon source for production of 3-HMG-CoA and sterols. HGML activity has been experimentally determined in *L. Mexicana,* since Ginger et al., observed ^{13}C originating from [^{13}C-U]-leucine in fatty acids[137]. This carbon source has been evaluated in *T. brucei* sterol synthesis [138], however study focused only on end products of sterol biosynthesis without evaluating ^{13}C incorporation into acyl-CoA species or fatty acids. Nonetheless, *T. brucei* PCF (strain 427) cultivated in SDM-79 supplemented with ^{13}C labeled leucine incorporated insignificant amount due to acetyl-CoA flux into sterols.

Alternative fate of acetoacetyl-CoA could be mediated via ACH, which has high substrate specificity towards acetoacetyl-CoA. The reaction produces acetoacetate, which could be excreted

directly into the cytosol and enter ELO pathway. In the next reaction, acetoacetate is reduced to β-OH-butyrate by activity of NADPH-dependent β-hydroxybutyrate dehydrogenase (HBDH) [139]. Putative orthologue of HBDH has been identified in *T. brucei,* its ablation lead to reduction of parasite growth. HBDH can utilize both NADPH and NADH for reduction of functional group, this unusual feature could play role in maintaining mitochondrial redox balance[139].

1.15 Objectives of the Thesis

During the past decade(s) combination of reverse genetic tools and isotope tracing into products of targeted gene (and enzyme) abolitions has advanced understanding of *T. brucei* metabolism. Despite the relevant position in metabolism, bridging catabolism of amino acids, carbohydrates and anabolic pathways, the mitochondrial network of acyl-CoA thioesters has not yet been resolved. The aim of this thesis was clarification of the topology and operation of mitochondrial acyl-CoA network of *T. brucei*. Several anabolic branches rely on the utilization of acetyl-CoA – FAS II, ELO and sterol biosynthesis, and the *in vivo* conversion rate of acetyl-CoA from various carbon sources into these pathways remains to be characterized. Historically, trypanosome metabolism was studied in glucose rich media, and organism significantly remodels its metabolism in absence of glucose[140,58,26]. Conditions mimicking true *tse-tse* environment, where glucose is consumed within 15 minutes of ingestion, are currently sought in order to clarify metabolism of procyclic form in its natural conditions. Any differences in context of acyl-CoA thioesters are not known yet in these conditions. Such elucidation is essential for understanding the metabolic adaptations of the organism during life cycle. That is why the aim was to first explore acyl-CoA thioesters with *T. brucei* on glucose, then on amino acids.

This task required to set up a complete methodological framework for functional investigation of acyl-CoA metabolism, which is presented in chapter 2. In chapter 3, we validate the biological applicability of the methodology on the bacterium *E. coli*, a model organism in systems and synthetic biology, for which we present the first comprehensive view of the functional interconnection between central metabolism and acyl-CoA metabolism. Finally, in chapter 4, we present the first results obtained on *T. brucei* metabolism.

Due to close relation between acyl-CoA thioesters to intermediary metabolism and anabolic pathways, the idea was to combine analytical method for acyl-CoA thioesters with already well established methodology for MS-based analysis of various groups of metabolites (phosphorylated sugars, organic acids, amino acids) with NMR-based quantification and isotopomers analysis of metabolic end products which has been extensively used in past years. The work aimed to enlarge observable metabolite groups (by adding acyl-CoAs to already established analyses of intracellular metabolites) in order to resolve abovementioned metabolic pathways using acyl-CoA thioesters.

2 *Application of Method for Analysis of Acyl-CoA Thioesters*

The objective of this chapter within scope of the whole thesis was to set up methodology for quantification and analysis of isotopic profile of acyl-CoA thioesters extracted from biological samples. Three main objectives for successful metabolite analysis are required: development and performance characterization of LC-MS method for quantitative analysis of acyl-CoAs concentration and isotopic profile and evaluation of sampling protocol.

First, the chapter aims to introduce methodology used for quantitation and isotopic profiling of short-polar Acyl-CoAs, with focus on the main parameters in preparing and analyzing Acyl-CoA extracts from cells growing in suspension published over last years. Numerous methods published show diversification of protocols into analysis of short and medium acyl-CoAs, or fatty acyl-CoAs in order to achieve acceptable level of sensitivty for quantitation. In a similar manner, presented analytical approach is focusing only on short polar Acyl-CoAs. Analytical method has been adapted from Peyraud *et al.* [141]. After the setting up and characterizing of method performance, sampling protocols were developed on *E. coli* as model organism and on *T. brucei*.

2.1 Introduction to Acyl-CoA Analytical Methodology

Pioneer studies on biosynthesis of CoA moiety were performed by feeding the cells with radiolabeled CoA precursors[142, 143]. Acyl-CoA thioesters of these extracts were separated and detected by HPLC coupled to a scintillator counter. Conversion of acyl-CoAs into radioactive molecule provides sensitive analysis, but requires radioactive material and careful sample handling. Due to health hazard, radioactive material cost and restricted disposal, such experiments are difficult to perform in large scale (*i.e.* bioreactor). Hyphenated techniques of coupling HPLC and UV detection (254-260 nm) have been in use since 80's and were frequently used for acyl-CoA analysis in various animal tissues [144,145,146,147,148,149]. UV detection is nonspecific and often hindered by numerous other metabolites that also absorb in the same wavelenght as the adenine moiety in the CoA. Compound identification relies on comparison of retention time (R_T) of acyl-CoAs in biological extrats with standards. Derivatization techniques were also applied to analyses of CoA thioesters. Acyl-CoAs were derivatized into fluorescent etheno-esters, this protocol has improved sensitivity compared to HPLC-UV, but preparation of etheno derivatives is laborious [150,151]. Derivatization to N-acylglycines [152] in order to increase volatile character of the molecule was used prior to GC-MS analysis.

The molecule of CoA contains 3 phosphate groups that enable its charged state and this characteristic was used to separate molecules by high resolution capillary electrophoresis (HPCE) [153,154]. Authors could successfully separate short-polar thioesters, but note that migration times and pH are sources of variability for this technique, which in the end is probably the reason why HPCE is not used more frequently. Furthermore, hydrophilic interaction liquid chromatography (HILIC) columns have emerged as alternative technique for separation of highly polar compounds and among other different classes of polar metabolites[155] also - allow separation acyl-CoA thioesters [156,157]. Separation by reversed phase HPLC is the most frequently used platform for acyl-CoA analysis, and vast majority of published methods use C-18 as stationary phase. Acyl-CoA thioesters are retained due to interactions of CoA carbohydrate skeleton with silica-bound oktadecyl groups. During analysis of acyl-CoA standards on C-18 columns two peaks elute per compound. This is due to presence of acyl-CoA isoforms [158], which differ only by position of phospate group on ribose-3'phosphate in *iso* acyl-CoA instead of ribose-2'phosphate of acyl-CoA. Isomers can be purified by preparatory HPLC [159]. Their function, if any, in biological systems is not known. It seems that *iso* acyl-CoAs are produced only artificially due to acidic preparation during CoA synthesis. In order to increase intensity of acyl-CoA signal, or to increase retention on a particular column ion pairing agents can be used. These are eluent additives present in mobile phase that bind to CoA moiety (*i.e.* to phosphate groups). Multiple publications use variety of ion pairing agents in analysis of acyl-CoAs, such as hexylamine [160], tributylamine [161], or trifluoroacetic acid [75]. One of the distadvantages is possible ion supression in the

ESI source and contamination of MS analyzer which might have significant impact on the robustness of the method.

I would like to highlight the main parameters in preparing and analyzing Acyl-CoA extracts from cells growing in suspension published over last couple of years, which are summed up in Table 2. Quantification of acyl-CoA thioesters, similarly as will be introduced in this work, is subjected to use of internal standards[162]. Different acyl-CoA species were used as internal standard – for example heptadecanoyl-CoA or propionyl-CoA were used[163, 164]. However, the choice of ^{13}C labeled internal standard is the most robust approach for quantification of metabolites. Of course, it is not the only option of internal standard production. Basu *et al*., used isotopes ^{13}C and ^{15}N coming from [$^{13}C_3{}^{15}N1$]-pantothenate incorporated within the CoA moiety for quantitation. Labeled [$^{13}C_3{}^{15}N_1$]-pantothenate was supplemented in the cultivation of mammalian cell lines as an essential dietary precursor since these cells are unable to synthetize CoA *de novo*[165, 166]. As a result, labeled pantothenate is incorporated into CoA moiety and its acyl thioesters of CoA.

Identification of acyl-CoA species is also facilitated by fragmentation of the molecule. All protonated acyl-CoAs undergo structure specific fragmentation that is why MRM mode is well-established method for MS identification and quantification (Table 2). Specific pattern has been observed by numerous authors in both positive and negative mode [163, 167, 168, 164, 169, 170, 171].

Table 2: Methods used in preparation and detection of short acyl-CoA extracts from cells in suspension.

Non-exhaustive list of methods used for sample preparation and analysis of Acyl-CoA thioesters applied to variety of biological matrices. Majority of methods are based on collecting cells either by sampling of whole broth or centrifugation. Due to rapid hydrolysis of the thioester bond, authors use acidic extraction to preserve the sample. Quenching and extraction in one step performed in acididified cold organic solvent is preferred protocol for cellular cultures. Chromatographic (Chrom) separation is almost uniquely done on C-18 columns. Use of ion pairing agent is relatively sparse. Selective detection in MRM mode is frequently used due to consistent fragmentation pattern.

Abbreviations: *Chrom, chromatography; C, centrifugation; WB, whole broth, F, fast filtration; FR, flash-freeze, F; filtration; TCA, trichloroacetic acid; SPE, solid phase extraction; full scan, monitoring all ions entering the detector (total ion current); MRM, multple reaction monitoring of targeted set of metabolites. SRM – selected reaction monitoring, MRM – multiple reaction monitoring, SPE – solid phase extraction. Use of ion pairing agent indicated by asterisk (*)*

Biological matrix	Sampling	Internal standard	Quenching, Extraction	Chrom.	MS Detector, polarity, scan type	Ref
E. coli (BAP1)	C	Glutaryl-CoA	45:45:10 (acetonitrile:methanol:water + 0.1% glacial acetic acid), -20°C	LC C-18	QqQ, pos, MRM	172
Hepatocytes (mouse)	C	no	Q+E: 10% TCA, sonication, SPE	LC C-18	QqQ, pos, MRM	173
HepG2 cells	C	no	Q+E: 10% TCA quench, sonication, SPE	LC C-18	QqQ, LTQ-Orbitrap XL, pos SRM	174

Human platelets	C	no	Q+E: 10% ice-cold TCA, SPE	LC C-18	QqQ, pos, SRM	[175]
M. elsdenii	C	^{13}C labeled extract of *Pichia pastoris*	Q: methanol -20°C, E: freeze thaw cycles	LC C-18	QqQ, pos, MRM	[176]
M. extorquens AM1	WB, F	^{13}C labeled extract of *M. extorquens*	Q+E: 95% acetonitrile + 25 mM formic acid, -20C	LC C-18	LTQ-Orbitrap, neg/pos, full scan	[141, 177]
R. eutropha H16	F	^{13}C extract of *R. eutropha*	Q+E: methanol: chloroform: water (5:2:2) 30min at room T, centrif	CE	Qtrap, neg, MRM	[178]
S. cerevisiae	WB	^{13}C extract of *S. cerevisiae*	Q:methanol:water at -40°C, E: 75% ethanol at 95°C	LC* C-18	QqQ, neg, MRM	[179]

2.1.1 Introduction to Acyl-CoA Extraction Methodology

Cells cultivated in suspension used for monitoring of short acyl-CoA profile were collected by routine protocols used in metabolomics studies – whole broth sampling, centrifugation or fast filtration (Table 2). Quenching and extraction is generally performed in cold acidified organic solvents. The length of acyl chain impacts the chemical propeties, thus short polar acyl-CoAs are extracted in aqueous polar solvents while long acyl-CoAs are mostly extracted with non-polar solvents and purified using solid phase extraction (SPE, C-18 type)[85]. Therefore, short polar acyl-CoAs are not routinely quantified by extraction together with fatty-acyl CoAs due to their different solubility. The molecule of acyl-CoA is alkali labile thus the extraction protocols are carried out in acidic conditions to preserve the thiester bond. Stability of short chain CoAs is temperature and pH dependent. Seifar *et al*. compared two extraction methods: boiling ethanol vs. methanol / chloroform/ water at room temperature. Applied to freshly prepared acyl-CoA standards in water author observed the loss of 95% succinyl-CoA within 3min with the first method and 65% with the second one[180]. Short-term stability of short polar acyl-CoA thioesters has been tested over short periods of time in different storage solutions by numerous authors.

All acyl-CoAs display measurable degradation over time in the autosampler at 4 °C [181] (Li *et al*., stored acyl-CoAs at pH 5). Especially succinyl-CoA was observed to be degraded rapidly. Succinyl-CoA decomposition by 77% in extracts of animal tissues was observed within 12h at pH 6 and 8°C [146]. This observation is in accordance with recent results by Neubauer *et al.,* who stored short polar acyl-CoAs standards in either water or 50 mM ammonium acetate (pH 6.9) and kept them in autosampler at 4°C over 29hours. Sucinyl-CoA decomposed by 30% in favor of CoA-SH in both conditions [176]. Succinyl-CoA was observed to be more stable at acidic pH than at neutral pH already in 1953 [182]. Stability of CoA thioesters in alkaline conditions is increased in the presence of magnesium ion[183]. In the literature, we can find different storage solutions, such as water [168, 74], 50% aq.methanol or acidic buffers 25 mM ammonium formate (pH 3.5) with 2% methanol [141].

2.2 Application of Separation and Detection of Acyl-CoA thioesters

2.2.1 HPLC Separation of Acyl-CoAs

In this work Phenomenex Kinetex C-18 with 1.7µmin particle size and trimethylsilyl (TMS) endcapping was the column of choice. This column setup was tested in three sizes (50×2.1 mm, 100×2.1 mm and 100×3.0 mm) in order to ameliorate separation of selected short-polar acyl-CoAs. Ion strenght and pH value of the aqueous phase were found to have major impact on the elution and peak shape. Acyl-CoAs were separated in flow of 50 mM formic acid with pH adjusted by addition of ammonium hydroxide. Tested pH of mobile phase was 4, 6, 8 and 10. Out of these, mobile phase adjusted to pH= 4 and 6 yielded broad non-gaussian peaks. Similar observation on separating short polar acyl-CoAs on C-18 column was made by Neubauer *et al*., [176]. At pH 10 the best peak shape (narrow, no tailing) and signal intensity was observed, however this value is at the end of pH range of the column, and prolonged exposure to such high pH would shorten its life.

Hence, the pH of mobile phase was kept as published previously (pH = 8.1)[141]. Loss of acyl-CoA signal due to degradation during the passage through the column is corrected with use of internal standard (described in section 2.3.2). Molecule of CoA contains several ionisable groups, in basic pH of the used mobile phase phosphoryl groups of CoA moiety are protonated, their pKa values are 4.3 and 6.5[184] (these values were measured with ATP). Most frequently used organic phase in separations of acyl-CoAs is acetonitrile and methanol. Both organic mobile phases were tested and compared for sepation properties and efficiency of ESI ionisation in positive mode. These two solvents have low surface tension, weak ion solvation properties, low viscosity and low heat of evaporation – these properties promote production of gas-phase ions. Major difference between acetonitrile and methanol is that methanol is protic and acetonitrile aprotic solvent. Elution strength of acetonitrile is greater than of methanol, thus compounds elute faster in acetonitrile. Acetonitrile produces narrow peaks and column backpressure is lower than with methanol (Fig. 6). However, ionisation was improved with methanol (Fig. 7). This could be related to the fact that compounds elute later and thus are ionized with higher amount of organic solvent that promotes analyte desolvation. Increase of retention time could be also beneficial for bioanalytical assays, because matrix interferences eluting in the void volume of the column (*i.e.* not retained on the stationary phase) could be diverted towards the waste in the first minutes of the LC-MS analysis. Matrix interferences could potentially lead to incorrect measurements due to their accumulation on the inner surface of the mass spectrometer and result in increase of the noise level. Since one of the objectives of the work is to ensure sensitive quantitation, the signal intensity (sensitivity) acquired in methanol was preffered over the convenient shorter analysis of acetonitrile.

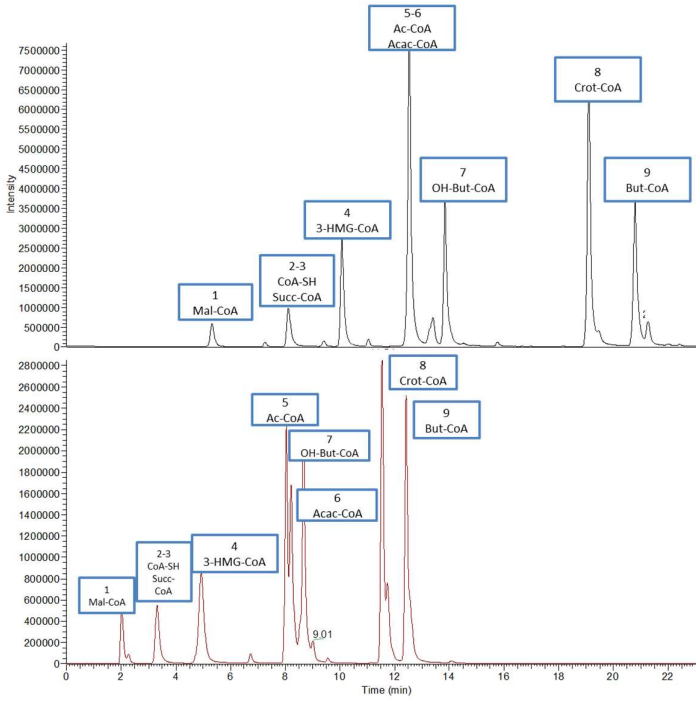

Figure 6: Acyl-CoA separation in methanol and acetonitrile

Representative chromatogram of a standard mixture of 9 commercially available short-polar acyl-CoA thioesters in 25 mM ammonium phosphate buffer (pH 3.5; 2 % methanol) at concentration c=5 µM separated and analyzed using HPLC-MS in full scan mode. Phenomenex kinetex 100×3.0 mm column used LC-MS setup parameters as described in Chapter 6. Depicted is comparison of separation in two different organic phases: top – methanol, bottom – acetonitrile.

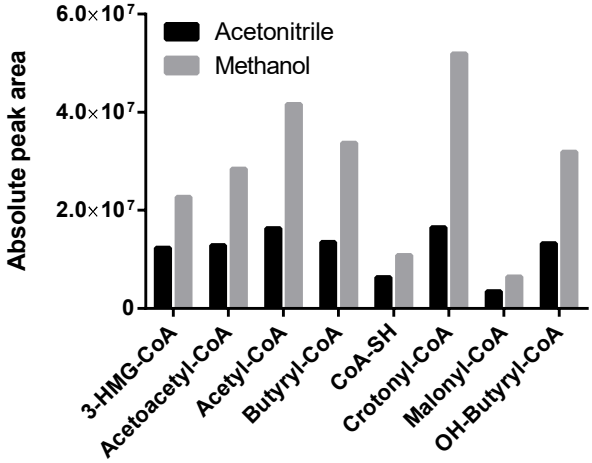

Figure 7: Absolute peak area of short-polar acyl-CoA thioesters

Comparison of absolute peak area of some of the acyl-CoA thioesters eluting in acetonitrile (black) and methanol (grey). Concentration of standards c = 10 µg/mL. Column Phenomenex kinetex 100×3.0 mm, flowrate 400 uL/min, LC-MS setup parameters as described in Chapter 6.

Main parameters considered in chromatographic separation of acyl-CoA thioesters were whether acyl-CoAs are retained on the column, length of LC-MS run and sufficient resolution of the column. Optimized gradient resulted in separation of 12 coenzymes A thioesters in 18 minutes. All the intended analytes are separated using Phenomenex Kinetex column with satisfactory repeatability of retention time (Table 3).

Table 3: Elution sequence of Acyl-CoAs

Elution of short polar Acyl-CoAs on Phenomenex Kinetex C-18 column. LC-MS setup parameters as described in Chapter 6; n=5

Metabolite	Average R_T [min]	CV R_T [%]
Malonyl-CoA	6.12	0.195%
CoA-SH	7.435	0.130%
Succinyl-CoA	7.443	0.090%
Methyl malonyl-CoA	8.085	0.180%
3-HMG-CoA	9.85	0.082%
Acetoacetyl-CoA	12.31	0.080%
Acetyl-CoA	12.37	0.084%
OH-Butyryl-CoA	13.68	0.082%
Propionyl-CoA	15.45	0.06%
Crotonyl-CoA	19.27	0.077%
Butyryl-CoA	21.06	0.075%
Methyl crotonyl-CoA	23.13	0.060%

2.2.2 MS-based Detection of Acyl-CoAs

Mass spectrometry is a detection technique widely used for metabolite identification and quantitation. The basic principle of mass spectrometric analysis is separation of charged ions based on their weight which are moving in electromagnetic field. Each ion is represented by own by mass-to-charge ratio (*m/z*). Due to structure and charge distribution in the molecule some compounds ionize better in positive or negative mode. For example amino acids are well detected in positive mode, while organic acids and phosphorylated compounds are usually detected in negative mode. Almost all neutral molecules yield ions in positive mode of ionization, while for production of negative ions presence of acidic group or electronegative element is required. This phenomenon can be exploited in selective analysis of types of compounds in biological extracts. Acyl-CoA thioesters can be analyzed in both modes (Table 2). In negative ionisaton mode acyl-CoA thioesters yield $[M-H]^-$ and $[M-2H]^{2-}$ ions [185], while positive mode yields only $[M+H]^+$ ions leading to better sensitivity. In this work, the chromatographic column was coupled to mass spectrometer LTQ-OrbiTrap operating in full-scan (750-1200 *m/z*), positive mode at resolution R = 60 000 at m/z 400 (details of ESI source parameters in Chapter 6 – Materials and Methods).

At resolution that is being used in the analytical method, minimal mass difference required for distinct differentiation of peaks is 0.006 Da. There are several acyl-CoAs which coelute (Fig. 6), such as acetyl-CoA and acetoacetyl-CoA which were partially separated only in acetonitrile. The mass difference between these two molecules is 42 *Da,* which is enough to distinguish the peaks in the mass spectrometer operating at sufficient resolution (Fig 8.). Another coeluting pair is free CoA (CoA-SH) and succinyl-CoA, both eluting at 7.4min, their mass difference is 100 *Da*. Isobaric compounds of succinyl-CoA and methylmalonyl-CoA (m/z = 867.13125) are baseline separated by approximately 30seconds.

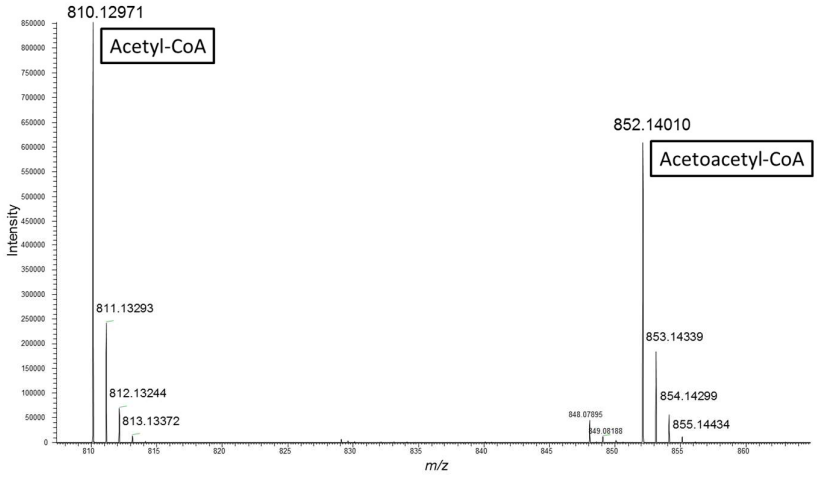

Figure 8: MS spectrum of coeluting compounds

Mass spectrum of coeluting compounds – acetyl-CoA and acetoacetyl-CoA. MS spectra obtained by LTQ-OrbiTrap operating in full scan mode at R=60 000 (m/z =400) in positive polarity. An increment 1.00336 m/z corresponds to exact mass of ^{13}C atom occuring naturally at 1.07% in isotopologues of these two acyl-CoAs annotated as M1, M2 and M3 (i.e. 1 up to 3 ^{13}C atoms detectable). Two compounds eluting in one peak from separation column are unambigously distinguished in mass spectrum.

2.3 Validation of Analytical method

This method was intended for quantification of short polar acyl-CoA thioesters with use of isotopically enriched extract. The selection of acyl-CoA thioesters for validation was based on the proposed pathway of beginning of sterol and fatty acid biosynthesis in mitochondria of *T. brucei* (Fig. 5). Process of validation is a proof that method yields analytical results within acceptable level of uncertainity. Any changes to components of analytical method require re-validation. Before starting any validation study, its scope and expected (or minimal) criteria should be defined. Extend of validation depend on the choice of performance; method can be fully or partially validated.

2.3.1 Parameters of Analytical Method

Method performance was evaluated based on following parameters: intraday precision (repeatability), interday precision (reproducibility), and accuracy. In practise, mixtures of short-polar acyl-CoA standards were injected several times at increasing concentration level. Standard mixtures were prepared by two different operators and injected in separate days. The method was considered to be acceptable if coefficient of variance (CV) of each concentration level in individual series was ≤ 10% for intraday and ≤ 20% for interday variability. This parameter describes the *precision* of the method. Method was acceptable, if measured value of concentration within two tested series of standards does not exceed ±15% from theoretical (*accurate)* value. This parameter described *bias* of the method. Furthermore, correlation coefficient of the calibration curves of individual compounds should be 0.99 at least. If any compound at any concentration level tested exceeded set limits in one or more parameters, this calibration point had to be excluded from validation.

2.3.2 Isotope Dilution Mass Spectrometry (IDMS)

2.3.2.1 Principle

Even with separation of analytes prior to detection in all hyphenated analytical techniques, biological extract may contain compounds of the same mass and similar retention time which can lead to misinterpretation of the data. Moreover, ESI ionization efficiency decreases for extracts containing salts (*i.e*. in samples collected as whole broth), causing reduction or even loss of analyte signal. Moreover, ionization in the ion source and detector response is not the same for all compounds, even structurally analogous. For these reasons, internal standards (IS) are required. Internal standard is a compound of very similar qualities as targeted analyte, *i.e.* a stable isotope labeled analogue of the metabolite of interest. This method is called isotope dilution mass spectrometry (IDMS) (Fig. 9).

Stable isotope enriched IS can be prepared either by chemical synthesis, which yields individual compounds; and for quantification of numerous metabolites participating in one or more pathways this procedure can become costly. Alternatively, internal standard can be prepared by cultivating cells with labeled substrate such as [U-^{13}C]-D-glucose for sufficient amount of time. During cultivation, cells incorporate ^{13}C from substrate into all relevant intermediates of metabolic pathways (Fig 9, section A). Internal standard is prepared by appropriate quenching and extraction of metabolites from the culture. Extract containing fully isotopically labeled metabolites should be first characterized in order to determine its quality and percentage of ^{12}C in analytes which can originate from incorporation of atmospheric CO_2 or residual carbon sources present in the cultivation broth. Characterization of internal standard is advised in order not to contaminate true biological samples

with non-labeled analytes of IS. Furthermore, approximate quantitation of ^{13}C-labeled analytes is useful for dosing, since ratio between ^{13}C:^{12}C should be approximately 1:1.

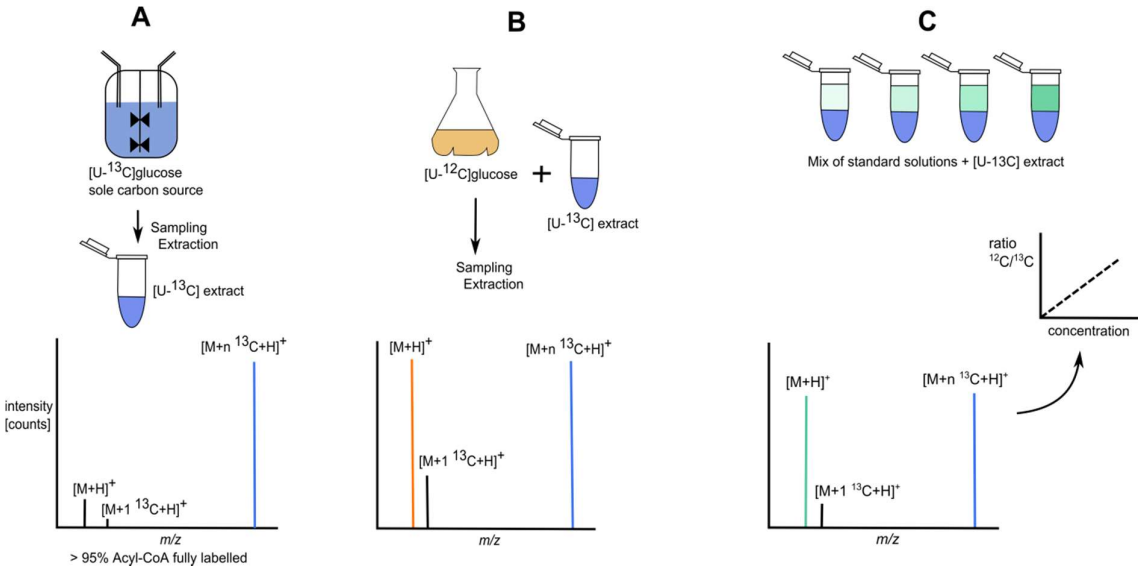

Figure 9: Principle of IDMS-based quantitation of metabolites

(A) Preparation of labeled internal standard by feeding cells with labeled substrate as sole carbon source. Followed by extraction of metabolites and characterization of quality of IS in order to determine percentage of non-labeled fraction. (B) Addition of internal standard to sample prior to extraction and analysis. (C) For quantitation purposes, stable isotope extract (blue) with constant fraction is spiked with non-labeled standards (green) with increasing concentration. Ratio of intensities of non-labeled and labeled analyte are plotted against known concentration in order to obtain linear regression. Ratio from biological extract is extrapolated onto individual regression curves.

Internal standard is applied during sample preparation since partial degradation of metabolites may occur during quenching, extraction, storage or other sample handling or any analytical bias towards targeted molecules during analysis (Fig. 9, section B). Degradation impacts all isotopologues equally, so ratio $^{12}C/^{13}C$ does not change. Moreover, multiple extractions in order to yield 100% recovery are not necessary with use of IS.

Quantitation of metabolites is accomplished by preparation of mix of non-labeled standards with increasing concentration and ^{13}C enriched internal standard in same ratio as used with biological samples (Fig.9 section C). Non-labeled and ^{13}C-labeled molecules are distinguished by a mass analyser operating with sufficient resolutive power. Analyte of interest elutes from chromatographic column at the same retention time as its stable isotope labeled analogue. Analysis of this standard calibration curve yields regression equations for each metabolite. Last step is analysis of biological extracts with added internal standard and extrapolation of $^{12}C/^{13}C$ ratio onto individual regression curves [162]. This strategy has been used in numerous quantitative studies – in *E. coli* [186,187] but also eukaryotic

organisms such as *S.cerevisiae* [188] or *Pencicillium chrysogenum* [189]. Applying IDMS improves quality of calibration lines, linear range of calibration and yields more reliable quantitative results.

2.3.3 Applied Procedure

In this study, the quantitation was performed with use of steady isotope enriched standards originating from *Methylobacterium extorquens* (Table 4). This facultative methylotroph with unusual carbon metabolism can utilize numerous carbon sources (acetate, succinate, ethanol, pyruvate). It also assimilates C1 from methanol in network of metabolic cyles involving serine cycle and TCA cycle together with ethymalonyl pathway which consists of numerous acyl-CoA thioesters[141]. This organism was chosen for the spectrum of produced acyl-CoAs. Some authors use yeast *Pichia pastoris* for production of ^{13}C labeled internal standard[176], however this organism only yields 4 Acyl-CoAs what seemed insufficient for use in *T. brucei*, where acyl-CoA metabolism has not yet been described.

Later, due to additional interest of acyl-CoA profile in *E. coli* additional compounds were added to validation – CoA-SH, succinyl-CoA, propionyl-CoA and methylmalonyl-CoA. Their quantitation was based on isotopically enriched extracts of *E. coli*. Preparation of *E. coli* IDMS is detailed in Chapter 6.

Table 4: Targeted metabolites

Summary of targeted analytes, exact mass of non-labeled molecule, exact mass of fully labeled molecule. IS source – source of internal standard, fully isotopically enriched extract.

Metabolite	Ion $[M+H]^+$	Ion $[M+H]^+$ U-^{13}C	IS compound for quantitation	IS source
3-HMG-CoA	912.16474	939.25532	U $^{13}C_{23}$ Acetyl-CoA	*M. extorquens*
Acetyl-CoA	810.13305	833.21020	U $^{13}C_{23}$ Acetyl-CoA	*M. extorquens*
Acetoacetyl-CoA	852.14361	877.22748	U $^{13}C_{23}$ Acetyl-CoA	*M. extorquens*
Butyryl-CoA	838.16434	863.24821	U $^{13}C_{25}$ Butyryl-CoA	*M. extorquens*
CoA-SH	768.12248	789.19293	U $^{13}C_{21}$ CoA-SH	*E. coli*
Crotonyl-CoA	836.14870	861.23256	U $^{13}C_{25}$ Butyryl-CoA	*M. extorquens*
Malonyl-CoA	854.12287	878.20339	U $^{13}C_{25}$ Malonyl-CoA	*M. extorquens*
Methylmalonyl-CoA	868.13852	893.22239	U $^{13}C_{25}$ Succinyl-CoA	*E. coli*
OH-butyryl-CoA	854.15926	879.24313	U $^{13}C_{25}$ OH-butyryl-CoA	*M. extorquens*
Propionyl-CoA	824.14869	848.22921	U $^{13}C_{24}$ Propionyl-CoA	*E. coli*
Succinyl-CoA	868.13852	893.22239	U $^{13}C_{25}$ Succinyl-CoA	*E. coli*

2.4 Results of Method Validation

The process of characterisation started with preparation of calibrant solutions by weighting powdered acyl-CoA salts. These were dissolved in 25 mM ammoniumn formate (pH = 3.5, 2% methanol)[141] stock solutions of 100 µg/mL were stored at -80°C. All dilutions were made from frozen stock solutions stored at -80°C with one freeze thaw cycle. Altogether, 7 concentration levels were prepared by mixing 50 µL ^{13}C stable isotope labeled extract of *M. extoruens* and 150 µL of standard solution with increasing concentration of acyl-CoA standards, as depicted in Fig 9 (section C).

Calibrant solutions at concentrations 0.05; 0.1; 0.25; 0.5; 1; 2.5; and 5 µM were freshly prepared by 2 operators to account for difference in manual preparation. 5 µL of the mixture of standards has been analyzed by HPLC-HRMS, and each level of calibrant solutions was injected 5 times starting from lowest concentration. Peak areas with mass accuracy of 5 ppm were extracted from ion chromatogram and integrated. Observed retention time for uniformly enriched compounds and non-labeled acyl-CoAs did not differ by more than 1%. In this particular method characterization, repeatability represents measurement of sample in one day (concentration 0.05 - 5µM). Variability of sample measurement between series 1 and 2 and operators is expressed as intermediate precision (reproducibility).

2.4.1 Carry Over

Carry over is concern in all cases where analytes adhere to needle surface and cause transfer of analyte from one sample another. Carry over is indication of cross-contamination between samples due to insufficient wash of needle and system fluidics that could lead to incorrect conclusions. It is specific to injection system that is implemented in particular chomatographic chain. In this work Dionex UltiMate U3000 chromatographic chain was used, it is equipped with an active external washing system. In our conditions, injection needle is washed with 3 mL 50% Methanol from external source. Carryover was calculated from peak area found in reagent blank (25 mM Ammonium formate, pH= 3.5, 2% Methanol) which was analyzed after the highest concentration (c = 5µg/mL) of mixture of standard acyl-CoAs. Minor carryover up to 0.35% was observed for almost all measured compounds (Table 5). Similar level of carryover into reagent blank samples (less than 1%) was observed also for fatty acyl-CoAs [190]. Method performance was not affected significantly by cross contamination.

Table 5: Calculated carry-over

Calculated carryover, estimation of cross-contamination between samples. n/a – value not available as compound was detected only in one repetition, n/d – not detected.

Acyl-CoA	Carryover [%]
3-HMG-CoA	0.13
Acetoacetyl-CoA	0.27
Acetyl-CoA	0.28
Butyryl-CoA	0.34
CoA-SH	*n/d*
Crotonyl-CoA	0.35
OH-Butyryl-CoA	0.21
Malonyl-CoA	*n/d*
Methylmalonyl-CoA	*n/d*
Propionyl-CoA	0.04
Succinyl-CoA	*n/d*

2.4.2 Mass Accuracy

Mass accuracy is the difference between known calculated monoisotopic mass *m/z* and measured *m/z* (Eq. 1). It is routinely expressed as relative measure *parts per million (ppm)*. This mass deviation from theoretical mass depends on the performance of mass spectrometer. Mass accuracy is closely linked to the resolution. Since resolution is function of mass, mass accuracy is improved with higher resolution, at the expense of reduced signal intensity (because less scans are performed)[191]. Increase in resolution (*i.e.* in OrbiTrap 10 000 – 30 000 – 60 000 or 100 000) does not change the relative intensity of peaks but requires longer acquisition time for one scan.

$$\Delta\, \boldsymbol{m/z} = \frac{(\boldsymbol{m/z\ accurate - m/z\ exact})}{\boldsymbol{m/z\ exact}} \times \mathbf{10^6}, \text{ unit } \textit{parts per million} \text{ (ppm)} \qquad \textbf{Equation 1}$$

Accuracy of mass measurement directly impacts quality of data which is reflected in peak areas. The MS spectras are data-mined based on exact mass (Extracted Ion Chromatogram, *EIC*). Mass measurement accuracy less than 3ppm during analyses performed for method characterization with OrbiTrap mass analyser is readily acquired for various types of analytes [192,193]. In presented analyses it signifies high level of condifence between theoretical (exact) and measured (accurate) mass of acyl-CoA thioesters (Fig 10).

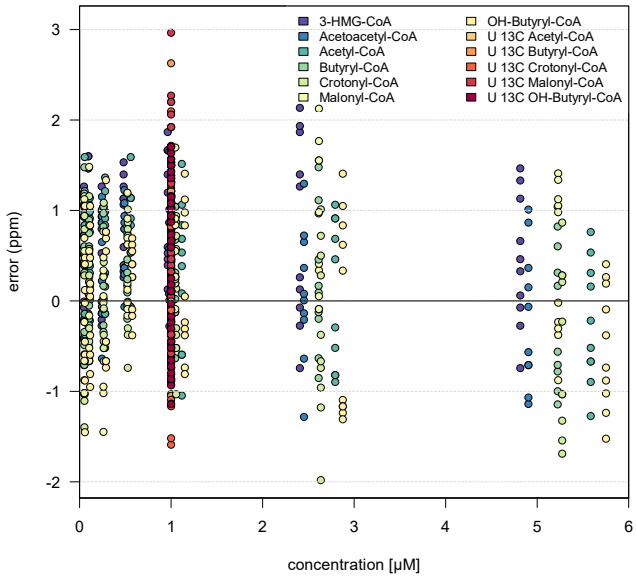

Figure 10: Mass accuracy of MS detection

Mass accuracy of Acyl-CoA thioesters originating from standards and isotopically enriched extract of Methylobacterium extorquens used as internal standard. Measured with LTQ-Orbitrap at R = 60 000 (m/z 400). Plotted as function of mass error (ppm) to concentration (µM). Isotopically enriched standard was given arbitrary concentration of 1. Plotted set of Acyl-CoA concentrations used for construction of calibration curves as described in Table 2.6 and 2.7. Mass error in ppm was calculated by Eq.1.

2.4.3 Repeatability and Reproducibility

Concentration calculated via regression parameters of both calibration curves has been submitted to comparisons of coefficient of variance (CV, %) calculated at every concentration level within each one of the series and between the two. Intraday precision is depicted on Fig. 11. The highest deviations are found in the lowest concentration level (c7, 0.05 µM) for most of the compounds, what highlights different preparation of calibrant solutions between operators, as lowest concentration is the most sensitive towards mistakes, *i.e.* pipetting. In cases, when CV exceeded value of 10% the particular concentration level would be removed from validation as it exceeds predefined acceptance criteria.

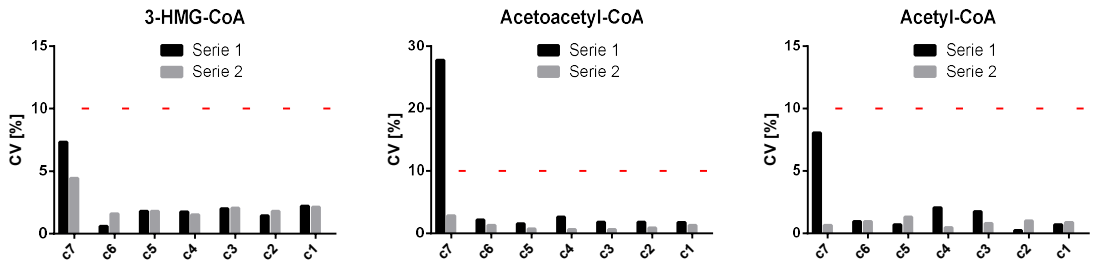

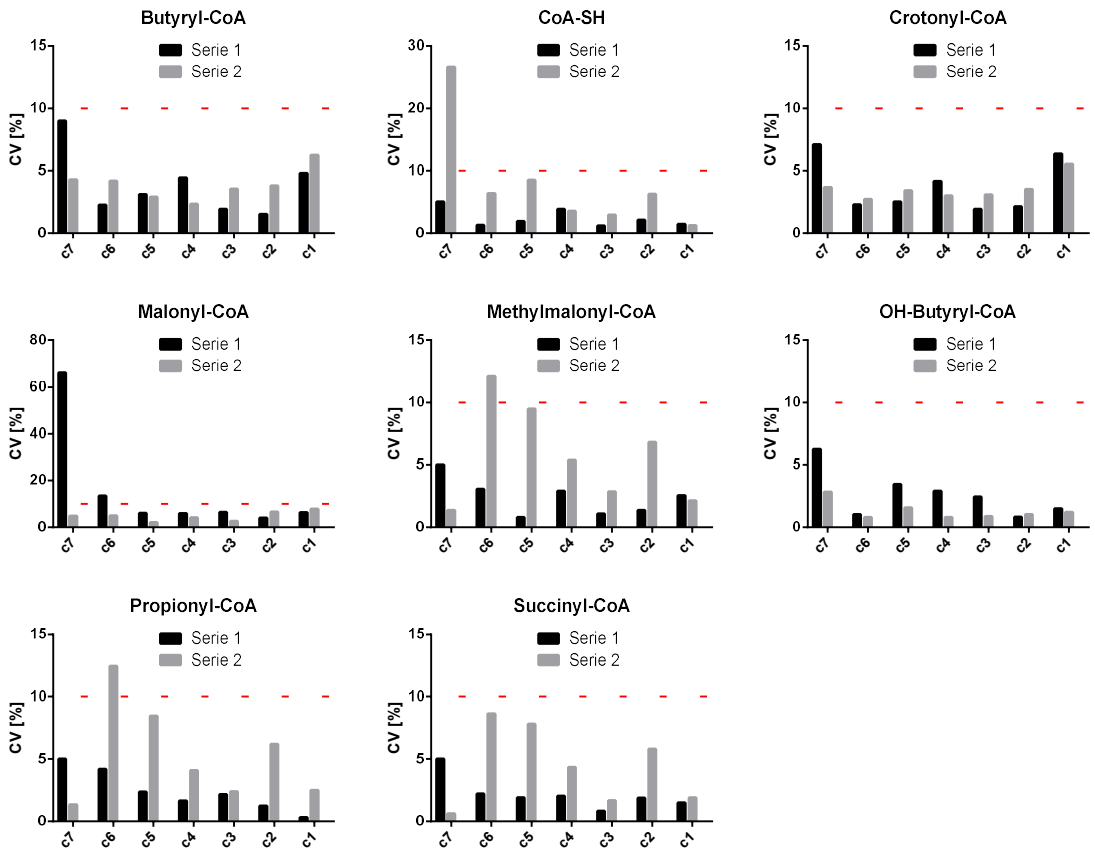

Figure 11: Precision - repeatability of measurement

Cofficients of variation (CV, %) acquired by repetitive injection of mix of acyl-CoA standard. Two series were measured in different days and prepared by different operator. Red dashed line represents 10% cutoff for acceptability of result dispersion.

Due to scope of this study, where inter laboratory tests were not performed, reproducibility encompasses only difference of individual analyst and day of measurement (Table 22, Annex). Similar rules apply to differences between the two series, *i.e.* CV different by more than 20%; the particular concentration level would not be included in the final validation. The main reason to test reproducibility is to verify, that analytical method yields the same reuslts in different laboratories or different operators. As observed in Fig 11 (repeatability, interday precision) the highest differences of CV (%) are related to lowest concentration values.

2.4.4 Calibration Curves and Linearity

Calibration curve represents relation between known concentrations and experimental response values which are represented by ratio of non-labeled standards and isotopically enriched internal standard (Fig 12). Ratio $^{12}C/^{13}C$ was plotted onto y axis and theoretical concentration onto x axis. Both series differ the most in highest concentration values. This can be attibuted to overcrowded ion source

and beginning of parabolic signal response for particular acyl-CoA. Highest concentration level (5 µM) had to be excluded from some calibration curves, thus effectively reducing linear range for quantificaiton in order to obtain correlation coefficient ≥0.99.

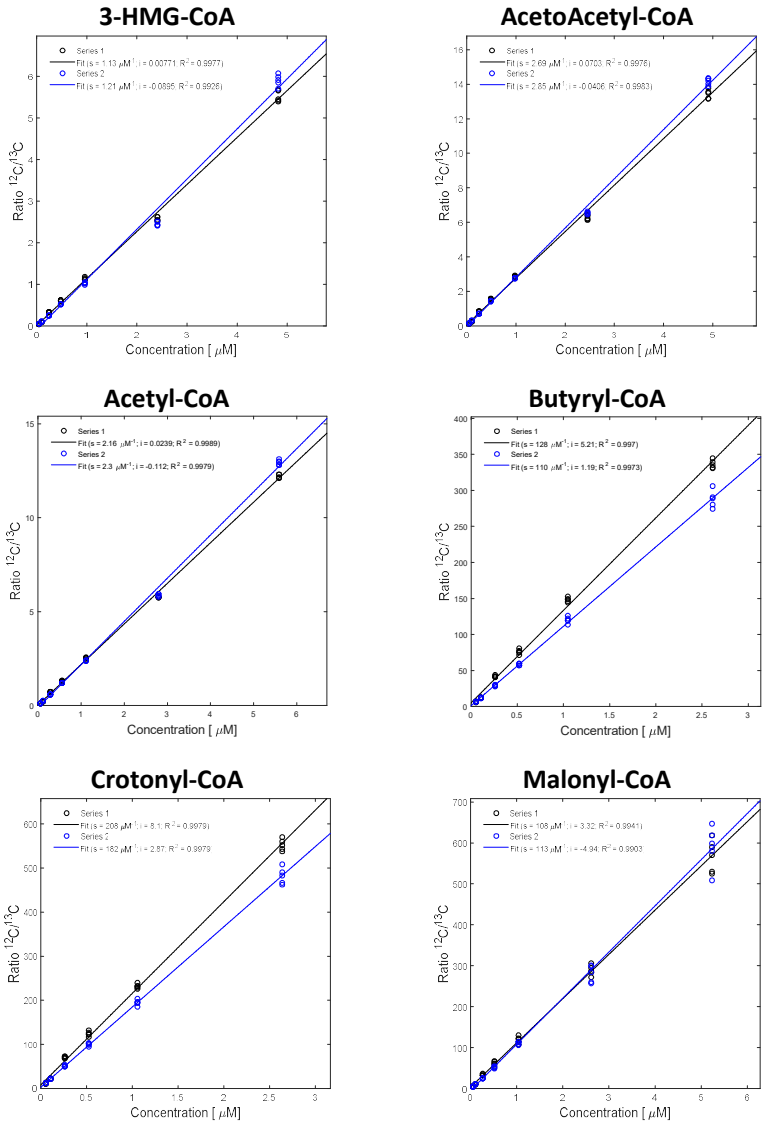

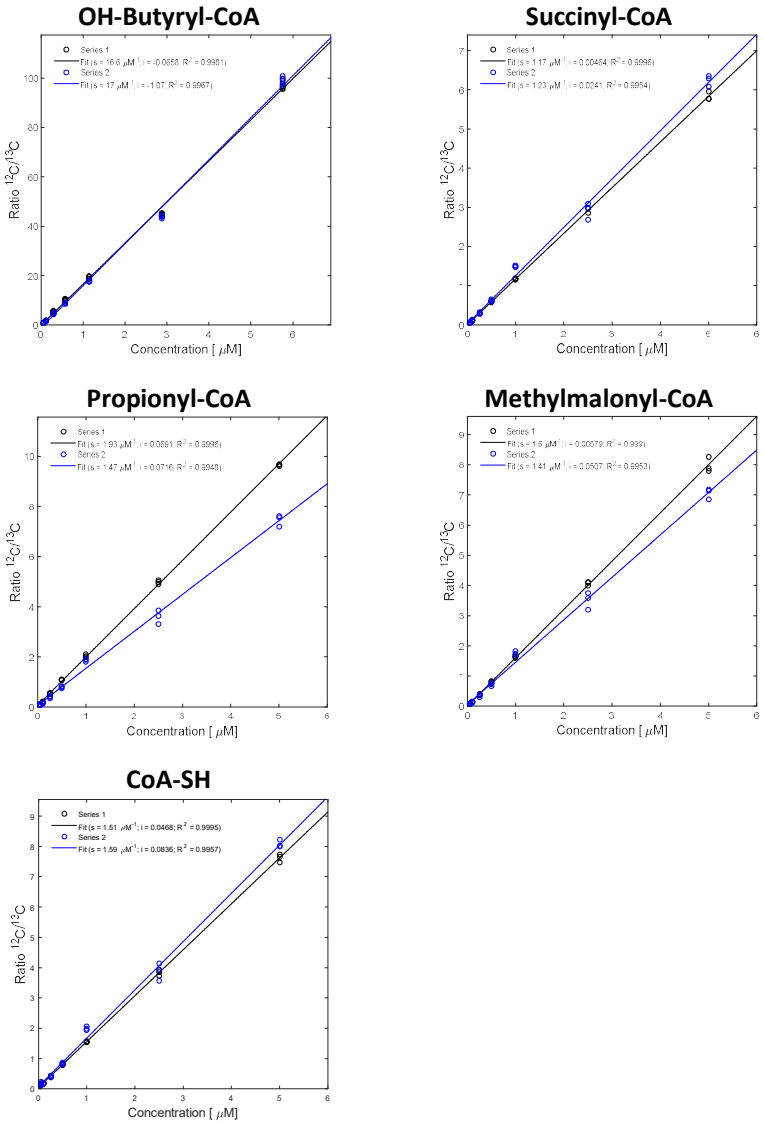

Figure 12 : Comparison of calibration curves for quantitation based on IDMS for chosen acyl-CoAs

Calibration curve graphs plotting ratio $^{12}C/^{13}C$ as function of concentration [µM]. Measured in two series of analyses (Serie1 - black, Serie2 - blue); s, slope; i, intercept

2.4.5 Accuracy

Bias of concentration is calculated as the difference between theoretical concentration and mean of measured concentrations of both series (Fig. 13).

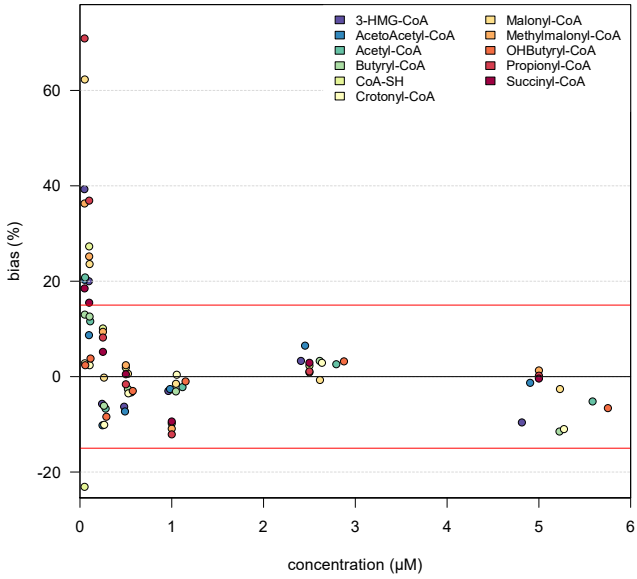

Figure 13 : Accuracy - bias of concentration

Acceptable difference between calculated mean of two series and theoretical concentration was ±15% (red line).

Dispersion of results at the lowest concentration (around 0.05 µM) can be explained by the fact, that these values are below LOQ of the analytical method, thus the difference between signal and noise is insignificant. Dispersion of the highest concentrations can be attributed to overcrowded ion source and higher impact of high concentration points on the slope of the calibration curve.

2.4.6 Limits of Detection and Quantitation

Limits of detection (LOD) and limit of quantitation (LOQ) were calculated from regression curve parameters. LOD was defined as signal to noise ratio 3:1 and LOQ was defined as signal to noise ratio 10:1 (Eq. 2 and 3, respectively)

$$LOD = \frac{3 \times SD_{intercept}}{slope}$$ **Equation 2**

$$LOQ = \frac{10 \times SD_{intercept}}{slope}$$ **Equation 3**

The lower limit of quantitation was determined as the lowest concentration of calibration curve that met all the predefined criteria. Upper limit of quantitation was defined as the highest concentration of the calibration curve meeting the same criteria, *i.e.* without necessity of being removed in order to attain acceptable correlation coefficient. The detection limit of all short polar acyl-CoA thioesters

was in low picomolar range per injection (Table 6, Fig. 14). Analytical method was validated within range of criteria for all targeted acyl-CoAs.

Table 6: Linear range of targeted acyl-CoAs

Coefficient of determination (R^2) from constructed regression lines of Serie 1 and 2. LLOQ, lower limit of quantitation; ULOQ, upper limit of quantitation.

CoA Name	R^2 mean	R^2 SD	LLOQ [µM]	ULOQ [µM]	LOD±SD [µM]	LOQ±SD [µM]
3-HMG-CoA	0.99840	0.00067	0.241	4.815	0.035± 0.017	0.117± 0.055
Acetoacetyl-CoA	0.99780	0.00037	0.245	4.904	0.061± 0.005	0.202± 0.017
Acetyl-CoA	0.99933	0.00047	0.112	5.585	0.026± 0.016	0.087± 0.054
Butyryl-CoA	0.99612	0.00120	0.052	2.612	0.067± 0.032	0.222± 0.107
CoA-SH	0.99763	0.00188	0.050	5.000	0.065± 0.032	0.216± 0.006
Crotonyl-CoA	0.99523	0.00269	0.053	2.636	0.076± 0.045	0.252± 0.15
Malonyl-CoA	0.99505	0.00157	0.261	5.229	0.066± 0.046	0.219± 0.154
Methylmalonyl-CoA	0.99713	0.00184	0.250	2.500	0.102± 0.027	0.249± 0.146
OH-Butyryl-CoA	0.99893	0.00088	0.058	2.876	0.034± 0.023	0.113± 0.078
Propionyl-CoA	0.99721	0.00238	0.250	5.000	0.069± 0.039	0.228± 0.128
Succinyl-CoA	0.99749	0.00209	0.250	5.000	0.066± 0.035	0.219± 0.118

HPLC-HRMS method for purpose of quantitation of short- polar acyl-CoAs has met all the predefined criteria of acceptance. The sensitivity of the method is within the range published by other authors (Fig. 14).

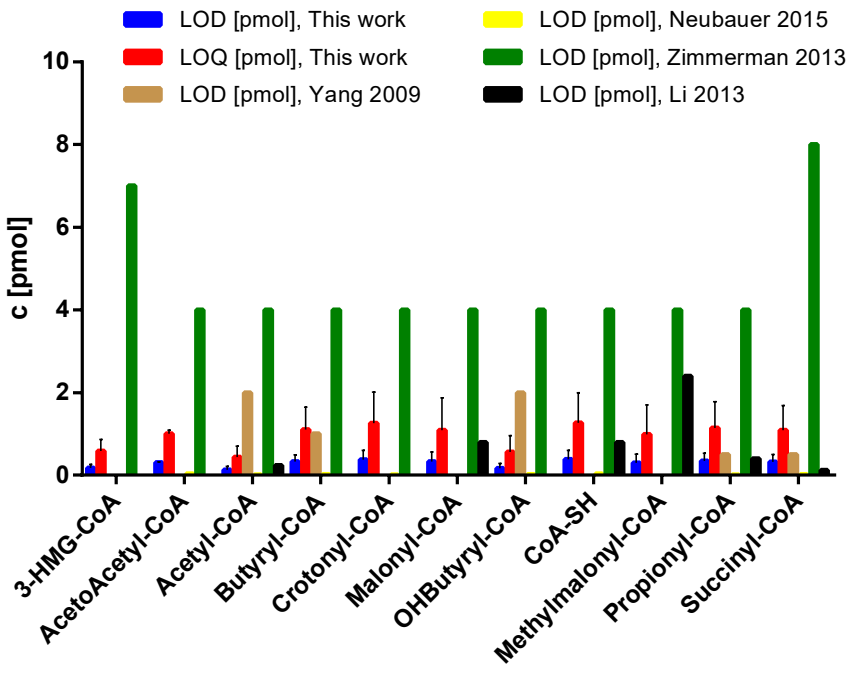

Figure 14 : Comparison of LOD, LOQ of this work with available literature

Non – exhaustive list of LOD values obtained by HPLC-MS (MS) analytical methods.

2.5 Extracting Acyl-CoA thioesters

The next goal was to determine, whether the analytical method is capable of detecting short polar chain acyl-CoA thioesters in *E. coli* K-12 MG1655. This prokaryote is used as model system for fundamental studies in biochemistry and molecular biology as it is easy to manipulate genetically and fast to grow. Sampling and extraction protocol is described in Chapter 6 (Materials and Methods).

2.5.1 Acyl-CoA Extraction in E. coli

Metholodogy for short acyl-CoA extraction relies mostly on acidified polar solvents (Table 2.) and due to degradation of thioester bond in neutral pH, the acidic conditions should be maintained throughout whole sample processing. For initial test of extraction solvent, *E. coli* growing on minimal synthetic media (M9) supplemented with glucose as only carbon source was used. Acyl-CoA thioesters are compounds known to be thermally unstable; therefore, extraction protocols involving boiling or hot solvents were dismissed. Furthermore, compounds are sensitive towards basic pH. Acyl-CoA thioesters were extracted following a modified protocol by Peyraud *et al*., [141]. Fast filtration was initially chosen for tests, because *T. brucei* cells were intended to be collected in the same manner. Extraction protocols yielded very similar results (Fig 15).

These extractions were performed at the same time as extractions of acyl-CoAs from *T. brucei*, where 125 mM formic acid in 80% methanol resulted in highest yield of acyl-CoAs (Fig. 34, Chapter 4), thus this extraction solution was used in further experiments. Extraction solutions were tested only for cells produced by fast filtration, in order to achieve appropriate evaluation of extraction protocol more rigorous examination of all sample fractions (whole broth, supernatant) needs to be acquired.

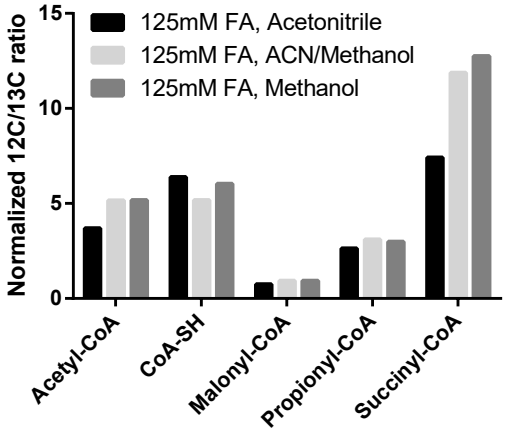

Figure 15: Comparison of extraction solutions applied to E. coli, prepared by fast filtration.

125 mM FA, acetonitrile: 125 mM formic acid dissolved in 80% aq. acetonitrile (20% water)

125 mM FA, methanol: 125 mM formic acid dissolved in 80% aq. methanol (20% water)

125 mM FA, acetonitrile, methanol: 125 mM formic acid dissolved in 40:40:20 acetonitrile: methanol: water

2.5.2 Acyl-CoA Profile in E. coli

Quantification of acyl-CoA thioesters in *E. coli* was accomplished by differential method developed by Taymaz-Nikerel[187] and extraction with acidified methanol. Protocol is described in detail in Chapter 6 (Materials and Methods).

E. coli growing on glucose as sole carbon substrate is not very rich source of different acyl-CoA species, unlike the more exotic *M.extorquens*. The most prominent is acetyl-CoA which is the main metabolic intermediate of pyruvate degradation, connecting glycolysis and TCA cycle. Apart from that, acetyl-CoA is also produced by β-oxidation of long and medium chain fatty acids and it can serve as substrate for de novo fatty acid biosynthesis. Second most abundand acyl-CoA thioester is succinyl-CoA, which takes part in TCA cycle, metabolic process of major importance in aerobically growing organisms. Free CoA is a known metabolic cofactor and carrier or acyl moieties in fatty acid biosynthesis where also malonyl-CoA is involved. Malonyl-CoA is formed by carboxylation of acetyl-CoA in the first step of fatty acid biosynthesis. Propionyl-CoA is known to be intermediary metabolite in degradation of branched amino acids and odd-chain fatty acids. Acyl-Coenzyme A thioesters are principially intracellular compounds, and due to charged phosphate groups present in CoA moiety the compounds cannot diffuse through the phospholipid bilayer freely. Unless their presence in the extracellular media is related to unspecific lysis of cells.

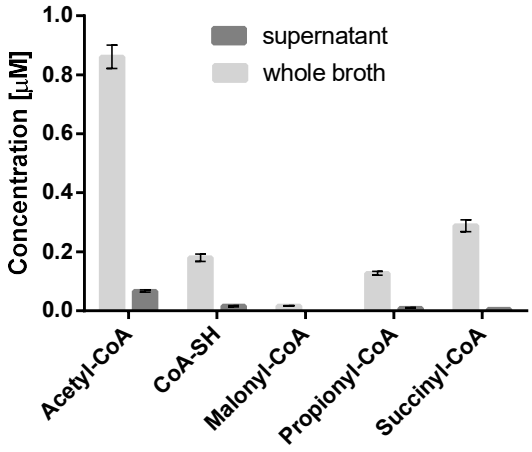

Figure 16: Acyl-CoA thioesters found in whole broth and supernatant, n=3

Differential method developed by Taymaz-Nikerel et al.[187], combined with acyl-CoA extraction was applied to E. coli K-12 MG1655 grown in minimal media on glucose as sole carbon source. Three species of acyl-CoA (dark grey) were quantified in supernatant. Their presence outside the cells might be explained by cell lysis during the cultivation because acyl-CoA is due to its charged nature membrane impermeable molecule.

Table 7: Calculated intracellular concentration of acyl-CoAs in *E. coli*

E. coli K-12 MG1655 strain grown in minimal media on glucose as sole carbon source. Intracellular concentration corrected for acyl-CoA amount found in supernatant.

Compound	Intracellular c [mM]	SD [mM]
Acetyl-CoA	0.940	0.044
CoA-SH	0.194	0.012
Malonyl-CoA	0.021	0.001
Succinyl-CoA	0.334	0.023
Propionyl-CoA	0.139	0.008

Absolute intracellular concentration has been compared to study performed in the same conditions – Bennet *et al*., used *E. coli* K-12 MG1655 grown anaerobically on glucose[186] sampled in exponential phase. As reported previously, the predominant thioester in *E. col*i growing on glucose is acetyl-CoA[117]. Acetyl-CoA pool is depleted rapidly if bacterial culture enters stationary phase and exhausts glucose. Furthermore, temperature affects pools of acetyl-CoA and malonyl-CoA, since fatty acids composition changes with temperature. Therefore, during sampling temperature fluctuation of culture broth in shake flask should be minimized[194]. Observed range of polar acyl-CoAs was found to be the most abundant coenzyme in extracts, unlike the free CoA observed by Bennet (Fig. 17). This discrepancy may be due to used quenching and extraction solution, Bennet used 2.5 mL of extraction solution 40:40:20 acetonitrile: methanol: water supplemented with 0.1 M formic acid cooled to -20°C. Moreover, cells were sampled in a different manner – whole broth (corrected for supernatant amount) in this work, versus fast filtration which is prone to metabolite alternation during stay on the filter surface until quenching of the enzymatic activity.

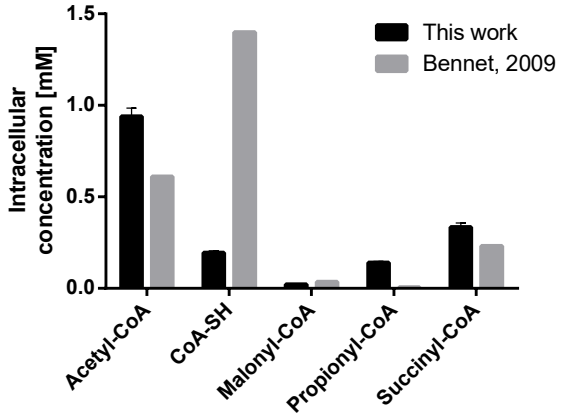

Figure 17: Comparison of intracellular concentration of acyl-CoAs with lit.

Intracellular acyl-CoA thioester composition was found qualitatively very similar to presented work with exception of propionyl-CoA which was not detected by Bennet[186]. Furthermore, the most obvious difference is ratio of acetyl-CoA/CoA-SH which opposite. This is most likely resulting from hydrolysis of thioester bond.

2.6 Analysis of Acyl-CoA Isotopic Profile

One of the objectives of the thesis was to refine the topology of metabolic network of acyl-CoA thioesters in *T. brucei*. This goal could be accomplished by tracing the incorporation of a chosen isotope, such as ^{13}C into the flexible acyl moiety of acyl-CoA thioesters. Isotopes of a compound might not have exactly the same analytical behaviour; therefore, evaluation of analytical performance for isotopic profile is required.

2.6.1 Isotopic Profile

Isotopic profile of a molecule is a sum of all isotopic species (isotopologues, isotopomers) which differ by number or position of isotopic atom. If stable isotope is supplemented within a substrate in the culture broth it is specifically incorporated into metabolic intermediates where it leaves an imprint based of involved biochemical reactions. Observation of the labeling pattern is a valuable tool used to describe metabolic network, this strategy can lead to identification of metabolites [195] or unravelling novel pathways[141] and clarification of the actual extend of for example glucose metabolism contribution to anabolic pathways[196]. Moreover, isotopic profile can be used for resolving the elementary composition and chemical structure. The term *labeling pattern (= isotopic pattern)* refers to mass isotopomers/isotopologue distribution (MID) which is a result of incorporation of any isotope into metabolic intermediates. In this work, only ^{13}C atoms were traced, therefore Carbon Isotopologue Distribution (CID) is used instead of MID. In principle, mass spectrometric detection does not differentiate the position(s) of the ^{13}C atom(s) as it only records difference in weight of the molecule (*m/z).* Mass isotopologue fractions observed in MS spectra are annotated M0, M1, M2 *etc*. what corresponds to a molecule containing 0, 1, 2 or more ^{13}C atoms. All isotopologues of a molecule are forming an *isotope cluster* with increments of *m/z* = 1.0033548Da, what corresponds to mass difference between ^{13}C and ^{12}C (Fig 18). In order to interpret labeling patterns correctly, it is important to correct for natural abundance of stable isotopes, *i.e.* ^{13}C (1.07%), ^{15}N (0.368%), etc. Otherwise, carbon isotopologue distribution would modify the metabolite enrichment pattern, which in turn would negatively impact the precision of metabolic flux calculation and result in biased interpretation of experimental data.

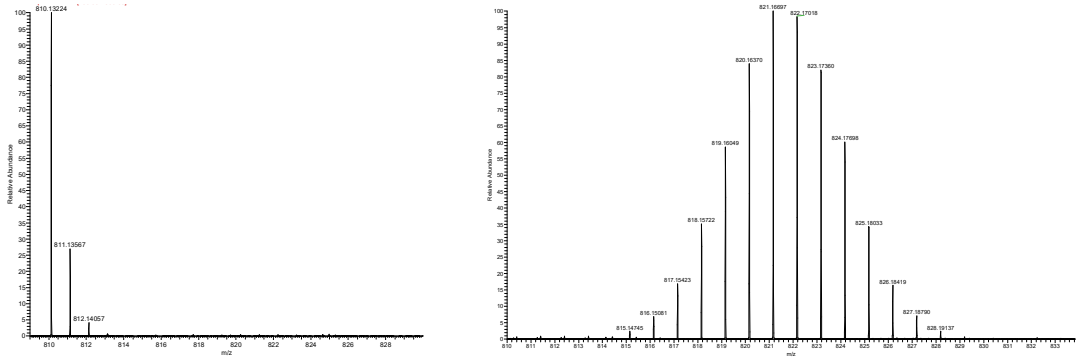

Figure 18: ^{13}C natural versus enriched amount in acyl-CoA molecule

Natural ^{13}C abundance in the molecule of acetyl-CoA (left) and isotopic profile of acetyl-CoA, binomic distribution (right). Comparison of isotopic profile of acetyl-CoA with only naturally abundant ^{13}C present versus extract of E. coli grown with defined mixture of ^{13}C-acetate[197] where the stable isotope tracer is incorporated into the molecule in a defined manner.

Due to different weight of isotopes, their analytical properties can differ. The *isotopic effect* was observed in numerous applications – it can be detected as a shift of protein binding to a molecule with ^{1}H and ^{2}H isotopes[198], altered growth rate and metabolite alternations of culture of ^{14}N and ^{15}N-labeled *E. coli*[199] and retention time shifts of ^{15}N labeled proteins[200]. Two types of impact could be derived from isotopes - biological, as enzymes are subjected to kinetic isotope effects that alter their reaction rates (KIE)[201] and analytical when isotope effect may occur at any part of the analytical process. Therefore, prior to drawing conclusions on topology of the network, it is important to acquire reliable isotopic information on all isotopologues. Errors of CID are originating from numerous sources – such as integration algorithm, concentration of the sample and mass accuracy which permits to distinguish overlapping peaks, as these are source of significant errors[202]. Standards for such comprehensive evaluation are not commercially available. To evaluate performance of the analytical method, extract of *E. coli* grown on defined mixture of acetate isotopologues was used to produce isotopic standards with controlled (predefined) fraction of isotopologues based on their distribution in metabolic network[197]. Such standard was used to test the fitness of the analytical method for accurate detection of each isotopologue by matching the measured CID and predicted CID (Fig. 19). The closest match to predicted CID was observed for isotopologues in the middle of the labeling pattern. Some of the experimental CID found in acyl-CoA thioesters did not match the predicted CID in malonyl-CoA. This compound is the first to elute, and its signal intensity is the lowest out of all acyl-CoAs analysed. Thus, isotopologues on the sides – the heaviest and the lightest are not detected due to lack of signal intensity. Isotopic cluster of butyryl-CoA was found to be coeluting with isotopic cluster of another molecule.

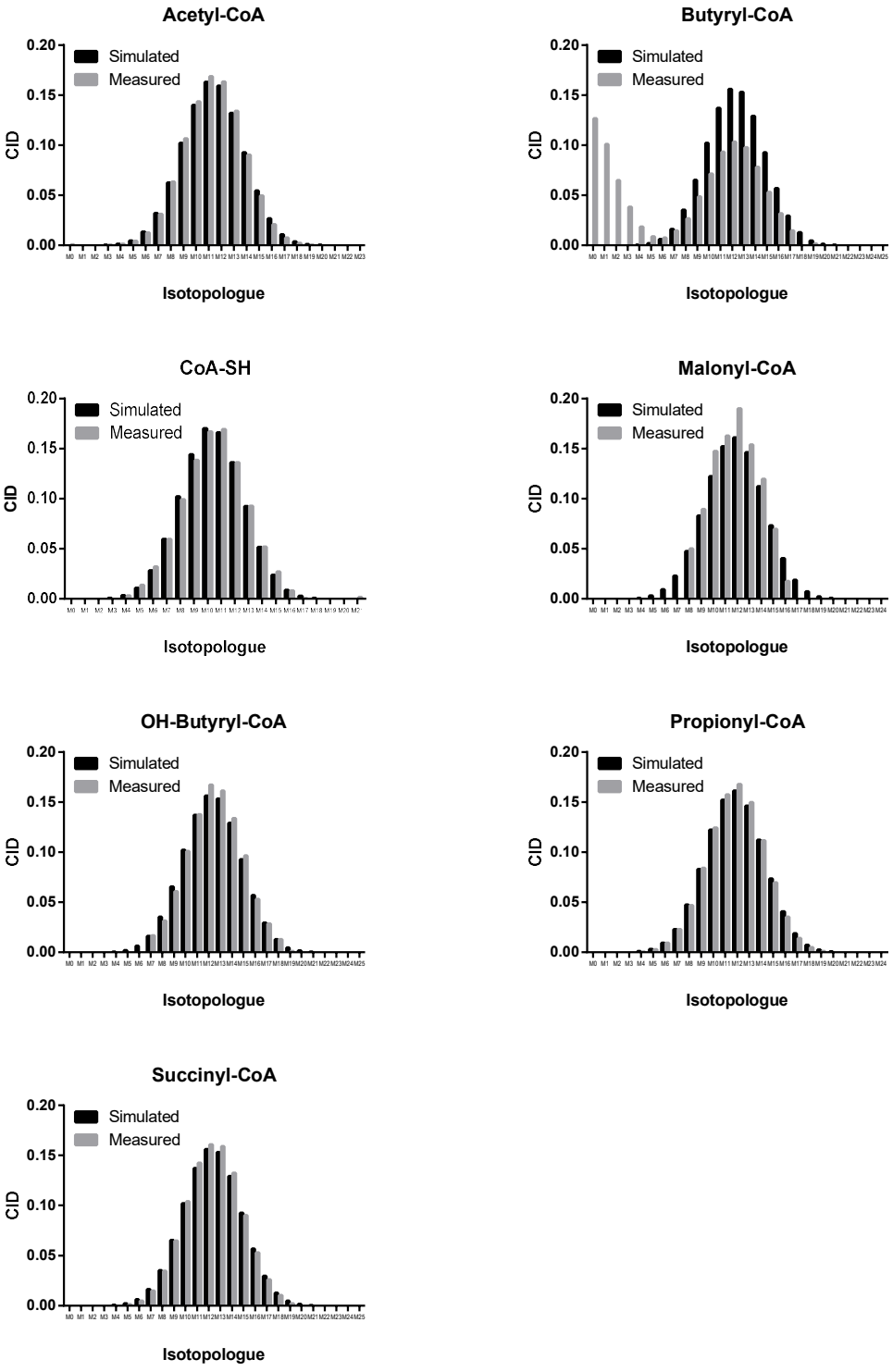

Figure 19 : Comparison of carbon isotopologue distribution in acyl-CoAs.

CID obtained by simulation and analysis of isotopic profile. *Simulated (black) and measured (grey).*

2.7 Conclusion

Adapted analytical method allows precise quantitation of short polar acyl-CoA thioesters based on principle of isotope dilution mass spectrometry (IDMS). All short-polar acyl-CoAs targeted for description of trypanosome's mitochondrial fatty acid and sterol biosynthesis were validated within set criteria. Sensitivity of the analytical method is also comparable to published literature, albeit it does not reach the LOD in range of attomol acquired by LC-MS with nano-ESI[161]. Absolute quantitation describes only one parameter of the metabolic network, for deciphering the topology ^{13}C tracer experiments are used. In order to evaluate fitness of analytical method to detect various 7 thioesters, isotopic profile produced with *E. coli* grown on defined mixture of labeled acetate producing all metabolic intermediates with predefined isotopic profile. This profile can be simulated, and carbon isotopologue distribution can be compared to measured values. For acyl-CoA thioesters, heaviest and lightest isotopologues were below LOD. Isotopologues in the middle of the pattern were in agreement with simulated values, except for butyryl-CoA which was found to be coeluting with an unknown molecule.

In agreement with vast majority of protocols published on extraction of short polar acyl-CoAs, sample handling was carried out at acidic pH in order to avoid pH-governed thioester bond hydrolysis. Ammonium formate was used as resolubilization solution as well as mobile phase, since its use as ionization reagent facilitates the detection of compounds in positive mode. Presented protocol determined concentration of acyl-CoAs in *E. coli* which were in agreement with previous findings by Bennet[186]. Although extraction protocol has been successfully employed to various types of cells (Gram negative bacteria, yeast and mammalian cells; not shown) in combination with different sample collection protocols - further evaluation of method extraction efficiency could be beneficial for acquisition of more reliable results.

Overall, the analytical method was evaluated as sensitive enough for intended application of quantification of intracellular acyl-CoA thioesters. Isotope tracing studies intended for deciphering the mitochondrial topology of acyl-CoA thioesters could be carried out. Extend of the difference of CID between prediced and measured isotopologues (bias) is compound-dependent.

3 *Investigation of Acyl-CoA Network in E. coli*

The first objective of the thesis is to investigate the operation of acyl-CoA metabolism in *T. brucei* using instationary ^{13}C-metabolic flux analysis. This requires integration of the analytical methods developed in the previous chapter within a complete instationary ^{13}C-metabolic flux analysis workflow, which must be validated first. In this chapter, we set up and present such workflow, and we tested its biological applicability on *E. coli*, a model organism in systems and synthetic biology. Despite the large number of flux studies carried out on *E. coli*, there is no model available that links central metabolism to acyl-CoAs metabolism. We thus developed such model, which was used i) to validate the proposed approach and ii) to investigate the acyl-CoAs metabolism in *E. coli*. Besides validating the metabolomics and isotopic data obtained using the presented methods, we clarified the routes that produce acetyl-CoA, malonyl-CoA, succinyl-CoA and propionyl-CoA *in vivo* in glucose-growing *E. coli* cells. This work provides the first comprehensive view of the functional interconnection between central metabolism and acyl-CoAs metabolism in *E. coli*.

Additional contribution: metabolomics experiments on the *E. coli* deletion mutants were carried out in collaboration with Mickael Dinclaux (MetaSys team, LISBP, Toulouse, France)

The analytical methods presented in the previous chapter were evaluated within the global framework of a complete instationary ^{13}C-metabolic flux analysis workflow, using *E. coli*, a model organism in systems and synthetic biology, as evaluation platform. After a brief introduction of the general principle of ^{13}C-metabolic flux analysis, we set up and validated a complete workflow for instationary ^{13}C-metabolic flux analysis in *E. coli* to investigate its acyl-CoA metabolism and its interconnection with the rest of metabolism. The measured kinetics of labeling in different acyl-CoAs intermediates highlighted two distinct kinetics of ^{13}C-incorporation for the (variable) acyl and the (conserved) CoA moieties, thereby revealing their very different turnover rates. Quantitative information on metabolic fluxes was then inferred by integrating the isotopic dataset with extracellular fluxes and metabolomics data, using a metabolic model developed in this work. Results validate the biological assumptions used for model construction, demonstrate the consistency between the different datasets, and clarify the biosynthetic origin of acetyl-CoA, malonyl-CoA, succinyl-CoA and propionyl-CoA *in vivo*. We show that propionyl-CoA is produced from decarboxylation of 2-oxobutyrate, an intermediate of the branched-chain amino acids biosynthetic pathway, by the pyruvate formate lyase PflB. This enzyme is thus active during aerobic growth of *E. coli*, contrary to current assumptions, and participates in its acyl-CoA metabolism. This work provides the first comprehensive view of the functional interconnection between central metabolism and acyl-CoAs metabolism in *E. coli*. The proposed framework is scalable both in terms of coverage and of resolution, hence paving the way towards global, comprehensive analysis of the entire acylCoA network of *E. coli* and other organisms.

3.1 Functional Studies of Metabolic Systems by Instationary ^{13}C-Metabolic Flux Analysis

^{13}C-metabolic flux analysis aims at the determination of the actual reaction rates within metabolic networks. This approach has become a powerful tool for functional investigations of metabolic systems, *e.g.* to identify metabolic pathways, to assist the discovery of novel regulatory interactions, to screen metabolic variants, to quantify flux responses to environmental and genetic perturbations, to support the construction of genome-scale metabolic models, or to identify metabolic bottlenecks to increase productivity in biotechnology [203]. In this section, we briefly present the general principle of ^{13}C-metabolic flux analysis, with a focus on the most comprehensive instationary approaches.

3.1.1 General Principle of ^{13}C-Metabolic Flux Analysis

Only extracellular metabolic fluxes can be measured directly (*i.e.* fluxes of substrates uptake and secreted metabolites) from the time-course concentrations of extracellular metabolites. In contrast, intracellular metabolic fluxes cannot be directly measured, but can be calculated by solving a network of stoichiometric reactions which represent the active set of biochemical reactions. Network topology is summarized as a stoichiometric matrix $S = m \times n$ where m is the number of metabolites and n is the number of reactions in the network. The overall change of any compound is then expressed as dynamic mass balance equation:

$$\frac{dM}{d\,t} = S.v \qquad \textbf{Equation 4}$$

where dM represents change of metabolite M over time, S is stoichiometric matrix and v is a vector of all metabolic reactions considered in the network[204].

This equation forms the basis of all the metabolic flux analysis approaches. Under metabolic steady-state, concentrations of metabolic intermediates are stable over time, then $\frac{dM}{d\,t} = S.v = 0$. In most cases the matrix contains more reactions than metabolites, the system is thus underdetermined and additional constrains need to be added in order to solve S. Several approaches were used to define constraints based on theoretical calculations, *e.g.* thermodynamic constrains that restrict metabolic flux through thermodynamically unfavourable reactions[205] or from *a priori* hypotheses where fluxes are optimized according to an arbitrary cellular objective (*e.g.* maximization of cell growth). However, metabolism is often suboptimal and differences may be observed between experimental and predicted behaviours.

^{13}C-MFA has been developed to overcome these limitations. In this approach, an organism is fed with a ^{13}C-labeled substrate, and the label distributes into the metabolites as function of pathways activities (*i.e.* metabolic fluxes). Since the isotopic content of metabolites can be measured using appropriate analytical tools, equations describing the mass balance of the isotopes can be established and provide additional constraints for calculation of intracellular fluxes.

3.1.2 Stationary and Instationary ^{13}C-Metabolic Flux Analysis

When cells are fed with (a mixture) of ^{13}C compound(s), a transient incorporation phase of ^{13}C tracer is first observed before reaching a steady state, as shown in Fig 20. Different frameworks have been developed to exploit isotopic data collected during each of these phases.

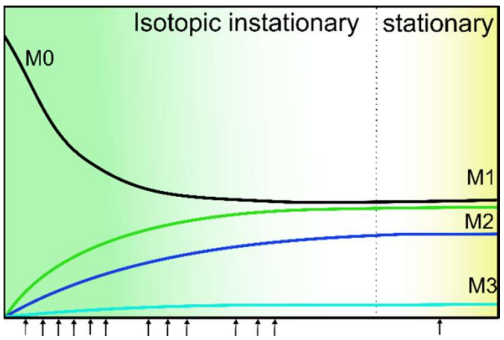

Figure 20 : Stationary and Instationary 13C-MFA

Propagation of isotope tracer through metabolic network causes isotopic instationary phase, which lasts until the biological system is allowed enough time to accumulare isotopic tracer into all metabolite pools. Depending on the size of metabolite pools, the time to reach isotopic stationary state varies. Annotated M0, M1, etc are isotopic species of a metabolite which are changing in the first phase but are constant in stationary phase. Thus sampling (depicted as arrows) is more frequent in isotopic instationary phase.

Stationary ^{13}C-metabolic flux analysis is well established method for estimation of intracellular fluxes. It is historically older approach and has been extensively reviewed [206,207]. Briefly, as shown in Fig. 21, cells are fed with ^{13}C compound(s) for sufficient time to reach a stable isotopic state before harvesting metabolites and measuring their labeling patterns. Fluxes are then estimated by fitting to these isotopic data, using appropriate mathematical frameworks[203]. Due to its simplicity and robustness, stationary ^{13}C-metabolic flux analysis is currently the most applied approach.

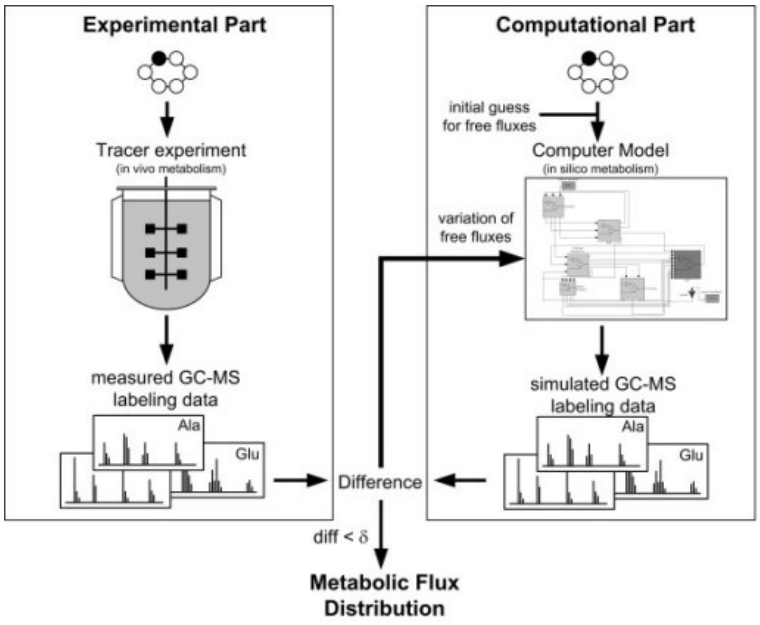

Figure 21: General principle of ^{13}C-MFA, combining experimental and computational parts

The flux estimation is based on minimizing the deviation (δ) between the measured and the simulated labeling data[206].

Exploiting the dynamic incorporation of isotopic tracer[208] allows to better resolve topology and operation of metabolic networks – in particular in compartmented biological systems[209]. Instationary ^{13}C-MFA is however more complex since it also requires to quantify of intracellular metabolite pools (labeling dynamics are function of metabolite concentrations) and to measure the tracer incorporation in metabolic intermediates with a sampling frequency sufficiently high. Since metabolic intermediates are present at low concentration and have a high turnover, specific sampling methods must be used to block metabolic activities and obtain samples representative of the *in vivo* metabolic state, as shown in previous studies [210]. Moreover, sensitive and rapid analytical tools are required to analyze the large number of samples that must be collected in these experiments. Finally, the large ODEs systems to solve during flux calculation are computationally expensive. Technological platforms are now mature enough to meet these challenges, as shown by the increasing number of flux studies carried out under the unstationary framework. Here, we set up such approach to investigate the acyl-CoA metabolism in *E. coli*.

3.2 Results

3.2.1 Workflow for Functional Analysis of Acyl-CoAs Metabolism in E. coli

The ^{13}C-metabolic flux analysis workflow developed in this work to investigate the interconnection between acyl-CoAs metabolism and central metabolism in *E. coli* is presented Fig 22. This workflow consists in i) cultivating *E. coli* under controlled conditions, ii) measuring extracellular fluxes from time-course concentrations of extracellular metabolites, iv) obtaining absolute quantification of intracellular metabolite pools, v) measuring time-course ^{13}C-incorporation into acyl-CoAs and central metabolites following a U-^{13}C-glucose pulse, and vi) integrating the different datasets for flux calculations, using a combined model of acyl-CoA and central metabolism which has been developed and is presented in this work.

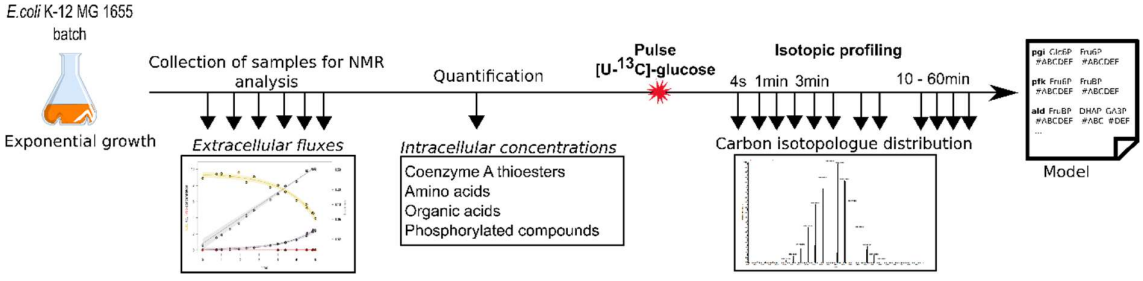

Figure 22: Workflow for functional analysis of acyl-CoA metabolism in *E. coli*

Schematic representation of experimental setup used for flux calculation. E. coli cultivated in batch was continuously sampled for extracellular flux calculation (supernatant analysed by ^{1}H-NMR). Prior to glucose pulse

samples for quantitative analysis were collected. After glucose pulse, samples were collected continuously from 4s to 60 min. All collected data on extracellular fluxes, intracellular concentrations and isotopic profile (up to 5 min) were introduced into model.

3.2.2 Quantitative Metabolomics and Isotopic Analyses of Acyl-CoA Thioesters in E. coli

At the experimental level, sampling of metabolic intermediates is one of the most complex steps. Intracellular metabolites have high turnover rates, hence the immediate blockage of all metabolic activities ("quenching") is required to obtain a picture representative of the *in vivo* metabolic state. Moreover, the chemical diversity of metabolites has important consequences on their stability to temperature, pH, and choice of extraction solvent. Metabolite degradation occurring during quenching or extraction would bias the measured concentrations and must be evaluated with respect to the class of metabolites analysed. In this work, the sampling step was therefore optimized for the analysis of acyl-CoA thioesters in *E. coli*. The optimal sampling procedure consisted in a single step where medium with or without cells – to analyze extracellular or total metabolite pools – was quenched and extracted in a solution of 125 mM formic acid in 80% methanol, maintained at -20°C. Detailed results of the evaluation and validation of the sampling method for acyl-CoAs analysis in *E. coli* can be found in Chapter 2.

Another important experimental challenge consists in quantitative analysis of pools and labeling of intracellular metabolites, which are found at low concentration in the cellular extracts and thus require highly sensitive analytical platforms. For metabolomics experiments, absolute intracellular concentrations were determined by mass spectrometry by combining the differential method and the IDMS approach. The LOD was about 0.1 µM, the LOQ about 0.2 µM, and the CV below 10%. Isotopic profiles measured in total broth samples were obtained after correcting isotopic patterns for the presence of naturally occuring isotopes. Accuracy and precision were within 2 %. The evaluation and validation of the quantitative analysis of CoA thioesters in *E. coli*, both in terms of absolute intracellular concentrations and of labeling patterns, is detailed in Chapter 2. Data were collected on the four acyl-CoAs which were detected (acetyl-CoA, propionyl-CoA, succinyl-CoA and malonylCoA), as well as on the free CoA-SH pool.

3.2.3 Labeling Kinetics of Acyl-CoAs and Central Metabolites

After quantifying the acyl-CoA thioesters in mid-exponential growth of *E. coli* on glucose, the instationary ^{13}C-labeling experiment was performed by adding uniformly labeled [U-^{13}C]-glucose (at a final concentration of 19 mM). The dynamic of label incorporation into central metabolites, amino acids and acyl-CoAs were monitored during the first hour with a sampling frequency of ~4s before 60s and then at 3, 5, 10, 20, 30 and 60 minutes. In total, 39 samples were taken out of which 27 were taken in first 3 minutes; results are shown in Figures 23-25.

Labeling kinetics of central metabolic intermediates (Fig. 23) were fast and were in excellent agreement with those observed in [210], with glycolytic and pentose phosphate pathway intermediates reaching isotopic steady state already within one minute, and slower label incorporation in TCA cycle metabolites. The low steady-state enrichments of some organic acids (citrate, aconitate and succinate) is caused by their significant amount outside the cells, which accumulate and have slower kinetics [210]. This is also observed, at a lower extent, for other metabolites.

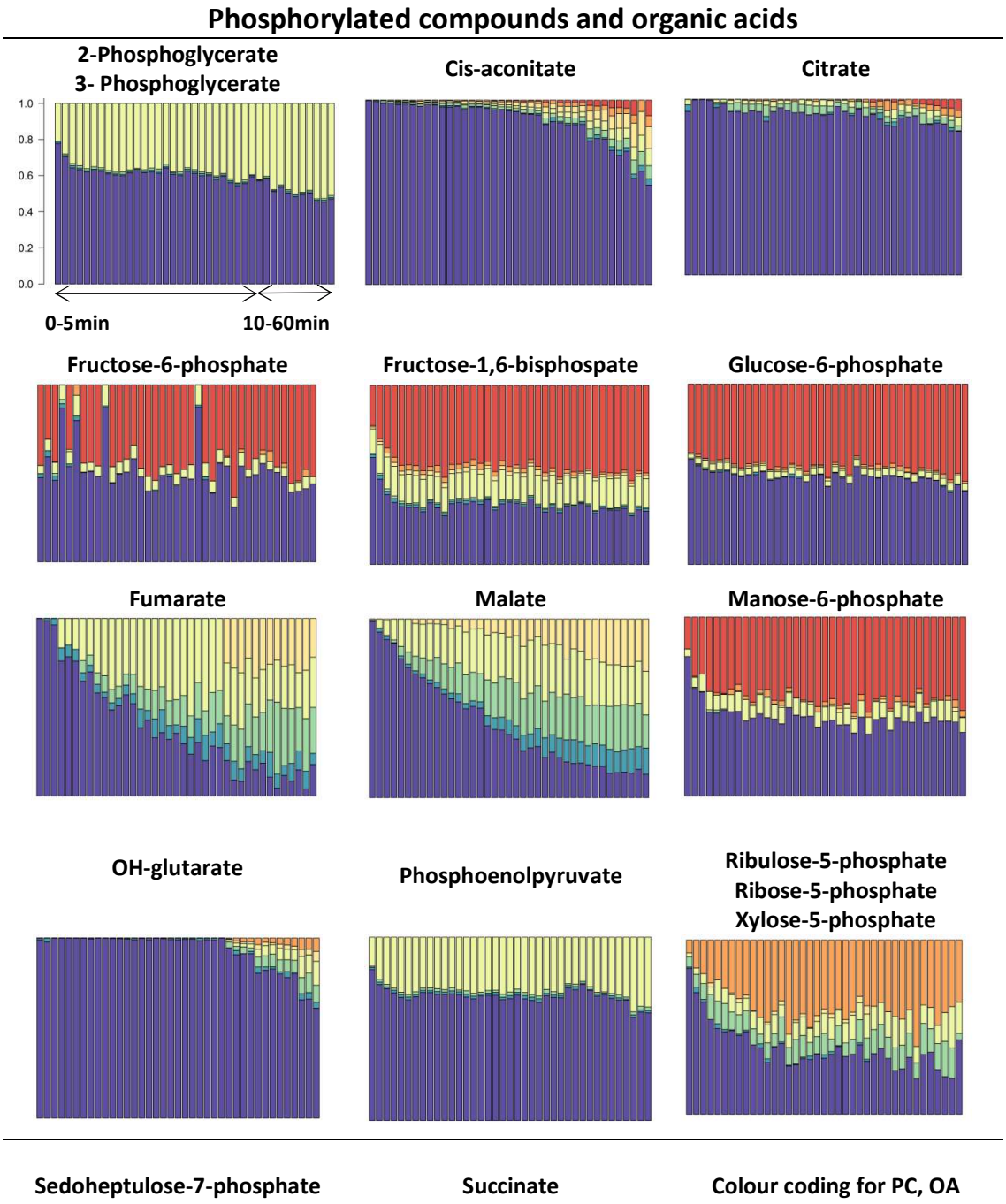

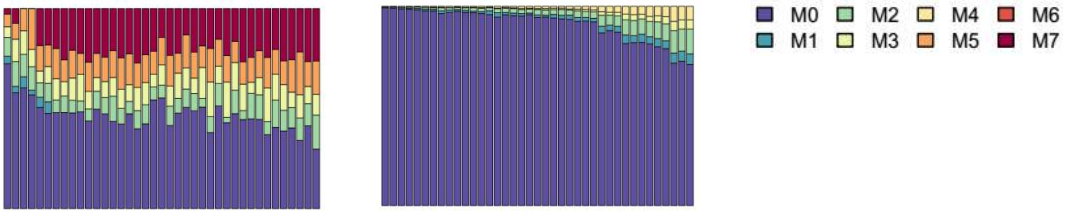

Figure 23: Dynamic label incorporation into organic acids and phosphorylated compounds.

Dynamic incorporation of 13C isotope tracer form uniformly labeled glucose [U-13C]-glucose in exponentially growing E. coli K12 MG1655. Time-scale 0-60min in 39 samples (x axis), carbon isotopologue distribution CID (y axis). Data corrected for natural abundance of ^{13}C. Compounds in alphabetical order.

Labeling kinetics of amino acids (Fig. 24) was slower compared to their precursors from central metabolism. Amino acids reached the steady isotopic state after approximately 20 minutes after the glucose pulse. Pools of glutamine and glutamate can be interconverted through glutamine synthetase (EC. 6.3.1.2), and this was reflected by their respective labeling kinetics, which are closely related. Glutathione and glutathione disulphide, a tripeptide synthesized from glutamate, cysteine and glycine, showed slower kinetics compared to their precursors.

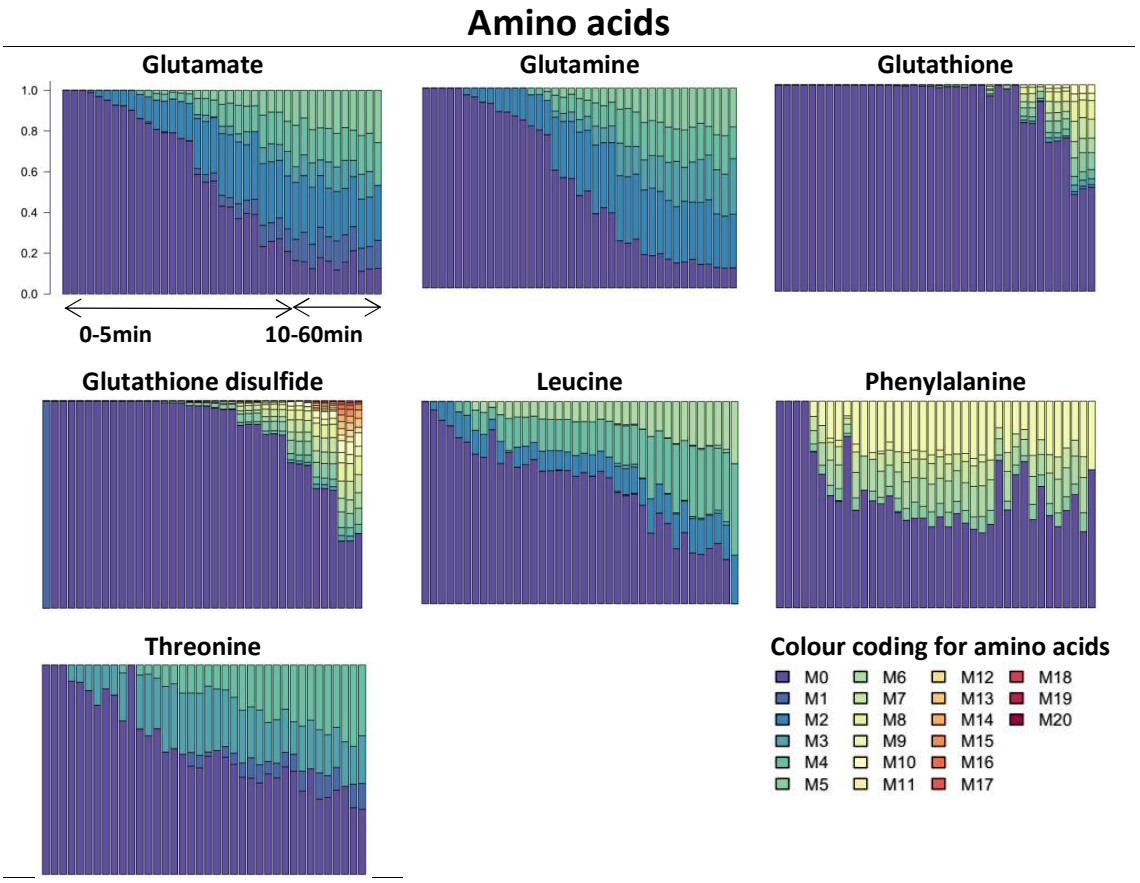

Figure 24: Dynamics of label incorporation in amino acids

Dynamic incorporation of 13C isotope tracer form uniformly labeled glucose [U-13C]-glucose in exponentially growing E. coli K12 MG1655. Time-scale 0-60min in 39 samples (x axis), carbon isotopologue distribution CID (y axis). Data corrected for natural abundance of ^{13}C. Compounds in alphabetical order.

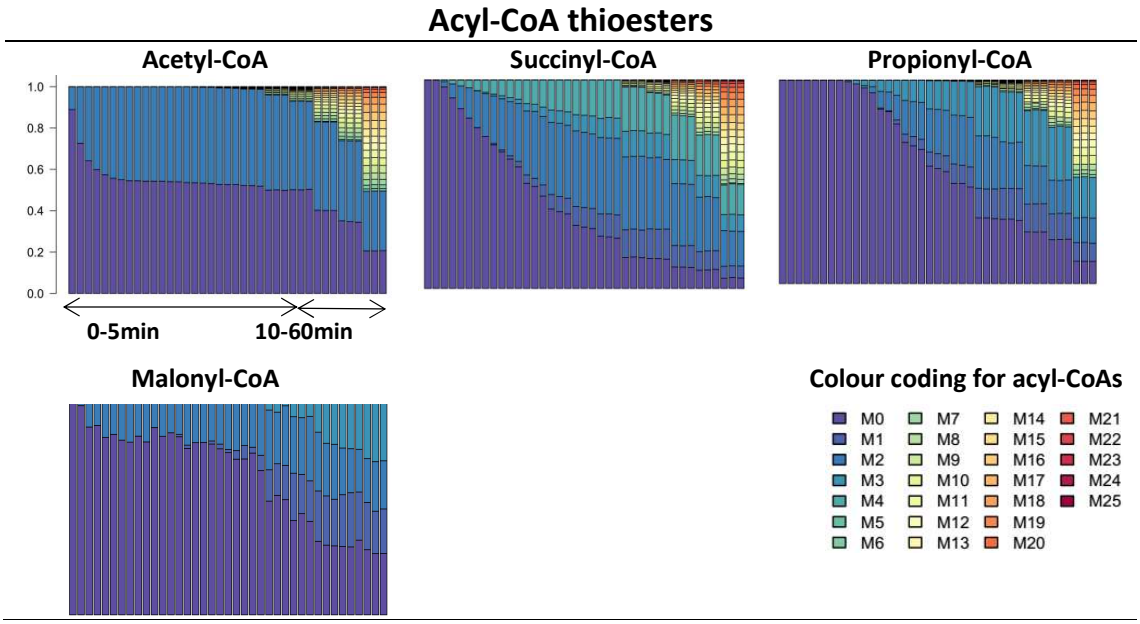

Figure 25: **Dynamic label incorporation into acyl-CoA thioesters**

Dynamic incorporation of 13C isotope tracer form uniformly labeled glucose [U-13C]-glucose in exponentially growing E. coli K12 MG1655. Time-scale 0-60min in 39 samples (x axis), carbon isotopologue distribution CID (y axis).. Data corrected for natural abundance of ^{13}C. Compounds in alphabetical order.

Finally, acyl-CoAs showed slower labeling incorporation than central metabolites and amino acids (Fig. 25), no isotopic steady-state was reached even after one hour. While distinct labeling patterns were observed for each of the CoAs, in all cases two labeling incorporation phases were observed (Fig. 26). The first phase is very short, with a plateau reached in the first minutes. This suggests a rapid ^{13}C-incorporation into the variable acyl parts while the CoA moiety has not yet incorporated ^{13}C tracer. Consistently, more complex labeling patterns are produced at a slower rate in the second phase, which may correspond to the ^{13}C incorporation into the CoA moiety. The labeling dynamics of free CoA-SH (Fig. 26) confirmed this hypothesis.

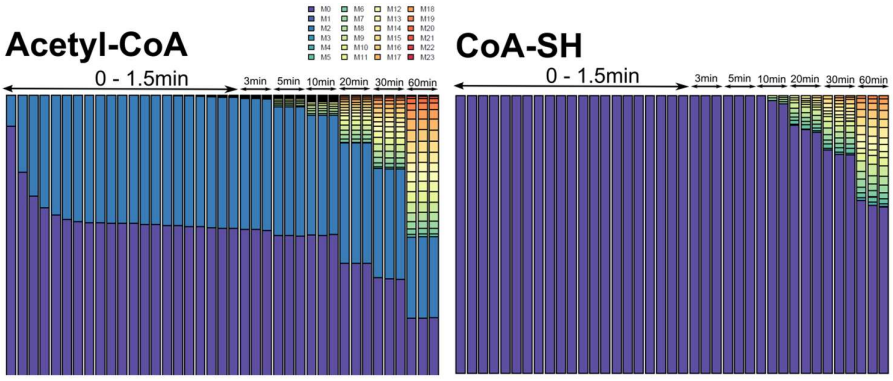

Figure 26: Distinct labeling incorporation kinetics is observed for all acyl-CoAs.

Depicted is acetyl-CoA, with higher turnover of the acetyl part which reached stationary state after approximately 20seconds. CoA moiety is synthetized de novo from pantothenate, ATP and cysteine.

Label incorporation into CoA moiety was not observed in malonyl-CoA due to low concentration and dilution of isotopic profile, which explains absence of the M+5 to M+24 isotopologues. The slow turnover of the CoA moiety indicates a low *de novo* biosynthesis flux of this central cofactor, while its recycling with the exchange of acyl moieties is much faster.

3.2.4 Metabolic Model Linking Central Metabolism to Acyl-CoAs Metabolism

Labeling kinetics contain rich information on metabolic fluxes, which can be inferred using a metabolic model. Since such model linking acyl-CoAs and central metabolites is lacking, it was developed in the present work. The topology of the central metabolic network was taken from the literature [210]. This network, which contains the glucose phosphotransferase systems, the glycolytic, Entner-Doudorrof, and pentose phosphate pathways, the acetate production pathway and the TCA cycle, was modified by adding a large extracellular acetate pool that may exchange between the cell and its environment, and thus dilute the acetyl-CoA labeling[211]. The resulting model was extended with reactions involved in acyl-CoA metabolism, as described in this section.

One of the main pathways related to acyl-CoA metabolism is the beta-oxidation cycle, a catabolic pathway for lipid degradation. Lipids are first activated by fixation to the CoA-SH moiety, resulting in the production of acyl-CoAs which are processed through the cycle. One C2 moiety is released per cycle turn in the form of acetyl-CoA, thus progressively shortening the acyl chain. This pathway is therefore capable of producing a large spectrum of CoAs intermediates, including those detected in this study. Besides this generic pathway, alternative routes are involved in the synthesis of the CoA esters detected in this work. **Acetyl-CoA** is part of central metabolism, where it is produced from decarboxylation of pyruvate by pyruvate dehydrogenase (EC 1.2.4.1) and is used to feed two ATP-generating processes: the TCA cycle and the acetate production pathway via activity of phosphate

acetyltransferase (EC 2.3.1.8) to produce intermediate acetyl-phosphate which is subsequently dephosporylated into acetate by acetate kinase (EC 2.7.2.1). **Succinyl-CoA** is an important metabolic intermediate of the TCA cycle, the main pathway for production of energy and several amino acids. Succinyl-CoA may be produced from succinate by the ATP-consuming succinyl-CoA synthetase (EC 6.2.1.5) or from propionyl-CoA by the propionyl-CoA/succinate-CoA transferase (EC 2.8.3.-). **Malonyl-CoA** is produced by carboxylation of acetyl-CoA, either by the acetyl-CoA carboxylase (EC 6.4.1.2) or consumed by the reverse reaction catalyzed by the malonyl-CoA decarboxylase (EC 4.1.1.9). Finally, **propionyl-CoA** may be formed from succinyl-CoA in two reaction steps catalysed by methylmalonyl-CoA racemase (EC 5.1.99.1) and methylmalonyl-CoA mutase (EC 5.4.99.2), or in a single step catalysed by two pyruvate formate lyases (EC 2.3.1.-). The latter reaction cleaves 2-oxobutyrate, an intermediate of the branched-chain amino acids (BCAAs) biosynthetic pathway formed during threonine degradation, into propionyl-CoA and formate. Alternatively, propionyl-CoA may be the last intermediate of odd-chain fatty acid degradation.

The rapid labeling incorporation observed in the variable acyl moiety following the U-^{13}C-glucose pulse suggests a negligible contribution of the beta oxidation cycle to acyl-CoAs production, since recycling of the large cellular lipid pools through this pathway would significantly delay ^{13}C propagation. The beta oxidation cycle was thus omitted from the model. The acetyl-CoA carboxylase and the malonyl-CoA decarboxylase involved in malonyl-CoA production result in identical carbon atom transitions and cannot be distinguised; they were thus lumped into a unique reaction (bs_accoa_1 in Fig. 27). All other routes were considered to be potentially active and were thus included in the present model, which contains a total of 105 reactions and 61 metabolites.

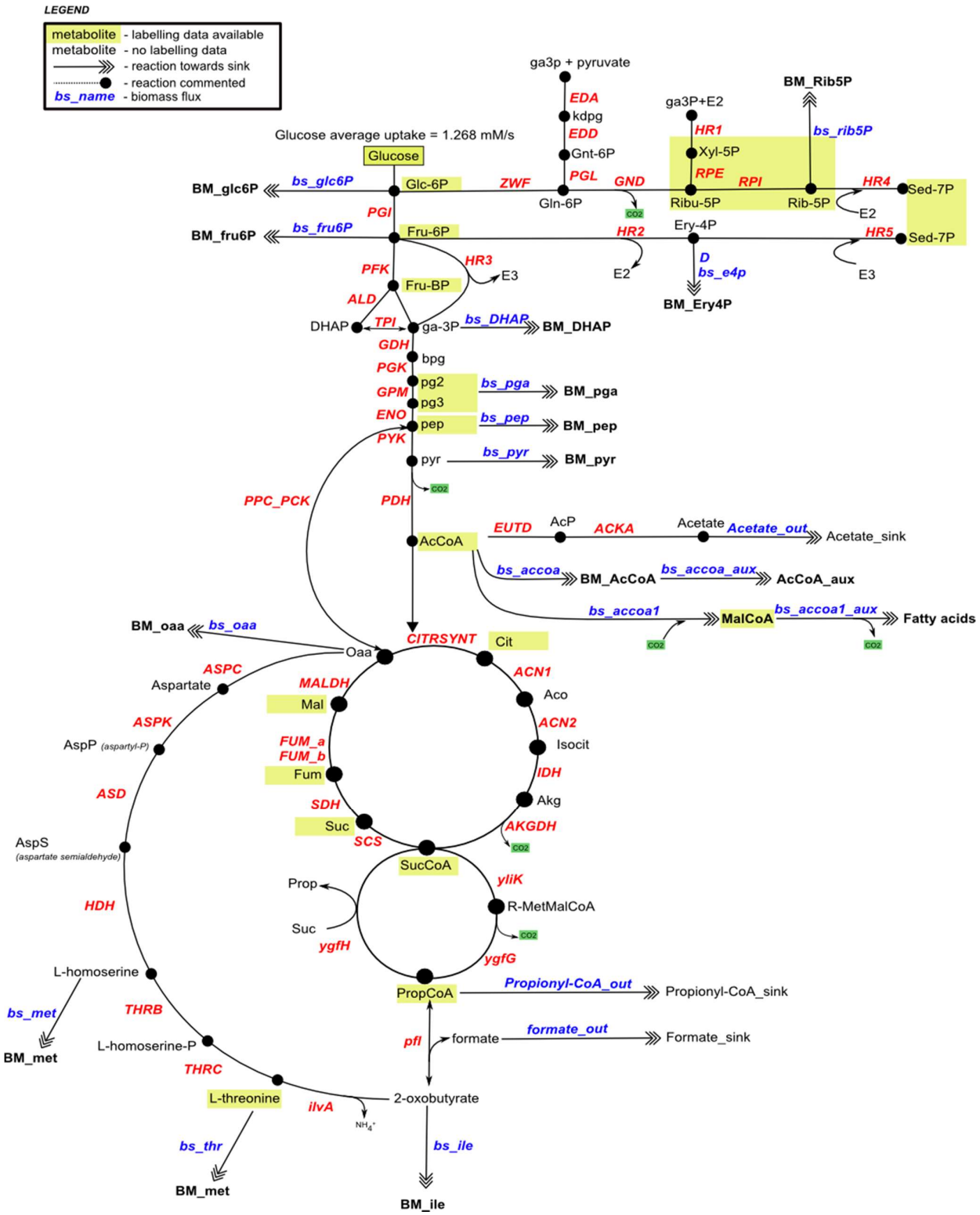

Figure 27: Representation of the metabolic network used for instationary ^{13}C-MFA

Schematic representation of the model used for flux calculation of two biological replicates

3.2.5 Metabolic Fluxes

The present model was used to investigate the interconnection between acyl-CoA metabolism and central metabolism in *E. coli*. Data input consisted in i) extracellular fluxes (calculated from the time-course concentrations of extracellular metabolites), ii) absolute concentrations of central metabolic intermediates and acyl-CoAs (quantified just before the ^{13}C pulse, as detailed in chapter 2), and iii) labeling kinetics of these metabolites during the first 3 minutes following the pulse. The different datasets were integrated into the metabolic model described above using *influx_i*, software developed in the team for instationary ^{13}C-metabolic flux analysis (metasys.insa-toulouse.fr/software/influx). Fluxes were thus calculated from a total of 2110 data points (16 metabolite concentrations, 2091 labeling data on 17 metabolite pools collected at 27 time points, and 3 extracellular fluxes). The contribution of unlabeled extracellular metabolites – which do not incorporate ^{13}C within the first 3 minutes – on the measured labeling kinetics was taken into account in the modeling step as described in[210] .

Plots of simulated versus measured data for the best fit are shown in Fig 28. A chi-squared (χ2) test evaluates the goodness of fit between experimental and simulated data, indicated that the model successfully fitted all the data, with a χ2 value of 2008. The χ2 tests can be used to determine whether hypothesized results are verified by an experiment[212].

The consistency between the model and the data indicates that the metabolic pathways considered here are sufficient to explain the observed labeling kinetics with respect to the measured intracellular pools and extracellular fluxes.

Experimental data fitting

AcCoA+AcCoA0

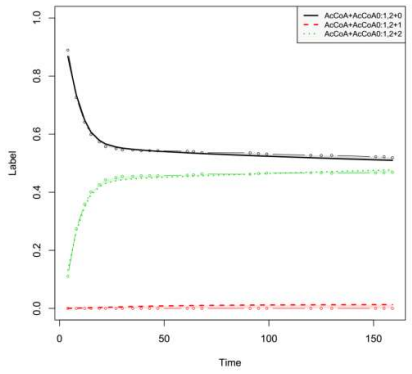

Aco+Aco0

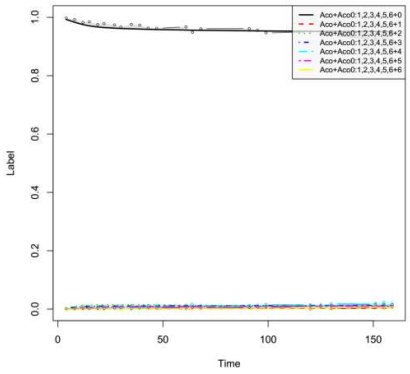

Cit + Cit0

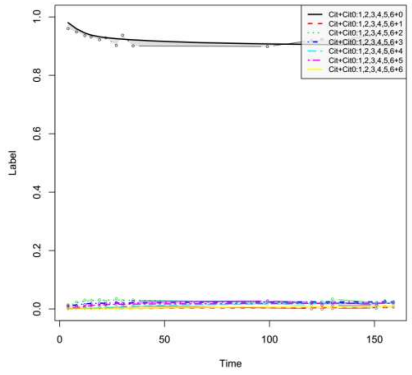

Fru6OP+Fru6P0

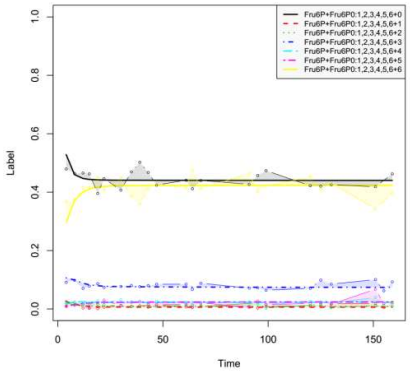

FruBP + FruBP0

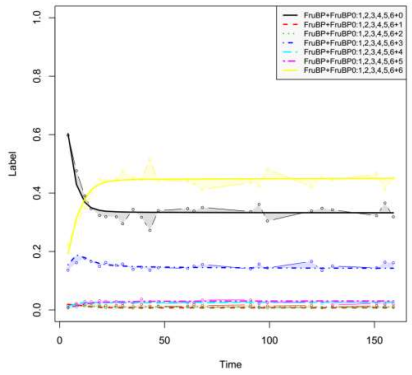

Fum+Fum0

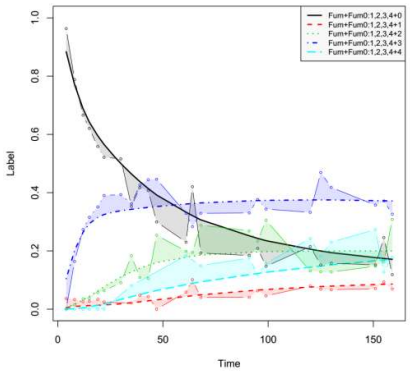

Glc6P+Glc6P0

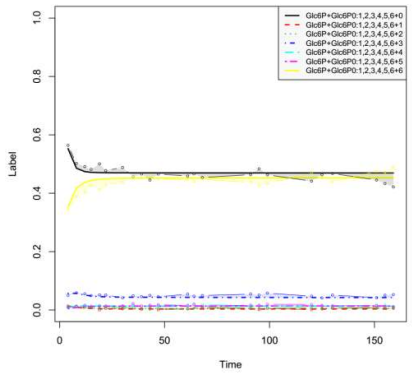

MalCoA+MalCoA0

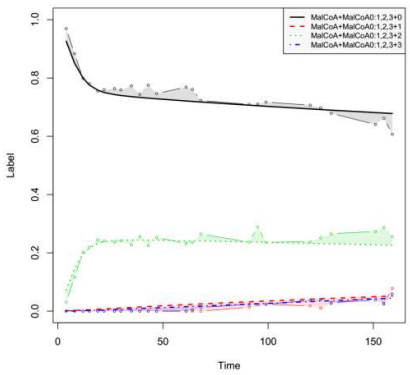

Mal + Mal0

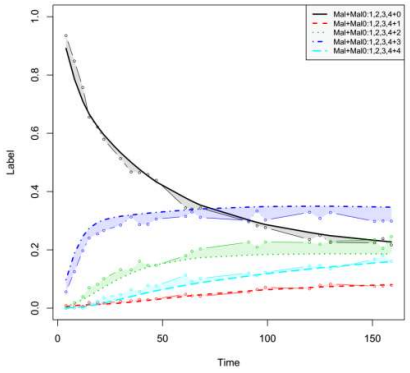

PEP+PEP0

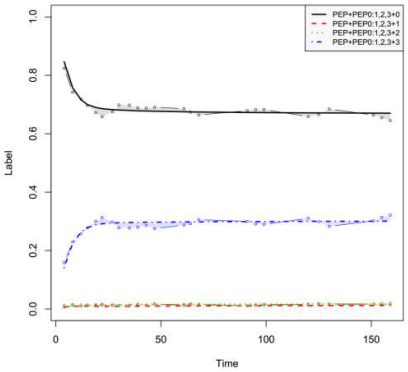

PG2+PG3+PG0

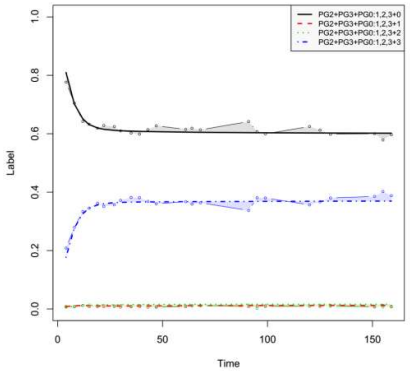

PropCoA+PropCoA0

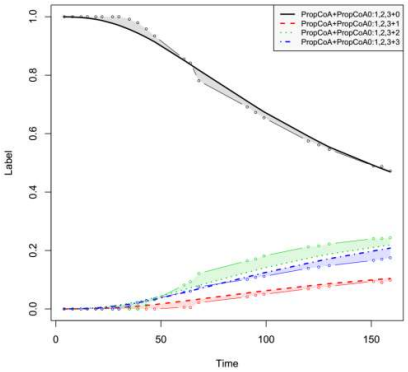

Ribu5 + Ribu5P0

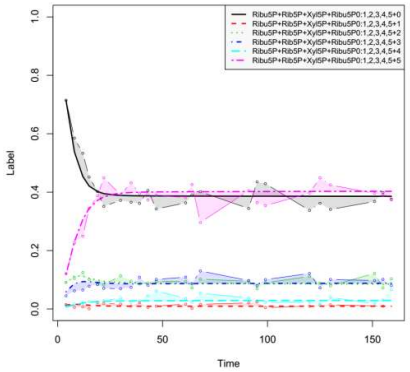

Sed7P + Sed7P0

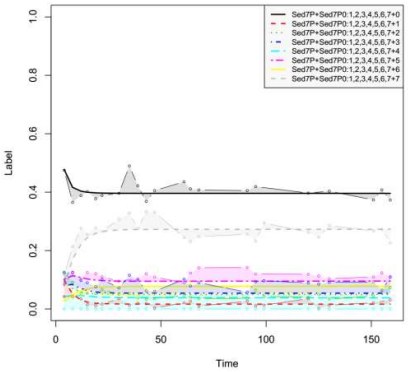

SucCoA + SucCoA0

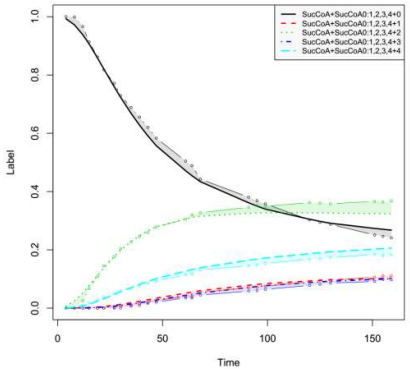

Suc + Suc0

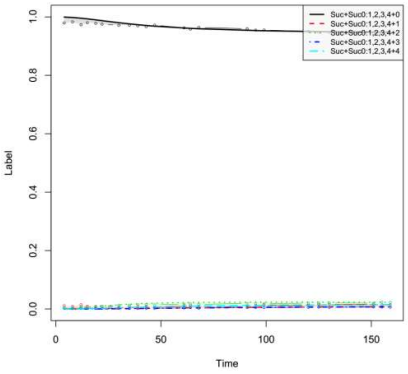

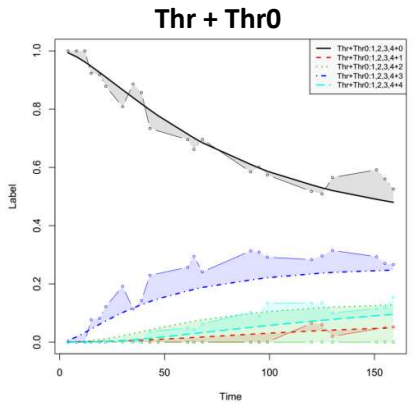

Figure 28: Comparison of measured and simulated CID

Comparison of carbon isotopologue distribution (CID, annotated as 'label') measured experimentally and simulated from the optimal set of fluxes. Graphs depict the fitting done by influx_i in order to minimize difference between measured and theoretical value. Coloured areas represent the difference between the two values.

Fluxes calculated from two independent biological replicates are shown in Fig. 29. The proportion of U-^{13}C-glucose was defined as a free parameter during flux calculation. The calculated and the experimental values (66% vs 69%, respectively) are in good agreement, which strenghtens the global consistency between the different datasets and the model. Central metabolic fluxes are also in excellent agreement with previous reports[210]. Interestingly, the CoAs producing fluxes span over a large range, from 0.03 mM/s for propionyl-CoA to 1.33 mM/s for acetyl-CoA. Acetyl- and succinyl-CoAs are part of central metabolism (intermediates of lower glycolysis and TCA cycle, respectively), which exhibits high fluxes responsible for their rapid turnover. Malonyl-CoA is formed directly by carboxylation of acetyl-CoA, at a lower rate. Finally, propionyl-CoA does not appear to be produced from succinyl-CoA through the methylmalonylCoA pathway but from decarboxylation of 2-oxobutyrate, and intermediate of the BCAAs pathway.

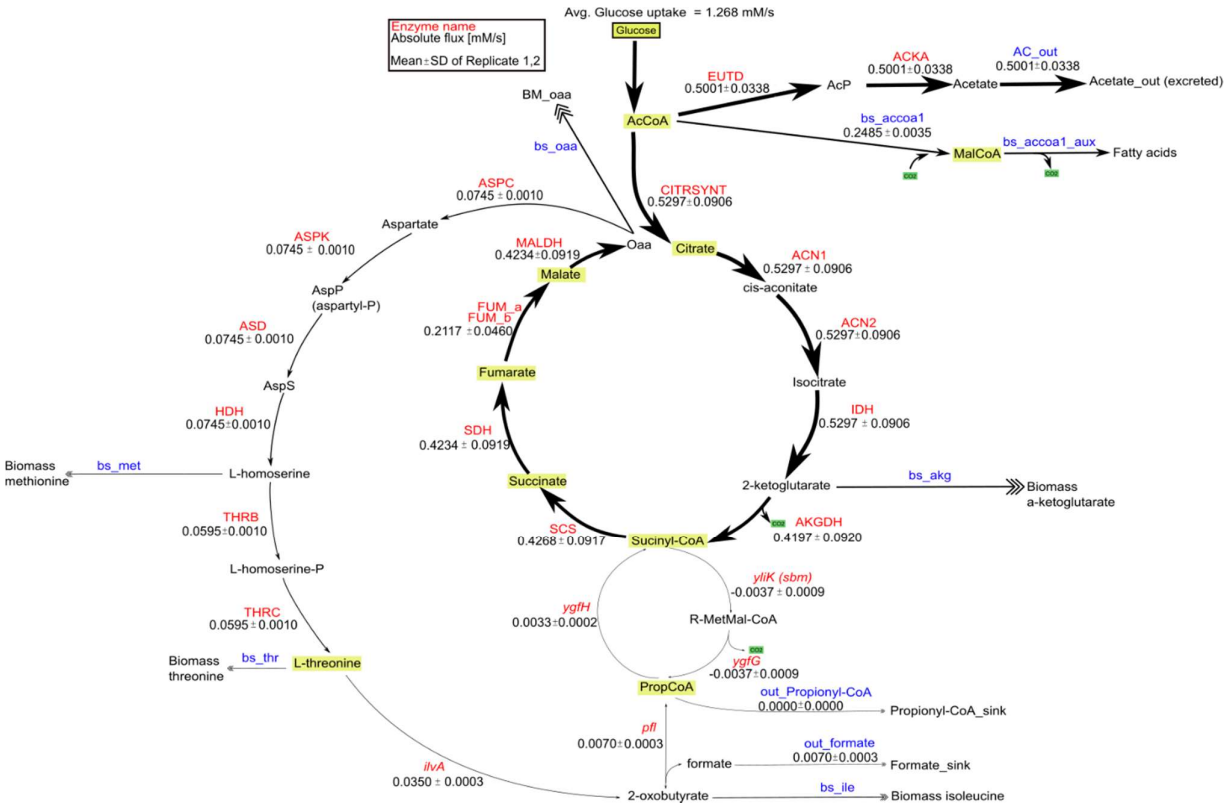

Figure 29: Flux map of *E. coli* K-12

Flux map with calculated metabolic flux values of E. coli growing exponentially on glucose as sole carbon source. Flux values (±sd) were calculated from two independent biological replicates.

3.2.6 Propionyl-CoA is Produced by The BCAAs Biosynthetic Pathway

The flux results indicate that propionyl-CoA is formed from the BCAAs biosynthetic pathway by decarboxylation of the 2-oxobutyrate produced during threonine degradation. This result is intriguing since the two pyruvate formate lyases that may catalyze this reaction, encoded by *pflB* and *tdcE* genes are considered to function only under anaerobic conditions. To test this model-driven hypothesis, we designed an experiment exploiting a feedback flux-regulatory mechanism of the BCAAs pathway. Isoleucine, a product of this pathway, is an allosteric inhibitor of L-threonine deaminase which catalyses the first step of the BCAAs pathway (production of alpha-oxobutyrate and ammonia from threonine), as shown in Fig 30. In presence of isoleucine, this pathway is expected to be blocked, and the propionyl-CoA formation should be abolished.

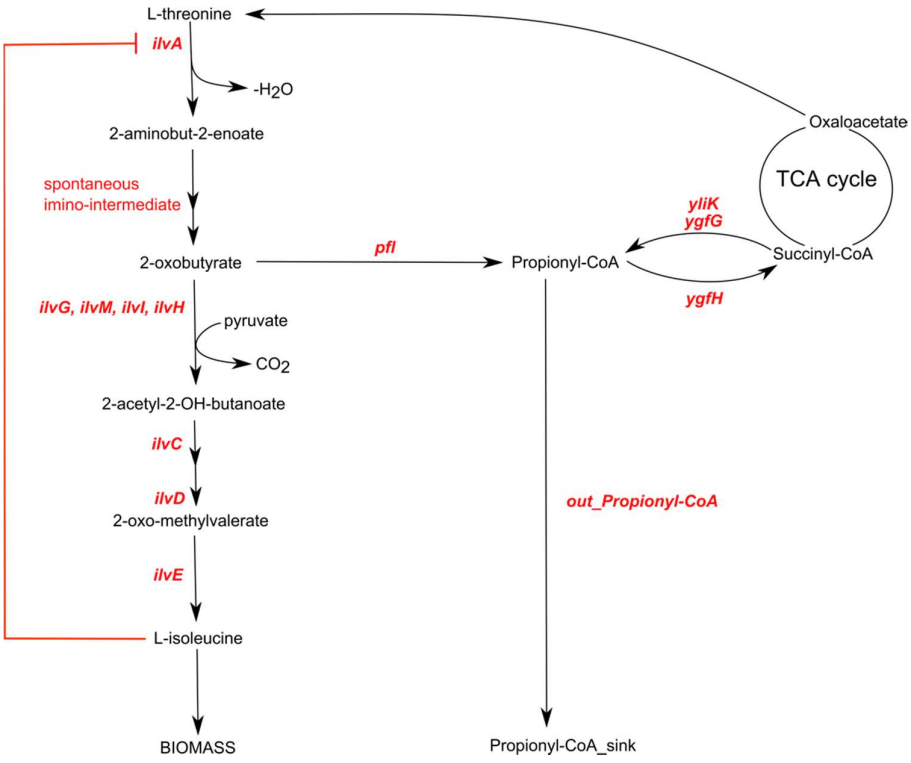

Figure 30: Regulation of the BCAAs biosynthetic pathway

L-isoleucine, an end-product of this pathway, inhibits the first step of threonine degradation

Propionyl-CoA was thus quantified in *E. coli* cells grown on glucose with or without isoleucine initially added to the medium (Fig. 31). Consistently with the flux results, propionyl-CoA was not detected when isoleucine was added to the medium, hence confirming the proposed origin.

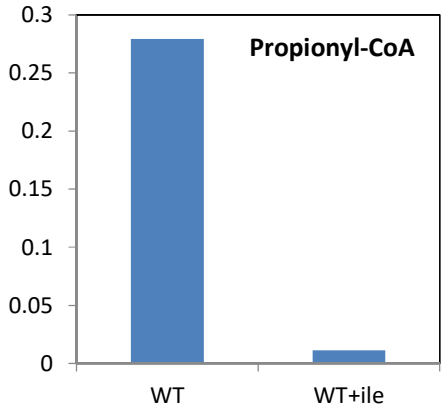

Figure 31: Normalized ratio of propionyl-CoA in *E. coli*

Barplot representation of propionyl-CoA in E. coli K-12 cultivation with and without L-isoleucine initially added to the medium.

3.2.7 *Propionyl-CoA is Produced by The Pyruvate Formate Lyase PflB Under Aerobic Conditions*

Two pyruvate formate lyases, encoded by genes *tdcE* and *pflB*, were proposed to catalyse propionyl-CoA production from 2-oxobutyrate *in vivo* under anaerobic conditions. Both enzymes are activated by the protein PflA (encoded by *pflA*) which generates a glycyl radical essential to their function. To identify if these pyruvate formate lyases are involved in propionyl-CoA formation in the present condition (*i.e.* under aerobic condition), propionyl-CoA was quantified in deletion mutants of each of these genes. To confirm further that succinyl-CoA is not involved in propionyl-CoA production, propionyl-CoA was also quantified in strains deleted for the *ygfG* and *ygfH* genes, which code for the methylmalonyl-CoA decarboxylase and the propionyl-CoA: succinate-CoA transferase, respectively.

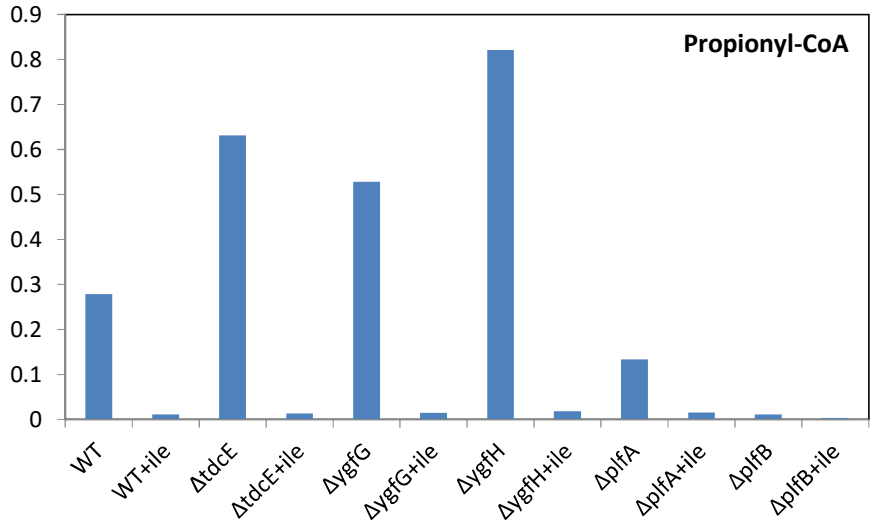

Figure 32: Normalized ratio of propionyl-CoA in all experiments

Barplot representation of of propionyl-CoA in E. coli K-12 cultivations with/without L-isoleucine

As expected from the flux results, propionyl-CoA concentration was not significantly impacted by the *ygfG* and *ygfH* deletion. Propionyl-CoA levels were similar in the wild-type strain and the *tdcE* mutants, suggesting that the corresponding enzyme is not involved in its formation. In contrast, propionyl-CoA concentration was reduced in the *pflA* mutant, and its production was abolished in the *pflB* mutant, demonstrating that the latter pyruvate formate lyase is the sole responsible for its production. PflB, considered to function only under anaerobic conditions, is thus involved in acyl-CoAs metabolism under aerobic condition.

3.3 Conclusion

A complete workflow for investigation of acyl-CoA metabolism was developed, validated, and applied on *E. coli*, a model organism in systems and synthetic biology and a platform organism in biotechnology. This workflow integrates optimized metabolomics and isotope labeling experiments with quantitative modelling. To the best of our knowledge, this work explores for the first time the functional interconnection between central metabolism and acyl-CoA metabolism in *E. coli*.

Labeling kinetics of acyl-CoA thioesters shows two successive dynamics. The variable acyl moiety is labeled very rapidly (in the minute range), while a much slower turnover of the CoA moiety (in the range of hours) is observed. Flux calculation results indicate that all the data – including extracellular fluxes, intracellular pools and labeling kinetics of acyl-CoAs – were consistent altogether and with the proposed network topology. Fluxes revealed large differences of turnover between the acyl moieties of the different acyl-CoAs, ranging from seconds to minutes. Labeling kinetics of succinyl-CoA and acetyl-CoA were fully explained assuming glycolysis and the TCA cyle were the sole production pathways. Flux results suggested that propionyl-CoA is mainly produced from the BCAAs biosynthetic pathway by decarboxylation of 2-oxobutyrate produced from threonine degradation. This result was supported by metabolomics data collected in presence of isoleucine, an inhibitor of the first step of threonine degradation. The analysis of different deletion mutants showed that decarboxylation of 2-oxobutyrate into propionyl-CoA is catalysed by PflB. This enzyme, considered to function only under anaerobic conditions, thus plays a role in the metabolism of acyl-CoAs under aerobic conditions. It is not clear yet if this reaction should be classified as a side reaction causing flux leakage due to imperfect regulation of PflB activity (either at the transcriptional, post-transcriptional, translational or post-translational levels), or if it actually plays a role under the present conditions or as an adaptive mechanism of *E. coli* metabolism to environmental perturbations.

A particular set of acyl-CoAs, reactions and conditions (both in terms of environmental parameters, carbon sources and label input) has been investigated here. The proposed workflow is scalable both in terms of coverage and of resolution, hence paving the way towards global, comprehensive analysis of the entire acyl-CoA network of *E. coli* and other organisms.

4 *Acyl-CoA Thioesters in Trypanosoma brucei*

T. brucei utilizes different types of carbon sources for growth and survival: carbohydrates as well as amino acids feed its energetic and biosynthetic needs. Mitochondrial network of acyl-CoA thioesters represents pivotal bridge between catabolism of these carbon sources and anabolic pathways leading to fatty acid and sterol biosynthesis has not yet been described. In order enlarge the understanding of cellular metabolism of *T. brucei*; the work aims to combine developed method for acyl-CoA analysis presented in chapter 2 with already established analytical methods for analysis of other groups of intracellular metabolites.

In previous years, majority of metabolic investigations in trypanosomes were carried out via the analysis of excreted compounds (exometabolome)[15], as these are available in sufficient amounts for NMR detection and appropriately reflect induced genetic changes. However, presented work aims at resolving topology and activity of a parts of the central metabolic network of *T. brucei*, which can hardly be done with few information coming from excreted compounds. Even though excreted metabolites or biomass are very good source of information on functional metabolism, metabolic networks are resolved in detail by use of intracellular metabolites. Pools of these compounds are smaller, thus require more sensitive analytical approach, but also respond to induced changes (environmental, genetic) dynamically what can help in resolving compartmentalized pools[213]. Analysis of central metabolism topology especially focused on acyl-CoA esters metabolism requires indeed a robust methodology able to identify, quantify these intracellular compounds and to obtain ^{13}C distribution resulting from ^{13}C labeling experiments. Apart from clarification of the network topology, ^{13}C labeling isotopic profiling is particularly useful for description of parallel pathways which are typical for parasitic organisms. Furthermore, ^{13}C-metabolic flux analysis can be used for resolution of compartmentalized fluxes, as compartmentalization is an essential condition for survival of *T. brucei*.

Combination of ^{13}C profiling and genetic perturbations (KO, *RNAi* mutants) is a well-established approach that yields detailed information on function of genes. In the presented work, the first acyl-CoA analyses were targeting main conversion reaction between acetyl-CoA and acetate.

The first objective of this work was application and validation of analytical method for quantitative and isotopic analysis of acyl-CoA thioesters which was applied to model organism *E. coli*. Complete methodological approach was introduced in chapters 2 and 3. This workflow was applied in *T. brucei* in order to obtain information on species and amount of acyl-CoAs present in *T. brucei* PCF grown on glucose. After first tests, developed workflow was intended to be applied to isotopic analysis of acyl-CoA species in order to resolve the dynamics of mitochondrial network and their associations with other metabolic intermediates. Sampling of intracellular metabolites in *T. brucei* can be established with two main approaches – with or without separation of cells and extracellular media by performing fast filtration[26, 27] or collecting the whole broth, respectively.

4.1 Adaptation of Fast-Filtration method for CoA analysis in T. brucei

All *T. brucei* cultivations were performed in collaboration with F. Bringaud's laboratory (CNRS, Bordeaux, France). Cultivation conditions are described in Chapter 6 (Materials and Methods).

4.1.1 Sampling and Quenching

To support the choice for sampling method, I will briefly remind the reader of the main parameters. Protocols for separation of cells and extracellular media are used in two main cases: i) when the targeted metabolites are accumulated during cultivation period and are abundantly present in the cultivation broth, thus true intracellular concentration can hardly be obtained or ii) if the composition of cultivation media is incompatible with intended analytical methodology (analytical platform) and presence would cause strong matrix effect or direct damage. Downside of separating of cells and media is due to strain in form of oxygen or substrate limitation and possibility of unwanted evolution of metabolism prior to quenching of all metabolic activity. Protocols for separation of cells and media, *i.e.* fast filtration also require several people to perform the experiment in short time-scale. Fast filtration method is a protocol previously used for intracellular metabolic quantification and their isotopic profiling in trypanosomes. This technique involves a rapid filtration of *T. brucei* culture broth through a filter by vacuum aspiration. Additional wash of the filtered cells with *e.g.* PBS supplemented with carbon sources (to minimize carbon limitation) aids in removal of residual cultivation broth and thus minimizing its matrix effect. Filter is then folded in aluminum and submerged in liquid nitrogen for quenching. Typically, time between end of filtration and quenching of metabolic activity in liquid nitrogen does not exceed 7-8seconds.

Eventually, protocol involving "quenching" of the cells in cooled ethanol (at 4°C) and their subsequent centrifugation (10min at 4°C) operates under assumption that metabolism is completely quenched and no unwanted enzymatic activities modify metabolite pools. And also, that *T. brucei* PCF

and cells do not significantly leak in these conditions. Subsequently, pellet is extracted in mixture of methanol: chloroform: water (1:3:1). This protocol has been applied to ^{13}C labeling of global metabolic pathways in trypanosomes fed with 50% uniformly labeled glucose[45]. Due to length of centrifugation step this protocol has not been tested in presented work, which intended to obtain isotopic profiles in significantly shorter time scale.

Previous investigations analyzing intracellular metabolite composition in trypanosomes relied on use of fast filtration. In this protocol of sample collection for analysis of intracellular metabolites – Ebikeme *et al.,* [27] collected 2×10^7 *T. brucei* PCF cells per filter, washed them with SDM-79 diluted in PBS (in ratio 1:9) and with use of isotopically enriched standard quantified organic acids and phosphorylated compounds in *T. brucei* PCF. Alternative of this protocol used in isotopic studies is sample preparation comprised of pre-growing cells in SMD-79 until the desired density, transfer of cells into phosphate buffered saline (PBS) supplemented with required carbon sources followed by short incubation prior to sample withdrawal (Fig. 33). This protocol has been established especially for isotopic investigations because it allows control of carbon sources and their isotopic composition targeting certain metabolic pathways. Allmann *et al.,* [26] applied this protocol for isotopic profiling of phosphorylated compounds collecting the same amount of cells as Ebikeme *et al,* [27].

Therefore, fast filtration is well-established method for *T. brucei* sample collection for quantitative and isotopic analyses and was therefore the first protocol of choice to evaluate CoA composition in *T. brucei*. This choice was also supported by the fact, that cultivation media SDM-79 is supplemented with fetal bovine serum together with rich mixture of amino acids, organic acids, and various buffers and colorants in large amounts (for media composition, please see Chapter 6). Residual cultivation broth has to be removed from samples prior to MS analyses in order to avoid ion suppression or detrimental effects towards analytical column by such rich matrix.

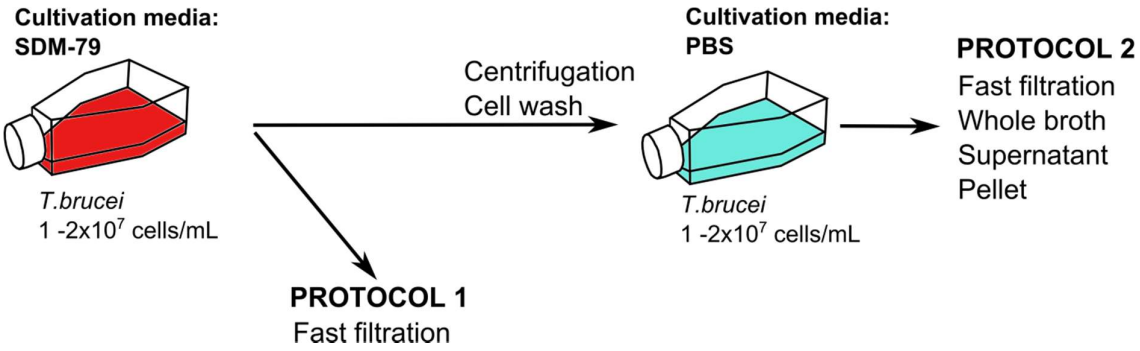

Figure 33: Scheme of procyclic *T. brucei* EATRO1125 sampling

Two protocols used for sample collection and subsequent quantification or isotopic profiling which were established in T. brucei PCF. Downside of cultivation in PBS supplemented with carbon sources is, that cells do not grow neither multiply. Thus the incubation in this media needs to be as short as possible to minimize changes

of metabolic state. Manipulation with cells, such as centrifugation and cell wash can trigger metabolic response as a result of oxygen or carbon substrate deprivation.

4.1.2 Extraction of Acyl-CoAs

The goal of the work was to combine already established methodology of cell collection of procyclic *T. brucei* by fast filtration in combination with extraction of acyl-CoA thioesters. The aim was to first obtain detailed information on identity and intracellular quantity of acyl-CoA thioesters present in trypanosomes growing in glucose-rich conditions. The focus was placed on short polar acyl-CoA thioesters, because these compounds represent the closest link between the catabolic reactions and sterol and lipid biosynthesis and are also involved in energy generation.

Extraction solution should sufficiently penetrate the cell membrane in order to release intracellular compounds; hence the primary choice was to use organic solvent. Since the focus was on short polar acyl-CoA thioesters, use of polar solvent was applied. Two polar organic solutions supplemented with equal amount of formic acid were tested – acetonitrile and methanol. Both are routinely used in as quenching/extraction (or combination of both) of intracellular metabolites in numerous microbial species. Both cause denaturation of proteins, and thus aid not only in penetration of the cellular membrane but also quenching of metabolism along with low temperature (-20°C). Since filters only contain only residue of water from cultivation media, it is essential to add water in order to restore the H^+ activity. Thus 20% of the quenching and extraction solution is constituted of water (MilliQ quality). As mentioned in chapter 1, acyl-CoA thioesters are prone to hydrolysis in basic pH.

Cultivation of *T. brucei*, sampling and extraction is described in detail in Chapter 6 (Materials and Methods). The intracellular metabolite content extracted with two protocols was analyzed for acyl-CoA thioester composition. In glucose-rich conditions, several acyl-CoA thioester species were detected in both extraction protocols (Fig. 34). As expected from high glycolytic flux, acetyl-CoA (produced by decarboxylation of pyruvate) was the highest observed compound in both. Apart from acetyl-CoA, other short-polar acyl-CoA species, such as succinyl-CoA and CoA-SH were found in rather small amounts considering extraction of 1×10^8 cells. Previously, for investigations of intracellular metabolites, 2×10^7 cells were sufficient[214]. Furthermore, exact mass of 3-HMG-CoA, butyryl-CoA, OH-butyryl and crotonyl-CoA were detected but could not be quantified in neither of the extraction solutions. The decision to use methanol as extraction solvent was based on the yield of acetyl-CoA which was found almost twice higher than with extraction with acetonitrile. Low signal intensity was likely not caused by matrix effect, as further dilution of the extract did not improve the detection.

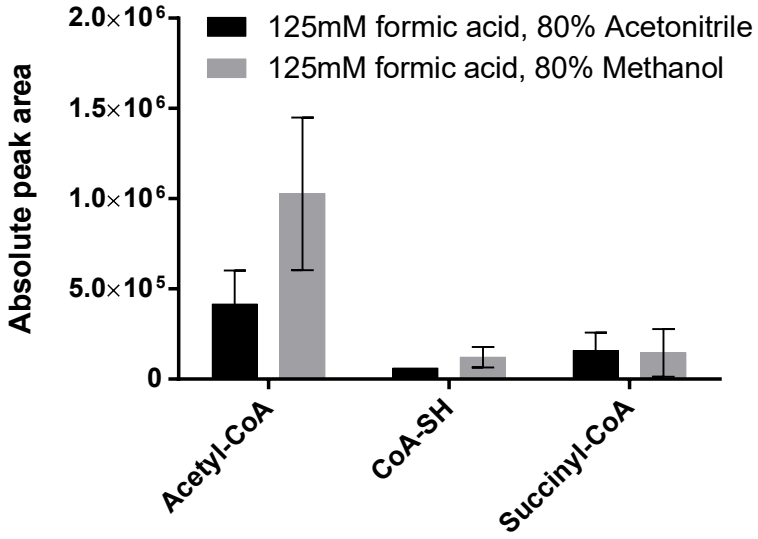

Figure 34: Comparison of extraction solutions applied to T. brucei PCF

Procyclic T. brucei cells cultivated in glucose rich SDM-79 media, cell collection done by fast filtration. 1×10^8 cells extracted per sample and extracted in two types of extraction solutions which were compared.

Our first hypothesis regarding these results was that acyl-CoA thioesters are not abundantly present compounds inside trypanosomes. In light of these results, for further experiments the cell number was increased 4-fold. Cultivation of such a high number of cells is laborious due to maximal allowed cell density inside the cultivation flask. If cell density exceeds 2x10^7 cells/mL for extended period of time trypanosomes start to form aggregates and lower their motility. Furthermore, pooling of filters is necessary in order to accumulate 4x10^8 cells per sample, as this number of cells cannot be filtered through a single filter due to time constrains needed for quick quenching and also maximum load of biomass that can be placed onto surface of the filter

In order to scan for unpredicted acyl-CoAs in *T. brucei* extracts, MS/MS scans with collision induced dissociation (CID) were acquired using normalized collision energy 35eV applied to each signal exceeding 10 000 counts. Fragmentation was tested in order to search for ions typical for CoA moiety; however, this strategy did not detect any other acyl-CoAs.

4.1.3 Acyl-CoA Profile and Quantitation in T. brucei: Evaluation of the Fast Filtration Method

4.1.2.1 Biological Context of the Experiment

Following experiment aimed for biological validation of the method, whether blocking acetate production from acetyl-CoA yields detectable changes. Specific mitochondrial mutants were chosen for this goal because mitochondrial network of acyl-CoA thioesters is closely related to metabolism of acetate, which is one of the main metabolic end products of glucose metabolism. Mitochondrial pool of acetyl-CoA is used by two enzymes (cf. Fig. 5, Chapter 1), namely Acetate: Succinyl-CoA Transferase (ASCT) (in cycle with Succinyl-CoA Synthase (SCoAS)), this enzyme facilitates conversion of succinyl-CoA to succinate with formation of ATP in *T. brucei*. Second enzyme participating on production of acetate from acetyl-CoA is acetyl-CoA transferase (ACH). These two enzymes, ACH and ASCT were targeted in order to investigate the re-routing of metabolic flux when acetate production is halted by genetic modification. As observed previously, acetate production decreased by 30% in *Δasct*, and no difference was found in *Δach* strain. Down regulation of ^{RNAi}ASCT in *Δach* null background was found to be lethal for trypanosomes[36] as rate of production of acetate is completely abolished. This double mutant strain does not die immediately but ceases to grow after approximately 8-10days.

It was assumed that *Δasct* and its downregulation ^{RNAi}ASCT in *Δach* null background would lead to accumulation of acetyl-CoA inside the cell and this accumulation would be possibly accompanied by re-direction of carbon flux into coenzymes which are presumed precursors of ketone bodies (Fig. 5). β-OH-butyrate was observed in *T. brucei* strains when acetate production is affected in *Δasct* and ^{RNAi}ASCT mutants[60], or when succinate production is abolished in *Δpepck* [27](therefore all metabolic flux from glucose degradation is redirected to mitochondrial acetate production) or when *T. brucei* grows on L-proline as sole carbon source[58]. In mammalian systems, ketone bodies (acetone, acetoaceatete and β-OH-butyrate) are produced when fatty acids are excessively metabolized (ketogenesis), ketone bodies can be reconverted back to acyl-CoAs to produce energy. In trypanosomes β-OH-butyrate is product of elimination of accumulated acetyl-CoA.

Due to reduction of acetate production in *Δasct*, small increase in acetyl-CoA accumulation was expected in this strain. And since *Δach* did not exhibit significant difference in production of acetate compared to wild type cells[36], it was expected that amounts of acyl-CoA thioesters in ACH strain will be comparable to amounts found in *T. brucei WT.* Individual impact of enzymatic activity of ASCT and ACH has not yet been described in context of acyl-CoA thioesters.

Upon applied gene perturbations, and collection of $4\times10e^8$ cells per sample the expected result was not observed and only acetyl-CoA could be detected above LOQ. Remaining acyl-CoA species were found below LOQ (3-HMG-CoA, not shown in Fig. 35) and no other acyl-CoA species could be detected in two separate experiments (Serie 1, Serie 2) (Fig. 35).

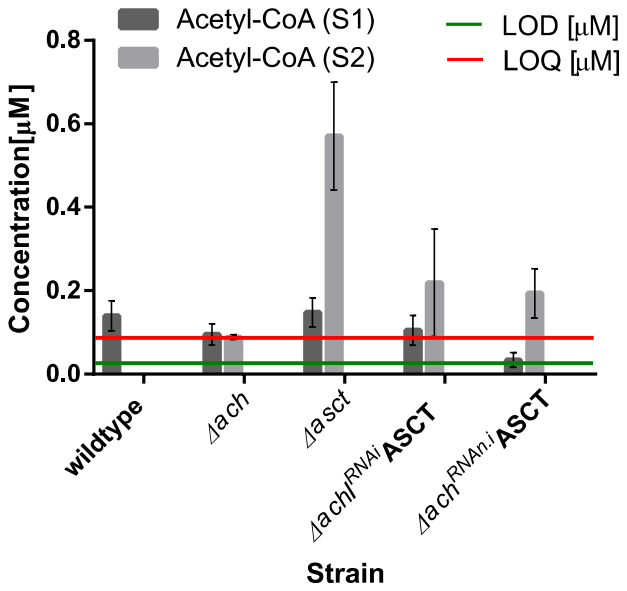

Figure 35: Comparison of acetyl-CoA quantification of *T. brucei* strains in two series

Experiment with 5 strains was performed in duplicate: series 1 (S1) and series 2 (S2). In both cases volume culture media SDM-79 corresponding to 2×10^8 cells per filter, which were subsequently pooled together of 4×10^8 cells was pooled together. S1 – Serie 1, experiment performed in February 2015 ; S2 –Serie 2, experiment performed in May 2015. Values LOD, LOQ from Table 6.

Reason for such discrepancy was not clear at first, as cells were collected, extracted and transported in the same manner. Special care was taken to fold the filter properly, *i.e*. fold it in half so the layer of cells does not stick to the aluminum folder and lead to loss of biological material during sample preparation.

Possible explanation was that during fast filtration, applied pressure causes damage to the cells which break and leak. Therefore, only minor number of cells stays intact for subsequent extraction. In hindsight, metabolites of glycolysis, PPP and organic acids/nucleotides[27] could have been analyzed using this protocol because they are sufficiently abundant, thus such losses may impact the absolute signal intensity but the compounds are still detected. Due to inconsistent results of the two replicates, no precise conclusions could be made on these mutant's phenotypes based on acetyl-CoA profiles. Though, negligible difference in acetyl-CoA amount found in *Δach*/^{RNAi} ASCT and *Δach*/$^{RNAn.i}$ ASCT is to

a high degree inconsistent with observed excreted amount of acetate in these strains by Millerioux *et al.,*[36]. Here, authors observed that production of acetate decreased by more than 90% in *Δach/*^{RNAi} ASCT therefore accumulation of acetyl-CoA in this strain should have exceed non-induced strain and single knockout in *Δasct* cell line. Therefore, the metabolic phenotype of this double strain is very noticeable. Since no such observation could be made from the data when comparing induced and non-induced double strain, which are almost identical - we concluded that fast filtration method is not suitable for sample collection for acyl-CoA thioester analysis because obtained acyl-CoA quantity was inconsistent with this expectation in both experiments. Described observation has prompted development of a new sampling method capable of reliable quantification of acyl-CoA thioesters in *T. brucei*.

4.2 Development of a New Sampling Method for Metabolomics and Isotopic Profiling Analyses of Acyl-CoA Thioesters

As stated in previous text, fast filtration was a method of choice because it was an established sample collection method for both quantitative and isotopic profiling studies in *T. brucei*. However, upon collection of unrepeatable results - it was obvious, that this type of sample collection not appropriate for CoA thioesters.

To set-up a new sampling strategy based on quenching and extraction in one step, we first tried to evaluate CoA-esters partitioning between intracellular, extracellular fractions and amounts in the whole broth, which comprise of both intra- and extracellular acyl-CoA amounts. For this reason, sampling was performed by collection of several fractions, that is – whole broth, supernatant, pellet and also filtered cells (Fig. 33, Protocol 2). In order to be able to analyze acyl-CoAs in whole broth and supernatant, the cells had to be transferred into PBS supplemented with same amount of carbon sources as are found in SDM-79 (but without fetal bovine serum and various buffers and additional compounds). Since cells are not multiplying in this type of cultivation, the intended residence time is as short as possible to perform whole experiment. Analysis of acyl-CoA in aforementioned fractions is the first application of differential method for quantification of intracellular metabolites in *T. brucei*. Differential method comprises of difference between metabolite concentration found in whole broth (end+exo metabolome) and concentration found in extracellular media (exometabolome). The difference is intracellular concentration of metabolites. This quantification is routinely used for many other microbial species[23]. Details of sample preparation and analytical methods are summarized in Chapter 6 (Materials and Methods).

4.2.3 *Results and Discussion*

The concentrations measured for 7 short polar acyl-CoAs are shown in Table 9 and Fig. 36 and represent averages of three replicate samples. From this data, it can be seen, that the total quantity of CoAs is significantly different in the four fractions collected. Acyl-CoA thioesters sampled by fast filtration were in much lower quantity than what has been found in the whole broth, confirming that indeed the fast filtration is not a suitable sample collection method. Unexpectedly, two acyl-CoA species, namely 3-HMG-CoA and OH-butyryl-CoA, were 3.5-fold and almost 6-fold, respectively higher in filtered samples than in whole broth. Furthermore, acetyl-CoA in filtered samples represents only 18% of the total acetyl-CoA found in whole broth, free CoA-SH represents 9.3% yet succinyl-CoA was found in almost equimolar amount. Reason for this is not clear, however extraction protocol has been previously adapted to filtered cells only, and its application to different fractions may not result in same efficiency of extraction, as methanol is diluted in volume of the broth. In regards to pH-related hydrolysis, amount of formic acid used in the quenching and extraction solution is sufficient to buffer phosphate salts to pH ~ 3.

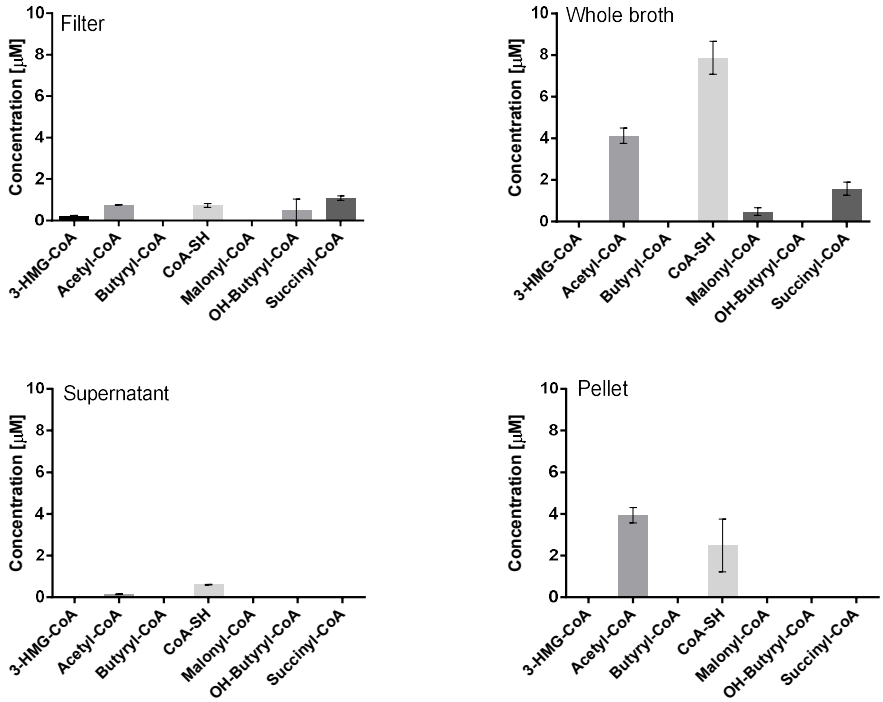

Figure 36: Acyl-CoA thioester quantification in sample fraction of *T. brucei* PCF

Acyl-CoA concentrations obtained from extracting 4×10^8 cells per sample in the whole broth, supernatant, pellet and filtered procyclic T. brucei cells. Due to nature of cell collection protocols, it currently not possible to

differentiate mitochondrial and cytosolic acyl-CoA thioester fraction, and obtained results comprise of thioesters of all compartments combined.

Table 8: Quantification of acyl-CoA thioesters in sample fractions of *T. brucei PCF*

Total of 4×10^8 cells collected in all sampling protocols. n/d, not detected; <LOQ, below limit of quantification – means that exact mass of compound could be detected but the amount could not be reliably quantified.

	Filter [µM]	Whole broth [µM]	Supernatant [µM]	Pellet [µM]
3-HMG-CoA	0.240 ± 0.006	< LOQ	n/d	n/d
Acetyl-CoA	0.752 ± 0.018	4.125 ± 0.373	0.152 ± 0.023	3.944 ± 0.370
Butyryl-CoA	< LOQ	< LOQ	n/d	n/d
CoA-SH	0.731 ± 0.097	7.864 ± 0.798	0.603 ± 0.017	2.479 ± 1.271
Malonyl-CoA	< LOQ	0.486 ± 0.188	< LOQ	< LOQ
OH-Butyryl-CoA	0.515 ± 0.522	< LOQ	n/d	n/d
Succinyl-CoA	1.075 ± 0.108	1.583 ± 0.314	< LOQ	< LOQ

Comparison of the acyl-CoA quantity in the whole broth and supernatant shows, that the most of metabolites are present inside the cells, as major compounds found in supernatant – free CoA and acetyl-CoA are only 7.6% and 3.7%, respectively, of total amount found in the whole broth. The fractions of metabolites present outside the cells seem to be compound-dependent and correspond to compounds in highest abundance in whole broth. Possible reasons why some acyl-CoAs were present in extracellular media could be unspecified metabolite leakage during centrifugation or unspecified cell lysis during cultivation. Since acetyl-CoA and free CoA are the most abundant intracellular compounds, their fraction is the highest detected in supernatants. No other metabolites were analyzed in these extracts, although it could be beneficial to analyze for example NAD^+ and NADH or fructose-1,6-bisphosphate, which are known to be strictly intracellular cofactors as a control of cell lysis. Supernatant samples were prepared by centrifugation that creates pellet. Interestingly while 96±3% of acetyl-CoA was present in pellet, only 31% of free CoA was found in the pellet, which does not add up to 100% together with fraction found in supernatant (7.6%). Reason for this could be metabolite evolution during centrifugation process, as the cells were centrifuged for 10min at room temperature and low speed to avoid cell damage. We can speculate that pool of acetyl-CoA found in pellet may be quantitatively similar to pool in whole broth, but could origin from different sources during exposition to limited oxygen and carbon substrate. That means we could observe a metabolome evolution during this centrifugation step. Quantitative difference of succinyl-CoA in sample fractions could be result of redistribution of metabolic flux inside the cells during centrifugation. This flux redistribution could be related to cell density. Such results were already observed with acetate and succinate ratios measured in supernatants for different cell densities[15]. Amount of excreted succinate and acetate depend on the cell density during sampling, almost no

succinate was detected when trypanosomes were cultivated at cell density 2×10^7 cells/mL compared to 4×10^8 cells/mL. This flux distribution between end products of succinate and acetate metabolic branched were interpreted by bioinformatics survey to be governed by NADH demand[215]. This metabolic flexibility is facilitated by cytosolic and mitochondrial $NADP^+$ dependent malic enzymes[26]. Increased NADPH requirement during oxidative stress such as oxygen limitation in pellet, results in increased acetate production.

4.3 Conclusion and Outlook

Until now, no studies of *T. brucei* have considered acyl-CoA thioesters. Short polar acyl-CoA thioesters in extracts of *T. brucei* could be qualitatively and quantitatively analysed by developed extraction and analytical methods. Presented work applies this methodology to procyclic forms for the first time. Sample collection protocol involving fast filtration resulted in unsatisfying results, where despite considerable efforts the metabolite pools were not adequately quantified.

Such results were puzzling at first, because this sample collection protocol was already used and published in multiple studies. At first, it was not apparent whether acyl-CoA thioesters degrade during sample handling, but identical handling of *E. coli* (chapter 3) yielded very reproducible results which could be integrated into mathematical model for flux calculation. Initially, we speculated that trypanosomes simply do not produce enough acyl-CoAs for reliable detection, but blocking of the main metabolic route of acetyl-CoA to acetate (^{RNAi} ASCT/ *Δach*) expecting elevated amount of (at least) acetyl-CoA and possibly detection of other species was not observed. Furthermore, the results of double mutant (^{RNAi} ASCT/ *Δach*, induced vs. non-induced) where amounts of acetyl-CoA were almost identical in two separate experiments were in clear discrepancy with amount of acetate measured in these two strains by Millerioux *et al*[36].

However, all these efforts were translated into differential method for quantitative analysis which was applied to *T. brucei* procyclic forms and acyl-CoA thioesters for the first time and which was presented in this chapter. Different metabolite profiles were observed in four collected fractions. Out of these, sampling by fast filtration yields the lowest concentrations likely due to physical damage of the cells. The major part of compounds was found in the whole broth, as was expected. During the cultivation, and possibly during manual handling of cells (*i.e.* during cell wash, centrifugation and transfer into PBS) the cells are damaged and leak into extracellular media. This is observed in two acyl-CoA thioesters found outside the cells. Since acyl-CoA is a membrane impermeable molecule due to charged state thanks to presence of three phosphate groups, its presence in extracellular media can

be explained by unspecific lysis. To my best knowledge, no CoA transporter has been reported for this organism as of yet.

Regarding quantification of CoA esters in the different fractions obtained, it seems that sampling whole broth is the most suitable method to acquire quantitative results of acyl-CoA thioesters in *T. brucei.* Indeed, because almost no acyl-CoA esters are found outside cells, whole broth composition reflects intracellular acyl-CoA esters composition. The choice of this method is also confirmed by the advantage that it combines quenching and extraction in one step, making it fast and reliable compared to other method requiring filtration or centrifugation steps which can affect metabolism before quenching, as we have seen previously (Fig 36).

Furthermore, this sampling method is adapted to short-term cultivation in PBS. Even though cells do not multiply in this minimal media and the "natural" metabolism is most probably altered, it is currently not possible to produce samples from media SDM-79. Attempts for fast filtration have been proven unsuccessful and composition of this cultivation media is not suitable for complete analysis by LC-MS. On the other hand, cultivation in PBS has been already established in metabolomics studies and also ^{13}C profiling because composition of ^{13}C substrates is controlled.

Lastly, due to aforementioned development, ^{13}C labeling has not yet been performed with *T. brucei*, however having reliable sampling method which is already compatible with analytical platform used – the transition to isotopic profiling ought to take shorter time than completion of this part of the work. Presented results, where the most abundant compounds were those related to acetate production (acetyl-CoA, succinyl-CoA and CoA-SH) confirm that acetate production is indeed the main reaction of acetyl-CoA. Having access to quantitative results, the next step is to evaluate the genetic modifications (ASCT, ACH) with adapted sample collection method in order to evaluate whether these actually had expected impact on redirection of metabolic flux.

5 Discussion and outlook

T.brucei is characterized by presence of metabolically important organelles – such as glycosome and mitochondria which respond to environmental changes (*e.g.* change of carbon substrate) by redirecting the metabolic flux (glycolysis from glucose, gluconeogenesis from proline, glutamine) and are interesting in studies of adaptation capabilities during rather complex life cycle. Some of active metabolic pathways are located in several organelles. Use of isotope tracing is an elegant way how to resolve topology as well as *in vivo* metabolic conversions in compartment fluxes and their distribution in light of applied genetic modifications. These reasons have inspired the topic of this thesis, which aimed to resolve the topology and the operation of the metabolic network of acyl-CoA thioesters, which are on the crossroad between catabolic and anabolic pathways, by emplying isotopic tracer experiments a network.

5.1 Perspectives from Analytical Point of View

In the first part of the work, qualitative and quantitative acyl-CoA analysis based on stable isotope ratio (IDMS) was adapted to available analytical instrumentation from work of Peyraud et al., [141]. Analytical method focused on short polar acyl-CoA thioesterters was then validated within defined set of criteria. Obtained method parameters of LOD and LOQ were in agreement with available literature. However, performance of the method could be enhanced by further improvements of chromatographic separation by using lower diameter particles, or using ion-pairing agents to increase signal intensity of acyl-CoA thioesters. Utilization of miniaturisation and nanoflow technique has been applied to analysis of acyl-CoAs with detection limit as low as 1fmol (versus 0.1 – 0.2pmol reported in this work)[161]. Recently, new mass spectrometers (Thermo Q Exactive, Waters Xevo G2-XS qTOF) have been introduced to MetaToul platform, where this work has been performed. Both are tandem mass spectrometers operating at high mass resolution (Q Exactive 140 000 at m/z 200) and are very suitable for isotopic profiling of complex molecules such as acyl-CoAs, and untargeted metabolomics aplications.

Subsequently, extraction method has been set up and validated for prokaryotic model organism *E. coli*. The extraction protocol used only polar solvents, in order to extract short polar acyl-CoAs, and as a result the procedure is discriminative towards long chain acyl-CoAs. Extraction method

can be improved in order to extract more non-polar acyl-CoA species to enlarge the coverage of this group of metabolites. Fatty acyl-CoAs were extracted from cells in liquid cultivations (*Mycobacterium*, *Streptomyces* and *Corynebacterium* species) via extraction with KH_2PO_4 buffer (pH 4.9), 2-propanol and triethylamine as ion pairing agent[216], alternatively mixture with methanol:chloroform:water (5:2:2) could be used to extract non-polar acyl-CoAs [178] as seen in Gram negative bacterium *Ralsolnia eutropha*. Alternatively, there are numerous protocols to start from available for extraction of fatty acyl CoAs from mammalian cells[85].

Untargeted screening for acyl-CoA thioesters using typical fragmentation pattern was used by Zimmermann et al. (Fig. 37)[86], using acyl pantetheine fragment for quantitation because it is characteristic to acyl-CoA molecule. Alternatively, this fragmentation pattern can be exploited for fragmentation of all signals above certain treshold in order to search for CoA-related fragments (*m/z* 428 and 410). In this manner, identification of novel acyl-CoAs by scanning for CoA-related fragment was used in studies of xenobiotics metabolism, *i.e.* in catabolic pathways of 4-hydroxy acids (including various drugs)[169].

Naturally, improvements to current methodological setup will be applied based on individual (organism-specific) demands and particular biological questions. Current adapted setup is able to separate 12 acyl-CoAs within 18minutes of LC-MS run. In combination with whole broth sampling into acidified mixture of organic solvent the procedure has been proven easy to use and fast to perform during short-time paced sampling needed for central acyl-CoA network in *E. coli*. In short-term perspective the aim is to improve the coverage of the LC and extraction method to increase number of acyl-CoA species.

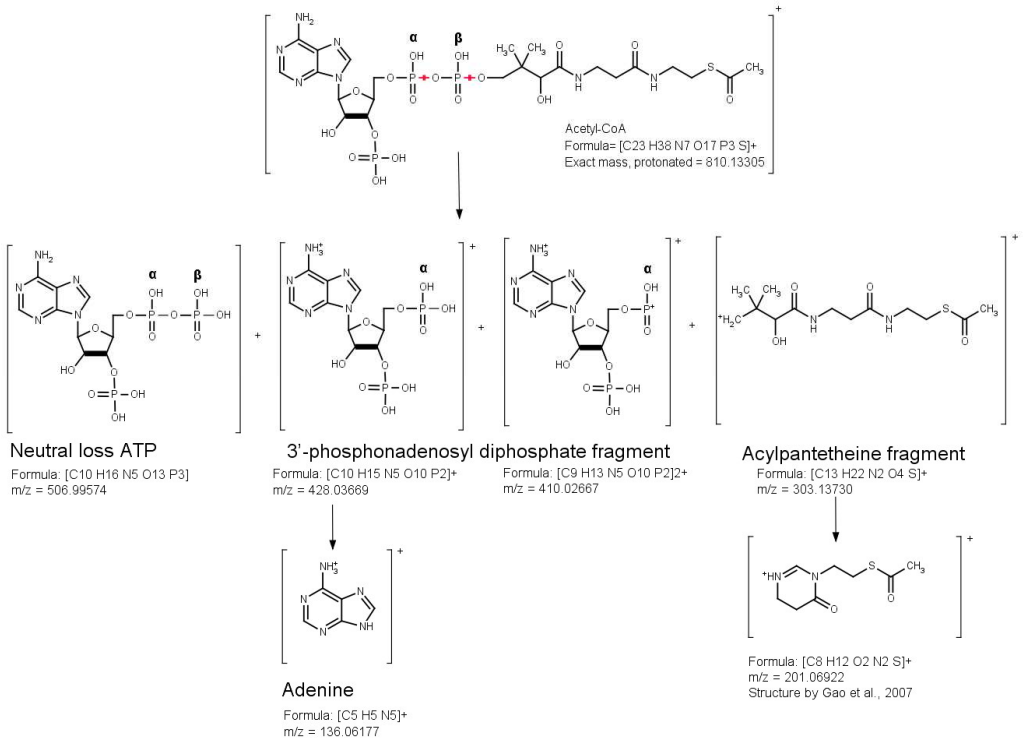

Figure 37: Fragmentation pattern of acetyl-CoA

In positive mode, observed fragments of CoA are 428.04 and 410.02 Da. The loss of H2O can occur in the phosphate backbone or in the ribose. Structure of acylpantetheine fragment suggested by Gao et al., [163].

5.2 Perspectives in Metabolic Flux Analysis of E. coli

A complete methodological workflow for incorporation of quantitative and isotopic data of acyl-CoA thioesters within central carbon metabolism has been established in well-known *E. coli*. Protocol comprised of cultivation of cells in minimal media, collection of data for extracellular fluxes, introduction of labeled substrate and subsequent sample collection by whole broth sampling.

Analysis of *in vivo* rates of metabolite conversions is useful tool in studies of organisms's capabilities to redirect pathway activity as a result of targeted genetic modifications or environmental changes. Flow of matter directly represents activity of metabolic pathways *in vivo* as metabolic fluxes and cells' ability to modulate them is central capability of the cell to respond to changing genetic or environmental changes. As a consequence, analysis of metabolic re-routing is increasingly popular in medical field in studies of cancer metabolism[217] as well as biotechnology[218]. Comparison of metabolic flux maps obtained under different conditions shows overall impact of these modifications on the celllar metabolism. Analysis of metabolic flux yields detailed information on topology of metabolism, as could be seen from the flux map obtained from *E. coli*. The main pathway active on glucose catabolism is production of acetate (excreted) and TCA cycle in order to maximize energy yield in

aerobic conditions. Acyl-CoA thioesters in this context enlarged observable metabolic fluxes, even if acyl-CoA related fluxes were of minor aspect. From the flux distribution, the origin and direction of one of acyl-CoAs could be explained. However, in presented work, only 4 acyl-CoA thioesters have been implemented in ^{13}C-MFA model of *E. coli* K-12. In order to increase the coverage of the metabolic network and the flux results, it is necessary to enlarge number of observable acyl-CoA species. Analysing a large number of conditions where acyl-CoA pathways are expected to be active will provide a more complete and detailed view of the acyl-CoA metabolism in this model organism. Furthermore, such clarification of acyl-CoA network is beneficial especially for industrial *E. coli* strains developed for polyketide production[219, 220].

5.3 Perspectives in Study of T. brucei Metabolism

Interest in study of Trypanosomes is governed by the medicinal importance as well as atypical features and easily accessible genetic manipulations. The genome of *T. brucei* was sequenced in 2005[110], however function of many genes is still not known. Successful strategy in deciphering operation of *T. brucei* metabolic network has been targeted disruption of gene transcription which ceases production of certain enzyme which induces blocking of certain pathways. Products of these pathways can be identified and quantified to provide information on flexibility of organism upon genetic perturbation. Metabolomics is especially informative in various systemic disorders (perturbations) caused either artificially by disrupting a gene, or naturally due to disease-related gene mutation. Furthermore, organisms respond to environmental conditions, thus cultivation with different carbon sources yields different metabolic profiles. So far, majority of studies focused on metabolic dissection of trypanosomes using NMR detection of metabolic end products.

The general perspective of this thesis has been to **enlarge number of observable metabolite groups** in *T. brucei*, for this reason analytical and extraction method have been adapted in the first phase. Quantitative analysis of acyl-CoAs could advance our understanding of targeted gene modifications, by observing accumulated product(s) of the targeted gene or their absence. Analysis of intracellular metabolites however requires sensitive analytical method. Sample collection method for acyl-CoA thioester analysis has been critical point of this work, and its modification lead to adaptation of cell collection compatible with NMR- based analyses.

Furthermore, application of ^{13}C isotope tracing for studies of **topology of acyl-CoA thioesters** and their placement within central carbon metabolism and anabolic pathways has not been deciphered. Overall, ^{13}C labeling of intracellular metabolites is, despite its popular use in microbiology, relatively less used protocol in trypanosomes given the number of studies [26,45]. This fact makes idea of

this work more interesting, as resolution of mitochondrial topology could be resolved by its application. *Trypanosoma bruc*ei is equipped with alternative pathways and unique features that are not found in model organisms like *E. coli*.

Furthermore, organism is known for its ability to adapt to surrounding environments (different carbon sources) in the course of its life cycle. The two main forms, bloodstream and procyclic differ in the composition of both sterols and fatty acids. Therefore, detailed description of pathways leading to biosynthesis of both in multiple compartments (cytosol, mitochondrion, microsomes, glycosomes) was aimed to advance our understading on adaptation possibilities of this organism. Acyl-CoA thioesters are at the very center between catabolic and anabolic pathways. The first goal was to describe the composition and acyl-CoA pools of *T. brucei* growing on glucose, and then compare with *T. brucei* growing on amino acids. In the obtained results so far, trypanosomes produce mainly acetyl-CoA, succinyl-CoA and free CoA which are part of acetate production. Deletion of genes participating on two reactions converting acetyl-CoA to acetate has not yet been fully evaluated in context of acyl-CoAs due to difficulties to obtain reproducible data. In short-term perspective, this is the first result to obtain.

In trypanosomes, some acyl-CoA thioesters are thought to participate in both lipid and sterol biosynthesis – such as 3-HMG-CoA, the central molecule between these two processes acording to Uttaro [118]. Long-term objective of this work was to evaluate participation of acyl-CoA thioesters also in mitochondrial mevalonate pathway.

Overall, the work established in model organism *E. coli* could be transferred to *T. brucei*. Given, that the current acyl-CoA sampling and analysis setup is compatible with NMR analyses – it allows collection of data on extracellular fluxes with subsequent quantification of intracellular metabolites followed by pulse of labeled substrate and time-appropriate collection of samples used for isotope analysis. Future direction for metabolic discoveries or detailed descriptions of metabolism under various induced conditions (environmental/genetic) may also explore the dynamic metabolic rearrangement in response to perturbation, such as changes in carbon nutrition.

6 *Materials and Methods*

Following chapter described protocols and methods used in this work.

6.1 E. coli cultivation

6.1.1 Pre-cultivation E. coli

Escherichia coli K12 MG1655 stock culture was stored in LB medium with glycerol (40% v/v) at T=-80°C. Cultivation was started by inoculating 10 mL of Lysogeny broth (LB) in 12 mL sterile tube with loose lid for culture aeration. This inoculum was used for overnight pre-cultivation of *E. coli* on minimal synthetic media "M9" containing: 3,03g/L KH_2PO_4, 17,4g/L Na_2HPO_4, 0.51g/L NaCl, 2.04g/L NH_4Cl, 0.49g/L $MgSO_4$, 4.38mg/L $CaCl_2$ and trace amounts of Zn^{2+}, Co^{2+}, Mn^{2+}, B^{3+}, Mo^{6-}, Fe^{2+}, Cu^{2+} which was sterilised by an autoclave. Carbon sources glucose and thiamine with concentration 3 g/L and 0.1 g/L, respectively, were sterilised by filtration (Ministart polyamide, 0.2 µm, Sartorius, Germany) prior to addition into media. Overnight M9 pre-culture was inoculated at very low OD (at 0.001) in 250 mL baffled shake-flask containing 50 mL of cultivation media, incubated at 37°C, 180RPM in orbital shaker (Innova 4230, New Brunswick Scientific, USA). Cell density was measured spectrophotometrically at 600 nm prior to extraction.

6.1.2 Cultivation E. coli

In order to prepare samples compatible with ion chromatography hyphenated with tandem mass spectrometric detection (IC-MS/MS) cultivation was carried out in synthetic media M9 with 5x reduced amount of phosphates, containing: 0,606 g/L KH_2PO_4, 3.48 g/L Na_2HPO_4, and same amounts of remaining mineral salts as described above. Glucose and thiamine with same concentration as described above were used in this media as well. Cells were transferred from overnight culture into reduced M9 media by centrifugation at 7600 g, at room temperature for 10min using centrifuge Sigma 3-18K (Sigma, Germany). Supernatant was discarded, cells were washed with 2 mL of fresh synthetic reduced M9 media containing carbon sources, after quick wash this liquid was discarded. Cell pellet was overlaid with 10 mL of M9 reduced media, vortexed and used to inoculate the culture. *E. coli* was incubated in 250 mL baffled shake-flasks containing 40 to 70 mL of culture incubated at 37°C, 180RPM in orbital shaker (Innova 4320, New Brunswick Scientific, USA). pH of this culture was continuously monitored and adjusted (approximately every 15 min) by 1 M NaOH to pH = 7.0. Sampling was carried out in exponential growth phase at OD 1.0-1.5.

6.1.3 Acyl-CoA Quantification in E. coli

6.1.3.1 E. coli: Fast Filtration Sampling

E. coli K-12 MG1655 bacterial culture at mid-exponential growth phase, corresponding to 0.63mg biomass (OD_{600}~1.6, 1mL culture sampled), was harvested by fast-filtration through polyamide filter (Sartolon polyamide, 0.2µm pore size, 45 mm diameter). Filter with layer of cells was wrapped in aluminium and rapidly placed into liquid nitrogen for quenching. Quenched cells were then extracted, all used solvents contained 125 mM formic acid in 80% of organic phase and 20% of water to restore pH, and total volume of extraction solution was 5 mL. Isotopically enriched *M. extorquens* extract (25µL) was used as internal standard and ratios of $^{12}C/^{13}C$ were compared for tested protocols. The absolute metabolite concentrations were determined by extrapolating ratio $^{12}C/^{13}C$ onto calibration curve analyzed together with each biological samples batch. All extraction solutions used were precooled to -20°C and amount of formic acid was increased 5-fold in order to avoid pH-related thioester hydrolysis since residual $[PO_4]^{3-}$ from culture media is present in dead volume of the filter. Sample was further processed as described in section "6.1.5 – Acyl-CoA additional preparation". All samples were evaporated overnight using SpeedVac (SC110A SpeedVac Plus, ThermoSavant, USA), re-solubilized in 100µL 25 mM ammonium formate with 2% methanol (pH = 3. 5). Liquid containing cell debris was transferred into 1.5 mL Eppendorf and centrifuged at 23 000g, 5 min at T=4°C. Supernatant was transferred into vials with inserts and stored at T=-21°C until analysis.

6.1.3.2 E. coli: Whole broth and Supernatant Sampling

E. coli K-12 MG1655 bacterial culture in exponential growth phase corresponding to 0.48 mg biomass (OD_{600}~1.3, 1 mL culture sampled) was used to prepare whole broth sample and filtrate (supernatant) sample. Whole broth sample was prepared by spraying culture broth with cells into pre-cooled 125 mM formic acid in 80% methanol at -20°C, V = 5 mL. Liquid was placed in 50 mL falcons in cryogenic bath. After placing whole broth into falcon, the mixture was briefly vortexed and placed on ice. Similarly, supernatant sample was prepared by spraying 1mL of filtered culture media into cold acidified methanol. Supernatant was produced by filtration of culture broth through a syringe filter (Sartorius Ministart polyamide filter, 0.2 µm). Isotopically enriched (*M. extorquens* 25µL*, E. coli* 50 µL) extract was used as internal standard. Quantitation of acyl-CoA in extracts was achieved by running a 7-point calibration curve. The absolute metabolite concentrations were determined by extrapolating ratio $^{12}C/^{13}C$ onto calibration curve analyzed together with each biological samples batch. All samples were evaporated overnight using SpeedVac (SC110A SpeedVac Plus, ThermoSavant, USA), re-solubilized in 100µL 25 mM ammonium formate with 2% methanol (pH = 3.5). Liquid containing cell

debris was transferred into 1.5 mL Eppendorf and centrifuged at 23 000g, 5 min at T=4°C. Supernatant was transferred into vials with inserts and stored at T=-21°C until analysis.

6.1.3.2.1 E. coli: Whole Broth and Supernatant Sampling with Isoleucine

E. coli K-12 was cultivated using robotic high-throughput platform as described by Heux et al., [221]. Samples were extracted and processed using acyl-CoA extraction protocol as described above.

6.1.4 Isotopic Profiling

6.1.4.1 Acyl-CoA isotopic profiling in E. coli

E. coli K-12 MG1655 bacterial culture in exponential growth phase corresponding to 0.48 mg biomass (OD_{600}~1.3, 1 mL culture sampled) was used to prepare whole broth samples for isotopic profiling of Acyl-CoAs.

Part of the cultivation broth (20 mL) was transferred into pre-heated plastic vessel with magnet placed onto magnetic stirrer to ensure proper aeration during short-term sampling. Isotopic instationary state was induced by single pulse of 1 mg/mL 99.9% U-[^{13}C-D-glucose] (Cambridge Isotope Laboratory, United Kingdom) pre-heated to 37°C. Final ratio between uniformly labeled glucose and non-labeled glucose was measured by ^{1}H-NMR to be 0.66, hence 66 % of consumed glucose was uniformly labeled and this is the maximum possible observable ratio in intracellular metabolites. Immediately after pulse introduction, 1mL of culture broth was sprayed into quenching and extraction solution (5 mL, 125 mM Formic acid in 80% aq. methanol) cooled to T = -20°C and placed on vortex to ensure immediate quench of enzymatic activity by rapid mixing. Falcon with quenched culture was placed on ice for 5 min. Whole broth samples were prepared in triplicates in following time points: 0s, 10s, 20s, 30s, 60s, 90s, 120s, 180s, 300s then at 10, 20, 30 and 60 minutes. In total, 39 samples were taken out of which 27 were taken in first 5 minutes. Precise time of quenching of the cell culture was read from camera footage. Due to very short time points at the beginning, samples are taken continuously every 2-3s. Three main metabolite groups were considered and separate analytical systems were used in isotopic analysis of amino acids (LC-HRMS) and organic acids/phosphorylated compounds (IC-MS/MS). All samples were evaporated overnight using SpeedVac (SC110A SpeedVac Plus, ThermoSavant, USA), re-solubilized in 100 µL 25 mM ammonium formate with 2% methanol (pH = 3.5). Liquid containing cell debris was transferred into 1.5 mL Eppendorf and centrifuged at 23 000g, 5 min at T= 4°C. Supernatant was transferred into vials with inserts and stored at T=-21°C until analysis.

6.1.5 Quantification of Amino Acids and Central Metabolites

E. coli K-12 MG1655 bacterial culture in exponential growth phase corresponding to 0.48mg biomass (OD_{600}~1.3, 1mL culture sampled) was used to prepare whole broth sample and filtrate (supernatant) sample. *E. coli* K-12 MG1655 cultivated as described above was sampled by whole broth as described with an exception, that quenching and extraction solution used was acetonitrile: methanol: 0.1% formic acid (2:2:1) cooled down to -20°C, V = 5 mL. Isotopically enriched standard of *E. coli* proteinogenic amino acids (100 µL) was used. Alternatively, for quantification of "central metabolites" (*i.e.* organic acids + phosphorylated sugars), 200 uL of isotopically enriched extract of *E. coli* was used. All samples were evaporated overnight using SpeedVac (SC110A SpeedVac Plus, ThermoSavant, USA), re-solubilized in 200µLwater (MilliQ). Liquid containing cell debris was transferred into 1.5 mL Eppendorf and centrifuged at 23 000g, 5 min at T=4°C. Supernatant was transferred into vials with inserts and stored at T=-21°C until analysis.

6.1.6 Calculation of Metabolite Intracellular Concentration in E. coli

Intracellular concentration was calculated by Eq.5. Cell growth was measured by monitoring the optical density at 600 nm (OD_{600}) in a spectrophotometer (Thermo Genesys 6). OD_{600} was converted into dry cellular weight (biomass concentration) using a standard curve (1 OD_{600} = 0.37 g/L of dry cellular weight)[222]. Intracellular volume was estimated to be 1.77mL per 1g dry weight[223].

$$c_{intra} = \frac{c\ [\mu M]}{1000} \times \frac{V_{sampled}}{\left(\frac{OD_{600} \times 0.37}{1000}\right) \times 1.77}$$ **Equation 5**

6.2 T. brucei PCF Cultivation

Procyclic EATRO1125.T7T, wild type (WT), null mutants of mitochondrial acetate: succinyl-CoA transferase (*Δasct*) and acetyl-CoA thioesterase (*Δach*) and their double mutant (*Δach/*^{RNAi}*ASCT)* induced for 5 days and non-induced (*Δach/*$^{RNAn.i}$*ASCT)* were grown at 27°C for 10 days in glucose rich media SDM-79 supplemented with 10% (*v/v*) heat-inactivated fetal calf serum and 35 µM hemin [224]. Composition of media SDM-79 detailed in Table 9. Gene knockouts and KO/RNAi cell lines were produced by replacement with blasticidin and puromicyn cassettes as described [36]. Prior to sample withdrawal, cell count was calculated via flow cytometry and motility of trypanosomes (and potential cell aggregates) were monitored with microscope and noted. All samplings were performed if viability was higher than 98%.

Table 9: Media SDM-79 composition

Complete composition of media used for cultivation of T. brucei PCF

Components	c [mM]
phenol red	0.031
NaCl	100.62
NaH2PO4.H2O	3.61
Mg SO4	0.34
KCl	4.64
CaCl2	0.28
Hepes	30.73
MOPS	23.89
ferric nitrate.9H2O	0.00037
Tween 80	0.0031
sodium acetate	0.122
L glutathione reduced	0.000033
D-ribose	0.00067
deoxy-D-ribose	0.00075
D-glucose	10.38
D-glucosamine.hcl	0.23
OH-proline	0.015
sodium pyruvate	0.897
L-threonine	3.42
L-arginine.hcl	1
L-methionine	0.6
L-phenylalanine	0.72
L-tyrosine	0.88
L-cysteine	0.00017
L-histidine.hcl.h20	0.19
L-isoleucine	0.45
L-leucine	0.52
L-lysine.hcl	0.42
L-tryptophane	0.064
L-valine	0.46
L-alanine	2.36
L-asparagine	0.68
L-aspartic acid	0.11
L-glutamic acid	0.13
L-serine	0.095
L-glycine	0.2
L-proline	5.34
L-glutamine	2.38
L-cystine	0.15
hypoxanthine	0.000514
xanthine.Na^+	0.0004
thymine	0.000476
adenine sulfate.2H2O	0.0055
adenosine	0.0374
guanine.hcl.2H2O	0.00268
guanosine	0.0353

Components	c [mM]
uracile	0.000535
cholesterol	0.0001
ascorbic acid	0.000057
ergocalciferol	0.00005
menadione	0.000012
niacin	0.000041
para-aminobenzoic acid	0.015
vit A acetate	0.000085
taurine	1.28
D-biotine	0.00083
choline chloride	0.0054
folic acid	0.0106
myo-inositol	0.0074
niacinamide	0.0055
Ca2+ d pantothenic acid	0.0014
pyridoxine.hcl	0.000024
pyridoxal.hcl	0.0032
riboflavine	0.00016
thiamine.2Cl	0.00162
FCS	10% (v/v)
DL-alpha-tocopherol-Na2PO4	0.0000035

6.2.1 T. brucei sample Collection

6.2.1.1 Fast Filtration

T. brucei EATRO 1125 cells were inoculated in SDM-79. Culture density did not exceed 2 × 10^7 cells/ mL at the time of sampling. Volume corresponding to 1 x 10^8 cells was directly filtered on a vacuum filtration unit through glass microfiber filter (Whatman, type GC/F, 25 mM diameter, and pore size 1.2 µm, Sigma-Aldrich). Layer of cells on the filter was washed with 1 mL of 10% of culture media SDM-79 diluted in PBS. Filter with layer of cells was wrapped in aluminum foil and rapidly placed into liquid nitrogen to quench metabolic activity. Sampling time from sample withdrawal until quenching did not exceed 8s on average. Two types of filters were initially tested – Whatman (type GF/C, 25 mM dimeter, pore size 1.2 µm) and Sartolon (cellulose polyamide, diameter 25 mM, pore size 0.45 µm), however filtration of 2 mL of culture media with cells in SDM-79 took more than 20s which was considered long enough for undesired changed in metabolic composition to occur in unquenched cells at room temperature. Thus, Whatman GF/C was used in every protocol involving sample collection by fast filtration.

Procyclic *T. brucei* EATRO1125.T7T was initially cultivated in SDM-79 until cell concentration approximately 2×10^7 cells/ mL was reached. In order to collect whole broth or supernatant which do not induce matrix effects, cells needed to be transferred from compound rich SDM-79 into PBS. Cells

were centrifuged (Multifuge Heratus 3L-R, Thermo Fisher Scientific) at 25°C, t = 10min, RCF = 987g. Supernatant was rapidly discarded and cell pellet was briefly washed with 2mL PBS supplemented with carbon sources. This washing solution was discarded and cells were re-suspended in PBS supplemented with carbon sources at cell density 2×10^7 cells/mL for 2-3hours. Filters with quenched cells were extracted in 5 mL 80% aq. methanol (or acetonitrile) with 125 mM formic acid cooled to T = -20°C, liquid with filter was thoroughly vortexed and incubated on ice for t=5 min.

All lyophilized samples were re-suspended in 100µL of 25 mM ammonium formate with 2% methanol (LC-MS grade). Sample was vortexed and sonicated (10s bursts) in 3cycles in order to dissolve the residues. Liquid was transferred into Eppendorf and centrifuged (t = 5 min, T = 4°C, RCF = 23 000; Sigma 3-18K centrifuge). Supernatant was transferred into glass vials and analyzed immediately or stored at -80°C until LC-MS analysis.

6.2.1.2 Quenching and Extraction in one Step

Procyclic *T. brucei* EATRO1125.T7T was initially cultivated in SDM-79 until cell concentration approximately 2×10^7 cells/ mL was reached. In order to collect whole broth or supernatant which do not induce matrix effects, cells needed to be transferred from compound rich SDM-79 into PBS. Cells were centrifuged (Multifuge Heratus 3L-R, Thermo Fisher Scientific) at 25°C, t = 10 min, RCF = 987 g. Supernatant was rapidly discarded and cell pellet was briefly washed with 2 mL PBS supplemented with carbon sources. This washing solution was discarded and cells were re-suspended in PBS supplemented with carbon sources at cell density 2×10^7 cells/mL for 2-3hours.

Whole broth sample collection was done by spraying 1×10^8 cultivation media with cells into 5 mL 80% aq. methanol with 125 mM formic acid cooled to T= -20°C. In practice, approximately 5 mL of culture broth was introduced into 5-fold of quenching and extraction solution in order to prevent thermic effect and insufficient quenching. In order to collect $4x10^8$ cells per sample, 4 samples were pooled together. Supernatant and cell pellet were obtained by centrifugation ((Multifuge Heratus 3L-R, Thermo Fisher Scientific) at 25°C, t = 10 min, RCF = 987g) of 4×10^8 cells. Both fractions pellet and supernatant were extracted in 5 mL, 25 mL respectively of 80% aq. methanol with 125 mM formic acid cooled to T = -20°C. Samples were thoroughly vortexed and incubated on ice for t=5 min. Afterwards, samples were lyophilized until dry and re-suspended with 100 µL 25 mM ammonium formate (pH = 3.5, 2% methanol). Internal standard, isotopically enriched extract of *M. extorquens* was added to each sample during sampling, total volume was 25 µL per $4x10^8$ cells in the sample. Acyl-CoA thioesters were analyzed with HPLC-HRMS (as detailed in chapter 6.4) and quantification was obtained by extrapolation of $^{12}C/^{13}C$ ratio onto calibration curve from set of 7 standard solutions.

6.3 Isotopically Enriched Standards

Two types of isotopically enriched standards were used in this work. Acyl-CoA extracts form *M.extorquens* used for quantification of acyl-CoA thioesters in *T. brucei*, grown on [1-^{13}C]-methanol was kindly provided by P.Kiefer.

6.4 IDMS E.coli

E. coli was cultivated in the same manner as described in subchapter 6.1.1 and 6.1.2, with exeption, that fully isotopically enriched glucose [U-^{13}C]-glucose (99% purity, Cambridge Isotope Laboratories, UK) was used in pre-cultivation and cultivation.

Bacteria broth corresponding to approx 1.8mg biomass was rapidly quenched in acidified methanol cooled down to -20°C, the mixture was vortexed and processed as described in subchapter 6.2.3. Since 5× the volume of culture broth was used, the volume of quenching and extraction solution was also 5× increased volume of quenching and extraction solution (*i.e.* 5 mL and 25 mL respectively). All lyophilized samples were re-suspended in 400µL of 25 mM ammonium formate with 2% methanol (LC-MS grade). Sample was vortexed and sonicated (10s bursts) in 3cycles in order to dissolve the residues. Liquid was transferred into Eppendorf and centrifuged (t = 5 min, T = 4°C, RCF = 23 000; Sigma 3-18K centrifuge). Supernatant was transferred into glass vials and analyzed immediately or stored at -80°C until LC-MS analysis.

Resuspended samples were collected, mixed together and aliqoted per 400uL into glass vials and stored in -80°C. Each vial was thawed only once prior to use.

6.5 Preparation of Solvents

Table 10: Preparation of quenching and extraction solution

	Value	SI unit
MetOH	0.24	L
water	0.06	L
Total	0.3	L
c formic acid	125	mM
V formic acid	1.415	mL
pH final (measured)	2.74	

Table 11: Preparation of resolubilization solution for Acyl-CoA thioesters

Adjusted to pH 3.0 – 3.5 for CoA storage.

	Value	SI unit
MetOH	0.002	L
water	0.098	L
Total	0.1	L
c formic acid	25	mM

V formic acid	0.09432377	mL
pH final (measured)	2.53	

6.6 HPLC-HRMS Analysis of Acyl-Coenzyme A Thioesters

Analysis of Coenzyme A thioesters was adapted from [141]. CoA thioesters are separated using Dionex UltiMate U3000 chromatographic system with UV/VIS detection equipped with guard column SecurityGuard Ultra (sub 2µm) and reversed phase C-18 column (Phenomenex Kinetex, 100mm×3mm, particle size 1.7µm) in gradient of 50 mM ammonium formate (adjusted to pH = 8.10 with ammonium hydroxide) and Methanol (LC-MS gr.) First two minutes of LC-MS eluent are diverted into waste via rheodyne 6-port switching valve followed by multi-step gradient lasting 36min. Mobile phase is always freshly prepared prior to analysis by adding formic acid into water (MILIQ quality, 18 mΩ) and titration with ammonium hydroxide until pH 8.1. Full loop injection was used, loop volume V = 5µL. Injection loop was washed with 50% methanol (LC-MS gr.). Samples were kept at temperature 4°C in autosampler.

Parameters of heated electrospray ion source were optimised by connecting HPLC eluent (98% 50 mM Ammonium formate, pH 8.10, 2% Methanol, flowrate 400 µL/min) and syringe pump with 10 µg/mL of each studied acyl-CoA thioester via T junction. The ion source parameters were as follows:

Table 12: Source parameters for Acyl-CoA thioesters analysis

Parameter	Value	Units
Ionisation mode	positive	-
Source temperature	250	°C
Capillary temp	275	°C
Sheath gas	50	U
Aux gas	10	U
Sweep gas	0	U
S lens level	70	%
Source voltage	4	kV

Table 13 : Acyl-CoA thioesters summary

Acyl-CoA	formula	m/z	[M+H]+	[U - 13C] acyl-CoA
CoA-SH	C21 H36 N7 O16 P3 S	767.1152079	768.122485	789.1929353
Acetyl-CoA	C23 H38 N7 O17 P3 S	809.1257725	810.133049	833.2102096
Acetoacetyl-CoA	C25 H40 N7 O18 P3 S	851.1363372	852.143614	877.2274838
Crotonyl-CoA	C25 H40 N7 O17 P3 S	835.1414226	836.148699	861.2325692
Malonyl-CoA	C24 H38 N7 O19 P3 S	853.1156017	854.122878	878.2033936
Methylmalonyl-CoA	C25 H40 N7 O19 P3 S	867.1312518	868.138528	893.2223984
Succinyl-CoA	C25 H40 N7 O19 P3 S	867.1312518	868.138528	893.2223984
3-HMG-CoA	C27 H44 N7 O20 P3 S	911.1574665	912.164743	939.2553228
Butyryl-CoA	C25 H42 N7 O17 P3 S	837.1570727	838.164349	863.2482193

OH-butyryl-CoA	C25 H42 N7 O18 P3 S	853.1519873	854.159264	879.2431339
Propionyl-CoA	C24 H40 N7 O17 P3 S	823.1414226	824.148699	848.2292144

Table 14: Elution gradient for Acyl-CoA thioesters

Time [min]	Flowrate [mL/min]	Mobile phase B [%]
0.0	0.4	2
2.0	0.4	2
23.0	0.4	25
23.1	0.4	95
28.0	0.4	95
28.1	0.4	2
36.0	0.4	2

Mass acquisition by furier transform mass spectrometry (FTMS) mode at resolution R=60 000 at m/z 400 was carried out using LTQ-OrbiTrap Velos (Thermo Fisher, company site, state) in positive full scan mode. LTQ-Orbitrap mass resolution in FTMS was calibrated every 3 days in running batch, or every time prior to starting analysis. Data acquisition by Xcalibur in centroid format and saved in .RAW format.

To exclude interrferences from matrix, sample blanks (only quenching and extractions solution processed in the same way as biological sample) were used. Aliquots of analyzed biological samples were pooled together to form a calibration standard (QC). Retention times of eluting peaks were not affected by high salt concentration from extraction solution due to redirection of first two minutes of HPLC eluent into waste.

6.7 HPLC-HRMS Analysis of Amino Acids

Quantitative analysis of free amino acid was developed by Maud Heuillet (LISBP-INSA de Toulouse). In this protocol amino acids are separated using pentafluorophenylpropyl silica (PFP) bound column. Dionex UltiMate U3000 coupled to mass spectrometer LTQ-Orbitrap (Thermo) are used for analysis.

HS F5 Discovery (150 × 2.1 mm, 5 µm particle size) was equipped with pre-column Supelguard kit HS F5 5µm (20×2.1 mm) both produced by Supelco (Pennsylvania, USA). Amino acids are separated in gradient of 0.1% formic acid in water (MILIQ quality, 18 mΩ) and 0.1% formic acid (pH 2.7) in acetonitrile (mobile phase B). Column compartment is tempered to 30°C, autosampler is tempered to 4°C. Injection loop of 50 µL was used to inject 20µL sample in partial mode. Injection loop was washed with 50% Methanol.

Table 15: Elution gradient for amino acids analysis

Time[min]	Flowrate [mL/min]	Mobile phase B [%]
0	0.25	2
2	0.25	2
10	0.25	5
16	0.25	35
20	0.25	100
24	0.25	100
24.1	0.25	2
30	0.25	2

Detection by LTQ-OrbiTrap Velos (Thermo Fisher) in full scan in positive mode. The ion source parameters are as follows:

Table 16: Source parameters for Amino acids analysis

Parameter	Value	Units
Ionisation mode	positive	-
Source temperature	250	°C
Capillary temp	275	°C
Sheath gas	45	U
Aux gas	20	U
Sweep gas	0	U
S lens level	40	%
Source voltage	5	kV

Table 17: Amino acids summary

Metabolite	Abbreviation	$[M+H]^+$	$[M+H]^+$ U-^{13}C	R_T [min]
Alanine	Ala	90,05480	93,06490	2,46
Arginine	Arg	175,1187	181,1389	3,69
Asparagine	Asn	133,0606	137,0741	2,15
Aspartate	Asp	134,0446	138,0580	2,15
Glutamate	Glu	148,0603	153,0771	2,42
Glutamine	Gln	147,0762	152,0930	2,23
Glycine	Gly	76,03930	78,04600	2,23
Histidine	His	156,0766	162,0967	3,25
Isoleucine	Ile	132,1018	138,1219	9,40
Leucine	Leu	132,1018	138,1219	10,70
Lysine	Lys	147,1127	153,1328	3,23
Methionine	Met	150,0582	155,0750	4,91
Phenylalanine	Phe	166,0859	175,1161	15,90
Proline	Pro	116,0703	121,0871	2,45

Metabolite	Abbreviation	$[M+H]^+$	$[M+H]^+$ U-^{13}C	R_T [min]
Serine	Ser	106,0498	109,0599	2,17
Threonine	Thr	120,0654	124,0788	2,32
Tryptophane	Trp	205,0966	216,1335	19,9
Tyrosine	Tyr	182,0810	191,1112	10,10
Valine	Val	118,0862	123,1030	4,45

6.8 IC-MS analysis of Organic Acids and Phosphorylated Compounds

Metabolic intermediates of glycolysis, TCA cycle and Pentose Phosphate pathway are quantitatively determined by ion chromatography coupled (Dionex ICS5000+, Dionex – now Thermo) to triple quadrupole (4000 Qtrap, AB Sciex) operating in multiple reactions monitoring mode (MRM) in negative mode. Analytes (anions) are separated in positively charged ion column (Dionex IonPac AS11, 250×2 mm) equipped with pre-column (Dionex AG11, 50×2 mm) in water (MILIQ quality, 18mΩ) and increasing concentration of OH- ions produced in potassium hydroxide cartridge (ECG III). Mobile phase flowrate is constant during analytical run at 035 mL/min. Column is tempered to 29°C. Ions from biological sample are supressed in supressor (ASRS-ULTRA II) maintaining ion current at 78 mA. Injection volume is 15 µL, injection loop is washed with water (MILIQ quality, 18 mΩ).

Table 18: Elution gradient in ion chromatography

Time[min]	Flowrate [mL/min]	Gradient of KOH [mM]
0	0.35	0.5
1	0.35	0.5
9.5	0.35	4.1
14.6	0.35	4.1
24	0.35	9.65
36	0.35	60
36.1	0.35	90
43	0.35	90
43.1	0.35	0.5
45	0.35	0.5

Table 19: Source settings

Parameter	Value	Units
Ionisation mode	negative	-
Scan type	MRM	-
Dwell time	25	ms
Pause	5.007	s
Duration	36.008	min
Nebulisation T	650	°C
Nebulizer gas pressure	50	psi
Desolvation gas pressure	60	psi
Source voltage	-3.3	kV

Table 20: MRM settings of IC-MS/MS analysis

Metabolites	Abbreviation	[M-H]-	MRM Transition	MRM Transition U-13C	DP	EP	CE	CXP
Fumarate	Fum	115,004	115/71	119/74	-30	-10	-15	-6
Succinate	Succ	117,019	117/73	121/76	-30	-10	-15	-6
Malate	Mala	133,014	133/71	137/74	-30	-10	-15	-6
Alfa-Ketoglutarate	Alfa-KG	145,015	145/101	150/105	-30	-6	-13	-6
Orotate	Oro	155,010	155/111	160/115	-28	-10	-29	-4
Phosphoenolpyruvate	PEP	166,975	167/79	170/79	-33	-4	-16	-6
Glycerol-3P	Gly3P	171,006	171/79	174/79	-35	-10	-22	-2
Cis-Aconitate	Cis-Aco	173,009	173/85	179/89	-35	-10	-28	-20
O-Phospho-L-Serine	P-Ser	183,800	184/97	187/97	-27	-3	-19	-7
2-Phosphoglycerate	2-PG	184,986	185/97	188/97	-30	-3	-22	-6
3-Phosphoglycerate	3-PG	184,986	185/97	188/97	-30	-3	-22	-6
Citrate	Cit	191,020	191/111	197/116	-35	-6	-20	-4
Isocitrate	IsoCit	191,020	191/111	197/116	-35	-6	-20	-4
Ribose-1P	R1P	229,012	229/97	234/97	-35	-8	-17	-6
Ribose-5P	Rib5P	229,012	229/97	234/97	-35	-8	-17	-6
Ribulose-5P	Ribu5P	229,012	229/97	234/97	-35	-8	-17	-6
Xylulose-5P	Xylu5P	229,012	229/97	234/97	-55	-10	-18	-5
Shikimate 3-Phosphate	Shiki3P	253,100	253/97	260/97	-35	-4	-22	-5
D-Glucosamine-6P	GluN-6P	258,000	258/97	264/97	-53	-8	-24	-5
Galactosamine-1P	GalacN-1P	258,000	258/79	264/79	-44	-10	-50	-2
Glucose-1P	G1P	259,022	259/97	265/97	-35	-10	-23	-6
Fructose-1P	F1P	259,022	259/97	265/97	-35	-10	-23	-6
Glucose-6P	G6P	259,022	259/97	265/97	-35	-10	-23	-6
Fructose-6P	F6P	259,022	259/97	265/97	-35	-10	-23	-6
Mannose-6P	Man6P	259,022	259/97	265/97	-35	-10	-23	-6
6-PhosphoGluconate	6-PG	275,017	275/97	281/97	-40	-10	-20	-6
Sedoheptulose-7P	Sed7P	289,030	289/97	296/97	-35	-8	-20	-6
N-acetyl-Glucosamine-1P	N-AcGluN-1P	301,000	300/79	308/79	-56	-8	-54	-5
N-acetyl-Glucosamine-6P	N-AcGluN-6P	301,000	300/79	308/97	-35	-3	-30	-5
Cytidine-5'-monophosphate	CMP	322,045	322/79	331/79	-60	-10	-40	-6
Uridine-5'-monophosphate	UMP	323,029	323/79	332/79	-70	-10	-70	-2
AMP cyclic	cAMP	328,045	328/134	338/139	-60	-6	-35	-6
Fructose-1,6-DP	FBP	338,989	339/97	345/97	-35	-10	-23	-6
GMP cyclic	cGMP	344,000	344/79	354/79	-65	-5	-70	-3
Adenosine 5'-monophosphate	AMP	346,056	346/79	356/79	-65	-10	-72	-1
Guanosine 5'-monophosphate	GMP	362,051	362/79	372/79	-55	-10	-42	-1
5-phosphoribosyl-pyrophosphate	PRPP	388,896	309/211	314/211	-35	-10	-20	-6
Cytidine Diphosphate	CDP	402,011	402/79	411/79	-65	-10	-100	-8
Uridine Diphosphate	UDP	402,995	403/79	412/79	-65	-10	-86	-2
Trehalose 6-Phosphate	Tre6P	421,200	421/79	433/79	-70	-8	-83	-5
Adenosine Diphosphate	ADP	426,022	426/79	436/79	-65	-10	-88	-2
Guanosine Diphosphate	GDP	442,017	442/79	452/79	-65	-10	-88	-2,11
Cytidine Triphosphate	CTP	481,977	482/79	491/79	-65	-10	-100	-6
Uridine Triphosphate	UTP	482,961	483/159	492/159	-55	-10	-40	-9
Adenosine Triphosphate	ATP	505,988	506/159	516/159	-70	-10	-50	-8
UDP-Glucose	UDP-Glu	565,048	565/79	580/79	-55	-10	-100	-1
ADP-Glucose	ADP-Glu	588,100	588/346	604/356	-50	-5	-35	-6
GDP-mannose	GDP-Man	604,200	604/79	620/79	-90	-9	-110	-5
UDP-acetylglucosamine	UDP-AcGluN	606,074	303/79	320/79	-44	-10	-75	-4
2-Hydroxy glutarate	2-OHGLu	146,800	147/103	152/107	-40	-8	-18	-7

6.9 Analysis of Extracellular Metabolites

E. coli supernatant harvested by filtraton of culture broth through syringe filter (Sartorius MiniStart syringe filter, celulose-acetate, pore size 0.2 µm). Subsequently, 1mL filtrate was frozen (corresponding to approx 0.37-0.55 mg biomass, T=-20°C) until NMR analysis. 540µL of sample diluted with 60 µL D_2O with 10mM TSP (Sigma-Aldrich, Germany), placed in glass tube (3mm diameter) and

analyzed by ^{1}H-NMR (500 MHz, Bruker). Total 36 scans were collected per sample, presaturation of the H_2O signal was performed using the zgpr30 Bruker sequence. After Fourier transformation, NMR spectra were phased, baselined and calibrated at 0ppm using TSP signal. Data were treated by TopSpin v3 and metabolites were quantified based on signal of TSP as internal standard.

6.10 Data Treatment Software

Acyl-CoA thioesters

Data were processed by TraceFinder (Thermo). Peak integration was carried out with ICIS algorithm, smoothing set to 5points, Data processing was within 5ppm mass range. Isotopic enrichment was calculated with IsoCor [44] to compensate for non-linearity of isotopic enrichment and natural abundance.

Amino Acids

Same as Acyl-CoA thioesters, but peak integration carried out with GENESIS algorithm in TraceFinder.

Organic acids and phosphorylated compounds

Data acquisition of Organic acids and phosphorylated compounds was done with Analyst software 1.5.2, data processing with Analyst 1.6 software.

6.11 Calculation of metabolic fluxes

The model was based on distribution of stable isotope of Carbon (^{13}C) introduced as a pulse of fully labelled glucose into culture of *E.coli* K-12 growing in exponential phase. Distribution of fluxes depends on the active metabolic pathways and type of input labelled molecule. The metabolic map of *E. coli* was based on model of central metabolic pathways [210] with addition of pathways contributing to coenzyme A metabolism originating from EcoCyc database search. The biomass fluxes (coding the endpoints of metabolism, metabolic sinks) were based on biomass requirements of *E. coli K-12* grown on glucose in aerobic conditions. Glucose consumption and acetate production was monitored during cells growth, measured using 1H-NMR and the resulting experimental flux (mmol/s/g biomass) was implemented into the model. The experimental data (i.e. carbon isotopologue distributions and metabolite pools) obtained from two biological replicates (*i.e.* two separate cultivations of *E.coli*) was implemented into mathematical model describing the metabolic network. Software used for metabolic flux application - "influx_si" was developed by Serguei Sokol (https://metasys.insa-toulouse.fr/software/influx/). In the scope of this work, the instationary fluxes were calculated from approximately 39 timepoints collected in 150seconds - *i.e* 39 ^{13}C isotopic ratios ranging from M0 (non-

labelled) to M_n (if n equals total number of carbons of a molecule, then molecule is fully ^{13}C labelled). All the labelling data obtained by mass spectrometry were corrected for natural abundance of ^{13}C using IsoCor[44] developed by Pierre Millard (http://metasys.insa-toulouse.fr/software/isocor/), the correction is a necessary prerequisite in order to obtain true metabolic fluxes as ^{13}C is a naturally occurring isotope. The ^{13}C ratios were collected for various types of molecules covering the central carbon metabolism – coenzyme A thioesters, free amino acids and components of the TCA cycle. Influx_i provides cumomer and EMU (elementary metabolite unit) nodes based on the input metabolic network which describes label distribution in metabolites. Influx_i uses ordinary differential equations (ODE) to calculate the statistically optimal condition of metabolic fluxes in order to obtain closest fit to with the measured carbon isotopologue distribution, the closeness of simulated and experimental data is characterized by $\chi 2$ statistical test. The procedure of "fitting" depends on the quality of the experimental MS data and size of metabolite pools. Series of reactions simulating ^{13}C label dilution with non-labelled metabolite were implemented in order to account for the type of sampling (whole broth) which caused under estimation of fluxes of TCA cycle due to large quantity of non-labelled organic acids found in the culture media.

Bibliography

1. Barrett, M. P., Boykin, D. W., Brun, R. & Tidwell, R. R. Human African trypanosomiasis: pharmacological re-engagement with a neglected disease. *Br. J. Pharmacol.* **152,** 1155–71 (2007).
2. Vickerman, K. Developmental cycles and biology of pathogenic Trypanosomes. *Br. Med. Bull.* **41,** 105–114 (1985).
3. Manna, P. T., Boehm, C., Leung, K. F., Natesan, S. K. & Field, M. C. Life and times: synthesis, trafficking, and evolution of VSG. *Trends Parasitol.* **30,** 251–8 (2014).
4. Roditi, I., Furger, a, Ruepp, S., Schürch, N. & Bütikofer, P. Unravelling the procyclin coat of Trypanosoma brucei. *Mol. Biochem. Parasitol.* **91,** 117–30 (1998).
5. Michels, P. M., Bringaud, F., Herman, M. & Hannaert, V. Metabolic functions of glycosomes in trypanosomatids. *Biochim. Biophys. Acta* **1763,** 1463–77 (2006).
6. Duffieux, F., Van Roy, J., Michels, P. a. M. & Opperdoes, F. Molecular characterization of the first two enzymes of the pentose-phosphate pathway of Trypanosoma brucei. Glucose-6-phosphate dehydrogenase and 6-phosphogluconolactonase. *J. Biol. Chem.* **275,** 27559–65 (2000).
7. Heise, N. & Opperdoes, F. Purification, localisation and characterisation of glucose-6-phosphate dehydrogenase of Trypanosoma brucei. *Mol. Biochem. Parasitol.* **99,** 21–32 (1999).
8. Stoffel, S. *et al.* Transketolase in Trypanosoma brucei. *Mol. Biochem. Parasitol.* **179,** 1–7 (2011).
9. Lee, S. H., Stephens, J. L. & Englund, P. T. A fatty-acid synthesis mechanism specialized for parasitism. *Nat. Rev. Microbiol.* **5,** 287–97 (2007).
10. Lee, S. H., Stephens, J. L., Paul, K. S. & Englund, P. T. Fatty acid synthesis by elongases in trypanosomes. *Cell* **126,** 691–9 (2006).
11. Krauth-Siegel, R. L. & Comini, M. a. Redox control in trypanosomatids, parasitic protozoa with trypanothione-based thiol metabolism. *Biochim. Biophys. Acta* **1780,** 1236–48 (2008).
12. Lindon, J. C. & Nicholson, J. K. Analytical technologies for metabonomics and metabolomics, and multi-omic information recovery. *TrAC - Trends Anal. Chem.* **27,** 194–204 (2008).
13. Mashego, M. R. *et al.* Microbial metabolomics: past, present and future methodologies. *Biotechnol. Lett.* **29,** 1–16 (2007).
14. Reaves, M. L. & Rabinowitz, J. D. Metabolomics in systems microbiology. *Curr. Opin. Biotechnol.* **22,** 17–25 (2011).
15. Bringaud, F. *et al.* Combining reverse genetics and NMR-based metabolomics unravels trypanosome-specific metabolic pathways. *Mol. Microbiol.* n/a–n/a (2015). doi:10.1111/mmi.12990
16. Beverley, S. M. Protozomics: trypanosomatid parasite genetics comes of age. *Nat. Rev. Genet.* **4,** 11–19 (2003).
17. Fiehn, O. Metabolomics–the link between genotypes and phenotypes. *Plant Mol. Biol.* **48,** 155–171 (2002).
18. Allen, J. *et al.* High-throughput classification of yeast mutants for functional genomics using metabolic footprinting. *Nat. Biotechnol.* **21,** 692–696 (2003).
19. Millard, P., Sokol, S., Letisse, F. & Portais, J.-C. IsoDesign: A software for optimizing the design of 13C-metabolic flux analysis experiments. *Biotechnol. Bioeng.* (2013).
20. Bolten, C. J., Kiefer, P., Letisse, F., Portais, J.-C. & Wittmann, C. Sampling for Metabolome Analysis of Microorganisms. *Anal. Chem.* **79,** 3843–3849 (2007).
21. Paczia, N. *et al.* Extensive exometabolome analysis reveals extended overflow metabolism in various microorganisms. *Microb. Cell Factories* **11,** 122 (2012).
22. Wittmann, C., Krömer, J. O., Kiefer, P., Binz, T. & Heinzle, E. Impact of the cold shock phenomenon on quantification of intracellular metabolites in bacteria. *Anal. Biochem.* **327,** 135–9 (2004).
23. Taymaz-Nikerel, H. *et al.* Development and application of a differential method for reliable metabolome analysis in Escherichia coli. *Anal. Biochem.* **386,** 9–19 (2009).

24. Duportet, X., Aggio, R. B. M., Carneiro, S. & Villas-Bôas, S. G. The biological interpretation of metabolomic data can be misled by the extraction method used. *Metabolomics* **8,** 410–421 (2012).
25. Creek, D. J., Anderson, J., McConville, M. J. & Barrett, M. P. Metabolomic analysis of trypanosomatid protozoa. *Mol. Biochem. Parasitol.* **181,** 73–84 (2012).
26. Allmann, S. *et al.* Cytosolic NADPH homeostasis in glucose-starved procyclic Trypanosoma brucei relies on malic enzyme and the pentose phosphate pathway fed by gluconeogenic flux. *J. Biol. Chem.* **288,** 18494–505 (2013).
27. Ebikeme, C. *et al.* Ablation of succinate production from glucose metabolism in the procyclic trypanosomes induces metabolic switches to the glycerol 3-phosphate/dihydroxyacetone phosphate shuttle and to proline metabolism. *J. Biol. Chem.* **285,** 32312–24 (2010).
28. Douma, R. D. *et al.* Intracellular metabolite determination in the presence of extracellular abundance: Application to the penicillin biosynthesis pathway in Penicillium chrysogenum. *Biotechnol. Bioeng.* **107,** 105–15 (2010).
29. Burgess, K. E. V., Creek, D., Dewsbury, P., Cook, K. & Barrett, M. P. Semi-targeted analysis of metabolites using capillary-flow ion chromatography coupled to high-resolution mass spectrometry. *Rapid Commun. Mass Spectrom. RCM* **25,** 3447–52 (2011).
30. Vincent, I. M. *et al.* Untargeted metabolomics reveals a lack of synergy between nifurtimox and eflornithine against Trypanosoma brucei. *PLoS Negl. Trop. Dis.* **6,** e1618 (2012).
31. van Gulik, W. M. Fast sampling for quantitative microbial metabolomics. *Curr. Opin. Biotechnol.* **21,** 27–34 (2010).
32. T'Kindt, R. *et al.* Towards an unbiased metabolic profiling of protozoan parasites: optimisation of a Leishmania sampling protocol for HILIC-orbitrap analysis. *Anal. Bioanal. Chem.* **398,** 2059–69 (2010).
33. Scheltema, R. A. *et al.* Increasing the mass accuracy of high-resolution LC-MS data using background ions: a case study on the LTQ-Orbitrap. *Proteomics* **8,** 4647–4656 (2008).
34. Rivière, L. *et al.* Acetate produced in the mitochondrion is the essential precursor for lipid biosynthesis in procyclic trypanosomes. *Proc. Natl. Acad. Sci. U. S. A.* **106,** 12694–9 (2009).
35. Millerioux, Y. *et al.* The threonine degradation pathway of the Trypanosoma brucei procyclic form: the main carbon source for lipid biosynthesis is under metabolic control. *Mol. Microbiol.* **90,** 114–29 (2013).
36. Millerioux, Y. *et al.* ATP synthesis-coupled and -uncoupled acetate production from acetyl-CoA by mitochondrial acetate:succinate CoA-transferase and acetyl-CoA thioesterase in Trypanosoma. *J. Biol. Chem.* **287,** 17186–97 (2012).
37. Mazet, M. *et al.* Revisiting the central metabolism of the bloodstream forms of Trypanosoma brucei: production of acetate in the mitochondrion is essential for parasite viability. *PLoS Negl. Trop. Dis.* **7,** e2587 (2013).
38. Patti, G. J. Separation strategies for untargeted metabolomics. *J. Sep. Sci.* **34,** 3460–3469 (2011).
39. Bharti, A., Ma, P. C. & Salgia, R. Biomarker discovery in lung cancer–promises and challenges of clinical proteomics. *Mass Spectrom. Rev.* **26,** 451–466 (2009).
40. Zhang, A., Sun, H., Wang, P., Han, Y. & Wang, X. Modern analytical techniques in metabolomics analysis. *The Analyst* **137,** 293–300 (2012).
41. Lämmerhofer, M. & Weckwerth, W. *NMR-based metabolomics analysis*. (2013).
42. Sumner, L. W. *et al.* Proposed minimum reporting standards for chemical analysis Chemical Analysis Working Group (CAWG) Metabolomics Standards Initiative (MSI). *Metabolomics Off. J. Metabolomic Soc.* **3,** 211–221 (2007).
43. Kiefer, P., Nicolas, C., Letisse, F. & Portais, J.-C. Determination of carbon labeling distribution of intracellular metabolites from single fragment ions by ion chromatography tandem mass spectrometry. *Anal. Biochem.* **360,** 182–8 (2007).
44. Millard, P., Letisse, F., Sokol, S. & Portais, J.-C. IsoCor: correcting MS data in isotope labeling experiments. *Bioinforma. Oxf. Engl.* **28,** 1294–6 (2012).

45. Creek, D. J. *et al.* Stable isotope-assisted metabolomics for network-wide metabolic pathway elucidation. *Anal. Chem.* **84,** 8442–8447 (2012).
46. Fan, T. W. M. & Lane, A. N. Structure-based profiling of metabolites and isotopomers by NMR. *Prog. Nucl. Magn. Reson. Spectrosc.* **52,** 69–117 (2008).
47. Massou, S., Nicolas, C., Letisse, F. & Portais, J.-C. NMR-based fluxomics: quantitative 2D NMR methods for isotopomers analysis. *Phytochemistry* **68,** 2330–40 (2007).
48. Durieux, P. O., Schutz, P., Brun, R. & Kohler, P. Alterations in Krebs cycle enzyme activities and carbohydrate catabolism in two strains of Trypanosoma brucei during in vitro differentiation of their bloodstream to procyclic stages. *Mol. Biochem. Parasitol.* **45,** (1991).
49. Turrens, J. F. The role of succinate in the respiratory chain of Trypanosoma brucei procyclic trypomastigotes. *Biochem. J.* **259,** 363–8 (1989).
50. Tielens, A. G. M. & Van Hellemond, J. J. More differences in energy metabolism between trypanosomatidae - Reply. *Parasitol. Today* **15,** 347–348 (1999).
51. Besteiro, S. *et al.* Succinate secreted by Trypanosoma brucei is produced by a novel and unique glycosomal enzyme, NADH-dependent fumarate reductase. *J. Biol. Chem.* **277,** 38001–12 (2002).
52. van Weelden, S. W. H. *et al.* Procyclic Trypanosoma brucei do not use Krebs cycle activity for energy generation. *J. Biol. Chem.* **278,** 12854–63 (2003).
53. Coustou, V. *et al.* Fumarate is an essential intermediary metabolite produced by the procyclic Trypanosoma brucei. *J. Biol. Chem.* **281,** 26832–46 (2006).
54. van Weelden, S. W. H., Van Hellemond, J. J., Opperdoes, F. R. & Tielens, A. G. M. New functions for parts of the Krebs cycle in procyclic Trypanosoma brucei, a cycle not operating as a cycle. *J. Biol. Chem.* **280,** 12451–60 (2005).
55. Coustou, V. *et al.* ATP generation in the Trypanosoma brucei procyclic form: cytosolic substrate level is essential, but not oxidative phosphorylation. *J. Biol. Chem.* **278,** 49625–35 (2003).
56. Deramchia, K. *et al.* Contribution of pyruvate phosphate dikinase in the maintenance of the glycosomal ATP/ADP balance in the Trypanosoma brucei procyclic form. *J. Biol. Chem.* **289,** 17365–78 (2014).
57. Coustou, V. *et al.* A mitochondrial NADH-dependent fumarate reductase involved in the production of succinate excreted by procyclic Trypanosoma brucei. *J. Biol. Chem.* **280,** 16559–70 (2005).
58. Coustou, V. *et al.* Glucose-induced remodeling of intermediary and energy metabolism in procyclic Trypanosoma brucei. *J. Biol. Chem.* **283,** 16342–54 (2008).
59. Spitznagel, D. *et al.* Alanine aminotransferase of Trypanosoma brucei--a key role in proline metabolism in procyclic life forms. *FEBS J.* **276,** 7187–99 (2009).
60. Rivière, L. *et al.* Acetyl:succinate CoA-transferase in procyclic Trypanosoma brucei. Gene identification and role in carbohydrate metabolism. *J. Biol. Chem.* **279,** 45337–46 (2004).
61. Opperdoes, F. R. Compartmentation of carbohydrate metabolism in Trypanosomes. *Annu. Rev. Microbiol.* **41,** 127–151 (1987).
62. Bakker, B. M. *et al.* Compartmentation protects trypanosomes from the dangerous design of glycolysis. *Proc. Natl. Acad. Sci. U. S. A.* **97,** 2087–92 (2000).
63. Gualdrón-López, M. *et al.* When, how and why glycolysis became compartmentalised in the Kinetoplastea. A new look at an ancient organelle. *Int. J. Parasitol.* **42,** 1–20 (2012).
64. Barrett, M. P. The pentose phosphate pathway and parasitic protozoa. *Parasitol. Today Pers. Ed* **13,** 11–16 (1997).
65. Balogun, R. A. Studies on the amino acids of the tsetse fly, Glossina morsitans, maintained on in vitro and in vivo feeding systems. *Comp. Biochem. Physiol. A* **49,** 215–222 (1974).
66. Shameer, S. *et al.* TrypanoCyc : a community-led biochemical pathways database for Trypanosoma brucei. *Nucleic Acids Res.* **43,** 637–644 (2015).
67. Wittmann, C. & Portais, J.-C. Metabolic Flux Analysis. in *Metabolomics in Practice* (eds. Lämmerhofer, M. & Weckwerth, W.) 285–312 (Wiley-VCH Verlag GmbH & Co. KGaA, 2013).

68. Wittmann, C. & Portais, J.-C. Metabolic Flux Analysis. in *Metabolomics in Practice* 285–312 (Wiley-VCH Verlag GmbH & Co. KGaA, 2013).
69. Lee, C.-Y. G. Co-purification of coenzyme-dependent enzymes by affinity chromatography. *Mol. Cell. Biochem.* **57,** 27–40 (1983).
70. Begley, T. P., Kinsland, C. & Strauss, E. The biosynthesis of coenzyme A in bacteria. *Vitam. Horm.* **61,** 157–71 (2001).
71. Keseler, I. M. *et al.* EcoCyc: fusing model organism databases with systems biology. *Nucleic Acids Res.* **41,** D605–D612 (2013).
72. Ruderman, N. B., Saha, A. K., Vavvas, D. & Witters, L. A. Malonyl-CoA, fuel sensing, and insulin resistance. *Am. J. Physiol.-Endocrinol. Metab.* **276,** E1–E18 (1999).
73. McGarry, J. D. Dysregulation of fatty acid metabolism in the etiology of type 2 diabetes. *Diabetes* **51,** 7–18 (2002).
74. Walker, K., Fujisaki, S., Long, R. & Croteau, R. Molecular cloning and heterologous expression of the C-13 phenylpropanoid side chain-CoA acyltransferase that functions in Taxol biosynthesis. *Proc. Natl. Acad. Sci.* **99,** 12715–12720 (2002).
75. Koetsier, M. J., Jekel, P. A., van den Berg, M. A., Bovenberg, R. A. L. & Janssen, D. B. Characterization of a phenylacetate–CoA ligase from Penicillium chrysogenum. *Biochem. J.* **417,** 467–476 (2009).
76. Kocharin, K., Siewers, V. & Nielsen, J. Improved polyhydroxybutyrate production by Saccharomyces cerevisiae through the use of the phosphoketolase pathway. *Biotechnol. Bioeng.* **110,** 2216–2224 (2013).
77. Szutowicz, A., Bielarczyk, H., Jankowska-Kulawy, A., Pawełczyk, T. & Ronowska, A. Acetyl-CoA the Key Factor for Survival or Death of Cholinergic Neurons in Course of Neurodegenerative Diseases. *Neurochem. Res.* **38,** 1523–1542 (2013).
78. Darnell, M. & Weidolf, L. Metabolism of xenobiotic carboxylic acids: Focus on coenzyme a conjugation, reactivity, and interference with lipid metabolism. *Chem. Res. Toxicol.* **26,** 1139–1155 (2013).
79. Knights, K. M. & Drogemuller, C. J. Xenobiotic-CoA Ligases : Kinetic and Molecular Characterization. 49–66 (2000).
80. Fasman, G. D. *Handbook of Biochemistry and Molecular Biology: Physical and Chemical Data*. (CRC Press, 1976).
81. Theodoulou, F. L., Sibon, O. C. M., Jackowski, S. & Gout, I. Coenzyme A and its derivatives: renaissance of a textbook classic. *Biochem. Soc. Trans.* **42,** 1025–1032 (2014).
82. Leonardi, R., Zhang, Y.-M., Rock, C. O. & Jackowski, S. Coenzyme A: back in action. *Prog. Lipid Res.* **44,** 125–53 (2005).
83. Spry, C., Kirk, K. & Saliba, K. J. Coenzyme A biosynthesis: an antimicrobial drug target. *FEMS Microbiol. Rev.* **32,** 56–106 (2008).
84. Lipmann, F. A Long Life in Times of Great Upheaval. *Annu. Rev. Biochem.* **53,** 1–34 (1984).
85. Haynes, C. a. Analysis of mammalian fatty acyl-coenzyme A species by mass spectrometry and tandem mass spectrometry. *Biochim. Biophys. Acta* **1811,** 663–8 (2011).
86. Zimmermann, M., Thormann, V., Sauer, U. & Zamboni, N. Nontargeted Profiling of Coenzyme A thioesters in biological samples by tandem mass spectrometry. *Anal. Chem.* **85,** 8284–8290 (2013).
87. Magnes, C. *et al.* Validated Comprehensive Analytical Method for Quantification of Coenzyme A Activated Compounds in Biological Tissues by Online Solid-Phase Extraction LC/MS/MS. *Anal. Chem.* **80,** 5736–5742 (2008).
88. Yun, M. *et al.* Structural Basis for the Feedback Regulation of Escherichia coli Pantothenate Kinase by Coenzyme A. *J. Biol. Chem.* **275,** 28093–28099 (2000).
89. Ivey, R. A. *et al.* The Structure of the Pantothenate Kinase·ADP·Pantothenate Ternary Complex Reveals the Relationship between the Binding Sites for Substrate, Allosteric Regulator, and Antimetabolites. *J. Biol. Chem.* **279,** 35622–35629 (2004).

90. Strauss, E., Kinsland, C., Ge, Y., McLafferty, F. W. & Begley, T. P. Phosphopantothenoylcysteine synthetase from Escherichia coli. Identification and characterization of the last unidentified coenzyme A biosynthetic enzyme in bacteria. *J. Biol. Chem.* **276,** 13513–13516 (2001).
91. Ottenhof, H. H. *et al.* Organisation of the pantothenate (vitamin B5) biosynthesis pathway in higher plants. *Plant J.* **37,** 61–72 (2004).
92. Raman, S. B. & Rathinasabapathi, B. Pantothenate synthesis in plants. *Plant Sci.* **167,** 961–968 (2004).
93. Tahiliani, A. G. & Beinlich, C. J. Pantothenic Acid in Health and Disease1. in *Vitamins & Hormones* (ed. Aurbach, G. D.) **46,** 165–228 (Academic Press, 1991).
94. Genschel, U. Coenzyme A biosynthesis: Reconstruction of the pathway in archaea and an evolutionary scenario based on comparative genomics. *Mol. Biol. Evol.* **21,** 1242–1251 (2004).
95. Saliba, K. J., Ferru, I. & Kirk, K. Provitamin B5 (pantothenol) inhibits growth of the intraerythrocytic malaria parasite. *Antimicrob. Agents Chemother.* **49,** 632–637 (2005).
96. Fletcher, S. *et al.* Biological characterization of chemically diverse compounds targeting the Plasmodium falciparum coenzyme A synthesis pathway. *Parasit. Vectors* **9,** 589 (2016).
97. Gerdes, S. *et al.* Plant B vitamin pathways and their compartmentation: a guide for the perplexed. *J. Exp. Bot.* **63,** 5379–5395 (2012).
98. Neuburger, M., Day, D. A. & Douce, R. Transport of coenzyme A in plant mitochondria. *Arch. Biochem. Biophys.* **229,** 253–258 (1984).
99. Prohl, C. *et al.* The yeast mitochondrial carrier Leu5p and its human homologue Graves' disease protein are required for accumulation of coenzyme A in the matrix. *Mol. Cell. Biol.* **21,** 1089–1097 (2001).
100. Vallari, D. S. & Jackowski, S. Biosynthesis and degradation both contribute to the regulation of coenzyme A content in Escherichia coli. *J. Bacteriol.* **170,** 3961–3966 (1988).
101. McLennan, A. G. The Nudix hydrolase superfamily. *Cell. Mol. Life Sci. CMLS* **63,** 123–143 (2006).
102. Xu, W., Dunn, C. A., O'Handley, S. F., Smith, D. L. & Bessman, M. J. Three New Nudix Hydrolases from Escherichia coli. *J. Biol. Chem.* **281,** 22794–22798 (2006).
103. Kleinkauf, H. The role of 4'-phosphopantetheine in t' biosynthesis of fatty acids, polyketides and peptides. *BioFactors Oxf. Engl.* **11,** 91–92 (2000).
104. Powell, G. L., Elovson, J. & Vagelos, P. R. Acyl carrier protein. XII. Synthesis and turnover of the prosthetic group of acyl carrier protein in vivo. *J. Biol. Chem.* **244,** 5616–24 (1969).
105. Jackowski, S., Edwards, H. H., Davis, D. & Rock, C. O. Localization of acyl carrier protein in Escherichia coli. *J. Bacteriol.* **162,** 5–8 (1985).
106. Vanaman, T. C., Wakil, S. J. & Hill, R. L. The Complete Amino Acid Sequence of the Acyl Carrier Protein of Escherichia coli. *J. Biol. Chem.* **243,** 6420–6431 (1968).
107. Lambalot, R. H. *et al.* A new enzyme superfamily - the phosphopantetheinyl transferases. *Chem. Biol.* **3,** 923–936 (1996).
108. Schulz, H. Beta oxidation of fatty acids. *Biochim. Biophys. Acta BBA - Lipids Lipid Metab.* **1081,** 109–120 (1991).
109. Færgeman, N. J. & Knudsen, J. Role of long-chain fatty acyl-CoA esters in the regulation of metabolism and in cell signalling. *Biochem. J.* **323,** 1–12 (1997).
110. Berriman, M. *et al.* The genome of the African trypanosome Trypanosoma brucei. *Science* **309,** 416–22 (2005).
111. Vidali, G., Gershey, E. L. & Allfrey, V. G. Chemical studies of histone acetylation. The distribution of epsilon-N-acetyllysine in calf thymus histones. *J. Biol. Chem.* **243,** 6361–6366 (1968).
112. Shahbazian, M. D. & Grunstein, M. Functions of Site-Specific Histone Acetylation and Deacetylation. *Annu. Rev. Biochem.* **76,** 75–100 (2007).
113. Kim, S. C. *et al.* Substrate and functional diversity of lysine acetylation revealed by a proteomics survey. *Mol. Cell* **23,** 607–618 (2006).
114. Hollebeke, J., Van Damme, P. & Gevaert, K. N-terminal acetylation and other functions of Nα-acetyltransferases. *Biol. Chem.* **393,** 291–298 (2012).

115. Pietrocola, F., Galluzzi, L., Bravo-San Pedro, J. M., Madeo, F. & Kroemer, G. Acetyl Coenzyme A: A Central Metabolite and Second Messenger. *Cell Metab.* **21,** 805–821 (2015).
116. Rock, C. O., Park, H.-W. & Jackowski, S. Role of Feedback Regulation of Pantothenate Kinase (CoaA) in Control of Coenzyme A Levels in Escherichia coli. *J. Bacteriol.* **185,** 3410–3415 (2003).
117. Vallari, D. S., Jackowski, S. & Rock, C. O. Regulation of pantothenate kinase by coenzyme A and its thioesters. *J. Biol. Chem.* **262,** 2468–2471 (1987).
118. Uttaro, A. D. Acquisition and biosynthesis of saturated and unsaturated fatty acids by trypanosomatids. *Mol. Biochem. Parasitol.* **196,** 61–70 (2014).
119. Tielens, a G. M., Van Grinsven, K. W. a, Henze, K., van Hellemond, J. J. & Martin, W. Acetate formation in the energy metabolism of parasitic helminths and protists. *Int. J. Parasitol.* **40,** 387–397 (2010).
120. van Hellemond, J. J., Opperdoes, F. R. & Tielens, A. G. M. Trypanosomatidae produce acetate via a mitochondrial acetate : succinate CoA transferase. **95,** 3036–3041 (1998).
121. Ong, H. B., Lee, W. S., Patterson, S., Wyllie, S. & Fairlamb, A. H. Homoserine and quorum-sensing acyl homoserine lactones as alternative sources of threonine: a potential role for homoserine kinase in insect-stage Trypanosoma brucei. *Mol. Microbiol.* **95,** 143–156 (2015).
122. Millerioux, Y. Etude fonctionnelle du métabolisme de l'acétyl-CoA chez Trypanosoma brucei. (Université Bordeaux Segalen, 2013).
123. Ferguson, M. A., Low, M. G. & Cross, G. A. Glycosyl-sn-1,2-dimyristylphosphatidylinositol is covalently linked to Trypanosoma brucei variant surface glycoprotein. *J. Biol. Chem.* **260,** 14547–14555 (1985).
124. Morita, Y. S. Specialized Fatty Acid Synthesis in African Trypanosomes: Myristate for GPI Anchors. *Science* **288,** 140–143 (2000).
125. Smith, T. K. & Bütikofer, P. Lipid metabolism in Trypanosoma brucei. *Mol. Biochem. Parasitol.* **172,** 66–79 (2010).
126. Allmann, S. *et al.* Triacylglycerol Storage in Lipid Droplets in Procyclic Trypanosoma brucei. 1–22 (2014). doi:10.1371/journal.pone.0114628
127. Stephens, J. L., Lee, S. H., Paul, K. S. & Englund, P. T. Mitochondrial fatty acid synthesis in Trypanosoma brucei. *J. Biol. Chem.* **282,** 4427–4436 (2007).
128. Vigueira, P. a & Paul, K. S. Requirement for acetyl-CoA carboxylase in Trypanosoma brucei is dependent upon the growth environment. *Mol. Microbiol.* **80,** 117–132 (2011).
129. Aslett, M. *et al.* TriTrypDB: a functional genomic resource for the Trypanosomatidae. *Nucleic Acids Res.* **38,** D457–D462 (2010).
130. Barber, M. C., Price, N. T. & Travers, M. T. Structure and regulation of acetyl-CoA carboxylase genes of metazoa. *Biochim. Biophys. Acta* **1733,** 1–28 (2005).
131. Guler, J. L., Kriegova, E., Smith, T. K., Lukes, J. & Englund, P. T. Mitochondrial fatty acid synthesis is required for normal mitochondrial morphology and function in Trypanosoma brucei. *Mol. Microbiol.* **67,** 1125–1142 (2008).
132. Zhou, W., Cross, G. A. M. & Nes, W. D. Cholesterol import fails to prevent catalyst-based inhibition of ergosterol synthesis and cell proliferation of Trypanosoma brucei. *J. Lipid Res.* **48,** 665–673 (2007).
133. Coppens, I. & Courtoy, P. J. Exogenous and endogenous sources of sterols in the culture-adapted procyclic trypomastigotes of Trypanosoma brucei. *Mol. Biochem. Parasitol.* **73,** 179–188 (1995).
134. Mazet, M. *et al.* The characterization and evolutionary relationships of a trypanosomal thiolase. *Int. J. Parasitol.* **41,** 1273–83 (2011).
135. Pena-Diaz, J. *et al.* Mitochondrial localization of the mevalonate pathway enzyme 3-hydroxy-3-methyl-glutaryl-CoA reductase in the trypanosomatidae. *Mol. Biol. Cell* **15,** 1356–1363 (2004).
136. Heise, N. & Opperdoes, F. R. Localisation of a 3-hydroxy-3-methylglutaryl-coenzyme A reductase in the mitochondrial matrix of Trypanosoma brucei procyclics. *Z. Naturforschung C- J. Biosci.* **55,** 473–477 (2000).

137. Ginger, M. L., Chance, M. L., Sadler, I. H. & Goad, L. J. The biosynthetic incorporation of the intact leucine skeleton into sterol by the trypanosomatid Leishmania mexicana. *J. Biol. Chem.* **276,** 11674–11682 (2001).
138. Nes, C. R. *et al.* Novel sterol metabolic network of Trypanosoma brucei procyclic and bloodstream forms. *Biochem. J.* **443,** 267–77 (2012).
139. Shah, T. D., Hickey, M. C., Capasso, K. E. & Palenchar, J. B. The characterization of a unique Trypanosoma brucei β-hydroxybutyrate dehydrogenase. *Mol. Biochem. Parasitol.* **179,** 100–106 (2011).
140. Lamour, N. *et al.* Proline metabolism in procyclic Trypanosoma brucei is down-regulated in the presence of glucose. *J. Biol. Chem.* **280,** 11902–10 (2005).
141. Peyraud, R. *et al.* Demonstration of the ethylmalonyl-CoA pathway by using 13C metabolomics. *Proc. Natl. Acad. Sci. U. S. A.* **106,** 4846–51 (2009).
142. Jackowski, S. & Rock, C. O. Metabolism of 4'-phosphopantetheine in Escherichia coli. *J. Bacteriol.* **158,** 115–120 (1984).
143. Jackowski, S. & Rock, C. O. Regulation of coenzyme A biosynthesis. *J. Bacteriol.* **148,** 926–932 (1981).
144. King, M. T. & Reiss, P. D. Separation and Measurement Rat Liver by Reversed-Phase of Short-Chain Coenzyme-A Compounds Liquid Chromatography in. **179,** 173–179 (1985).
145. King, M. T., Reiss, P. D. & Cornell, N. W. Determination of short-chain coenzyme A compounds by reversed-phase high-performance liquid chromatography. *Methods Enzymol.* **166,** 70–79 (1988).
146. Hosokawa, Y., Shimomura, Y., Harris, R. A. & Ozawa, T. Determination of short-chain acyl-coenzyme A esters by high-performance liquid chromatography. *Anal. Biochem.* **153,** 45–49 (1986).
147. Demoz, A., Garras, A., Asiedu, D. K., Netteland, B. & Berge, R. K. Rapid method for the separation and detection of tissue short-chain coenzyme A esters by reversed-phase high-performance liquid chromatography. *J. Chromatogr. B. Biomed. Sci. App.* **667,** 148–152 (1995).
148. Corkey, B. E., Brandt, M., Williams, R. J. & Williamson, J. R. Assay of short-chain acyl coenzyme A intermediates in tissue extracts by high-pressure liquid chromatography. *Anal. Biochem.* **118,** 30–41 (1981).
149. Deutsch, J., Grange, E., Rapoport, S. I. & Purdon, A. D. Isolation and quantitation of long-chain Acyl-Coenzyme A esters in brain tissue by Solid Phase Extraction. *Anal. Biochem.* (1994).
150. Larson, T. R. & Graham, I. a. Application of a new method for the sensitive detection and quantification of acyl-CoA esters in Arabidopsis thaliana seedlings and mature leaves. *Biochem. Soc. Trans.* **28,** 575–7 (2000).
151. Larson, T. R. & Graham, I. A. Technical Advance: A novel technique for the sensitive quantification of acyl CoA esters from plant tissues. *Plant J.* **25,** 115–125 (2001).
152. Tamvakopoulos, C. S. & Anderson, V. E. Detection of acyl-coenzyme A thioester intermediates of fatty acid beta-oxidation as the N-acylglycines by negative-ion chemical ionization gas chromatography-mass spectrometry. *Anal. Biochem.* **200,** 381–387 (1992).
153. Jiang, Y., Nikolau, B. & Ma, Y. Separation and quantification of short-chain coenzyme A in plant tissues by capillary electrophoresis with laser-induced fluorescence detection. *Anal. Methods* **2,** 1900–1904 (2010).
154. Liu, G., Chen, J., Che, P. & Ma, Y. Separation and Quantitation of Short-Chain Coenzyme A's in Biological Samples by Capillary Electrophoresis. *Anal. Chem.* **75,** 78–82 (2003).
155. Bajad, S. U. *et al.* Separation and quantitation of water soluble cellular metabolites by hydrophilic interaction chromatography-tandem mass spectrometry. *J. Chromatogr. A* **1125,** 76–88 (2006).
156. Liu, X. *et al.* High-Resolution Metabolomics with Acyl-CoA Profiling Reveals Widespread Remodeling in Response to Diet. *Mol. Cell. Proteomics MCP* **14,** 1489–1500 (2015).

157. Qualley, A. V., Cooper, B. R. & Dudareva, N. Profiling hydroxycinnamoyl-coenzyme A thioesters: Unlocking the back door of phenylpropanoid metabolism. *Anal. Biochem.* **420,** 182–184 (2012).
158. Burns, K. L., Gelbaum, L. T., Sullards, M. C., Bostwick, D. E. & May, S. W. Iso-coenzyme A. *J. Biol. Chem.* **280,** 16550–16558 (2005).
159. Minkler, P. E., Anderson, V. E., Maiti, N. C., Kerner, J. & Hoppel, C. L. Isolation and identification of two isomeric forms of malonyl-coenzyme A in commercial malonyl-coenzyme A. *Anal. Biochem.* **328,** 203–9 (2004).
160. Coulier, L. *et al.* Simultaneous quantitative analysis of metabolites using ion-pair liquid chromatography-electrospray ionization mass spectrometry. *Anal. Chem.* **78,** 6573–82 (2006).
161. Kiefer, P., Delmotte, N. & Vorholt, J. a. Nanoscale ion-pair reversed-phase HPLC-MS for sensitive metabolome analysis. *Anal. Chem.* **83,** 850–5 (2011).
162. Wu, L. *et al.* Quantitative analysis of the microbial metabolome by isotope dilution mass spectrometry using uniformly 13C-labeled cell extracts as internal standards. *Anal. Biochem.* **336,** 164–71 (2005).
163. Gao, L. *et al.* Simultaneous quantification of malonyl-CoA and several other short-chain acyl-CoAs in animal tissues by ion-pairing reversed-phase HPLC/MS. *J. Chromatogr. B Analyt. Technol. Biomed. Life. Sci.* **853,** 303–13 (2007).
164. Magnes, C., Sinner, F. M., Regittnig, W. & Pieber, T. R. LC/MS/MS method for quantitative determination of long-chain fatty Acyl-CoAs. *Anal. Chem.* **77,** 2889–2894 (2005).
165. Frey, A. J. *et al.* LC-quadrupole/Orbitrap high-resolution mass spectrometry enables stable isotope-resolved simultaneous quantification and C-13-isotopic labeling of acyl-coenzyme A thioesters. *Anal. Bioanal. Chem.* **408,** 3651–3658 (2016).
166. Basu, S. S. & Blair, I. a. SILEC: a protocol for generating and using isotopically labeled coenzyme A mass spectrometry standards. *Nat. Protoc.* **7,** 1–12 (2012).
167. Hayashi, O. & Satoh, K. Determination of acetyl-CoA and malonyl-CoA in germinating rice seeds using the LC-MS/MS technique. *Biosci. Biotechnol. Biochem.* **70,** 2676–2681 (2006).
168. Dalluge, J. J. *et al.* Separation and identification of organic acid-coenzyme A thioesters using liquid chromatography/electrospray ionization-mass spectrometry. *Anal. Bioanal. Chem.* **374,** 835–40 (2002).
169. Zhang, G.-F. *et al.* Catabolism of 4-Hydroxyacids and 4-Hydroxynonenal via 4-Hydroxy-4-phosphoacyl-CoAs. *J. Biol. Chem.* **284,** 33521–33534 (2009).
170. Park, J. W., Jung, W. S., Park, S. R., Park, B. C. & Yoon, Y. J. Analysis of intracellular short organic acid-coenzyme A esters from actinomycetes using liquid chromatography-electrospray ionization-mass spectrometry. *J. Mass Spectrom.* **42,** 1136–1147 (2007).
171. Purves, R. W., Ambrose, S. J., Clark, S. M., Stout, J. M. & Page, J. E. Separation of isomeric short-chain acyl-CoAs in plant matrices using ultra-performance liquid chromatography coupled with tandem mass spectrometry. *J. Chromatogr. B-Anal. Technol. Biomed. Life Sci.* **980,** 1–7 (2015).
172. Armando, J. W., Boghigian, B. A. & Pfeifer, B. A. LC-MS/MS quantification of short-chain acyl-CoA's in Escherichia coli demonstrates versatile propionyl-CoA synthetase substrate specificity. *Lett. Appl. Microbiol.* **54,** 140–148 (2012).
173. Basu, S. S., Mesaros, C., Gelhaus, S. L. & Blair, I. A. Stable Isotope Labeling by Essential Nutrients in Cell Culture for Preparation of Labeled Coenzyme A and Its Thioesters. *Anal. Chem.* **83,** 1363–1369 (2011).
174. Snyder, N. W., Basu, S. S., Worth, A. J., Mesaros, C. & Blair, I. A. Metabolism of propionic acid to a novel acyl-coenzyme A thioester by mammalian cell lines and platelets. *J. Lipid Res.* **56,** 142–150 (2015).
175. Worth, A. J. *et al.* Stable isotopes and LC-MS for monitoring metabolic disturbances in Friedreich's ataxia platelets. *Bioanalysis* **7,** 1843–1855 (2015).
176. Neubauer, S. *et al.* LC-MS/MS-based analysis of coenzyme A and short-chain acyl-coenzyme A thioesters. *Anal. Bioanal. Chem.* **407,** 6681–6688 (2015).

177. Schneider, K. *et al.* The ethylmalonyl-CoA pathway is used in place of the glyoxylate cycle by Methylobacterium extorquens AM1 during growth on acetate. *J. Biol. Chem.* **287,** 757–66 (2012).
178. Fukui, T. *et al.* Metabolite profiles of polyhydroxyalkanoate-producing Ralstonia eutropha H16. *Metabolomics* **10,** 190–202 (2014).
179. Seifar, R. M. *et al.* Quantitative analysis of intracellular coenzymes in Saccharomyces cerevisiae using ion pair reversed phase ultra high performance liquid chromatography tandem mass spectrometry. *J. Chromatogr. A* **1311,** 115–20 (2013).
180. Seifar, R. M. *et al.* Quantitative analysis of intracellular coenzymes in Saccharomyces cerevisiae using ion pair reversed phase ultra high performance liquid chromatography tandem mass spectrometry. *J. Chromatogr. A* **1311,** 115–20 (2013).
181. Li, Q., Zhang, S., Berthiaume, J. M., Simons, B. & Zhang, G.-F. Novel approach in LC-MS/MS using MRM to generate a full profile of acyl-CoAs: discovery of acyl-dephospho-CoAs. *J. Lipid Res.* **55,** 592–602 (2014).
182. Simon, E. J. & Shemin, D. The Preparation of S-Succinyl Coenzyme A. *J. Am. Chem. Soc.* **75,** 2520–2520 (1953).
183. De Spiegeleer, B. M., Sintobin, K. & Desmet, J. High performance liquid chromatography stability study of malonyl-coenzyme A, using statistical experimental designs. *Biomed. Chromatogr. BMC* **3,** 213–216 (1989).
184. Stockbridge, R. B. & Wolfenden, R. The Intrinsic Reactivity of ATP and the Catalytic Proficiencies of Kinases Acting on Glucose, N-Acetylgalactosamine, and Homoserine. *J. Biol. Chem.* **284,** 22747–22757 (2009).
185. Kalderon, B. Modulation by nutrients and drugs of liver acyl-CoAs analyzed by mass spectrometry. *J. Lipid Res.* **43,** 1125–1132 (2002).
186. Bennett, B. B. D. *et al.* Absolute metabolite concentrations and implied enzyme active site occupancy in Escherichia coli. *Nat. Chem. Biol.* **5,** 593–9 (2009).
187. Taymaz-Nikerel, H. *et al.* Development and application of a differential method for reliable metabolome analysis in Escherichia coli. *Anal. Biochem.* **386,** 9–19 (2009).
188. Cipollina, C. *et al.* A comprehensive method for the quantification of the non-oxidative pentose phosphate pathway intermediates in Saccharomyces cerevisiae by GC-IDMS. *J. Chromatogr. B Analyt. Technol. Biomed. Life. Sci.* **877,** 3231–3236 (2009).
189. Nasution, U., van Gulik, W. M., Proell, a, van Winden, W. a & Heijnen, J. J. Generating short-term kinetic responses of primary metabolism of Penicillium chrysogenum through glucose perturbation in the bioscope mini reactor. *Metab. Eng.* **8,** 395–405 (2006).
190. Haynes, C. a *et al.* Quantitation of fatty acyl-coenzyme As in mammalian cells by liquid chromatography-electrospray ionization tandem mass spectrometry. *J. Lipid Res.* **49,** 1113–25 (2008).
191. Gross, J. *Mass Spectrometry*. (2006).
192. Glauser, G., Veyrat, N., Rochat, B., Wolfender, J.-L. & Turlings, T. C. J. Ultra-high pressure liquid chromatography–mass spectrometry for plant metabolomics: A systematic comparison of high-resolution quadrupole-time-of-flight and single stage Orbitrap mass spectrometers. *J. Chromatogr. A* **1292,** 151–159 (2013).
193. Heras, R. M.-L., Quifer-Rada, P., Andrés, A. & Lamuela-Raventós, R. Polyphenolic profile of persimmon leaves by high resolution mass spectrometry (LC-ESI-LTQ-Orbitrap-MS). *J. Funct. Foods* **23,** 370–377 (2016).
194. CHOHNAN, S., IZAWA, H., NISHIHARA, H. & TAKAMURA, Y. Changes in Size of Intracellular Pools of Coenzyme A and Its Thioesters in Escherichia coli K-12 Cells to Various Carbon Sources and Stresses. *Biosci. Biotechnol. Biochem.* **62,** 1122–1128 (1998).
195. Kind, T. & Fiehn, O. Seven Golden Rules for heuristic filtering of molecular formulas obtained by accurate mass spectrometry. **20,** 1–20 (2007).

196. Creek, D. J. *et al.* Probing the Metabolic Network in Bloodstream-Form Trypanosoma brucei Using Untargeted Metabolomics with Stable Isotope Labelled Glucose. *PLOS Pathog.* **11,** e1004689 (2015).
197. Millard, P., Massou, S., Portais, J.-C. & Letisse, F. Isotopic Studies of Metabolic Systems by Mass Spectrometry: Using Pascal's Triangle To Produce Biological Standards with Fully Controlled Labeling Patterns. *Anal. Chem.* **86,** 10288–10295 (2014).
198. Cherrah, Y. *et al.* Study of deuterium isotope effects on protein binding by gas chromatography/mass spectrometry. Caffeine and deuterated isotopomers. *Biol. Mass Spectrom.* **14,** 653–657 (1987).
199. Filiou, M. D. *et al.* The N-15 isotope effect in Escherichia coli: A neutron can make the difference. *Proteomics* **12,** 3121–+ (2012).
200. Webhofer, C. *et al.* 15N metabolic labeling: Evidence for a stable isotope effect on plasma protein levels and peptide chromatographic retention times. *J. Proteomics* **88,** 27–33 (2013).
201. Millard, P., Portais, J.-C. & Mendes, P. Impact of kinetic isotope effects in isotopic studies of metabolic systems. *BMC Syst. Biol.* **9,** (2015).
202. Antoniewicz, M. R., Kelleher, J. K. & Stephanopoulos, G. Accurate Assessment of Amino Acid Mass Isotopomer Distributions for Metabolic Flux Analysis. *Anal. Chem.* **79,** 7554–7559 (2007).
203. Heux, S., Bergès, C., Millard, P., Portais, J.-C. & Létisse, F. Recent advances in high-throughput (13)C-fluxomics. *Curr. Opin. Biotechnol.* **43,** 104–109 (2017).
204. Edwards, J. S. & Palsson, B. O. Robustness analysis of the Escherichia coli metabolic network. *Biotechnol. Prog.* **16,** 927–939 (2000).
205. Henry, C. S., Broadbelt, L. J. & Hatzimanikatis, V. Thermodynamics-based metabolic flux analysis. *Biophys. J.* **92,** 1792–1805 (2007).
206. Wittmann, C. Fluxome analysis using GC-MS. *Microb. Cell Factories* **6,** 6 (2007).
207. Zamboni, N., Fendt, S.-M., Rühl, M. & Sauer, U. (13)C-based metabolic flux analysis. *Nat. Protoc.* **4,** 878–92 (2009).
208. Wahrheit, J., Nicolae, A. & Heinzle, E. Eukaryotic metabolism: Measuring compartment fluxes. *Biotechnol. J.* **6,** 1071–1085 (2011).
209. Wiechert, W. 13C metabolic flux analysis. *Metab. Eng.* **3,** 195–206 (2001).
210. Millard, P., Massou, S., Wittmann, C., Portais, J.-C. & Létisse, F. Sampling of intracellular metabolites for stationary and non-stationary (13)C metabolic flux analysis in Escherichia coli. *Anal. Biochem.* **465C,** 38–49 (2014).
211. Enjalbert, B., Millard, P., Dinclaux, M., Portais, J.-C. & Létisse, F. Acetate fluxes in Escherichia coli are determined by the thermodynamic control of the Pta-AckA pathway. *Sci. Rep.* **7,** 42135 (2017).
212. Greenwood, P. E. & Nikulin, M. S. *A Guide to Chi-Squared Testing*.
213. Allen, D. K., Shachar-Hill, Y. & Ohlrogge, J. B. Compartment-specific labeling information in 13C metabolic flux analysis of plants. *Phytochemistry* **68,** 2197–2210 (2007).
214. Ebikeme, C. *et al.* Ablation of succinate production from glucose metabolism in the procyclic trypanosomes induces metabolic switches to the glycerol 3-phosphate/dihydroxyacetone phosphate shuttle and to proline metabolism. *J. Biol. Chem.* **285,** 32312–32324 (2010).
215. Ghozlane, A. *et al.* Flux analysis of the trypanosoma brucei glycolysis based on a multiobjective-criteria bioinformatic approach. *Adv. Bioinforma.* **2012,** (2012).
216. Cabruja, M., Lyonnet, B. B., Millán, G., Gramajo, H. & Gago, G. Analysis of coenzyme A activated compounds in actinomycetes. *Appl. Microbiol. Biotechnol.* **100,** 7239–7248 (2016).
217. Zielinski, D. C. *et al.* Systems biology analysis of drivers underlying hallmarks of cancer cell metabolism. *Sci. Rep.* **7,** 41241 (2017).
218. Iwatani, S., Yamada, Y. & Usuda, Y. Metabolic flux analysis in biotechnology processes. *Biotechnol. Lett.* **30,** 791–799 (2008).
219. Luo, H. *et al.* Production of 3-Hydroxypropionic Acid via the Propionyl-CoA Pathway Using Recombinant Escherichia coli Strains. *Plos One* **11,** e0156286 (2016).

220. Zhang, H., Boghigian, B. A. & Pfeifer, B. A. Investigating the role of native propionyl-CoA and methylmalonyl-CoA metabolism on heterologous polyketide production in Escherichia coli. *Biotechnol. Bioeng.* **105,** 567–573 (2010).
221. Heux, S., Juliette, P., Stéphane, M., Serguei, S. & Jean-Charles, P. A novel platform for automated high-throughput fluxome profiling of metabolic variants. *Metab. Eng.* **25,** 8–19 (2014).
222. Hernández-Montalvo, V., Valle, F., Bolivar, F. & Gosset, G. Characterization of sugar mixtures utilization by an Escherichia coli mutant devoid of the phosphotransferase system. *Appl. Microbiol. Biotechnol.* **57,** 186–191 (2001).
223. Volkmer, B. & Heinemann, M. Condition-Dependent Cell Volume and Concentration of Escherichia coli to Facilitate Data Conversion for Systems Biology Modeling. *PLOS ONE* **6,** e23126 (2011).
224. Brun, R. & Schönenberger. Cultivation and in vitro cloning or procyclic culture forms of Trypanosoma brucei in a semi-defined medium. Short communication. *Acta Trop.* **36,** 289–292 (1979).

Annex

Annex A: Repeatability, reproducibility and bias of calibration solutions

Precision and Accuracy measurements of 11 Acyl-CoA thioesters in 7 concentration levels ranging from 0.05 to 5µM. Values marked red exceed parameters of acceptance. Repeatability < 10% (intra-day precision), reproducibility < 20% (inter-day precision), bias <15% (difference between measured and theoretical value of concentration).

		Repeatability		Reproducibility	Bias	Bias
		Serie 1 CV [%]	Serie 2 CV [%]	CV [%]	[uM]	%
c7	3-HMG-CoA	7.33%	4.45%	11.18%	0.014	39.32%
c6	3-HMG-CoA	0.59%	1.59%	10.53%	0.016	20.01%
c5	3-HMG-CoA	1.81%	1.79%	10.86%	-0.015	-5.71%
c4	3-HMG-CoA	1.73%	1.52%	3.85%	-0.033	-6.35%
c3	3-HMG-CoA	2.00%	2.06%	2.18%	-0.030	-3.02%
c2	3-HMG-CoA	1.44%	1.81%	3.38%	0.076	3.26%
c1	3-HMG-CoA	2.20%	2.13%	9.32%	-0.514	-9.64%
c7	AcetoAcetyl-CoA	27.77%	2.80%	73.96%	0.008	20.32%
c6	AcetoAcetyl-CoA	2.16%	1.28%	36.23%	0.008	8.74%
c5	AcetoAcetyl-CoA	1.51%	0.71%	2.72%	-0.028	-10.22%
c4	AcetoAcetyl-CoA	2.62%	0.59%	2.73%	-0.039	-7.31%
c3	AcetoAcetyl-CoA	1.77%	0.58%	2.80%	-0.027	-2.64%
c2	AcetoAcetyl-CoA	1.80%	0.85%	1.50%	0.150	6.50%
c1	AcetoAcetyl-CoA	1.73%	1.26%	1.59%	-0.064	-1.30%
c7	Acetyl-CoA	8.04%	0.65%	11.47%	0.010	20.79%
c6	Acetyl-CoA	0.96%	0.96%	10.02%	0.012	11.60%
c5	Acetyl-CoA	0.70%	1.31%	8.00%	-0.020	-6.71%
c4	Acetyl-CoA	2.04%	0.46%	3.26%	-0.019	-3.26%
c3	Acetyl-CoA	1.74%	0.79%	1.91%	-0.025	-2.17%
c2	Acetyl-CoA	0.23%	0.99%	2.64%	0.070	2.57%
c1	Acetyl-CoA	0.69%	0.87%	4.61%	-0.308	-5.23%
c7	Butyryl-CoA	9.01%	4.28%	9.09%	0.006	12.99%
c6	Butyryl-CoA	2.26%	4.18%	6.87%	0.012	12.65%
c5	Butyryl-CoA	3.12%	2.90%	9.92%	-0.017	-6.10%
c4	Butyryl-CoA	4.44%	2.33%	5.08%	-0.014	-2.62%
c3	Butyryl-CoA	1.93%	3.54%	3.00%	-0.033	-3.09%
c2	Butyryl-CoA	1.51%	3.81%	4.36%	0.084	3.34%
c1	Butyryl-CoA	4.79%	6.25%	12.51%	-0.680	-11.52%
c7	CoA-SH	5.00%	26.61%	59.24%	0.442	23.09%
c6	CoA-SH	1.30%	6.37%	17.56%	0.027	27.26%
c5	CoA-SH	1.89%	8.52%	9.35%	0.025	10.15%
c4	CoA-SH	3.83%	3.57%	5.02%	0.009	1.85%
c3	CoA-SH	1.19%	2.90%	9.36%	-0.098	-9.79%
c2	CoA-SH	2.08%	6.27%	5.09%	0.058	2.33%
c1	CoA-SH	1.47%	1.27%	1.39%	-0.012	-0.24%
c7	Crotonyl-CoA	7.12%	3.67%	8.76%	0.001	2.76%
c6	Crotonyl-CoA	2.30%	2.73%	2.82%	0.002	2.40%
c5	Crotonyl-CoA	2.50%	3.42%	10.39%	-0.029	-10.05%
c4	Crotonyl-CoA	4.16%	3.00%	4.73%	-0.019	-3.52%
c3	Crotonyl-CoA	1.92%	3.10%	2.77%	0.004	0.42%
c2	Crotonyl-CoA	2.13%	3.52%	4.33%	0.074	2.91%
c1	Crotonyl-CoA	6.36%	5.55%	12.08%	-0.651	-10.99%
c7	Malonyl-CoA	66.09%	4.91%	96.09%	0.020	62.28%
c6	Malonyl-CoA	13.43%	5.04%	40.71%	0.020	23.60%
c5	Malonyl-CoA	6.03%	2.05%	7.14%	-0.001	-0.21%
c4	Malonyl-CoA	5.93%	4.08%	6.52%	0.003	0.57%
c3	Malonyl-CoA	6.50%	2.68%	5.27%	-0.016	-1.47%

		Repeatability		Reproducibility	Bias	Bias
		Serie 1 CV [%]	Serie 2 CV [%]	CV [%]	[uM]	%
c2	Malonyl-CoA	4.01%	6.54%	5.72%	-0.018	-0.67%
c1	Malonyl-CoA	6.30%	7.91%	8.18%	-0.141	-2.62%
c7	Methylmalonyl-CoA	5.00%	1.37%	10.77%	0.688	36.30%
c6	Methylmalonyl-CoA	3.06%	12.10%	27.43%	0.025	25.22%
c5	Methylmalonyl-CoA	0.79%	9.51%	11.47%	0.024	9.42%
c4	Methylmalonyl-CoA	2.91%	5.39%	4.75%	0.012	2.38%
c3	Methylmalonyl-CoA	1.09%	2.85%	9.45%	-0.109	-10.89%
c2	Methylmalonyl-CoA	1.35%	6.83%	4.95%	0.023	0.91%
c1	Methylmalonyl-CoA	2.56%	2.14%	2.55%	0.063	1.26%
c7	OH-Butyryl-CoA	6.27%	2.83%	5.92%	0.001	2.37%
c6	OH-Butyryl-CoA	1.05%	0.79%	4.89%	0.004	3.80%
c5	OH-Butyryl-CoA	3.46%	1.58%	9.54%	-0.026	-8.36%
c4	OH-Butyryl-CoA	2.90%	0.80%	4.27%	-0.018	-2.97%
c3	OH-Butyryl-CoA	2.46%	0.87%	1.99%	-0.012	-1.02%
c2	OH-Butyryl-CoA	0.83%	1.04%	3.44%	0.090	3.21%
c1	OH-Butyryl-CoA	1.51%	1.21%	5.77%	-0.406	-6.59%
c7	Propionyl-CoA	5.00%	1.35%	1.97%	0.457	70.86%
c6	Propionyl-CoA	4.21%	12.45%	14.26%	0.037	36.92%
c5	Propionyl-CoA	2.37%	8.45%	7.90%	0.021	8.21%
c4	Propionyl-CoA	1.64%	4.10%	4.73%	-0.008	-1.58%
c3	Propionyl-CoA	2.15%	2.41%	9.17%	-0.121	-12.12%
c2	Propionyl-CoA	1.26%	6.20%	5.32%	0.027	1.06%
c1	Propionyl-CoA	0.33%	2.50%	1.84%	0.010	0.19%
c7	Succinyl-CoA	5.00%	0.62%	2.80%	0.213	18.51%
c6	Succinyl-CoA	2.21%	8.63%	10.52%	0.015	15.49%
c5	Succinyl-CoA	1.91%	7.81%	7.08%	0.013	5.16%
c4	Succinyl-CoA	2.03%	4.35%	4.03%	0.003	0.54%
c3	Succinyl-CoA	0.83%	1.68%	8.86%	-0.094	-9.43%
c2	Succinyl-CoA	1.89%	5.81%	5.37%	0.073	2.91%
c1	Succinyl-CoA	1.50%	1.91%	1.78%	-0.019	-0.38%

Annex B: Isotopic cluster of butyryl-CoA coeluting with isotopic cluster of another compound.

HRMS spectra of isotopic cluster of butyryl-CoA with controlled label incorporation (blue) coeluting with isotopic cluster of unknown compound (red). Exact m/z of butyryl-CoA is 838.16435 and detected m/z in this isotopic cluster is 838.16514, the mass difference is -0.00079 m/z.

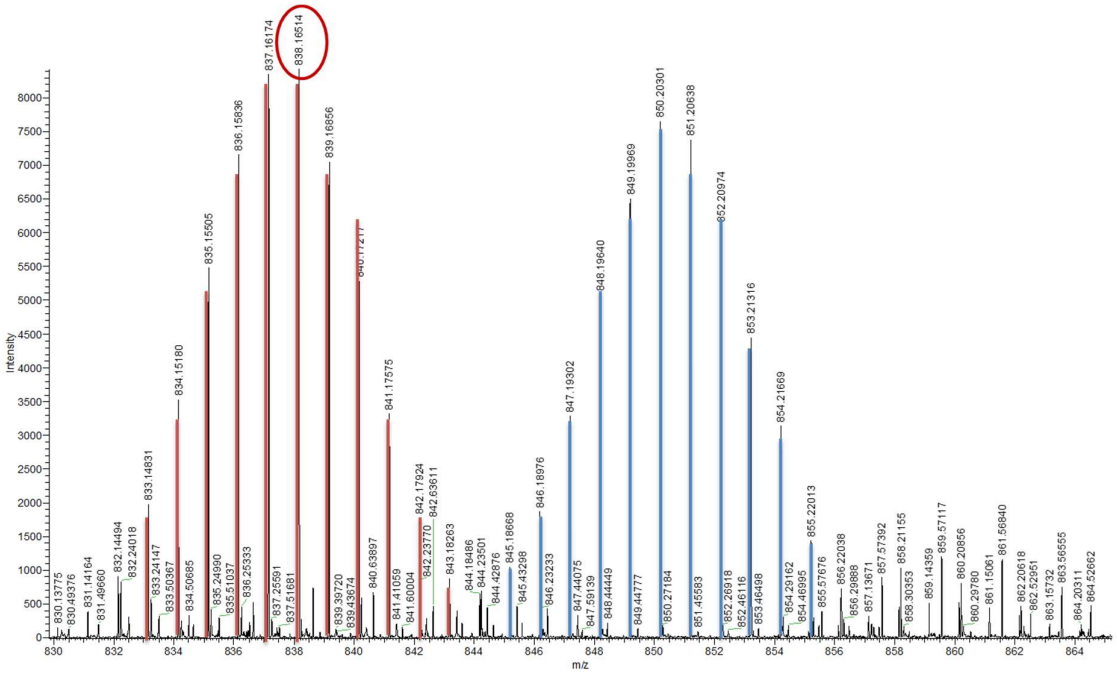

Annex C: LC-MS analysis of standard solutions

LC-MS analysis of Acyl-CoA stadnard solutions tested in method adaptation. Extracted ion chromatogram (XIC) created by selecting exact mass of Acyl-CoA ±5ppm. Succinyl-CoA elutes before methylmalonyl-CoA

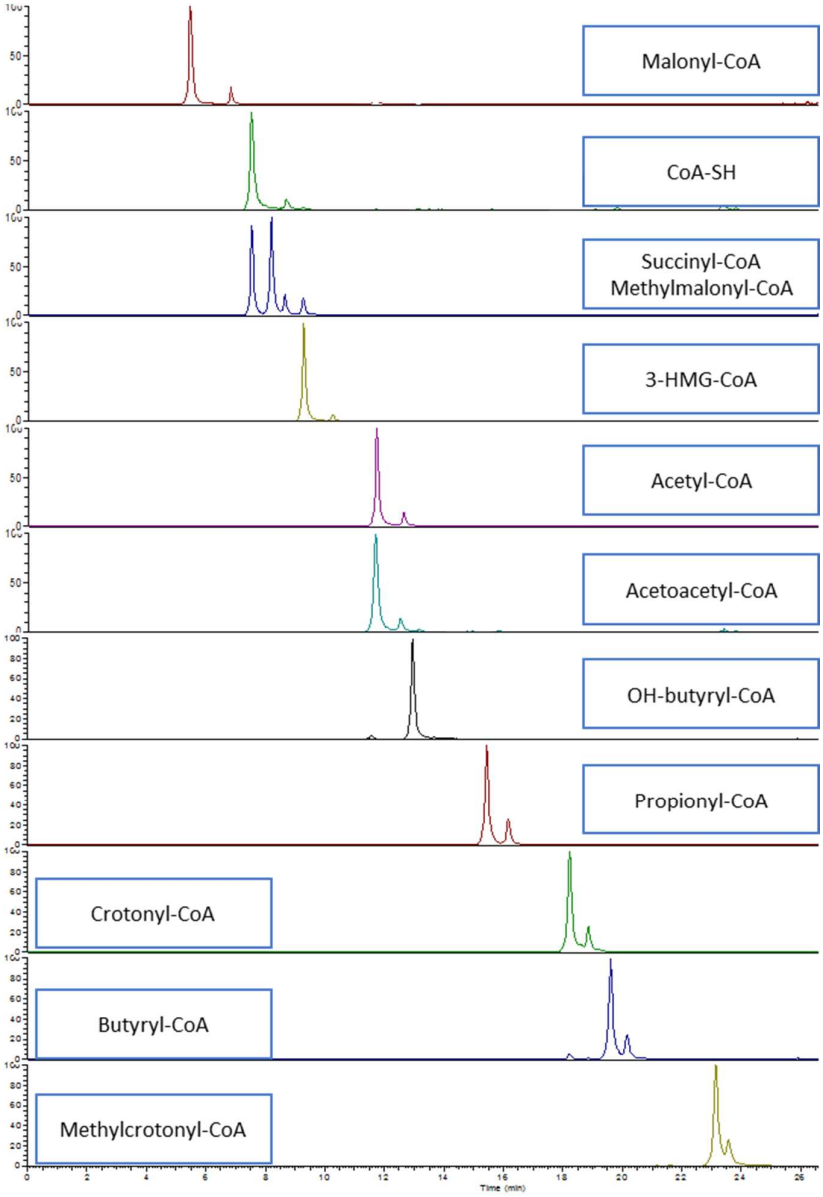

Annex D: Table of reactions included in the E. coli K-12 model

List of reactions used in flux calculation including the stoichiometry. Reactions grouped as "decoupling M0" describe metabolite dilution with non-labelled isotopes to account for the type of sampleg (total broth), which collects extracellular media that can contain non-labeled metabolites from time period before ^{13}C-glucose pulse. Influx_i offers possibility to deal with metabolite pool confusion appearing either in compartmentation or in coelution.

Pathway	Reaction name	Substrat(es)	Product(s)	Coding of carbon transfer
glycolysis	pgi	Glc-6P	Fru6P	ABCDEF → ABCDEF
glycolysis	pfk	Fru6P	FruBP	ABCDEF → ABCDEF
glycolysis	ald	FruBP	DHAP + GA3P	ABCDEF → ABC + DEF
glycolysis	tpi	DHAP	GA3P	ABC → CBA
glycolysis	gdh	GA3P	BPG	ABC → ABC
glycolysis	pgk	BPG	PG2	ABC → ABC
glycolysis	gpm	PG2	PG3	ABC → ABC
glycolysis	eno	PG3	PEP	ABC → ABC
glycolysis	pyk	PEP	Pyr	ABC → ABC
PPP	zwf	Glc6P	Gnl6P	ABCDEF → ABCDEF
PPP	pgi	Gnl6P	Gnt6P	ABCDEF → ABCDEF
PPP	gnd	Gnt6P	CO2 + Ribu5P	ABCDEF → A BCDEF
PPP	rpe	Ribu5P	Xyl5P	ABCDE → ABCDE
PPP	rpi	Ribu5P	Rib5P	ABCDE → ABCDE
PPP	edd	Gnt6P	KDPG	ABCDEF → ABCDEF
PPP	eda	KDPG	Pyr + GA3P	ABCDEF → ABC + DEF
PPP	HR1	Xyl5P	GA3P + E2	ABCDE → CDE + AB
PPP	HR2	Fru6P	Ery4P + E2	ABCDEF → CDEF + AB
PPP	HR3	Fru6P	GA3P + E3	ABCDEF → DEF + ABC
PPP	HR4	Rib5P	E2 + Sed7P	ABCDE → ab + abABCDE
PPP	HR5	Ery4P	E3 + Sed7P	ABCD → abc + abcABCD
TCA	citsynth	AcCoA + OAA	Cit	AB + abcd → dcbaBA
TCA	acn1	Cit	Aco	ABCDEF → ABCDEF
TCA	acn2	Aco	Icit	ABCDEF → ABCDEF
TCA	idh	Icit	AKG + CO2	ABCDEF → ABCEF + D
TCA	akgdh	AKG	SucCoA + CO2	ABCDE → BCDE + A
TCA	scs	SucCoA	Suc	ABCD → ABCD
TCA	sdh	Suc	Fum	ABCD → ABCD
TCA	fum_a	Fum	Mal	ABCD → ABCD
TCA	fum_b	Fum	Mal	ABCD → DCBA
TCA	maldh	Mal	OAA	ABCD → ABCD
Anaplerotic reactions	pdh	Pyr	AcCoA + CO2	ABC → BC + A
Anaplerotic reactions	ppc_pck	PEP + CO2	OAA	ABC + a → ABCa
Acetate metabolism	eutD	AcCoA	AcP	AB → AB
Acetate metabolism	ackA	AcP	Acetate	AB → AB
Acetate metabolism	ac_out	Acetate	Acetate_out	AB → AB
CoA metabolism	yliK	SucCoA	MetmalCoa	ABCD → ABCD
CoA metabolism	ygfG	MetmalCoa	PropCoA + CO2	ABCD → ABC D
CoA metabolism	ygfH	PropCoA + Suc	Prop + SucCoA	ABC + EFGH → ABC + EFGH
CoA metabolism	aspC	OAA	AsP	ABCD → ABCD
CoA metabolism	aspk	AsP	AspS	ABCD → ABCD
CoA metabolism	asD	AspS	AspP	ABCD → ABCD
CoA metabolism	hdh	AspP	Lhom	ABCD → ABCD
CoA metabolism	thrb	Lhom	LhomP	ABCD → ABCD
CoA metabolism	thrc	LhomP	Thr	ABCD → ABCD
CoA metabolism	ilvA	Thr	2Oxbut	ABCD → ABCD
CoA metabolism	tdce	2Oxbut	PropCoA + formate	ABCD → ABC + D
CoA metabolism	out_form	formate	formate_sink	A → A
biosynthetic reactions	bs_glc6P	Glc6P	BM_Glc6P	ABCDEF → ABCDEF
biosynthetic reactions	bs_fru6P	Fru6P	BM_Fru6P	ABCDEF → ABCDEF
biosynthetic reactions	bs_DHAP	GA3P	Glp	ABC → ABC
biosynthetic reactions	bs_pga	PG3	BM_PGA	ABC → ABC

Pathway	Reaction name	Substrat(es)	Product(s)	Coding of carbon transfer
biosynthetic reactions	bs_pep	PEP	BM_PEP	ABC → ABC
biosynthetic reactions	bs_pyr	Pyr	BM_Pyr	ABC → ABC
biosynthetic reactions	bs_e4p	Ery4P	BM_Ery4P	ABCD → ABCD
biosynthetic reactions	bs_rib5p	Rib5P	BM_Rib5P	ABCDE → ABCDE
biosynthetic reactions	bs_akg	AKG	BM_AKG	ABCDE → ABCDE
biosynthetic reactions	bs_oaa	OAA	BM_OAA	ABCD → ABCD
biosynthetic reactions	bs_ile	2Oxbut	BM_Ile	ABCD → ABCD
biosynthetic reactions	bs_met	Lhom	BM_Met	ABCD → ABCD
biosynthetic reactions	bs_thr	Thr	BM_Thr	ABCD → ABCD
biosynthetic reactions	bs_accoa	AcCoA	BM_AcCoA	AB → AB
biosynthetic reactions	bs_accoa1	AcCoA + CO2	MalCoA	AB +C → ABC
biosynthetic reactions	bs_accoa1_aux	MalCoA	FattyAcids + CO2	ABC → AB + C
decoupling M0	Glc6P_in	Glc6P_out	Glc6P0	abcdef → abcdef
decoupling M0	Glc6P_dilution	Glc6P0	Glc6P_decoupled	abcdef → abcdef
decoupling M0	Fru6P_in	Fru6P_out	Fru6P0	abcdef → abcdef
decoupling M0	Fru6P_dilution	Fru6P0	Fru6P_decoupled	abcdef → abcdef
decoupling M0	FruBP_in	FruBP_out	FruBP0	abcdef → abcdef
decoupling M0	FruBP_dilution	FruBP0	FruBP_decoupled	abcdef → abcdef
decoupling M0	PG2_in	PG2_out	PG0	abc → abc
decoupling M0	PG2_dilution	PG0	PG2_decoupled	abc → abc
decoupling M0	PG3_in	PG3_out	PG0	abc → abc
decoupling M0	PG3_dilution	PG0	PG3_decoupled	abc → abc
decoupling M0	PEP_in	PEP_out	PEP0	abc → abc
decoupling M0	PEP_dilution	PEP0	PEP_decoupled	abc → abc
decoupling M0	AcCoA_in	AcCoA_out	AcCoA0	ab → ab
decoupling M0	AcCoA_dilution	AcCoA0	AcCoA_decoupled	ab → ab
decoupling M0	Cit_in	Cit_out	Cit0	abcdef → abcdef
decoupling M0	Cit_dilution	Cit0	Cit_decoupled	abcdef → abcdef
decoupling M0	Aco_in	Aco_out	Aco0	abcdef → abcdef
decoupling M0	Aco_dilution	Aco0	Aco_decoupled	abcdef → abcdef
decoupling M0	SucCoA_in	SucCoA_out	SucCoA0	abcd → abcd
decoupling M0	SucCoA_dilution	SucCoA0	SucCoA_decoupled	abcd → abcd
decoupling M0	Suc_in	Suc_out	Suc0	abcd → abcd
decoupling M0	Suc_dilution	Suc0	Suc_decoupled	abcd → abcd
decoupling M0	Fum_in	Fum_out	Fum0	abcd → abcd
decoupling M0	Fum_dilution	Fum0	Fum_decoupled	abcd → abcd
decoupling M0	Mal_in	Mal_out	Mal0	abcd → abcd
decoupling M0	Mal_dilution	Mal0	Mal_decoupled	abcd → abcd
decoupling M0	MalCoA_in	MalCoA_out	MalCoA0	abc → abc
decoupling M0	MalCoA_dilution	MalCoA0	MalCoA_decoupled	abc → abc
decoupling M0	PropCoA_in	PropCoA_out	PropCoA0	abc → abc
decoupling M0	PropCoA_dilution	PropCoA0	PropCoA_decoupled	abc → abc
decoupling M0	Thr_in	Thr_out	Thr0	abcd → abcd
decoupling M0	Thr_dilution	Thr0	Thr_decoupled	abcd → abcd
decoupling M0	Ribu5P_in	Ribu5P_out	Ribu5P0	abcde → abcde
decoupling M0	Ribu5P_dilution	Ribu5P0	Ribu5P_decoupled	abcde → abcde
decoupling M0	Sed7P_in	Sed7P_out	Sed7P0	abcdefg → abcdefg
decoupling M0	Sed7P_dilution	Sed7P0	Sed7P_decoupled	abcdefg → abcdefg

Annex E:

Experimentally measured intracellular metabolite concentrations of glucose-grown E.coli prior to ^{13}C-glucose pulse. Metabolite concentrations were established using IDMS-based LC-HRMS quantification.

Central metabolites	**Mean [mM]**	**SD [mM]**
Fru6P	0.43	0.24
FruBP	1.86	0.34
Glc6P	1.44	0.22
PEP	0.11	0.06
PG23	0.89	0.04
Ribu5P+Rib5P+Xyl5P	0.43	0.12
Gnt6P	0.1	0.06
Acetate	1000	100
AcP	0.3	0.05
Coenzymes	**Mean [mM]**	**SD [mM]**
AcCoA	1.6869	0.0695
PropCoA	0.1418	0.0087
SucCoA	0.2109	0.0061
MalCoA	0.02	0.0012
Amino Acids	**Mean [mM]**	**SD [mM]**
Ala	13.1586	1.48
Arg	1.0724	0.18
Asn	0.4724	0.189
Asp	8.5738	0.784
Glu	57.3853	1.537
Gln	68.8052	7.629
Gly	8.2799	0.9996
ile	0.27839	0.102
Leu	5.461993	1.082
Lys	0.755731	0.265
Met	0.2963	0.106
Phe	0.3007	0.039
Pro	0.4051	0.076
Ser	1.456	0.347
Thr	4.5045	0.326
Trp	0.01612	0.001
Tyr	0.454	0.087
Val	0.8706	0.3

Annex F: Measured Carbon isotopologue distribution, Experiment 1

Carbon isotopologue distribution of ^{13}C in each metabolite measured by LC-MS. Column numbers represent time in seconds when the sample has been withdrawn from the culture vessel.

Metabolitel	4	8	12	15	19	22	27	30	35	39	43	47	61	64	68	91	95	99	120	125	130	151
Glc6P:M0	0.56415	0.5023	0.49129	0.48166	0.5006	0.47751	NA	0.48817	0.45608	0.46593	0.4452	0.46555	0.45914	0.46626	0.45379	0.46366	0.48356	0.46293	0.4414	0.46345	0.4675	0.44502
Glc6P:M1	0.00862	0.01148	0.00957	0.00947	0.00017	0.00525	NA	0.0037	NA	0.00255	0.006	0.00078	0.00446	NA	0.00971	0.0049	0.00106	0.00561	0.00094	0.00354	0.00722	NA
Glc6P:M2	0.01411	0.01166	0.00986	0.00774	0.00577	0.01032	NA	NA	NA	0.00619	0.00307	0.00584	0.00329	0.00698	0.00768	0.00735	0.00572	0.00661	0.0071	0.00642	0.00733	0.0067
Glc6P:M3	0.05013	0.05891	0.05549	0.04952	0.0517	0.05165	NA	0.04158	0.04834	0.04578	0.05015	0.04541	0.05417	0.0475	0.04965	0.0544	0.05124	0.05768	0.04753	0.04123	0.05123	0.04213
Glc6P:M4	0.00831	0.01331	0.01498	0.01437	0.01595	0.01612	NA	0.01538	0.01755	0.01392	0.01675	0.01576	0.01661	0.01848	0.0185	0.01526	0.01784	0.01398	0.01309	0.01631	0.0157	0.01461
Glc6P:M5	0.01019	0.01368	0.01636	0.01153	0.01302	0.01215	NA	0.01337	0.02238	0.01357	0.01598	0.01829	0.01594	0.0202	0.01294	0.0171	0.01472	0.01984	0.01932	0.01526	0.01317	0.01598
Glc6P:M6	0.34449	0.38866	0.40245	0.42571	0.41278	0.42699	NA	0.4378	0.45565	0.45207	0.46285	0.44836	0.44639	0.4406	0.44773	0.43733	0.42587	0.43335	0.47062	0.4538	0.43784	0.47556
Fru6P:M0	0.47924	0.46371	0.46538	0.46256	0.39575	0.44631	NA	0.40694	0.46935	0.5024	0.46733	0.42404	0.44076	0.41132	0.43989	0.42658	0.457	0.47368	0.42174	0.42031	0.4256	0.41841
Fru6P:M1	0.01001	0.01593	0.00309	0.00178	0.00071	0.00573	NA	0.01188	0.00941	NA	NA	0.01416	0.00693	0.00549	0.01148	0.00862	0.00296	0.0096	0.01052	0.01017	0.01751	0.01914
Fru6P:M2	0.02533	0.02285	0.01473	0.0159	0.01699	0.01381	NA	0.01085	0.00831	0.01141	0.00525	0.00882	0.0127	0.01313	0.00841	NA	0.02088	0.00316	NA	0.01555	0.00413	0.01161
Fru6P:M3	0.09103	0.09814	0.07039	0.07818	0.08681	0.07369	NA	0.07714	0.08033	0.07665	0.07988	0.08457	0.08477	0.06704	0.08834	0.07106	0.07249	0.06409	0.07052	0.09891	0.08499	0.10066
Fru6P:M4	0.01873	0.01395	0.01434	0.0212	0.0284	0.02255	NA	0.03158	0.02428	0.02694	0.02034	0.02626	0.02392	0.02254	0.0187	0.02479	0.01686	0.01484	0.0264	0.0249	0.02008	0.03962
Fru6P:M5	0.00832	0.01273	0.01737	0.00428	0.02153	0.03039	NA	0.0115	0.02259	0.02359	0.0159	0.01377	0.0164	0.00502	0.02116	0.0049	0.02712	0.01441	0.01855	0.02094	0.01604	0.06774
Fru6P:M6	0.36735	0.3727	0.41469	0.41609	0.44982	0.40752	NA	0.45012	0.38573	0.35901	0.4113	0.42837	0.41451	0.47546	0.41201	0.46406	0.40269	0.42023	0.45227	0.40921	0.43164	0.34282
FruBP:M0	0.59746	0.47643	0.39035	0.34656	0.32287	0.31896	0.31871	0.29474	0.34448	0.31702	0.27226	0.33985	0.34682	0.33906	0.35077	0.3366	0.36119	0.30415	0.33888	0.34823	0.34265	0.32238
FruBP:M1	0.01709	0.02197	0.01857	0.02137	0.01688	0.01466	0.01572	0.01469	0.01115	0.01969	0.01313	0.01267	0.01264	0.01812	0.01553	0.01744	0.01001	0.01346	0.01546	0.00805	0.01046	0.01382
FruBP:M2	0.00679	0.01016	0.0139	0.01513	0.01282	0.00744	0.00937	0.00851	0.0061	0.0074	0.00814	0.01074	0.00964	0.01052	0.00857	0.00992	0.00766	0.00668	0.00772	0.007	0.00861	0.00844
FruBP:M3	0.13602	0.16153	0.17676	0.16584	0.14894	0.16259	0.15313	0.15716	0.13862	0.14627	0.13553	0.14451	0.14241	0.14968	0.15578	0.14049	0.15698	0.14366	0.16617	0.1344	0.15028	0.14431
FruBP:M4	0.01091	0.0162	0.02191	0.02131	0.02015	0.02307	0.02562	0.02731	0.02279	0.02563	0.02864	0.02099	0.02186	0.02633	0.02238	0.02581	0.01738	0.02581	0.02344	0.02144	0.02756	0.02331
FruBP:M5	0.00836	0.01709	0.02889	0.02845	0.03179	0.02989	0.02911	0.02178	0.02466	0.03696	0.02851	0.02928	0.02598	0.02462	0.03414	0.03441	0.0224	0.02468	0.0274	0.02801	0.01638	0.02244
FruBP:M6	0.22336	0.29662	0.34961	0.40135	0.44655	0.44339	0.44835	0.47582	0.4522	0.44703	0.51379	0.44195	0.44065	0.43165	0.41283	0.43532	0.42438	0.48157	0.42094	0.45286	0.44405	0.4653
PG2+PG3:M0	0.77675	0.7045	0.6421	0.63292	0.61889	0.62836	0.62432	0.60974	0.60216	0.59845	0.61393	0.62721	0.61492	0.61879	0.61328	0.64169	0.60721	0.59955	0.62481	0.61244	0.59832	0.60016
PG2+PG3:M1	0.00864	0.00728	0.01237	0.00803	0.00766	0.00751	0.0086	0.00629	0.0072	0.00799	0.006	0.00769	0.00769	0.01081	0.01214	0.00784	0.00982	0.00851	0.00953	0.00854	0.01271	0.00655
PG2+PG3:M2	0.00607	0.00863	0.01172	0.0138	0.01152	0.01297	0.01048	0.012	0.00867	0.0126	0.01193	0.00527	0.01001	0.01154	0.01107	0.01334	0.00211	0.01192	0.00927	0.01198	0.00894	0.00787
PG2+PG3:M3	0.20855	0.27959	0.33381	0.34524	0.36193	0.35116	0.35659	0.37197	0.38196	0.38097	0.36814	0.35983	0.36738	0.35887	0.3635	0.33713	0.38087	0.38003	0.35639	0.36704	0.38002	0.38542
PEP:M0	0.82402	0.74185	0.71886	0.69674	0.67195	0.65781	0.67499	0.69826	0.6979	0.68869	0.68761	0.69086	0.68587	0.67365	0.66397	0.67902	0.68234	0.68261	0.65875	0.66525	0.68488	0.66374
PEP:M1	0.0117	0.01337	0.00974	0.01385	0.01499	0.01585	0.01235	0.01162	0.01132	0.01486	0.01332	0.01615	0.01576	0.01548	0.01396	0.01021	0.01255	0.01644	0.01395	0.0157	0.01389	0.01744
PEP:M2	0.0059	0.01525	0.01408	0.01165	0.0128	0.01312	0.01454	0.01233	0.01365	0.01657	0.01327	0.01794	0.01111	0.0191	0.01634	0.01086	0.01459	0.01208	0.01657	0.01987	0.01864	0.01723
PEP:M3	0.15838	0.22953	0.25732	0.27776	0.30025	0.31322	0.29812	0.2778	0.27713	0.27989	0.2858	0.27506	0.28726	0.29178	0.30574	0.29991	0.29051	0.28887	0.31073	0.29918	0.28259	0.30159
AcCoA:M0	0.88943	0.72612	0.64114	0.59895	0.57381	0.55687	0.54971	0.54527	0.54518	0.54323	0.54316	0.54309	0.54096	0.54025	0.53645	0.53574	0.5331	0.53136	0.52734	0.52672	0.52715	0.52222
AcCoA:M1	0	0	0	0	0	0	0	0	0	0	0	0	0	0	0	0	0	0	0	0	0	0
AcCoA:M2	0.11057	0.27388	0.35886	0.40105	0.42619	0.44313	0.45029	0.45473	0.45482	0.45677	0.45684	0.45691	0.45904	0.45975	0.46309	0.46186	0.46429	0.46573	0.46656	0.46654	0.46541	0.46631
Cit:M0	0.96004	0.94859	0.93581	0.93125	0.92175	0.92815	0.90219	0.93744	0.90075	NA	NA	NA	NA	NA	NA	NA	NA	0.89832	0.91941	0.92334	0.9146	0.94147
Cit:M1	0.01382	0.01001	0.00741	0.004	0.00607	0.00657	0.00809	NA	0.01024	NA	NA	NA	NA	NA	NA	NA	NA	NA	0.00066	0	0.00122	0.00249
Cit:M2	0.01229	0.02371	0.03037	0.02968	0.0318	0.02577	0.0359	0.02851	0.03061	NA	NA	NA	NA	NA	NA	NA	NA	0.02251	0.02032	0.02495	0.0339	0.02154
Cit:M3	0.00864	0.01089	0.01465	0.01774	0.0198	0.01747	0.02296	0.01773	0.02591	NA	NA	NA	NA	NA	NA	NA	NA	0.02774	0.02355	0.01338	0.02247	0.01368
Cit:M4	0.00262	0.00166	0.00239	0.00422	0.00478	0.00565	0.009	0.00359	0.00951	NA	NA	NA	NA	NA	NA	NA	NA	0.01744	0.01086	0.01909	0.01197	0.00207
Cit:M5	0.00222	0.00486	0.00901	0.01242	0.01451	0.01527	0.01965	0.01273	0.01979	NA	NA	NA	NA	NA	NA	NA	NA	0.02725	0.01897	0.01155	0.01326	0.01174
Cit:M6	0.00037	0.00028	0.00036	0.00069	0.00128	0.00111	0.00222	NA	0.00318	NA	NA	NA	NA	NA	NA	NA	NA	0.00675	0.00623	0.0077	0.00257	0.007
Aco+Aco0:M0	0.99757	0.99275	0.98269	0.98484	0.97556	0.97889	0.97403	0.96707	0.97633	0.9731	0.96345	0.96255	0.96754	0.94869	0.9614	0.96165	0.95557	0.94681	0.94962	0.94246	0.93778	0.92514
Aco+Aco0:M1	0	0	0.00392	0	0.00652	0	0.0025	0	0	0.00425	0.00566	0.00761	0.00231	0.0074	0.00569	0.00466	0.00557	0.0071	0	0.00713	0.00145	0.00422
Aco+Aco0:M2	0.00243	0.00516	0.01027	0.00972	0.00803	0.01004	0.00982	0.01068	0.01136	0.0083	0.01257	0.01332	0.01376	0.01688	0.01175	0.01286	0.01309	0.01594	0.0148	0.01418	0.01698	0.02039
Aco+Aco0:M3	0	0.00209	0.00177	0.00116	0.00326	0.00213	0.00495	0.00487	0.00267	0.00427	0.00464	0.00393	0.00585	0.00614	0.0057	0.00474	0.00612	0.00942	0.01051	0.01054	0.01285	0.01572
Aco+Aco0:M4	0	0	0	0.00428	0.0047	0.00568	0.00362	0.0106	0.00646	0.00578	0.0093	0.00922	0.00474	0.01667	0.01119	0.00996	0.01165	0.01252	0.0129	0.01233	0.01836	0.01931
Aco+Aco0:M5	0	0	0.00134	0	0.00192	0.00327	0.0044	0.00678	0.00318	0.00431	0.00438	0.00337	0.0058	0.00422	0.00427	0.00613	0.00799	0.00519	0.00952	0.00922	0.00893	0.00681
Aco+Aco0:M6	0	0	0	0	0	0	NA	0	0	0	0	0	0	0	0	0	0	0.00303	0.00265	0.00414	0.00365	0.00841
SucCoA:M0	1	0.99899	0.96641	0.91391	0.86225	0.81743	0.77134	0.72926	0.68838	0.65533	0.62036	0.5834	0.50462	0.48888	0.44278	0.38083	0.36858	0.35787	0.30298	0.29433	0.28751	0.25101
SucCoA:M1	0	0	0	0	0	0	0	0	0.00682	0.0087	0.01612	0.02562	0.04037	0.03958	0.05441	0.06969	0.07178	0.07507	0.08997	0.09399	0.09579	0.10649
SucCoA:M2	0	0	0.02531	0.0667	0.10932	0.14455	0.17628	0.20446	0.22723	0.24546	0.25914	0.27793	0.30598	0.32031	0.32741	0.34618	0.35188	0.34941	0.36228	0.3606	0.35804	0.36646
SucCoA:M3	0	0	0	0	0	0	0.00124	0.00701	0.00975	0.01464	0.01897	0.02037	0.03532	0.03492	0.04467	0.05827	0.05982	0.06422	0.07789	0.08142	0.08568	0.09148
SucCoA:M4	0	0.00101	0.00828	0.0194	0.02843	0.03803	0.05113	0.05928	0.06782	0.07587	0.08541	0.09268	0.11372	0.11632	0.13073	0.14502	0.14794	0.15344	0.16687	0.16965	0.17299	0.18456
Suc:M0	0.97922	0.98291	0.97293	0.97996	0.97797	0.97501	NA	0.97106	0.97145	0.96966	0.96663	0.97189	0.96233	0.95823	0.9639	0.95966	0.95468	0.95489	0.95058	0.94753	0.94681	0.94419
Suc:M1	0.01113	0.00897	0.01432	0.00923	0.00742	0.00949	NA	0.00751	0.00746	0.00815	0.00916	0.00575	0.01098	0.01124	0.00931	0.00737	0.01146	0.01373	0.01347	0.0152	0.01521	0.01612
Suc:M2	0.00405	0.00391	0.00664	0.00577	0.00885	0.00954	NA	0.0127	0.01334	0.01385	0.01487	0.01391	0.01577	0.01781	0.01556	0.01854	0.01879	0.01721	0.02013	0.02039	0.02044	0.01976
Suc:M3	0.00237	0.00142	0.00226	0.00172	0.00177	0.00174	NA	0.00247	0.00184	0.00207	0.00247	0.0026	0.00342	0.00472	0.00308	0.00506	0.00491	0.00445	0.00564	0.0064	0.00538	0.00727
Suc:M4	0.00322	0.0028	0.00385	0.00333	0.00398	0.00422	NA	0.00626	0.00591	0.00627	0.00687	0.00586	0.0075	0.00799	0.00815	0.00937	0.01015	0.00972	0.01019	0.01048	0.01217	0.01266
Fum:M0	0.96337	0.78827	0.66606	0.62063	0.55846	0.52116	NA	0.51597	0.35269	0.41711	0.40701	0.29961	0.22992	0.42035	0.1927	0.18425	0.20838	0.14734	0.21478	0.15166	0.15765	0.15194
Fum:M1	0.03663	0.03296	0.02582	0.02706	0.03357	0.02524	NA	NA	0.02094	0.04769	0.04348	0	0.05882	0.10148	0.04024	0.04085	0.06285	0.04561	0.07906	0.06859	0.06658	0.07034
Fum:M2	0	0.01481	0.03468	0.03674	0.05685	0.06334	NA	0.09073	0.1834	0.10873	0.1052	0.25401	0.19889	0.19499	0.28839	0.26878	0.23393	0.30528	0.13116	0.1281	0.12745	0.14729
Fum:M3	0	0.16395	0.27344	0.31557	0.35111	0.39026	NA	0.3933	0.36169	0.42647	0.44431	0.44638	0.32883	0.28318	0.32919	0.33043	0.37652	0.34367	0.33231	0.46912	0.41803	0.35717
Fum:M4	0	0	0	0	0	0	NA	NA	0.08128	NA	NA	NA	0.18354	NA	0.14948	0.17569	0.11833	0.15809	0.24269	0.18254	0.23028	0.27326
Mal:M0	0.935	0.84787	0.75728	0.65521	0.62125	0.57953	NA	0.5132	0.4672	0.46492	0.45842	0.43889	0.34396	0.34014	0.34335	0.29666	0.2825	0.27629	0.23533	0.24935	0.22538	0.22404
Mal:M1	0.00903	0.00831	0.00633	0.01945	0.01808	0.01683	NA	0.02332	0.02515	0.0297	0.02896	0.03222	0.04789	0.04254	0.04072	0.05544	0.06414	0.07148	0.06628	0.0783	0.08278	0.07558
Mal:M2	0	0.01852	0.03937	0.06995	0.08197	0.10111	NA	0.13199	0.13137	0.16108	0.14697	0.14695	0.18028	0.1951	0.2033	0.22669	0.20966	0.22725	0.22529	0.21943	0.22955	0.23481
Mal:M3	0.05597	0.12529	0.19702	0.24052	0.2546	0.26633	NA	0.2848	0.31285	0.28651	0.28757	0.30555	0.31469	0.32974	0.31109	0.30052	0.33297	0.3022	0.32884	0.30762	0.32795	0.29761
Mal:M4	0	0	0	0.01486	0.02409	0.0362	NA	0.04669	0.06343	0.05779	0.07809	0.07639	0.11319	0.09247	0.10154	0.12068	0.11073	0.12277	0.14426	0.1453	0.13435	0.16796
RibuS P+Rib5P+Xyl5P:M0	0.71465	0.58502	0.53315	0.45173	0.40184	0.35145	NA	0.37188	0.36538	0.36134	0.40574	0.34242	0.36325	0.39062	0.40146	0.34399	0.43508	0.42892	0.33755	0.36193	0.34072	0.3681
RibuS P+Rib5P+Xyl5P:M1	0.01528	0.00546	0.00699	0.00068	0.02198	0.01838	NA	0.01685	0.01008	0.02217	0.00538	0.01006	0.0165	0.00215	0.01597	0.02084	0.02497	0.00449	0.00979	0.01367	0.01406	NA
RibuS P+Rib5P+Xyl5P:M2	0.09187	0.10447	0.12534	0.10062	0.08332	0.08242	NA	0.1135	0.09533	0.08515	0.08925	0.0946	0.09406	0.07172	0.10206	0.09499	0.06916	0.08996	0.11153	0.08868	0.07953	0.12183
RibuS P+Rib5P+Xyl5P:M3	0.04489	0.06206	0.06509	0.07788	0.0841	0.07064	NA	0.06938	0.07399	0.10872	0.08128	0.10124	0.10904	0.08669	0.13019	0.09725	0.07972	0.1005	0.12171	0.07194	0.10094	0.09743
RibuS P+Rib5P+Xyl5P:M4	0.01211	0.01659	0.01992	0.02506	0.02103	0.02799	NA	0.03744	0.02316	0.02742	0.04508	0.06221	0.03601	0.02273	0.05431	0.03769	0.02725	0.02231	0.02292	0.0146	0.04017	0.01714
RibuS P+Rib5P+Xyl5P:M5	0.1212	0.2264	0.24951	0.34404	0.38773	0.44912	NA	0.39095	0.43207	0.39521	0.37328	0.38948	0.38114	0.42608	0.296	0.40525	0.36383	0.35382	0.39651	0.44918	0.42457	0.39551
Sed7P:M0	0.47514	0.36481	0.388	0.40189	0.37743	0.3883	NA	0.39585	0.48998	0.42195	0.36828	0.40546	0.43544	0.41122	0.40749	0.40552	0.41913	NA	0.39689	NA	0.40331	0.37334
Sed7P:M1	0.04264	0.04147	0.03447	0.01406	0.01171	0.01665	NA	0.03503	0.01306	0.02003	0.01804	0.00354	0.02104	0.02702	0.00992	0.02651	0.01095	0.01304	0.03536	0.00103	0.01283	0.02113
Sed7P:M2	0.12642	0.09111	0.05292	0.05369	0.05313	0.06665	NA	0.05039	0.05291	0.0372	0.03285	0.03528	0.04625	0.04033	0.03595	0.03619	0.06453	0.04316	0.04012	0.04915	0.03365	0.04441
Sed7P:M3	0.12344	0.12563	0.09752	0.09014	0.07657	0.10097	NA	0.07214	0.11569	0.09921	0.06233	0.06008	0.10189	0.07859	0.08996	0.05725	0.09366	0.09669	0.08903	0.08533	0.09124	0.09285
Sed7P:M4	0	0	0	0	0	0	NA	0	0	0	0	0	0	0	0	0	0	0	0	0	0	0

Metabolite	4	8	12	15	19	22	27	30	35	39	43	47	61	64	68	91	95	99	120	125	130	151
Sed7P:M5	0.08524	0.12435	0.10185	0.12466	0.12092	0.11028	NA	0.09513	NA	0.10303	0.12061	0.10925	0.08999	0.123	0.14095	0.14198	0.12006	NA	0.11898	0.11326	0.10374	0.10969
Sed7P:M6	0.03021	0.03858	0.04929	0.06016	0.08212	0.05162	NA	0.04412	NA	0.04326	0.06476	0.0551	0.06051	0.08938	0.06811	0.07649	0.05985	NA	0.05701	0.0624	0.0693	0.09159
Sed7P:M7	0.11692	0.21407	0.27595	0.25538	0.27813	0.26553	NA	0.30734	0.32837	0.27532	0.33312	0.33128	0.24488	0.23046	0.24762	0.25606	0.23182	0.29456	0.26262	0.24581	0.28593	0.26698
MalCoA:M0	0.96914	0.88347	0.79866	0.78033	0.75514	0.7597	0.76369	0.75894	0.77302	0.74412	0.77549	0.74677	0.76855	0.76082	0.72298	0.70934	0.71105	0.71722	0.70675	0.69759	0.67868	0.64035
MalCoA:M1	0	0	0	0	0	0	0	0	0	0	0	0	0	0	0	0.01297	NA	0.02328	0.01761	0.0104	0.02727	0.04803
MalCoA:M2	0.03086	0.11653	0.20134	0.21967	0.24486	0.2403	0.23631	0.24106	0.22698	0.25588	0.22451	0.25323	0.23145	0.23526	0.26469	0.23632	0.28895	0.23638	0.23826	0.25139	0.26531	0.27364
MalCoA:M3	0	0	0	0	0	0	0	0	0	0	0	0	0	0.00393	0.01233	0.02359	NA	0.02312	0.03739	0.04063	0.02874	0.03799
PropCoA:M0	1	1	1	1	1	1	1	1	0.99159	0.97944	0.95837	0.93433	0.85511	0.84153	0.781	0.69099	0.67249	0.65434	0.57459	0.56147	0.54596	0.48926
PropCoA:M1	0	0	0	0	0	0	0	0	0	0	0	0	0.00553	0.00439	0.02121	0.04129	0.04678	0.0501	0.06872	0.07315	0.07718	0.09424
PropCoA:M2	0	0	0	0	0	0	0	0	0	0	0.01269	0.03119	0.0819	0.09326	0.12155	0.1648	0.17102	0.18158	0.21267	0.21604	0.22243	0.24055
PropCoA0:M3	0	0	0	0	0	0	0	0	0.00841	0.02056	0.02895	0.03449	0.05745	0.06082	0.07592	0.10111	0.10764	0.11143	0.1392	0.14322	0.14802	0.16621
Thr:M0	1	1	1	0.923	0.91817	0.87828	NA	0.80834	0.88589	0.85681	0.73333	NA	0.69523	0.66159	0.69615	0.58451	0.60098	0.57394	0.51755	0.50883	0.56507	0.59184
Thr:M1	0	0	0	0	0	0	NA	0	0	0	0	0	0	0	0	0	0	0	0.06489	0.06008	0.01967	NA
Thr:M2	0	0	0	0	0	0	NA	0	0	0	0	0	0	0	0	0	0	0	0	0	0	0
Thr:M3	0	0	0	0.077	0.08183	0.12172	NA	0.19166	0.11411	0.14319	0.22959	NA	0.25694	0.29453	0.24119	0.31343	0.30912	0.29169	0.28348	0.29597	0.31476	0.29352
Thr:M4	0	0	0	0	0	0	NA	0	0	0	0.03707	NA	0.04783	0.04388	0.06267	0.10206	0.0899	0.13437	0.13408	0.13512	0.1005	0.11464
Ohglut:M0	0.99913	0.997	0.99582	0.99353	0.98519	0.97664	NA	0.98188	0.96743	0.97072	0.97592	0.98872	0.97468	0.95476	0.97381	0.96026	0.95952	0.96191	0.97082	0.94825	0.93856	0.96791
Ohglut:M1	0.00087	0.003	0.00201	0.00115	0.00384	0.01048	NA	0.00112	0.00832	0.01096	0.00399	0.00127	0.00204	0.01481	0.00192	0.00778	0.00456	0.00632	0	0.01427	0.00028	0
Ohglut:M2	0	0	0	0	0.0019	NA	NA	NA	0.00469	0.00074	NA	NA	0.00089	0.0023	NA	NA	0.00842	0.00353	NA	NA	0.01606	NA
Ohglut:M3	0	0	0.00217	0.0031	0.00188	0.00432	NA	0.0051	0.00576	0.005	0.00696	0.00418	0.00623	0.00765	0.00564	0.00978	0.00729	0.00754	0.01347	0.01918	0.01543	0.01491
Ohglut:M4	0	0	0	0	0	0	NA	0	0	0	0	0	0	0	0	0	0	0	0.00317	0.00544	0.00235	0.00416
Ohglut:M5	0	0	0	0.00222	0.00719	0.00855	NA	0.01189	0.0138	0.01258	0.01313	0.00584	0.01616	0.02048	0.01862	0.02218	0.02021	0.02071	0.01255	0.01287	0.02733	0.01302
Glu:M0	0.99977	0.99821	0.95703	0.91707	0.87984	0.84091	NA	0.75789	0.71922	0.6956	0.65316	0.77198	0.55844	0.48666	0.49723	0.43415	0.42209	0.38901	0.33964	0.34435	0.34095	0.29117
Glu:M1	0	0	0	0	0	0	NA	0.00531	0.00752	0.01111	0.0108	NA	0.02624	0.02668	0.03769	0.04855	0.04726	0.04241	0.06583	0.06447	0.06544	0.06991
Glu:M2	0	0	0.03771	0.06676	0.0942	0.12036	NA	0.16785	0.18879	0.20046	0.21899	0.13952	0.26094	0.23484	0.27931	0.29885	0.30423	0.2983	0.32356	0.31834	0.32061	0.32177
Glu:M3	0	0	0	0	0	0	NA	0.00325	0.00844	0	0.00916	0	0	0.10264	0	0	0	0.04816	0	0	0	0.02385
Glu:M4	0.00023	0.00179	0.00526	0.01126	0.01909	0.02729	NA	0.04586	0.05042	0.06285	0.07265	0.08849	0.10032	0.09637	0.11928	0.13596	0.13691	0.138	0.16198	0.16135	0.16288	0.17228
Glu:M5	0	0	0	0.00491	0.00687	0.01144	NA	0.01985	0.02562	0.02998	0.03524	0	0.05407	0.05282	0.0665	0.08248	0.08951	0.08413	0.10899	0.11149	0.11012	0.12101
Gln:M0	0.70555	0.49592	0.77169	0.89041	0.57426	0.52836	NA	0.78948	0.8202	0.46552	0.75742	0.66145	0.64562	0.62241	0.56409	0.50917	0.48364	0.44602	0.28105	0.40121	0.37781	0.34291
Gln:M1	0.29445	0.50408	0.22831	0.09279	0.41555	0.45481	NA	0.07098	NA	0.43292	NA	NA	NA	NA	0.02092	NA	NA	0.07048	0.32222	NA	NA	0.00418
Gln:M2	0	0	0	0.01506	0.00632	0.01102	NA	0.09487	0.12118	0.05913	0.15242	0.11075	0.20244	0.21108	0.22158	0.24767	0.25776	0.23025	0.17101	0.26501	0.28502	0.28379
Gln:M3	0	0	0	0	0	0	NA	0.01288	0.01235	0.01092	0.02804	0.2278	0.04779	0.0563	0.06238	0.08564	0.08983	0.09232	0.0871	0.13048	0.12517	0.1247
Gln:M4	0	0	0	0.00175	0.00387	0.00581	NA	0.02194	0.03167	0.02268	0.04135	NA	0.07115	0.07059	0.08582	0.10005	0.10665	0.09836	0.0846	0.12694	0.13119	0.14655
Gln:M5	0	0	0	0	0	0	NA	0.00987	0.0146	0.00883	0.02078	NA	0.033	0.03962	0.0452	0.05748	0.06212	0.06256	0.05403	0.07636	0.08081	0.09786

Annex G: Measured Carbon Isotopologue Distribution, Experiment 2

Carbon isotopologue distribution of ^{13}C in each metabolite measured by LC-MS. Column numbers represent time in seconds when the sample has been withdrawn from the culture vessel.

Metabolite	6	11	17	21	24	30	36	40	47	53	60	71	77	85	89	95	99	107	114	121	126	133	150
Glc6P:M0	0.37434	0.37676	0.33978	0.37046	0.33463	0.33132	0.32743	0.33475	0.33936	0.33113	0.33676	0.33648	0.34324	0.33428	0.3382	0.3105	0.34404	0.33673	0.3276	0.33127	0.33545	0.32754	0.32336
Glc6P:M1	0	0	0	0	0	0	0	0	0	0	0	0	0	0	0	0	0	0	0	0	0	0	0
Glc6P:M2	0	0	0	0	0	0	0	0	0	0	0	0	0	0	0	0	0	0	0	0	0	0	0
Glc6P:M3	0.01039	0.01242	0.01042	0.01224	0.01057	0.01117	0.01296	0.01272	0.01088	0.01222	0.00941	0.0112	0.01293	0.01449	0.01391	0.01478	0.01458	0.01579	0.01771	0.01846	0.01931	0.01995	0.01872
Glc6P:M4	0.00044	0.00067	0.00054	0.00088	0.00067	0.00053	0.00074	0.00109	0.00082	0.00067	0.00115	0.00122	0.00185	0.00189	0.0017	0.0014	0.00198	0.00268	0.0021	0.00292	0.0032	0.00334	0.00367
Glc6P:M5	0	0	0	0	0	0	0	0	0	0	0	0	0	0	0	0	0	0	0	0	0	0	0
Glc6P:M6	0.61482	0.61015	0.64926	0.61643	0.65412	0.65698	0.65888	0.65144	0.64894	0.65598	0.65268	0.65111	0.64198	0.64935	0.64619	0.67333	0.63939	0.6448	0.65259	0.64735	0.64204	0.64917	0.65425
Fru6P:M0	0.40576	0.34245	0.30477	0.33429	0.29306	0.28529	0.22939	0.29972	0.31786	0.32982	0.2931	0.29053	0.2691	0.30252	0.37184	0.12721	0.31489	0.20788	0.273	0.27867	0.20339	0.30701	0.29038
Fru6P:M1	0.00244	0.00104	0.01408	0	0.00625	0.01502	0.01634	0.01573	0.01114	0.00886	0.01073	0.01988	0.0254	0.00804	0	0.01777	0.01155	0.01627	0.00883	0.01176	0.02472	0.00123	0.00595
Fru6P:M2	0	0	0	0	0	0	0	0	0	0	0	0	0	0	0	0	0	0	0	0	0	0	0
Fru6P:M3	0.077	0.07047	0.06959	0.06231	0.08258	0.0888	0.10442	0.07518	0.07402	0.0707	0.12409	0.11399	0.07928	0.08944	0.09806	0.05128	0.06341	0.11863	0.09331	0.09874	0.09096	0.08262	0.08634
Fru6P:M4	0	0	0	0	0	0	0	0	0	0.00105	0	0	0.00029	0.00023	0	0	4.00E-04	0.00138	0.00231	0.00497	0.003	0.00327	0.00714
Fru6P:M5	0.01409	0.00016	0.00011	0	0.02715	0	0	0	0	0	4.00E-04	0	0	0.00053	0.00766	0	0.02313	0	0	0	0.00054	0	0
Fru6P:M6	0.50072	0.58588	0.61145	0.6034	0.59095	0.61089	0.64985	0.60937	0.59699	0.58958	0.57168	0.57561	0.62593	0.59924	0.52244	0.80374	0.58661	0.65584	0.62254	0.60585	0.67739	0.60588	0.61018
FruBP:M0	0.73807	0.34444	0.26404	0.23642	0.21974	0.20443	0.20419	0.21323	0.19743	0.20384	0.1952	0.19274	0.20506	0.20624	0.19944	0.20203	0.20692	0.19119	0.18912	0.19481	0.19612	0.1859	0.17862
FruBP:M1	0	0.00418	0.00581	0.00313	0.00337	0.0043	0.0016	0.00222	0.0025	0.00206	0.00251	0.00185	0.00233	0.00266	0.00284	0.00352	0.00334	0.00392	0.00193	0.00377	0.00426	0.00421	0.00393
FruBP:M2	0	0.00739	0.00577	0.00559	0.0043	0.00411	0.00385	0.00326	0.00275	0.00292	0.00238	0.00166	0.00167	NA	0.00069	0.00037	0.00276	NA	0.00059	0.0017	0.00329	0.00427	0.00432
FruBP:M3	0.07371	0.18829	0.17685	0.16662	0.15057	0.14839	0.14429	0.14061	0.14219	0.14088	0.13352	0.1373	0.13861	0.14477	0.14098	0.13605	0.14087	0.14293	0.14591	0.14502	0.14314	0.14621	0.15084
FruBP:M4	0.00144	0.00739	0.01011	0.01017	0.01082	0.0113	0.01085	0.01073	0.01058	0.01135	0.01185	0.01143	0.0108	0.0096	0.01029	0.0132	0.01334	0.01256	0.01389	0.01537	0.01634	0.01678	0.01745
FruBP:M5	0	0	0	0	0	0	0	0.00074	0	0	0.00066	0	0	0	0	0.00015	0.00106	0	0	0.001	0.00682	0.0024	0.01163
FruBP:M6	0.18678	0.44832	0.53742	0.57806	0.6112	0.62747	0.63521	0.62921	0.64455	0.63895	0.65388	0.65502	0.64153	0.63673	0.64576	0.64468	0.63172	0.6494	0.64856	0.63832	0.63003	0.64024	0.6332
6PG:M0	0.8857	0.89393	0.90948	0.90989	0.89334	0.89526	0.87227	0.87851	0.90578	0.89713	0.87708	0.88808	0.8714	0.87813	0.86542	0.87402	0.86856	0.84563	0.84605	0.84641	0.84292	0.83864	0.85543
6PG:M1	0	0	0	0	0	0	0	0	0	0	0	0	0	0	0	0	0	0	0	0	0	0	0
6PG:M2	0	0	0	0	0	0	0	0	0	0	0	0	0	0	0	0	0	0	0	0	0	0	0
6PG:M3	0	0	0	0	0	0	0	0	0	0	0	0	0	0	0	0	0	0	0	0	0	0	0
6PG:M4	0	0	0	0	0	0	0	0	0	0	0	0	0	0	0	0	0	0	0	0	0	0	0
6PG:M5	0	0	0	0	0	0	0	0	0	0	0	0	0	0	0	0	0	0	0	0	NA	0	0
6PG:M6	0.1143	0.10607	0.09052	0.09011	0.10666	0.10474	0.12773	0.12149	0.09422	0.10287	0.12292	0.11192	0.1286	0.12187	0.13458	0.12598	0.13144	0.15437	0.15395	0.15359	0.15604	0.16136	0.14457
PG2+PG3:M0	0.89275	0.68986	0.61684	0.58792	0.58195	0.56308	0.55468	0.54994	0.54973	0.54723	0.54602	0.54483	0.5381	0.50844	0.53251	0.50384	0.50681	0.52065	0.50658	0.51267	0.49808	0.50643	0.49406
PG2+PG3:M1	0	0	0	0	0	0	0	0	0	0	0	0	0	0	0	0	0	0	0	0	0	0	0.00014
PG2+PG3:M2	0	0	0	0	0	0	0	0	0	0	0	0	0	0	0	0	0	0	0	0	0	0	0
PG2+PG3:M3	0.10725	0.31014	0.38316	0.41208	0.41805	0.43692	0.44532	0.45006	0.45027	0.45277	0.45398	0.45517	0.4619	0.49156	0.46749	0.49616	0.49319	0.47935	0.49342	0.48733	0.50192	0.49357	0.50581
PEP:M0	1	0.82166	0.69711	0.77811	0.70923	0.69853	0.64551	0.66927	0.63651	0.67956	0.67924	0.63334	0.6918	0.68741	0.72919	0.66237	0.67669	0.67764	0.69652	0.69794	0.68895	0.71445	0.65885
PEP:M1	0	0	0	0	0	0	0	0	0	0	0	0	0	0	0	0	0	0	0	0	0	0	0
PEP:M2	0	0	0	0	0	0	0	0	0	0	0	0	0	0	0	0	0	0	0	0	0	0	0
PEP:M3	0	0.17834	0.30289	0.22189	0.29077	0.30147	0.35449	0.33073	0.36349	0.32044	0.32076	0.36666	0.3082	0.31259	0.27081	0.33763	0.32331	0.32236	0.30348	0.30206	0.31105	0.28555	0.34115
Cit:M0	0.92739	0.96799	0.9708	0.96955	0.96463	0.96078	0.93825	0.95098	0.95489	0.94976	0.86116	0.89449	0.8918	0.91357	0.91408	0.91644	0.90924	0.90624	0.89672	0.8961	0.88278	0.87898	0.87795
Cit:M1	0	0	0	0	0	0	0	0	0	0.00078	NA	NA	NA	NA	NA	NA	0.00053	NA	0.00108	NA	0.00206	0.00656	0.00222
Cit:M2	0.01079	0.00191	0.00468	0.00364	0.00457	0.00464	0.01373	0.00778	0.00344	0.00413	0.02886	0.02077	0.01973	0.01115	0.01159	0.00783	0.00929	0.01205	0.01249	0.01515	0.01772	0.01413	0.01611
Cit:M3	0.02813	0.0142	0.01251	0.01217	0.01356	0.01459	0.0205	0.0166	0.01536	0.01634	0.04929	0.03771	0.03186	0.02788	0.02465	0.02646	0.02587	0.0268	0.02816	0.02785	0.03144	0.03236	0.03355
Cit:M4	0.02364	0.01081	0.00484	0.00555	0.00494	0.00502	0.00627	0.00469	0.00695	0.00658	0.03169	0.01771	0.02018	0.01708	0.01733	0.01644	0.02029	0.0182	0.02108	0.02272	0.02482	0.0267	0.0273
Cit:M5	0.00817	0.00424	0.00644	0.0083	0.01167	0.01402	0.02002	0.01846	0.01793	0.0203	0.02606	0.02659	0.03208	0.0254	0.02715	0.02767	0.0288	0.02883	0.0322	0.0304	0.03174	0.03279	0.03202
Cit:M6	0.00186	0.00086	0.00075	8.00E-04	0.00063	0.00095	0.00122	0.00149	0.00142	0.00212	0.00293	0.00272	0.00435	0.00492	0.00521	0.00516	0.00598	0.00788	0.00827	0.00778	0.00942	0.00848	0.01084
Aco:M0	0.99822	1	1	1	1	1	1	1	1	1	0.99947	1	1	1	1	1	1	1	1	1	1	1	1
Aco:M1	0.00178	0	0	0	0	0	0	0	0	0	0.00053	0	0	0	0	0	0	0	0	0	0	0	0
Aco:M2	0	0	0	0	0	0	0	0	0	0	0	0	0	0	0	0	0	0	0	0	0	0	0
Aco:M3	0	0	0	0	0	0	0	0	0	0	0	0	0	0	0	0	0	0	0	0	0	0	0
Aco:M4	0	0	0	0	0	0	0	0	0	0	0	0	0	0	0	0	0	0	0	0	0	0	0
Aco:M5	0	0	0	0	0	0	0	0	0	0	0	0	0	0	0	0	0	0	0	0	0	0	0
Aco:M6	0	0	0	0	0	0	0	0	0	0	0	0	0	0	0	0	0	0	0	0	0	0	0
Suc:M0	0.99317	0.99906	0.99936	0.99643	0.99781	0.9965	0.9969	0.9945	0.99423	0.99419	0.97328	0.98465	0.98871	0.99081	0.98968	0.98936	0.98762	0.98926	0.98938	0.98664	0.98849	0.98563	0.98386
Suc:M1	0	0	0	0	0	0	0	0	0	0	0.00237	0	0	0	0	0	0	0	0	0	0	0	0
Suc:M2	0	0	0	0	0	0	0	0	0	0	0.01045	0.00523	0.00265	0.00065	0.00138	0.00136	0.00194	0.00213	0.00182	0.0031	0.00263	0.00359	0.00376
Suc:M3	0.0023	0.00094	0.00064	0.00064	0.00057	0.00089	0.00039	0.00089	0.00138	0.00144	0.00499	0.00319	0.00181	0.0021	0.00181	0.00175	0.00197	0.00178	0.00198	0.00205	0.00216	0.00272	0.00268
Suc:M4	0.00453	0	0	0.00293	0.00162	0.00261	0.00272	0.00461	0.00439	0.00437	0.0089	0.00693	0.00682	0.00644	0.00713	0.00753	0.00847	0.00683	0.00682	0.00821	0.00671	0.00806	0.00969
Fum:M0	0.9894	0.93117	0.89367	0.7636	0.74632	0.69595	0.72477	0.55223	0.63048	0.6371	0.44413	0.41643	0.49388	0.54579	0.50182	0.37922	0.41846	0.44185	0.44221	0.34957	0.39264	0.37741	0.38728
Fum:M1	0.0106	0	0	0	0	0	0	0.00607	0.0018	NA	0.01436	0.00838	NA	0.00042	0.00415	NA	0.00791	0.00315	0.00268	0.02225	0.02106	0.03426	0.01577
Fum:M2	0	0	0	0.01981	NA	0.03521	0.02533	0.08868	0.07667	0.06529	0.10521	0.10432	0.09772	0.08333	0.11436	0.13153	0.1156	0.15198	0.13016	0.12165	0.15622	0.15923	0.16956
Fum:M3	0	0.06883	0.10633	0.21659	0.25368	0.26884	0.2499	0.35302	0.29104	0.2976	0.33279	0.33224	0.26006	0.2371	0.23113	0.27599	0.25187	0.22554	0.19398	0.21633	0.19742	0.20668	0.22011
Fum:M4	0	0	0	0	0	0	0	0	0	0	0.10352	0.13863	0.14834	0.13336	0.14854	0.21326	0.20616	0.17748	0.23097	0.2902	0.23266	0.22242	0.20727
Mal:M0	0.96499	0.89377	0.80793	0.72951	0.68193	0.62987	0.59454	0.53478	0.50128	0.49157	0.45246	0.42352	0.40649	0.39752	0.37351	0.35823	0.3597	0.36079	0.34377	0.34021	0.32998	0.3051	0.30697
Mal:M1	0.01048	0.00239	0.00316	0.00609	0.0061	0.01209	0.01111	0.02112	0.01437	0.01665	0.03339	0.02783	0.02895	0.03035	0.03627	0.03427	0.03088	0.03381	0.03484	0.04242	0.03933	0.04198	0.05115
Mal:M2	0.00636	0.00634	0.01619	0.02489	0.03681	0.04597	0.06064	0.0742	0.08219	0.09085	0.11285	0.11063	0.11938	0.13094	0.13488	0.14385	0.15598	0.15524	0.16297	0.16819	0.18803	0.18108	0.19351
Mal:M3	0.01484	0.09455	0.16883	0.23408	0.26522	0.29805	0.31472	0.3448	0.36642	0.36456	0.35436	0.38403	0.37723	0.36352	0.36845	0.36396	0.36589	0.34929	0.34893	0.32721	0.3203	0.34362	0.31032
Mal:M4	0.00332	0.00295	0.00389	0.00542	0.00994	0.01402	0.01899	0.02509	0.03574	0.03637	0.04694	0.05399	0.06795	0.07767	0.08689	0.09968	0.08755	0.10087	0.10949	0.12196	0.12236	0.12821	0.13805
Ribu5P+Rib5P+Xyl5P:M0	0.9995	0.99456	0.99253	0.98331	0.98203	0.97791	0.97432	0.96903	0.96948	0.96485	0.96074	0.94427	0.91988	0.93237	0.91928	0.9243	0.90792	0.91861	0.90909	0.88949	0.87487	0.86984	0.85381
Ribu5P+Rib5P+Xyl5P:M1	0	0	0	0	0	0	0	0	0	0	0	0	0	0	0	0	0	0	0	0	0	0	0
Ribu5P+Rib5P+Xyl5P:M2	0	0	0	0	0	0	0	0	0	0	0	0	0.00355	0.00077	0.00268	0.00162	0.00304	0.00243	0.0034	0.00605	0.00869	0.01003	0.01201
Ribu5P+Rib5P+Xyl5P:M3	0	0	8.00E-05	0.00201	0.0021	0.0028	0.00329	0.00421	0.00428	0.00538	0.00588	0.00932	0.01336	0.01173	0.01313	0.01245	0.01476	0.01332	0.0154	0.01727	0.02091	0.02131	0.02377
Ribu5P+Rib5P+Xyl5P:M4	0	0	0	0.00011	0	0.00031	0.00034	0.00071	0.00083	0.00093	0.00085	0.00152	0.00223	0.00185	0.00214	0.00208	0.00172	0.00208	0.00234	0.0027	0.00356	0.00373	0.00408
Ribu5P+Rib5P+Xyl5P:M5	5.00E-04	0.00544	0.00739	0.01457	0.01586	0.01897	0.02205	0.02604	0.02541	0.02884	0.03253	0.04489	0.06098	0.05327	0.06278	0.05954	0.07256	0.06355	0.06977	0.0845	0.09198	0.09509	0.10633
Sed7P:M0	0.81726	0.64294	0.58916	0.56952	0.55405	0.51728	0.50656	0.50411	0.51722	0.53909	0.5133	0.52841	0.5	0.43261	0.46469	0.4864	0.46898	0.40068	0.40614	0.37944	0.3803	0.37707	0.3679
Sed7P:M1	0	0	0	0	0	0	0	0	0	0	0	0	0	0	0	0	0	0	0	0	0	0	0
Sed7P:M2	0	0	0	0	0	0	0	0	0	0	0	0	0	0	0	0	0	0	0	0	0	0	0
Sed7P:M3	0.08382	0.078	0.09363	0.07416	0.09317	0.11063	0.10114	0.1021	0.09368	0.10399	0.10256	0.10701	0.08315	0.10182	0.09729	0.09104	0.0752	0.09524	0.11028	0.10831	0.09405	0.09569	0.10331

metabolite	6	11	17	21	24	30	36	40	47	53	60	71	77	85	89	95	99	107	114	121	126	133	150
Sed7P:M4	0.05298	0.09967	0.11215	0.08811	0.10485	0.10379	0.11079	0.11695	0.11523	0.11446	0.10921	0.09989	0.10053	0.11879	0.0848	0.11864	0.0946	0.12404	0.12027	0.11307	0.11559	0.12168	0.13004
Sed7P:M5	0.01377	0.047	0.03748	0.0511	0.04151	0.03517	0.03734	0	0.03292	0	0.03262	0	0.04108	0.04621	0.04603	0	0.04348	0.0427	0.03605	0.04526	0.04292	0.04946	0.04747
Sed7P:M6	0	0	0	0.00933	0	0.00864	0	0	0	0	0.02211	0.01009	0.00064	0	0.02117	0	0.01472	0.02832	0.0252	0.03151	0.02845	0.03135	0.03575
Sed7P:M7	0.03218	0.13239	0.16758	0.20778	0.20643	0.2245	0.24418	0.27683	0.24094	0.24246	0.2202	0.25461	0.27459	0.30057	0.28601	0.30393	0.30302	0.30902	0.30206	0.3224	0.33869	0.32475	0.31553
Ohglut:M0	1	0.99684	0.99736	0.99788	0.99683	0.99622	0.99599	0.99667	0.9967	0.99612	0.99474	0.99471	0.99578	0.99382	0.99501	0.99352	0.99254	0.99279	0.99255	0.99133	0.9901	0.99101	0.98942
Ohglut:M1	0	0	0	0	0	0	0	0	0	0	0	0	0	0	0	0	0	0	0	0	0	0	0
Ohglut:M2	0	0	0	0	0	0	0	0	0	0	0	0	0	0	0	0	0	0	0	0	0	0	0
Ohglut:M3	0	0	0	0	0	0	0	0	1.00E-04	0.00034	0.00024	0.00043	0.00057	0.00114	0.00063	0.00124	0.00123	0.00124	0.00157	0.00142	0.0023	0.0023	0.00238
Ohglut:M4	0	0	0	0	0	0	0	0	0	7.00E-05	0.00058	0.00032	0	0.00101	0.00077	0.00163	0.00148	0.00159	0.00172	0.00189	0.00248	0.0023	0.00271
Ohglut:M5	0	0.00316	0.00264	0.00212	0.00317	0.00378	0.00401	0.00333	0.0032	0.00347	0.00443	0.00454	0.00365	0.00404	0.00358	0.00361	0.00476	0.00438	0.00416	0.00535	0.00512	0.0044	0.00549
Man6P:M0	0.80591	0.60271	0.63315	0.60307	0.58027	0.57797	0.54717	0.52059	0.53132	0.5542	0.54669	0.52106	0.48032	0.47985	0.46886	0.49611	0.46971	0.47874	0.4664	0.41993	0.42333	0.41086	0.39543
Man6P:M1	0	0	0	0	0	0	0	0	0	0	0	0	0	0	0	0	0	0	0	0	0	0	0
Man6P:M2	0	0	0	0	0	0	0	0	0	0	0	0	0	0	0	0	0	0	0	0	0	0	0
Man6P:M3	0	0	0	0	0	0	0.0046	0.00592	NA	NA	NA	NA	0.00253	0.01052	0.01268	0.00955	0.01147	NA	0.01182	0.01272	0.01401	0.01476	0.01805
Man6P:M4	0	0	0	0	0	0	0.00455	0.00389	0.00734	NA	0.00638	NA	0.00212	0.00855	0.01102	0.00817	0.00966	NA	0.00968	0.01058	0.01038	0.01194	0.01402
Man6P:M5	0.02056	0.07328	0.0092	0.009	0.01838	0.01518	0.01192	0.0435	0.02194	0.02501	0.0119	0.0179	0.01987	0.01903	0.02355	0.01375	0.01193	0.01293	0.01689	0.01809	0.03343	0.01295	0.01852
Man6P:M6	0.17353	0.324	0.35764	0.38794	0.40135	0.40685	0.43176	0.4261	0.4394	0.42079	0.43504	0.46104	0.49517	0.48205	0.48388	0.47243	0.49722	0.50833	0.49521	0.53867	0.51885	0.5495	0.55398
Rib1P:M0	0.9995	0.99456	0.99253	0.98331	0.98203	0.97791	0.97432	0.96903	0.96948	0.96485	0.96074	0.94427	0.91988	0.93237	0.91928	0.9243	0.90792	0.91861	0.90909	0.88949	0.87487	0.86984	0.85381
Rib1P:M1	0	0	0	0	0	0	0	0	0	0	0	0	0	0	0	0	0	0	0	0	0	0	0
Rib1P:M2	0	0	0	0	0	0	0	0	0	0	0	0	0.00355	0.00077	0.00268	0.00162	0.00304	0.00243	0.0034	0.00605	0.00869	0.01003	0.01201
Rib1P:M3	0	0	8.00E-05	0.00201	0.0021	0.0028	0.00329	0.00421	0.00428	0.00538	0.00588	0.00932	0.01336	0.01173	0.01313	0.01245	0.01476	0.01332	0.0154	0.01727	0.02091	0.02131	0.02377
Rib1P:M4	0	0	0	0.00011	NA	0.00031	0.00034	0.00071	0.00083	0.00093	0.00085	0.00152	0.00223	0.00185	0.00214	0.00208	0.00172	0.00208	0.00234	0.0027	0.00356	0.00373	0.00408
Rib1P:M5	5.00E-04	0.00544	0.00739	0.01457	0.01586	0.01897	0.02205	0.02604	0.02541	0.02884	0.03253	0.04489	0.06098	0.05327	0.06278	0.05954	0.07256	0.06355	0.06977	0.0845	0.09198	0.09509	0.10633
Ala:M0	0.97814	0.94075	0.88615	0.87101	0.83545	0.83449	0.81596	0.80061	0.78034	0.79431	0.7648	0.72588	0.70565	0.7419	0.71004	0.75776	0.76258	0.74136	0.71408	0.70408	0.72224	0.73471	0.71506
Ala:M1	0	0	0	0	0	0	0	0	0	0	0	0	0	0	0	0	0	0	0	0	0	0	0
Ala:M2	0	0	0	0	0	0	0	0	0	0	0	0	0.0031	0	0.00489	0.00155	0.00328	NA	NA	0.00269	NA	0.00134	0.00618
Ala:M3	0.02186	0.05925	0.11385	0.12899	0.16455	0.16551	0.18404	0.19939	0.21966	0.20569	0.2352	0.27412	0.29126	0.2581	0.28507	0.24068	0.23415	0.25864	0.28592	0.29323	0.27776	0.26395	0.27876
Arg:M0	1	1	1	1	1	1	1	1	1	1	1	0.96964	0.95162	0.93596	0.91535	0.90282	0.82192	0.84329	0.81079	0.75663	0.76705	0.67355	0.62538
Arg:M1	0	0	0	0	0	0	0	0	0	0	0	0	0	0	0	0	0	0	0	0	0	0	0
Arg:M2	0	0	0	0	0	0	0	0	0	0	0	0.03036	0.04838	0.06404	0.08465	0.09718	0.1234	0.12631	0.14573	0.15139	0.17864	0.17527	0.18369
Arg:M3	0	0	0	0	0	0	0	0	0	0	0	0	0	0	0	0	0.01017	0.00549	0.01032	0.02471	0	0.04638	0.05674
Arg:M4	0	0	0	0	0	0	0	0	0	0	0	0	0	0	0	0	0.03511	0.02492	0.03316	0.04849	0.05431	0.07081	0.09138
Arg:M5	0	0	0	0	0	0	0	0	0	0	0	0	0	0	0	0	0.00941	NA	NA	0.01879	NA	0.034	0.0428
Arg:M6	0	0	0	0	0	0	0	0	0	0	0	0	0	0	0	0	0	0	0	0	0	0	0
Glu:M0	1	1	0.98636	0.96007	0.93968	0.89854	0.86167	0.81767	0.7822	0.75272	0.70529	0.65968	0.62282	0.60155	0.55817	0.56027	0.53918	0.51373	0.492	0.4672	0.44515	0.4415	0.39861
Glu:M1	0	0	0	0	0	0	0	0	0	0	0	0.00158	0.00763	0.00802	0.01117	0.00952	0.0126	0.01606	0.01823	0.01876	0.023	0.02504	0.02829
Glu:M2	0	0	0.01364	0.03103	0.0449	0.07014	0.09016	0.11658	0.13042	0.14836	0.16514	0.19017	0.20238	0.20132	0.22889	0.22497	0.23356	0.23289	0.24817	0.25287	0.26443	0.25555	0.27217
Glu:M3	0	0	0	0	0	0	0	0	0	0	0	0	0	0	0	0	0	0	0	0	0	0	0
Glu:M4	0	0	0	0.0089	0.01542	0.02136	0.03271	0.04441	0.0564	0.06249	0.08216	0.09369	0.10347	0.12049	0.12287	0.12484	0.13202	0.14615	0.14808	0.16366	0.15823	0.16811	0.1782
Glu:M5	0	0	0	0	0	0.00996	0.01547	0.02133	0.03098	0.03644	0.04741	0.05487	0.06371	0.06862	0.07891	0.0804	0.08264	0.09116	0.09352	0.09751	0.10919	0.1098	0.12273
Gln:M6	1	1	1	1	1	1	0.98695	0.96988	0.98042	0.90868	0.8798	0.74724	0.75254	0.79452	0.69839	0.84421	0.66525	0.66574	0.55124	0.55872	0.5391	0.49338	0.45784
Gln:M0	0	0	0	0	0	0	0	0	0	0	0	0	0	0	0	0	0	0	0	0	0	0	0
Gln:M1	0	0	0	0	0	0	0	0.01031	0.01958	0.03158	0.05345	0.13893	0.14155	0.10405	0.16487	0	0.09276	0.11351	0.13603	0.14376	0.17797	0.23891	0.18583
Gln:M2	0	0	0	0	0	0	0.01305	0	0	0	0	0	0	0.01624	0.00508	NA	0.13774	0.00553	0.07994	0.02308	0.01059	0.00617	0.02651
Gln:M3	0	0	0	0	0	0	0	0.01981	0	0.04735	0.05559	0.06724	0.0771	0.08519	0.09833	0.08229	0.10426	0.14386	0.15476	0.17489	0.18081	0.19652	0.22943
Gln:M4	0	0	0	0	0	0	0	0	0	0.01239	0.01116	0.0466	0.02882	NA	0.03332	0.0735	NA	0.07136	0.07803	0.09955	0.09153	0.06502	0.10039
Glut:M0	1	1	1	1	1	1	1	1	1	1	1	1	1	1	1	1	1	1	1	1	1	1	1
Glut:M1	0	0	0	0	0	0	0	0	0	0	0	0	0	0	0	0	0	0	0	0	0	0	0
Glut:M2	0	0	0	0	0	0	0	0	0	0	0	0	0	0	0	0	0	0	0	0	0	0	0
Glut:M3	0	0	0	0	0	0	0	0	0	0	0	0	0	0	0	0	0	0	0	0	0	0	0
Glut:M4	0	0	0	0	0	0	0	0	0	0	0	0	0	0	0	0	0	0	0	0	0	0	0
Glut:M5	0	0	0	0	0	0	0	0	0	0	0	0	0	0	0	0	0	0	0	0	0	0	0
Glut:M6	0	0	0	0	0	0	0	0	0	0	0	0	0	0	0	0	0	0	0	0	0	0	0
Glut:M7	0	0	0	0	0	0	0	0	0	0	0	0	0	0	0	0	0	0	0	0	0	0	0
Glut:M8	0	0	0	0	0	0	0	0	0	0	0	0	0	0	0	0	0	0	0	0	0	0	0
Glut:M9	0	0	0	0	0	0	0	0	0	0	0	0	0	0	0	0	0	0	0	0	0	0	0
Glut:M10	0	0	0	0	0	0	0	0	0	0	0	0	0	0	0	0	0	0	0	0	0	0	0
Ile:M0	1	0.87802	0.76833	0.67331	0.75722	0.68306	0.69851	0.62282	0.63982	0.6411	0.52573	0.53803	0.42229	0.54993	0.47939	0.57887	0.46217	0.50432	0.56009	0.50989	0.43689	0.49686	0.49357
Ile:M1	0	0	0	0	0	0	0	0	0	0	0	0	0	0	0	0	0	0	0	0	0	0	0
Ile:M2	0	0.12198	0.23167	0.32669	0.24278	0.31694	0.30149	0.34692	0.29654	0.2822	0.32426	0.29874	0.31828	0.22643	0.26178	0.19606	0.24528	0.21183	0.17557	0.19497	0.20644	0.18239	0.161
Ile:M3	0	0	0	0	0	0	0	0	0.00681	0.00306	0.02656	0.02516	0.03995	0.04656	0.03894	0.03618	0.04108	0.04288	0.04331	0.04031	0.04903	0.05126	0.04389
Ile:M4	0	0	0	0	0	0	0	0	0	0	0	0.00976	0.01525	0.01598	0.03875	0.03724	0.04961	0.04609	0.04332	0.05636	0.07471	0.07124	0.07417
Ile:M5	0	0	0	0	0	0	0	0.03026	0.05683	0.07365	0.12345	0.12831	0.20424	0.16111	0.18114	0.15165	0.20187	0.19487	0.15963	0.17966	0.2191	0.17993	0.19016
Ile:M6	0	0	0	0	0	0	0	0	0	0	0	0	0	0	0	0	0	0	0.01809	0.01881	0.01384	0.01832	0.03721
Leu:M0	1	0.96272	0.90441	0.84578	0.82523	0.77709	0.74639	0.71017	0.68826	0.68372	0.65007	0.65061	0.61588	0.63646	0.61582	0.61122	0.61247	0.61227	0.60438	0.6169	0.59239	0.60089	0.60124
Leu:M1	0	0	0	0	0	0	0	0	0	0	0	0	0	0	0	0	0	0	0	0	0	0	0
Leu:M2	0	0.03728	0.08523	0.11938	0.11556	0.12991	0.12317	0.12388	0.11706	0.10782	0.10464	0.09355	0.09916	0.0899	0.09097	0.09159	0.08952	0.08743	0.09036	0.08296	0.09328	0.08969	0.08641
Leu:M3	0	0	0	0	0	0	0	0	0	0	0	0	0	0	0.00015	0	0	0.00018	0	0.00092	0.00049	0.00049	0.00114
Leu:M4	0	0	0.01036	0.02883	0.0424	0.06678	0.08971	0.10969	0.12221	0.1293	0.14721	0.15211	0.16888	0.16324	0.17364	0.17618	0.17128	0.17445	0.18146	0.17795	0.18057	0.18256	0.18187
Leu:M5	0	0	0	0	0	0	0	0	0	0	0	0	0	0	0	0	0	0	0	0	0.00086	NA	NA
Leu:M6	0	0	0	0.00601	0.01681	0.02621	0.04074	0.05626	0.07248	0.07916	0.09807	0.10374	0.11608	0.11041	0.11942	0.12101	0.12673	0.12568	0.1238	0.12128	0.13242	0.12637	0.12934
Phe:M0	1	0.95612	0.88902	0.82168	0.80357	0.73872	0.7056	0.6815	0.66819	0.62569	0.61642	0.59078	0.55271	0.58771	0.5449	0.57307	0.53499	0.53883	0.54088	0.55925	0.51639	0.51512	0.53209
Phe:M1	0	0	0	0	0	0	0	0	0	0	0	0	0	0	0	0	0	0	0	0	0	0	0
Phe:M2	0	0	0	0	0.00247	0	0.00078	0.00069	0.00074	0.00207	0.00014	0.00108	0.00729	0.00227	0.00289	0	0.00513	0.00039	0.00488	0.00116	0.00563	0.00267	0.00257
Phe:M3	0	0.03852	0.08257	0.095	0.086	0.06901	0.05692	0.04985	0.03344	0.03164	0.02414	0.02557	0.02818	0.02019	0.02264	0.01976	0.03172	0.0182	0.01874	0.02178	0.01932	0.02505	0.02069
Phe:M4	0	0.00536	0.01765	0.0309	0.03357	0.03192	0.03068	0.0327	0.02801	0.02528	0.02354	0.02785	0.02354	0.02199	0.02617	0.0229	0.02265	0.02765	0.02646	0.01961	0.02741	0.02529	0.02047
Phe:M5	0	0	0	0	0	0	0	0	0	0	0	0	0	0	0	0	0	0	0	0.0071	0.0032	0.00693	0.01517
Phe:M6	0	0	0	0.01768	0.03203	0.04415	0.06099	0.06236	0.07109	0.07213	0.08426	0.08487	0.09514	0.08765	0.10018	0.09434	0.09397	0.10549	0.09194	0.09569	0.10367	0.10256	0.09744
Phe:M7	0	0	0.01076	0.03474	0.04235	0.04771	0.0502	0.05318	0.05546	0.05875	0.06332	0.05822	0.06498	0.05995	0.07136	0.05985	0.06615	0.06965	0.06319	0.05885	0.06561	0.06138	0.06728
Phe:M8	0	0	0	0	0	0	0	0	0	0.01206	0.02198	0.0096	0.01631	0.01631	0.01846	0.01691	0.02884	0.02782	0.03948	0.02062	0.024	0.02653	0.0256
Phe:M9	0	0	0	0	0	0.06849	0.09483	0.11971	0.14308	0.17237	0.16619	0.20204	0.21185	0.20394	0.2134	0.21318	0.21654	0.21199	0.21442	0.21594	0.23478	0.23449	0.21867
Pro:M0	1	1	1	1	1	1	1	1	1	0.968	0.92873	0.88385	NA	0.87376	0.84052	0.85352	0.83717	0.77566	0.76373	0.71657	0.59761	0.77841	0.55923

metabolite	6	11	17	21	24	30	36	40	47	53	60	71	77	85	89	95	99	107	114	121	126	133	150
Pro:M1	0	0	0	0	0	0	0	0	0	0	0	0	0	0	0	0	0	0	0	0	0	0	0
Pro:M2	0	0	0	0	0	0	0	0	0	0.032	0.07127	0.11615	NA	0.12624	0.15948	0.14648	0.16283	0.14106	0.1746	0.19992	0.24979	0.22159	0.29945
Pro:M3	0	0	0	0	0	0	0	0	0	0	0	0	0	0	0	0	0	0	0	0	0	0	0
Pro:M4	0	0	0	0	0	0	0	0	0	0	0	0	0	0	0	0	0	0.08328	0.06168	0.08351	0.1526	NA	0.14132
Pro:M5	0	0	0	0	0	0	0	0	0	0	0	0	0	0	0	0	0	0	0	0	0	0	0
Thr:M0	1	1	1	1	1	1	1	1	1	1	1	0.77154	1	1	0.7982	0.73805	0.56178	0.80619	0.70686	0.73557	0.80511	0.55923	1
Thr:M1	0	0	0	0	0	0	0	0	0	0	0	0	0	0	0	0	0	0	0	0	0	0	0
Thr:M2	0	0	0	0	0	0	0	0	0	0	0	0	0	0	0	0	0	0	0	0	0	0	0
Thr:M3	0	0	0	0	0	0	0	0	0	0	0	0.22846	0	0	0	0	0.2603	0	0	0	0	0.23813	0
Thr:M4	0	0	0	0	0	0	0	0	0	0	0	0	0	0	0.2018	0.26195	0.17792	0.19381	0.29314	0.26443	0.19489	0.20264	0
Trp:M0	1	1	1	1	1	1	0.95929	0.86564	0.89465	0.88928	0.80019	0.76011	0.67598	0.71846	0.68339	0.68808	0.69425	0.71325	0.65481	0.70317	0.68949	0.64445	0.6317
Trp:M1	0	0	0	0	0	0	0	0	0	0	0	0	0	0	0	0	0	0	0	0	0	0	0
Trp:M2	0	0	0	0	0	0	0	0	0	0	0	0	0	0	0	0	0	0	0	0	0	0	0
Trp:M3	0	0	0	0	0	0	0	0	0	0	0	0	0	0	0	0	0	0	0	0	0	0	0
Trp:M4	0	0	0	0	0	0	0	0	0	0	0	0	0	0	0	0	0	0	0	0	0	0	0
Trp:M5	0	0	0	0	0	0	0	0	0	0	0	0	0	0	0	0	0	0	0	0	0	0	0
Trp:M6	0	0	0	0	0	0	0	0	0	0	0	0	0	0	0	0	0	0	0	0	0	0	0
Trp:M7	0	0	0	0	0	0	0	0	0	0	0	0	0	0	0	0	0	0	0	0	0	0	0
Trp:M8	0	0	0	0	0	0	0	0	0	0	0	0	0.05218	0.0341	0.08146	0.07146	0.06983	0	0.03921	0.02798	0.06859	0.07001	0.05994
Trp:M9	0	0	0	0	0	0	0.04071	0.1069	NA	0.05621	0.06904	0.09894	0.12303	0.10813	0.05039	0.0844	0.1097	0.08713	0.10317	0.08592	0.10097	0.08651	0.1428
Trp:M10	0	0	0	0	0	0	0	0	0	0	0	0	0	0	0	0	0	0	0	0	0	0	0
Trp:M11	0	0	0	0	0	0	0	0.02746	0.10535	0.05451	0.13077	0.14095	0.14882	0.13931	0.18475	0.15606	0.12622	0.19963	0.20281	0.18293	0.14095	0.19903	0.16556
Tyr:M0	1	0.97675	0.9094	0.83935	0.80495	0.69326	0.64119	0.58739	0.55893	0.5356	0.50358	0.46313	0.41953	0.44403	0.40671	0.42388	0.40296	0.37923	0.40321	0.36942	0.39441	0.39727	0.36492
Tyr:M1	0	0	0	0	0	0	0	0	0	0	0	0	0	0	0	0	0	0	0	0	0	0	0
Tyr:M2	0	0	0	0	0	0	0	0	0	0	0	0	0	0	0	0	0	0	0	0	0	0	0
Tyr:M3	0	0.02325	0.07444	0.09324	0.06352	0.07642	0.05508	0.04692	0.02573	0.02244	0.01646	0.02572	0.02952	0.01395	0.02214	0.02305	0.01646	0.02982	NA	0.01875	NA	NA	0.01429
Tyr:M4	0	0	0.01616	0.0249	0.02768	0.02917	0.02811	0.02861	0.02708	0.01649	0.02133	NA	0.01155	0.02207	NA	0.02356	0.02704	0.02842	0.02207	0.01845	0.03067	0.01909	0.02403
Tyr:M5	0	0	0	0	0	0	0	0	0	0	0	0	0	0	0.00951	0.01105	0.01163	0.0029	0.01766	0.02293	NA	0.01104	0.02099
Tyr:M6	0	0	0	0.02453	0.02503	0.05575	0.09201	0.09651	0.10882	0.12321	0.12909	0.13191	0.15044	0.13577	0.13718	0.12526	0.14011	0.15788	0.14614	0.13535	0.14518	0.14367	0.14536
Tyr:M7	0	0	0	0.01798	0.02928	0.0493	0.05317	0.06072	0.05997	0.07775	0.06604	0.0602	0.07746	0.07557	0.07665	0.07808	0.05887	0.08568	0.07186	0.08025	0.07082	0.07087	0.09227
Tyr:M8	0	0	0	0	0	0	0	0	0	0	0	0	0	0	0	0	0	0	0	0	0	0	0
Tyr:M9	0	0	0	0	0.04955	0.09609	0.13043	0.17985	0.21947	0.22451	0.26351	0.31904	0.31151	0.3086	0.34782	0.31512	0.34294	0.31607	0.33906	0.35486	0.35891	0.35805	0.33814

Annex H: Result of flux calculation

Values of flux net calculated by influx_i from network of stoichiometric reactions (Annex D), metabolite pools (concentrations, Annex E) and experimental carbon isotopologue data (Annex F, G) collected in glucose-grown E.coli K-12. Mean Absolute mean value in mmol/s/g biomass, standard deviation calculated from the two biological replicates.

Flux net	Mean [mM/s/g]	SD [mM/s/g]
ackA	0.5001	0.0338
acn1	0.5297	0.0906
acn2	0.5297	0.0906
ac_out	0.5001	0.0338
akgdh	0.4197	0.0920
ald	1.0346	0.1390
asD	0.0745	0.0010
aspC	0.0745	0.0010
aspk	0.0745	0.0010
bs_accoa1	0.2485	0.0035
citsynth	0.5297	0.0906
eda	0.0501	0.0706
eno	1.9693	0.2299
eutD	0.5001	0.0338
fum_a	0.2117	0.0460
fum_b	0.2117	0.0460
gdh	2.1213	0.2285
gpm	2.1213	0.2285
hdh	0.0745	0.0010
HR1	0.0668	0.0413
HR2	-0.0152	0.0210
HR3	-0.0517	0.0203
HR4	0.0517	0.0203
HR5	-0.0517	0.0203
idh	0.5297	0.0906
maldh	0.4234	0.0919
out_form	0.0070	0.0003
pdh	1.3289	0.1201
pfk	1.0346	0.1390
pgi	0.9749	0.0975
pgk	2.1213	0.2285
pgl	0.2506	0.0234
ppc_pck	0.3285	0.0434
rpe	0.0668	0.0413
rpi	0.1338	0.0060
sdh	0.4234	0.0919
ilvA	0.0350	0.0003
tdce	0.0070	0.0003
thrb	0.0595	0.0010
thrc	0.0595	0.0010
tmp	0.0033	0.0002
tpi	1.0346	0.1390
zwf	0.2506	0.0234
CO2upt	22.4742	31.5038
edd	0.0501	0.0706
Glc_upt	1.2466	0.0742
gnd	0.2006	0.0473
out_co2	24.6210	31.1971
pta2	0.0000	0.0000
pyk	1.5673	0.1872
scs	0.4268	0.0917
yliK	-0.0037	0.0009
ygfG	-0.0037	0.0009
ygfH	0.0033	0.0002